

ABSTRACT

Title of Document: REVERSE GENETICS OF INFLUENZA B
AND THE DEVELOPMENT OF A NOVEL
LAIV VACCINE

Courtney L. Finch, Doctor of Philosophy, 2014

Directed By: Professor Daniel R. Perez, Department of
Veterinary Medicine

Due to the disease burden of influenza virus types A and B, vaccines, which are manufactured as formalin-inactivated killed virus (KV) and live-attenuated virus (LAIV), are produced to provide coverage against currently circulating influenza A (IAV) and B (IBV) viruses. Although the licensed LAIV vaccine provides enhanced coverage over the KV vaccine, it is only licensed for immunocompetent individuals ages 2-49 years without pre-existing conditions, so individuals who are most at risk cannot receive it. Previously, our lab showed that incorporation of an 8 amino acid HA tag in frame at the C-terminus of the PB1 open-reading frame (ORF) in addition to the mutations found in the PB2 and PB1 segments of the licensed LAIV vaccine yielded a stable, efficacious alternative LAIV vaccine for IAV; however, to develop a complete vaccine, a corresponding IBV candidate is required. Towards this goal, a contemporary IBV strain, B/Brisbane/60/2008, was cloned and recovered by reverse genetics (RG-B/Bris). Subsequently, it was demonstrated that the parental and RG-

B/Bris show similar growth kinetics *in vitro*. An initial vaccine attempt, which combined PB2 cap-binding mutants with the HA tag in PB1, was made but led to the realization of the PB2 cap-binding mutations, PB2 W359F and F406Y, as virulence factors. In a subsequent vaccine attempt, mutations analogous to those found only in segment 2 of the A/Ann Arbor/6/60 cold-adapted LAIV backbone were introduced into the homologous segment of RG-B/Bris. The following mutations were introduced into the PB1 gene segment of RG-B/Bris, either in the presence or absence of a C-terminal HA tag: K391E, E580G, and S660A. Two viruses were rescued, referred to as RG-B/Bris *ts* and RG-B/Bris *att*, both containing the set of three amino acid mutations but differing in the absence or presence of the HA tag, respectively. Both viruses showed ideal attenuation, safety, and immunogenicity in DBA/2 mice and conferred protection against lethal IBV challenge. More importantly, RG-B/Bris *att*, but not RG-B/Bris *ts*, showed ideal stability with no reverting mutations over 8 passages in eggs. Taken together, a stable, immunogenic, and live attenuated virus alternative to the current live influenza B virus vaccine was produced.

REVERSE GENETICS OF INFLUENZA B AND THE DEVELOPMENT OF A
NOVEL LAIV VACCINE

By

Courtney L. Finch

Dissertation submitted to the Faculty of the Graduate School of the
University of Maryland, College Park, in partial fulfillment
of the requirements for the degree of
Doctor of Philosophy
2014

Advisory Committee:
Professor Daniel R. Perez, Chair
Assistant Professor Georg Belov
Professor Jeffery DeStefano
Associate Professor Yanjin Zhang
Professor Xiaoping Zhu

© Copyright by
Courtney L. Finch
2014

Dedication

I dedicate this dissertation to my family, namely my parents, Joseph and Carolyn, my husband, Nathan, and my in-laws. Mom and Dad, you taught me long ago that I could achieve anything. During my graduate career whenever I was in doubt, you believed. You gave me the strength and encouragement to continue believing in myself. I hope that seeing the acquisition of a PhD finally come to fruition will give you great pride. I regret that this achievement has been at the expense of time with the family. I hope that as my career progresses I can rectify this.

To Nathan, my ever supportive, everloving husband, your unrelenting optimism and your unwavering belief in me have meant everything over these years. You alone know how truly difficult this process has been at times. You know my joys and my sorrows. You have been there for me the entire way. Thank you for tolerating the long nights and early mornings all of these years, thank you for never complaining and always understanding. This achievement also belongs to you.

To the Finch family, especially Bud, Pat and Justin, you welcomed me into your family with open arms. You are more than just my in-laws; you are an extension of my immediate family. The love, support and acceptance you have shown me have been immeasurable. Thank you for always treating me like one of your own.

Acknowledgements

There are many who deserve thanks for the support and guidance provided to me during the course of my graduate career. Firstly, I would like to thank Dr. Daniel Perez. Thank you for the opportunity to work, learn and mature as a scientist in your laboratory. Thank you for the freedom you gave me to pursue my own ideas and to direct my own research. I know that I am a better scientist for having been in your laboratory. Few labs can rival the expertise in reverse genetics, transmission and animal models that the Perez lab offers, and I am proud to say that my most formative years as a scientist were spent in your lab.

Secondly, I would like to thank my committee members, Dr. Belov, Dr. Culver, Dr. DeStefano, Dr. Zhang and Dr. Zhu. Thank you for your invaluable input in guiding my research progress. Thank you for pushing me to be better. Thank you for your time. Each committee meeting gave me more to consider and opened my eyes to new perspectives, strengthening my research.

Thirdly, I would like to thank all members of the Perez lab, past and present, for the knowledge and skills that were imparted to me. In particular, I would like to thank Dr. Troy Sutton. The time you spent in mentoring and training me is unparalleled. I will never forget the role you played in my professional development. I will forever use 70% ethanol in excess and I have you to thank. In all sincerity, thank you. Additionally, I would like to thank Ana Silvia Gonzalez Reiche. It is difficult to describe how much your friendship and support have meant throughout the years. Having someone in the same year, someone with similar work ethic and interests has been amazing.

Table of Contents

Dedication.....	ii
Acknowledgements.....	iii
Table of Contents.....	iv
Abbreviations List.....	viii
List of Tables.....	x
List of Figures.....	xi
Chapter 1: Introduction to Influenza B, Reverse Genetics and LAIV Vaccines	1
<u>1.1. General Introduction to Orthomyxoviridae</u>	1
<u>1.2. General introduction to influenza B</u>	2
<u>1.3. Genomic organization and encoded proteins of influenza B</u>	5
1.3.1. Genomic organization.....	5
1.3.2. Influenza B encoded proteins.....	8
<u>1.4. Influenza B virus life cycle and immune response to infection</u>	11
1.4.1. Virus attachment and entry	11
1.4.2. Nuclear import.....	14
1.4.3. Transcription, replication and translation	15
1.4.4. Nuclear export.....	16
1.4.5. Virus assembly and budding.....	17
1.4.6. Host immune response to infection.....	18
<u>1.5. Influenza B host-range, evolution and restriction</u>	23
1.5.1. Host range.....	23
1.5.2. Evolution.....	23
1.5.3. Host restriction of influenza B.....	25
<u>1.6. Introduction to Influenza B Reverse Genetics</u>	27
1.6.1. HA receptor binding, egg-adapted mutations and the significance of the HA cytoplasmic tail	30
1.6.2. Antiviral resistance of NA and the role of NB	32
1.6.3. Transcription of BM1 and BM2 and implications for vaccine development and experimentation.....	34
1.6.4. BNS1 antagonism of the innate immune response	37
<u>1.7. Introduction to LAIV Vaccines</u>	39
1.7.1. Review of the B/Ann Arbor ca vaccine backbone.....	43
1.7.2. Modifying the NS Gene Segment.....	48
1.7.3. Modifications in the HA Cleavage Site	49
1.7.4. Conclusions and Commentary: LAIV vaccines.....	51
<u>1.8. Summary of Research Objectives</u>	52
1.8.1. Dissertation outline	53
Chapter 2: Development of a Contemporary B/Brisbane/60/2008 Reverse Genetics System.....	55
<u>2.1. Abstract</u>	55

2.2. Introduction.....	56
2.3. Materials and Methods.....	62
2.3.1. Maintenance of cells	62
2.3.2. Cloning and sequencing of B/Brisbane/60/2008	62
2.3.3. Cloning of a <i>Gaussia</i> Luciferase reporter construct	70
2.3.4. Virus rescue	73
2.3.5. Virus stocks and titration	74
2.3.6. Virus rescue over time	77
2.3.7. Mini-genome assays.....	78
2.3.8. Growth kinetics.....	80
2.3.9. Mouse Lethal Dose 50 (MLD ₅₀).....	81
2.3.10. Phylogenetic analysis of influenza B HA and NA.....	83
2.4. Results.....	85
2.4.1. Polymerase activity shows that RG-Bris polymerase is functional	85
2.4.2. Virus rescue over time shows RG-B/Bris rescues efficiently.....	85
2.4.3. WT and RG-B/Bris grow to similar titers in tissue culture	86
2.4.4. RG-B/Bris is virulent in mice	87
2.4.5. Phylogenetic analysis of RG-B/Bris shows it is a member of the most recent B/Victoria-like virus clade	91
Chapter 3: Development of an Alternative Influenza B LAIV Vaccines: PB2/PB1 mutants.....	98
3.1. Abstract.....	98
3.2. Introduction.....	100
3.3. Materials and Methods.....	105
3.3.1. Cloning and confirmation of mutations	105
3.3.2. Virus rescue and stocks.....	108
3.3.3. Virus titrations	109
3.3.4. Mini-genome assays.....	109
3.3.5. Growth kinetics.....	110
3.3.6. Western blot.....	110
3.3.7. Mouse study	112
3.4. Results.....	114
3.4.1. Similar GLuc expression of PB2/PB1 mutants compared to WT.....	114
3.4.2. Growth curves of PB2/PB1 mutant viruses are similar to WT.....	116
3.4.3. PB2/PB1 mutant viruses express the HA tag from the PB1 ORF	119
3.4.4. PB2/PB1 mutant viruses are lethal in mice at 10 ⁶ EID ₅₀	119
3.5. Discussion.....	122
Chapter 4: PB2 Cap-binding Mutants as Influenza B Virulence Factors in Mice....	124
4.1. Abstract.....	124
4.2. Introduction.....	125
4.3. Materials and Methods.....	129
4.3.1. Cloning of cap-binding mutants by site-directed mutagenesis, virus rescue, and stocks.....	129
4.3.2. Titrations	130

4.3.3. Mini-genome assays.....	131
4.3.4. Growth kinetics.....	132
4.3.5. Mouse studies.....	132
4.3.6. Tissues.....	133
4.3.7. Statistical analyses	134
<u>4.4. Results.....</u>	<u>135</u>
4.4.1. Polymerase assays and growth kinetics of cap-binding mutants show trend towards increased activity and replication at 37°C.....	135
4.4.2. Increased weight loss and mortality with cap-binding mutant viruses in DBA/2 mice	139
4.4.3. Pulmonary virus titers early during infection trend toward increased replication of cap-binding mutants	141
4.4.4. PB2 cap-binding mutant viruses show enhanced lung pathology	143
<u>4.5. Discussion.....</u>	<u>147</u>

Chapter 5: Development of Alternative Influenza B LAIV Vaccines based on three amino acid mutations and an C-terminal HA tag in PB1.....	151
<u>5.1. Abstract.....</u>	<u>151</u>
<u>5.2. Introduction.....</u>	<u>153</u>
<u>5.3. Materials and Methods.....</u>	<u>159</u>
5.3.1. Cloning and confirmation of mutations	159
5.3.2. Virus rescue and stocks.....	160
5.3.3. Virus titrations	161
5.3.4. Mini-genome assays.....	161
5.3.5. Growth kinetics.....	162
5.3.6. Western blot.....	163
5.3.7. Assessing stability of vaccine candidates	165
5.3.8. Vaccine safety studies.....	166
5.3.9. Vaccine study.....	167
5.3.10. Tissues for pathology.....	168
5.3.11. Hemagglutination Inhibition assays.....	169
5.3.12. Statistical analyses	170
<u>5.4. Results.....</u>	<u>171</u>
5.4.1. B/Bris <i>ts</i> and B/Bris <i>att</i> polymerase complexes have the highest GLuc expression at low temperatures.....	171
5.4.2. B/Bris <i>ts</i> and <i>att</i> viral titers are undetectable at 37 and 39°C	175
5.4.3. B/Bris <i>att</i> expresses the HA tag.....	178
5.4.4. Vaccine safety studies show B/Bris <i>ts</i> and <i>att</i> viruses are safe and immunogenic in mice.....	181
5.4.5. Vaccine study: no weight loss post-vaccination	182
5.4.6. B/Bris <i>att</i> and <i>ts</i> vaccine replication is restricted to growth in nasal turbinates.....	182
5.4.7. Pre-challenge HI assays reveal detectable HI titers in B/Bris <i>att</i> and <i>ts</i> vaccinated mice.....	185
5.4.8. No weight loss in B/Bris <i>att</i> or <i>ts</i> vaccinated mice post-challenge.....	185

5.4.9. No virus detected in tissues of B/Bris <i>att</i> or <i>ts</i> vaccinated mice post-challenge, suggests sterilizing immunity	188
5.4.10. Increased HI titers in vaccinated mice post-challenge.....	188
5.4.11. Increased pulmonary pathology in PBS/C group post-challenge	189
5.4.12. Enhanced stability of B/Bris <i>att</i> virus over the B/Bris <i>ts</i> virus.....	193
<u>5.5. Discussion</u>	194
<u>6.1. Conclusions</u>	197
6.1.2. Chapter 2 conclusions: A contemporary reverse genetics system for B/Brisbane/60/2008 grows to high titers and is virulent in mice.....	198
6.1.3. Chapter 3 conclusions: PB2/PB1 mutant vaccine strategy is lethal in mice	199
6.1.4. Chapter 4 conclusions: PB2_F406Y and PB2_W359F are virulence factors of B/Brisbane/60/2008	200
6.1.5. Chapter 5 conclusions: B/Bris <i>att</i> is stable, safe and immunogenic in mice	200
<u>6.2. Future Directions</u>	202
6.2.1. Determine efficacy of the B/Bris <i>att</i> backbone in the context of a quadrivalent vaccine	202
6.2.2. Assess IgG, IgA and innate responses to vaccination.....	202
6.2.3. Evaluate the B/Bris <i>att</i> backbone in a quadrivalent vaccine for ferrets..	203
6.2.4. Analyze the immune response conferred by the B/Bris <i>att</i> vaccine in an aged mouse model.....	204
6.2.5. Adapt B/Bris <i>att</i> to birds for use as a DIVA vaccine.....	205
Appendices.....	206

Abbreviations List

AF	Allantoic Fluid
Ca	Cold-adapted
cRBC	Chicken Red Blood cells
CTL	Cytotoxic T Lymphocyte
DIVA	Differentiating Infected from Vaccinated Animals
DMEM	Dulbecco's Modification of Eagle's Medium
Dpc	Days post-challenge
Dpi	Days post-infection
Dpv	Days post-vaccination
EID ₅₀	Egg Infectious Dose 50
ER	Endoplasmic Reticulum
GFP	Green Fluorescent Protein
GISRS	Global Influenza Surveillance and Response System
GLuc	<i>Gaussia</i> Luciferase
HA	Hemagglutinin
HE	Hemagglutinin-esterase
H&E	Hematoxylin and Eosin
HI	Hemagglutination Inhibition
Hpi	Hours post-infection
Hpt	Hours post-transfection
Hsp40	Heat shock protein 40
IAV	Influenza A Virus
IBV	Influenza B Virus
IFN	Interferon
IL	Interleukin
IRF	Interferon Regulatory Factor
ISG	Interferon Stimulated Gene
KV	Killed Virus
LAIV	Live-attenuated Influenza Virus
MDCK	Madin-Darby Canine Kidney
MLD ₅₀	Mouse Infectious Dose 50
MOI	Multiplicity of Infection
Mx	Myxovirus gene
NA	Neuraminidase
NFDM	Non-fat Dry Milk
NEP	Nuclear Export Protein
NLS	Nuclear Localization Signal
NOS2	Nitric Oxide Synthase 2
NP	Nucleoprotein
NS1	Non-structural Protein 1
NT	Nasal Turbinates
ORF	Open Reading Frame
PA	Polymerase Acid protein 1

PAMP Pathogen Associated Molecular Pattern
PB1 Polymerase Basic protein 1
PB2 Polymerase Basic protein 2
Pfu Plaque-forming units
PI3K Phosphatidylinositol 3-Kinase
PKC Protein Kinase C
Pol I RNA Polymerase I
Pol II RNA Polymerase II
PRR Pathogen Recognition Receptor
RDE Receptor Destroying Enzyme
RdRp RNA Dependent RNA Polymerase
RG Reverse Genetics
RIG-I Retinoic acid inducible gene-I
rRNA Ribosomal RNA
RT Reverse Transcription
SEAP Secreted Alkaline Phosphatase
SPF Specific Pathogen Free
TCID₅₀ Tissue Culture Infectious Dose 50
Th T helper cell
TLR Toll-like Receptor
TNF Tumor Necrosis Factor
UTR Untranslated Region
VAERD Vaccine Associated Enhanced Respiratory Disease
vRNA Viral RNA
vRNP Viral Ribonucleoprotein complex
WHO World Health Organization
WT Wild-type

List of Tables

1. Table 2.1. Universal primers for influenza B reverse transcription
2. Table 2.2. Cloning primers for influenza B
3. Table 2.3. Scoring explanations of signs and symptoms of disease in mice
4. Table 2.4. BLAST results for B/Brisbane/60/2008 plasmid sequences
5. Table 5.1. B/Bris *att* and *ts* inoculated mice HI titers (21dpi)
6. Table 5.2. Tissue pathology post-challenge
7. Appendix. Table 1. HA accession numbers for phylogenetic tree
8. Appendix. Table 2. NA accession numbers for phylogenetic tree

List of Figures

1. Figure 1.1. Influenza B genome
2. Figure 1.2. Influenza B virus life cycle
3. Figure 1.3. 8-plasmid reverse genetics
4. Figure 2.1. B/Brisbane/60/2008 plasmid maps
5. Figure 2.2. Cloning of a GLuc reporter: steps 1-3
6. Figure 2.3. Cloning of a GLuc reporter: steps 4-6
7. Figure 2.4. Polymerase activity of RG-B/Brisbane/60/2008
8. Figure 2.5. Virus rescue over time of RG-B/Brisbane/60/2008
9. Figure 2.6. Growth kinetics of WT and RG-B/Brisbane/60/2008
10. Figure 2.7. Survival of RG-B/Brisbane/60/2008 inoculated mice
11. Figure 2.8. HA and NA phylogenetic trees
12. Figure 3.1. Diagram of the HA tag
13. Figure 3.2. Polymerase activity of PB2/PB1 mutant complexes
14. Figure 3.3. Growth kinetics of PB2/PB1 mutant viruses
15. Figure 3.4. Expression of HA Tag from PB2/PB1 mutant viruses
16. Figure 3.5. Survival of PB2/PB1 mutant inoculated mice at 10^6 EID₅₀
17. Figure 4.1. Mini –genome assays of B/Brisbane/60/2008 cap-binding mutants
18. Figure 4.2. Viral growth kinetics of B/Brisbane/60/2008 cap-binding mutants
19. Figure 4.3. Weight loss and survival of B/Brisbane/60/2008 infected mice
20. Figure 4.4. Tissue titers of cap-binding mutant infected mice
21. Figure 4.5. Lung pathology of cap-binding mutant infected mice

22. Figure 4.6. Representative lung pathology of cap-binding mutant infected mice
23. Figure 5.1. Mini-genome assay results for B/Bris *att* and *ts* polymerase complexes
24. Figure 5.2. Growth kinetics assay results for B/Bris *att* and *ts* vaccine candidates
25. Figure 5.3. B/Bris *att* expression of HA tag
26. Figure 5.4. Vaccine safety studies: weight loss of B/Bris *ts* and B/Bris *att* inoculated mice
27. Figure 5.5. Weight loss post-vaccination
28. Figure 5.6. Post-vaccination tissue titers
29. Figure 5.7. HI titers 20 days post-vaccination
30. Figure 5.8. Weight loss and survival post-challenge
31. Figure 5.9. Post-challenge tissue titers
32. Figure 5.10. Post-challenge HI titers
33. Figure 5.11. Post-challenge representative pulmonary pathology images

Chapter 1: Introduction to Influenza B, Reverse Genetics and LAIV Vaccines

1.1. General Introduction to Orthomyxoviridae

Influenza B virus (IBV) causes respiratory disease in humans and belongs to the *Orthomyxoviridae* family of viruses (3, 4). As part of group V in the Baltimore scheme of virus classification, IBV has a negative-sense, single-stranded RNA genome (5). In addition to influenza B, there are five other virus types belonging to this family: influenza A virus, influenza C virus, Thogotovirus, Isavirus and Quarantivirus (3, 6-9). All virus types within the family *Orthomyxoviridae* possess segmented genomes, each gene segment encoding at least 1 protein; influenza A virus, influenza B virus, and Isavirus have 8 RNA gene segments, while the influenza C virus genome has only 7 segments (3, 6, 10). Thogotovirus and Quarantivirus possess even fewer segments, having just 6 RNA gene segments (8, 9). The segmented nature of the genome enables rapid divergence of each virus type through the swapping of virus segments amongst like virus types, and by increasing diversity of the virus genome, virus host range may also increase.

Orthomyxoviruses infect a wide host range, from oviparous animals to mammals, and all orthomyxoviruses, excepting Isavirus, cause disease in humans. While Thogotovirus and Quarantivirus are known to infect humans, they are unique

among orthomyxoviruses in that they may use insect vectors. Influenza C virus infects humans but is not considered a major human pathogen, as it causes mild infection only in young children, and children beyond age 6 typically have protective antibodies against influenza C (11-13). Influenza A has the broadest host range of all orthomyxoviruses. The influenza A virus (IAV) reservoir is thought to be waterfowl, but it is also known to infect dogs, horses, swine, and bats among other species (14-17). Both IAV and IBV are considered major human pathogens; furthermore, although influenza B has been isolated in birds and seals, the IBV host range is thought to be limited primarily to humans (18-23). Indeed, vaccines are manufactured each year to protect against IAV and IBV illness in humans (24, 25).

1.2. General introduction to influenza B

IBV is most closely related to influenza A and C viruses within the *Orthomyxoviridae* family, and IAV and IBV are more closely related. The IAV and IBV major antigenic surface gene, hemagglutinin (HA), diverged 4,000 years ago while the major antigenic surface gene of influenza C, hemagglutinin-esterase (HE), diverged 8,000 years ago (26). These divergence times are earlier than previous estimates but have high bootstrap values indicating that these values are reliable (27).

IBV is one of the major causes of respiratory illness in humans. Symptoms associated with IBV infection are fever, cough, muscle aches, malaise, congestion and sore throat (28, 29). The incidence of IBV-related illness varies seasonally, as cold and dry conditions have been shown to facilitate transmission of influenza (30,

31). Each year, the significant morbidity and mortality influenza B causes is profound, particularly in infants and the elderly. For example, in the U.S. from 2004-2011 (excluding the 2009-10 influenza A pandemic), 22-44% of all pediatric influenza-related deaths were IBV-related (28). Additionally, hospitalization rates due to influenza B illness from 1979/80-2000/01 occurred at a rate of 83.4/100,000 cases, making IBV hospitalization rates during this period higher than seasonal influenza A H1N1 virus but lower than influenza A H3N2 virus (4).

The prevalence of IBV virus tends to be lower than that of IAV; however, this does not diminish its impact on human health. Indeed, every 3 years influenza B is actually more prevalent than influenza A (32). Even during years when influenza B is less prevalent, it has been documented to account for a disproportionately large number of pediatric fatalities. For example, during the 2010-11 influenza season, IBV accounted for 38% of all influenza-associated pediatric deaths despite accounting for only 26% of all circulating influenza viruses (33). For this reason, regardless of the prevalence of influenza B in a given year, it is represented in the seasonal influenza vaccine (24).

IBV vaccine manufacture is complicated by the fact that the virus has an error-prone RNA polymerase with no proofreading capabilities, as well as a segmented genome. These features generate diversity by the accumulation of mutations, antigenic drift, and the exchange of viral RNA (vRNA) segments, reassortment (34). Multiple strains of IBV circulate throughout the year, leading to antigenic changes by both mechanisms.

Due to the high mutability of these viruses, virus surveillance is carried out throughout the year to determine the most prevalent strains of IBV in circulation (35). Each fall, the World Health Organization (WHO) makes recommendations as to which viruses should be included in the seasonal influenza vaccine, which is comprised of 2 strains of IAV and 2 strains of IBV (35-37). Vaccines are produced in two primary formulations, formalin-treated inactivated/killed virus (KV) and live-attenuated virus (LAIV) vaccine (24).

1.3. Genomic organization and encoded proteins of influenza B

1.3.1. Genomic organization

The IBV genome is 14.548 kb in length, making it the largest viral genome of the influenza virus types (38). The 8 segments of its genome are numbered 1-8 based on the movement of each RNA segment in a polyacrylamide gel (39, 40). Segments 1-8 correspond to the PB1, PB2, PA, HA, NP, NA, M and NS segments, respectively (39, 40)(Fig. 1.1). Segments 1-3, the PB1, PB2 and PA genes, correspond to the viral RNA-dependent RNA polymerase (RdRp) (41, 42). Segments 4 and 6 correspond to the HA and NA surface genes, respectively; segment 6 also encodes NB, an ion channel protein (43-45). NP, the nucleoprotein that coats and stabilizes the vRNA segments, is encoded by segment 5 (46). Segment 7, the M gene, encodes BM1 and BM2 by a stop-start translation mechanism (47). The eighth and final segment, NS, encodes BNS1, an antagonist of the innate immune response, and BNS2 (also known as NEP), the nuclear export protein, by a post-transcriptional splicing mechanism (48-50).

Each of the 8 vRNA gene segments consists of a coding region flanked by 5' and 3' untranslated regions (UTRs). The first 9 nucleotides at the 3' end UTR of the vRNA of all IBV gene segments are highly conserved, as are the extreme termini of the 5' end of the vRNA (2, 51-53). These conserved 5' and 3' ends have partial inverted complementarity and have been shown to interact (51, 54). The interaction of these ends is crucial, as it creates a promoter and docking site for the viral RdRp,

forming a panhandle structure (54-56). It has been proposed that IBV may also assume a corkscrew structure; this is based on studies demonstrating that IAV, which has similar partial inverted complementarity of its UTRs, forms both panhandle and corkscrew structures (39, 51, 56, 57).

IBV 5' and 3' UTRs are unique in length, being on average longer than those of IAV, a feature that may affect transcription. Indeed, mutational analyses of the influenza B panhandle region have shown that IBV tolerates greater variability in sequence than has been shown for IAV without any detrimental effects on transcription (53, 55).

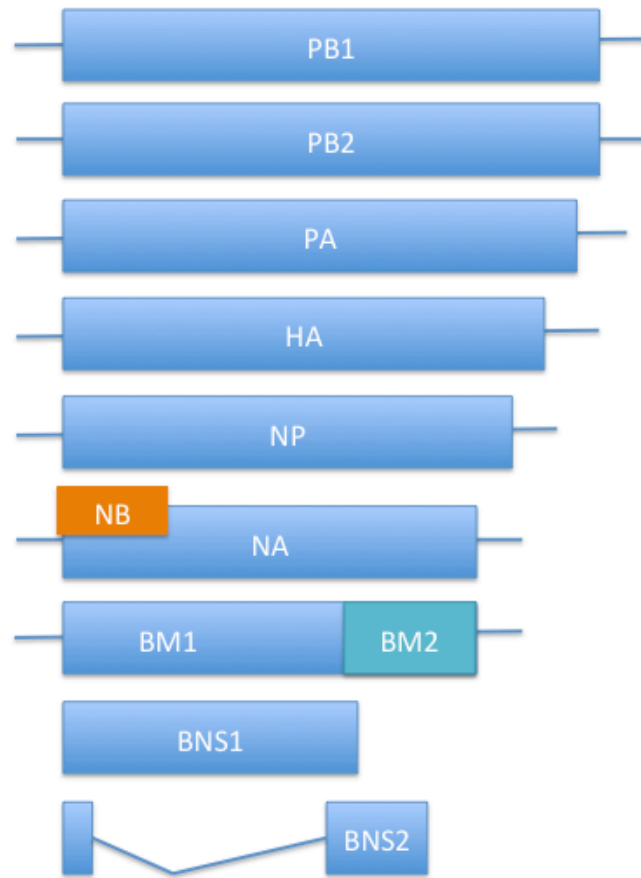


Figure 1.1. Influenza Genome. All 8 RNA segments and the encoded proteins are shown. Segments are 1, 2, 3, 4, 5, 6, 7, and 8 (from top to bottom). NB is shown in orange. BM2 is shown in teal.

1.3.2. Influenza B encoded proteins

The 8 vRNA segments of influenza B virus encode 11 proteins. Each gene segment encodes at least 1 protein with 3 segments encoding 2 proteins each (40, 44, 47, 48). The gene segments can be divided into backbone genes (PB1, PB2, PA, HA, NP, M and NS) and surface genes (HA and NA).

PB1, polymerase basic protein 1, contains the polymerase active site and catalyzes cRNA, vRNA and mRNA transcription (41, 58, 59). PB1 works synergistically with PB2, polymerase basic protein 2, and PA, polymerase acidic protein, to perform these functions. PB2 is responsible for binding the host 5' pre-mRNA cap, which is a crucial step for viral mRNA transcription as the cap acts as a primer for extension (60, 61). Once PB2 binds the cap, PA, an endonuclease, cleaves the cap, and then, PB1 initiates transcription (41, 58, 59, 62). Together, PB1, PB2 and PA form the RdRp which is bound to every vRNA segment, and the RdRp interacts with NP, a nucleoprotein that coats and stabilizes each segment, to form the viral ribonucleoprotein complex (vRNP)(63-66).

The remaining segments of the virus backbone, M and NS, encode 2 proteins each. The M segment encodes BM1 and BM2 via a stop-start translation mechanism, in which the start signal of BM2 overlaps the stop signal of BM1 (47). BM1 is a matrix protein that provides structure to the influenza B virion but is also involved in nuclear import and export (49, 67, 68). BM2, in contrast, is an integral membrane ion channel protein whose primary function is the acidification of the influenza B virion upon entry (69, 70). Finally, NS encodes BNS1, non-structural protein 1, and

BNS2/NEP, nuclear export protein, via a post-transcriptional splicing mechanism (48-50, 71). The splicing mechanism functions such that BNS1 and BNS2 share a 5' leader sequence in the mRNA that is 75 nucleotides in length. The remainder of BNS2 is translated by a +1 frame shift in the BNS1 open reading frame, and then the BNS2 transcript is spliced at the 5' and 3' ends to yield a smaller product than BNS1 (ORF)(48, 72).

Segment 4 is a surface gene that encodes just one protein, hemagglutinin (HA) (40). HA is a major antigenic protein and is also responsible for binding the host cell receptor, alpha 2,6 sialic acid on the surface of host respiratory epithelial cells (43, 73, 74). In the 1980s, the antigenicity of the HA of influenza B virus diverged into two lineages (75). This divergence led to the categorization of IBV strains based on the sequence homology and antigenicity of the HA to either B/Yamagata/16/88 or B/Victoria/2/87, the prototypical strains of the B/Yamagata-like and B/Victoria-like lineages, respectively (75). As the major antigenic protein, HA is key in vaccine development; nevertheless, due to the lack of cross-reactivity between these lineages, a vaccine with an HA mismatched to the currently circulating strain will not protect vaccinees (28, 76, 77).

The two remaining IBV proteins, NA and NB, are encoded from segment 6. NA, neuraminidase, is a surface protein which is responsible for cleaving sialic acid moieties from glycoproteins that coat the surface of the host cell releasing newly budded virions (78-80). In addition to being a sialidase, NA is immunogenic, although it is not considered to be a major antigenic protein (81, 82). Unlike NA, NB, which is encoded from an alternate ORF in segment 6, is an integral membrane ion

channel protein (44, 83, 84). Although the function of NB within the viral life cycle has not been elucidated, the structure of NB is similar to BM2, so it is speculated that NB functions in the same manner as BM2 (45, 84, 85).

1.4. Influenza B virus life cycle and immune response to infection

1.4.1. Virus attachment and entry

The IBV life cycle begins with the attachment of the HA homotrimer to the host cell surface (Fig. 1.2) (43). In order to be infectious, however, HA must first be cleaved by trypsin-like proteases located in the human upper respiratory tract; consequently, prior to attachment, HA0 is cleaved into the HA1 globular head and HA2 stalk region, which remain bound by disulfide bonds (86-91). Attachment occurs via HA recognition of the terminal alpha 2,6 sialic acid bound to glycoproteins of *human* respiratory epithelial cells. Mutations in the HA sialic acid binding sites alter the HA preference for sialic acid from alpha 2,6 to alpha 2,3 sialic acid (the receptor for *avian* IAV); regions identified as important for receptor binding are located in the HA1 globular head, particularly in the 120, 150 and 160 loops and the 190 helix region (92, 93). Although influenza B virus is known to bind primarily to alpha 2,6 sialic acids, it should be noted that B/Victoria-like viruses, in particular, are capable of naturally binding alpha 2,3 and alpha 2,6 sialic linkages (74). Despite some variability in sialic acid preference, the base of the receptor binding site is highly conserved at 4 amino acids in all IBV strains: F95, Y158, H191 and Y202 (92).

Entry of the influenza B virion is thought to occur via receptor-mediated endocytosis (89-91, 94). Upon HA binding with sialic acid on the surface of the host cell, endocytosis of influenza B occurs. It is likely that this process is clathrin-

dependent, as IAV entry has been shown to be clathrin-mediated and all known mechanisms of IBV entry are also found in influenza A (86, 94-98). Upon endocytosis of the virion, the successful trafficking of the endosome requires protein kinase C (PKC), which has been shown to regulate the function of the late endosome (99). Indeed, inhibition of PKC inhibits IBV entry (98). As the endosome matures into the low pH environment of the late endosome (pH 5.5), a conformational change is triggered in the HA protein in which the fusion peptide present in the HA2 stalk region becomes exposed and inserts itself into the endosomal membrane (94, 95, 97). Fusion of the viral and the endosomal membranes exposes the contents of the virion, the vRNPs, to the cytoplasm (95, 100). During this process, proton pumps, BM2 and likely also NB, pump protons into the virion, acidifying it and causing the release of the vRNPs by BM1 (45, 69, 85, 101-103). At this stage, the contents of the virion are released into the cytoplasm leaving them available for import into the nucleus.

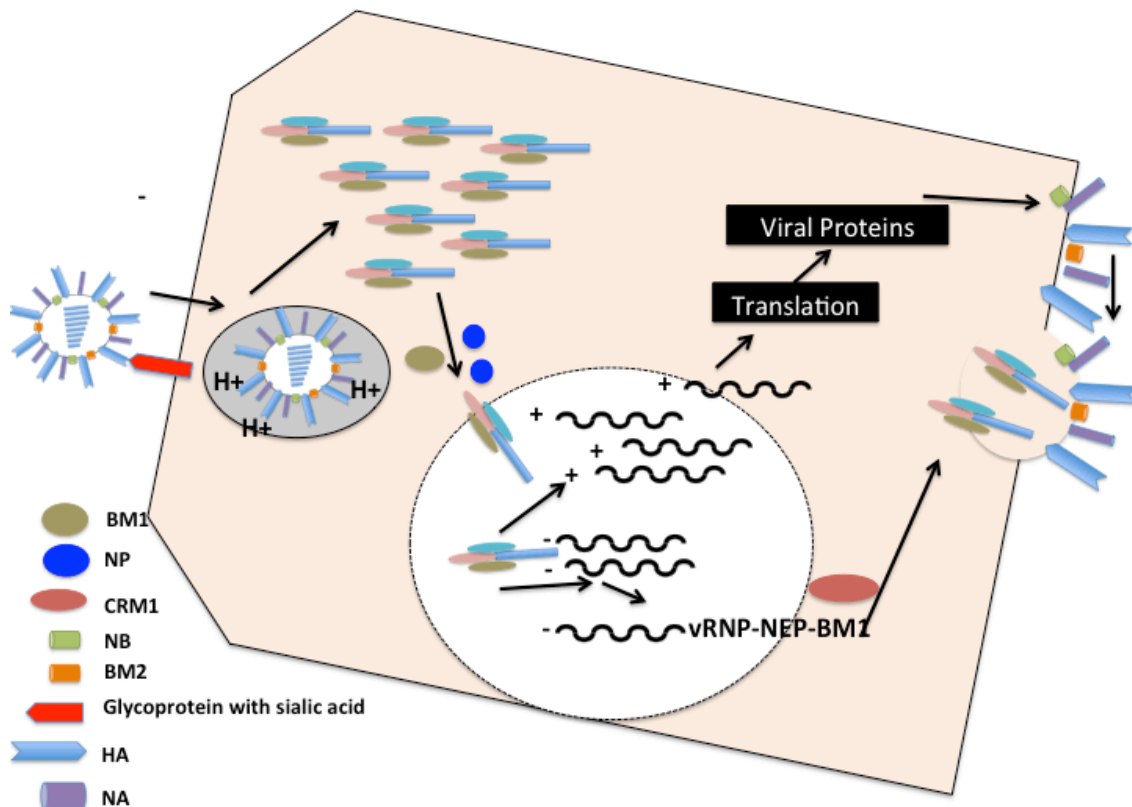


Figure 1.2. Influenza B virus life cycle. HA of influenza B binds to sialic acid, and the virus particle is endocytosed. The endosome matures and acidifies. Then, BM2 and NB pump protons into the influenza virion, and acidification causes a conformational change in the HA. Next, the HA2 fusion peptide fuses the endosomal and the viral membranes, exposing the vRNPs to the cytoplasm. BM1 releases the vRNPs into the cytoplasm. Then, NP and BM1 facilitate the import of vRNPs into the nucleus using a series of host proteins. Once in the nucleus, the viral RdRp, snatches the host pre-mRNA caps, and viral mRNAs are transcribed. vRNA is also synthesized. Next, viral mRNA and vRNPs are exported from the nucleus. vRNPs are exported through an association with BM1 and NEP, and NEP interacts with CRM1 to export the vRNPs out of the nucleus. Viral mRNAs are translated using host machinery at the ER and are subsequently packaged in the Golgi and sent to the plasma membrane (HA, NA, BM2, and NB). Finally, vRNPs are then assembled into the budding virion.

1.4.2. Nuclear import

The IBV life cycle relies on host cell machinery in the nucleus, thus nuclear import of viral proteins and vRNA is required. Indeed, NP, BM1, and the polymerase proteins of influenza B virus have all been shown to enter the nucleus (68, 104, 105).

Localization to the nucleus requires nuclear localization signals (NLS). The nuclear localization signals of NP and BM1 have recently been defined, and while nuclear localization signals for PB2, PB1 and PA remain undefined, these polymerase proteins have been shown to localize to the nucleus in binary complexes PA-PB1, PA-PB2 and PB1-PB2 (68, 104, 105). Interestingly, although PB2 localizes exclusively to the nucleus, PA and PB1 have been identified in the cytoplasm (105).

The elucidation of host and viral proteins involved in mediating nuclear import of influenza B vRNP complexes requires further study; however, BM1 seems to play an important role. It has been shown to interact with host protein, importin α , part of the nuclear import machinery, and has also been shown to be a nuclear shuttle protein, having been identified moving back and forth between the cytoplasm and the nucleus during the early stages of viral replication (68). Based on influenza A research, in which importin α recognizes the NLS on the vRNP complex and interacts with importin β to shuttle the vRNPs across the nuclear pores of the nuclear envelope into the nucleus, it is possible that BM1 mediates the interaction between the vRNP complex and importin α through its NLS which would be consistent with BM1 acting as a shuttle protein (68, 106, 107). In this way, BM1 may transport the complex into the nucleus before releasing the vRNP only to move back to the cytoplasm and interact with another vRNP complex. NP may also mediate the import of the vRNPs

through an interaction with importin α as has been shown in influenza A. Once the vRNP complexes have entered the nucleus, viral transcription and replication can begin.

1.4.3. Transcription, replication and translation

Once in the nucleus, IBV must produce viral mRNA, cRNA and vRNA in order to produce progeny virion. Viral mRNA is produced first, and its transcription is initiated by the viral RdRp. Transcription of the viral genome begins with PB2 cap-binding to the host 5' pre-mRNA cap and cleavage of the cap by PA as described previously (60-62). IBV cleaves methylated and unmethylated 5' caps, m^7 GpppG⁻ RNA and GpppG-RNA, respectively (61). The cap acts as a primer for transcription and is also required for the viral transcripts to be translated by host ribosomes. In addition to possessing a cap, all viral mRNA transcripts are polyadenylated by a stuttering mechanism in which the polymerase moves back and forth over a stretch of uracils generating a Poly-A tract at the 3' end of each mRNA transcript (108, 109). Viral mRNA transcripts are then either further processed by the spliceosome, as in the case of segment 8, or immediately exported out of the nucleus to be translated by the ribosome (48).

Transcription of cRNA and vRNA occurs after viral mRNA transcription, although it is unclear how the transition occurs. It has been hypothesized that NP may play a role in switching from mRNA transcription to cRNA transcription, as NP has been shown to be required for full length cRNA transcription of IAV (110, 111).

cRNA transcripts are transcribed to serve as templates for the production of vRNA but are not incorporated into the virion; only vRNA transcripts become incorporated into the virion (112). During cRNA and vRNA transcription, neither transcripts are capped or polyadenylated. Given the absence of a cap, the promoter region for cRNA and vRNA synthesis is the binding region of the 5' and 3' ends of the UTRs of each gene segment, although the cRNA promoter is complementary, not identical, to the vRNA promoter (51, 55, 113, 114). After the vRNA segments are transcribed, vRNP complexes are exported out of the nucleus (115).

1.4.4. Nuclear export

Much like nuclear import, the IBV nuclear export process relies on host proteins. The vRNPs are exported from the nucleus using the CRM1 nuclear export pathway (49). NEP interacts with CRM1 and nucleoporins to export the vRNP complexes out of the nucleus (49). Although NEP is capable of directly interacting with vRNP complexes, the interaction of NEP with the nuclear export machinery is typically mediated by BM1 (116). The BM1 nuclear export signals (NES) have recently been defined, and it is thought that at least 1 of the 2 NESs in BM1 is CRM1 dependent, although this has not been shown definitively (68). Export of the vRNP complexes has also been shown to utilize the Ref/MEK/ERK signaling cascade (117). Inhibition of MEK interferes with nuclear export, but the mechanism of action has not been elucidated (117).

Exported viral mRNA transcripts HA, NA, BM2 and NB are translated by the ribosome at the endoplasmic reticulum (ER) (118-121). Following translation, the proteins are folded and then sent to the Golgi apparatus for further modification (118, 119, 121). While in the Golgi, HA is glycosylated and its signal peptide is cleaved; furthermore, new evidence has suggested that HA0 is cleaved by proteases within the Golgi into HA1 and HA2 (122-124). NB is also modified in the Golgi through the addition of fatty acids to cysteine residues in a process known as palmitoylation, and these modifications are required for proper trafficking of NB to the cell membrane (118). All of these proteins, HA, NA, BM2 and NB, are targeted for the apical side of the cell membrane of polarized epithelial cells where they accumulate at lipid raft regions to form a platform for budding viral progeny (125).

1.4.5. Virus assembly and budding

Assembly and budding of viral progeny occurs at lipid rafts where HA, NA, BM2 and NB have incorporated into the cell membrane. Viral proteins and vRNPs must then be recruited to the site of assembly. For example, BM2 is known to recruit BM1 to the plasma membrane and to enhance BM1 association with the plasma membrane (103, 126). Additionally, BM2, through interactions with BM1-vRNP complexes, facilitates the assembly of the vRNP complexes into the viral bud (127).

There are likely two types of BM1 that assemble into the virion, BM1 with and without vRNP (127). There is evidence to suggest that BM1 without vRNP associates with the cytoplasmic tail of HA to facilitate HA assembly (128). This is

based on findings which show that a deletion of the HA cytoplasmic tail that disrupts HA incorporation can be compensated with mutations in BM1 (128). Such mutations may restore the HA-BM1 interaction (129).

Assembly and packaging of the vRNP complexes has been the subject of extensive research seeking to determine whether or not the vRNPs are assembled specifically or randomly into the budding virion. Each vRNA gene segment contains packaging signals at the 5' and 3' ends, and although IBV packaging signals have not been defined, IAV packaging signals are known and have been conclusively shown to employ specific incorporation (130-134). Given the similarity of the influenza A and B vRNP and RNA structures, it is likely that packaging of influenza B vRNP complexes is also specific (46, 51, 58, 135).

Once the virion has been assembled, budding occurs. The viral bud forms with the aid of at least NA and BM1, although HA may be involved as in influenza A virus; nonetheless, the primary protein involved in bud formation and virion morphology is BM1(136-139). Once the bud has formed, it is excised and released from the cell surface by NA sialidase activity (78, 82).

1.4.6. Host immune response to infection

Entry of influenza into a host cell stimulates an immune response, as host proteins sense a foreign presence in the cell via pathogen recognition receptors (PRR), which recognize pathogen associated molecular patterns (PAMPs) present on

a foreign body (140, 141). The resultant immune response can be broken down into two branches, innate and adaptive, which differ in the time required to mount a response and the specificity of the response. The innate immune response uses PRRs to recognize PAMPs, and thus acts as the host's first line of defense against infection (141). The adaptive immune response is stimulated by the innate response but relies on T cells and B cells to mount a specific immune response against a particular pathogen primarily via CTL (cytotoxic T lymphocyte) and antibody production, a process that can take weeks to develop (142).

Influenza virus stimulates a robust innate immune response. PRRs of the innate immune system recognize single-stranded and double-stranded RNA as PAMPs. These PRRs include toll-like receptors (TLRs), retinoic acid inducible gene-I (RIG-I) and NOD-like receptors (143). Each PRR recognizes a distinct feature of influenza virus. For example, TLR7 recognizes single-stranded RNA while TLR3 and RIG-I recognize double-stranded RNA generated transiently during the virus life cycle. Recognition of the foreign RNA by PRRs leads to stimulation of pro-inflammatory cytokines as well as type I interferon (IFN) (144-146). IFN stimulation then leads to expression of a plethora of other genes with antiviral activity.

As IFN has strong antiviral activity and can control gene expression, it is key in stimulating the expression of other antiviral genes and even immune cells. Induction of interferon-stimulated genes (ISGs) by IFN occurs via the JAK/STAT pathway (147). An important ISG induced via this pathway is the Mx (myxovirus) gene, which encodes MxA, a protein that is capable of inhibiting influenza virus replication (148, 149).

In addition to stimulating ISGs, IFN stimulates cell types of the innate immune system such as macrophages and dendritic cells. When alveolar macrophages become activated, they phagocytose infected cells; however, macrophages can also produce NOX2 (nitric oxide synthase 2) and TNF alpha (tumor necrosis factor alpha) when they become infected, contributing to influenza-induced pathology (150-154). In contrast, stimulation of dendritic cells by IFN leads to the stimulation of adaptive immune pathways as dendritic cells present influenza virus antigen to CD4+ and CD8+ T cells, ultimately leading to antibody production (155, 156).

The adaptive immune response can be divided into cell-mediated and humoral branches, which are governed by T cells and B cells, respectively. The humoral branch leads to the production of antibodies by B cells, while the cell-mediated branch utilizes T cells that are virus-specific and remain present even after the clearance of viral infection. CD4+ and CD8+ T cells are both activated by the presentation of virus antigens from antigen presenting cells (primarily dendritic cells) but have different functions (155, 156). CD8+ T cells are directly cytolytic and capable of killing virally infected cells (157). While CD4+ T cells have some cytolytic activity, they function primarily as T helper cells (Th), with Th1 and Th2 cells being of particular importance after virus infection (158). Th1 cells produce IFN gamma and IL-2 to control macrophage and CD8+ T cell responses to infection (159). Th2 cells, in contrast, produce IL-4 (IL, interleukin), IL-5 and IL-6, which stimulate the proliferation and differentiation of B cells into plasma cells (159, 160).

The primary immunoglobulins produced after influenza virus infection are IgA, IgG and IgM. IgA is present in the mucosa, and IgG is present in serum (but can

enter the respiratory tract). IgM is present in the circulatory system and is capable of mediating neutralization of influenza virus infection via the complement pathway (161-165). Influenza virus-specific antibody responses are produced primarily against the HA and NA surface glycoproteins. Indeed, the presence of HA specific antibodies against a particular influenza virus has historically been used as a correlate of protection against re-infection with the same or similar virus at a later date (166-168). Traditionally, influenza vaccines have been produced in a KV vaccine formulation known to generate IgG primarily against the globular head of the HA protein. More recently, live-attenuated vaccines have been made available and these vaccines produce a broader immune response, inducing IgA and IgG responses to vaccination as well as an increased IFN and T cell responses (169, 170).

Influenza viruses have evolved mechanisms to evade the host innate immune responses discussed above. IBV BNS1 protein is one such adaptation, as it possesses a variety of different functions related to the evasion of the innate immune response. BNS1 has been shown to antagonize ISG15, which is involved in the activation of an antiviral state within the host cell, and interact with dsRNA at its N-terminus. It also prevents activation of host proteins, protein kinase R (PKR) and interferon regulatory factor-3 (IRF-3) (50, 171-173). Finally, it is crucial for the down-regulation of interferon beta (IFN- β). Given its ability to bind dsRNA, it would seem that BNS1 regulatory functions are carried out via RNA binding and sequestration; however, this is not always the case. While BNS1 dsRNA binding and sequestration results in the down-regulation of PKR, BNS1 down-regulation of IFN occurs independent of dsRNA binding (172).

Regardless of the means by which BNS1 regulates gene expression of the host innate immune response, regulation is crucial to the completion of the IBV life cycle. For instance, by sequestering RNA from PKR, BNS1 prevents PKR from carrying out its function (174). Without intervention by BNS1, PKR would be activated by the presence of dsRNA and would halt viral protein synthesis by phosphorylating eIF2, a translation initiation factor (174). In summary, without BNS1, IBV is unable to use the host translation machinery to translate its genome. In addition, BNS1 inhibits activation of IRF-3. IRF-3 is an interferon regulatory transcription factor which, when activated, translocates to the nucleus from the cytoplasm and initiates transcription of antiviral cytokines. The inhibition of IRF-3 prevents these cytokines from being produced; conversely, without BNS1, the host cell is better able to mount an immune response (175). Indeed, the degree of virus attenuation has been shown to correlate with the length of BNS1, and BNS1 truncated viruses have been shown experimentally to serve as effective LAIV vaccine candidates (176, 177).

1.5. Influenza B host-range, evolution and restriction

1.5.1. Host range

IBV has a narrow host-range that is thought to be limited primarily to humans. Although these viruses have been isolated in seals and pheasants, these hosts are not believed to be natural reservoirs (18-23, 178). Interestingly, IBV strains that have been repeatedly isolated from seals in the Dutch coastal regions are distinct from those virus strains circulating in the surrounding humans populations, suggesting that some other reservoir exists for these viruses (19, 20). Harbor porpoises residing near these seals were initially suspected to be the reservoir of these influenza B viruses; nonetheless, recent research has confirmed that there is no serological evidence of influenza B virus in the harbor porpoises, so the search for a reservoir continues (20).

1.5.2. Evolution

Novel influenza viruses can arise by either antigenic shift or antigenic drift. The emergence of a novel influenza virus by antigenic shift occurs through the exchange (or reassortment) of influenza virus gene segments after the infection of a single host cell with 2 or more viruses (179). Through reassortment, viruses can evolve more rapidly than by antigenic drift, the accumulation of mutations over generations of viral replication. IBV is well documented to reassort; indeed,

reassortment of influenza B strains has been linked to the emergence of new epidemic strains (180-185). For example, outbreaks of the same antigenic lineage reported in the same geographic region over a short span of years were initially puzzling because protection against infection is thought to be based primarily on the HA protein; however, phylogenetic analyses in these cases revealed the cause to be a reassortant virus carrying an NA from a virus of the opposite lineage (180). Importantly, influenza viruses can only reassort with like virus types conceivably due to differences in packaging signal requirements; therefore, IBV strains only reassort with other strains of IBV (34, 186-188).

Influenza B, due to an error-prone viral RNA polymerase, also evolves readily by antigenic drift. Antigenic drift differs from antigenic shift in that it occurs over many cycles of viral replication, whereas antigenic shift can occur after a single cycle of replication. The rate of antigenic drift is determined by selective pressures exerted on each gene segment and the mutation rate of the viral RdRp. IBV has a mutation rate of $.6 \times 10^{-6}$ /replication cycle (189). Additionally, influenza B evolution is not governed by antigenic changes on HA or NA, as none of the gene segments experience positive selection (189-191). The percentage of mutations (regardless of the mutation rate) resulting in nonsynonymous mutations in influenza B HA and NA proteins is much lower than, for instance, human influenza A, a virus that experiences positive selection on the HA (189, 192, 193). In fact, it has been shown that only 30% of mutations in HA and NA of IBV result in amino acid changes which is in stark contrast to the 50% seen in human IAV (190). This finding is reasonable if one again considers the limited host range of influenza B. For example, since Influenza B

viruses do not switch from one host species to another (like influenza A), changes in highly mutable regions like the receptor binding region of HA are less likely to occur, as influenza B viruses already possess the ability to bind well to the human influenza virus receptor, alpha 2,6 sialic acid.

1.5.3. Host restriction of influenza B

Influenza B host restriction is due to virus preference for and recognition of human specific proteins. One major factor recently elucidated is the specificity of BNS1 for human and non-human primate ISG15 mentioned previously (194, 195). BNS1 protein evades the host innate immune response during infection by binding directly to ISG15, thereby interfering with the establishment of an antiviral state in the host cell (50, 194, 196-198). BNS1 binds specifically to five amino acid residues present in the hinge region of ISG15 (194). In a pull-down assay of BNS1 and human, mouse, canine and monkey ISG15, only human and monkey BNS1/ISG15 complexes were detected. Further, mutating the canine and mouse ISG15 to carry the 5 amino acid human hinge region resulted in BNS1/ISG15 complexes for both canine and mouse ISG15 mutants (194). Thus, the species specificity of this reaction relies on the sequence of the 5 amino acid hinge.

Although ISG15 is the only host factor that has clearly been determined to have a species-specific interaction with IBV, there are other host proteins that could also interact with influenza B in a species-specific manner. For example, BM2 is

known to interact with human Hsp40 (heat shock protein 40), a chaperone protein, through its C-terminal domain (199). Hsp40 is a regulator of PKR (protein kinase R), which, as has been previously described, is crucial in the host response to infection (174). Other proteins of the host innate immune response, such as RIG-I and MDA5 (melanoma differentiation-associated gene), have been shown to differ among species. Interactions between these proteins and IBV may offer additional opportunities for species-specific interactions (200-202).

A recent study has suggested that influenza B host restriction is related to the low binding affinity of the HA to the sialic acid receptor. Compared to IAV, IBV has lower overall receptor-binding affinity (203). This may be due to a conserved phenylalanine residue at position 95 of the influenza B HA (95). When this position is mutated to a tyrosine, receptor binding to synthetic glycans dramatically increases (204). Interestingly, when a tyrosine at an analogous residue of influenza A HA (amino acid residue 98) is mutated to a phenylalanine, receptor-binding affinity decreases (205). These findings suggest an association between the presence of tyrosine at position 95/98 resulting in enhanced receptor binding and a broad host range of infection.

1.6. Introduction to Influenza B Reverse Genetics

The development of a reverse genetics system for IBV has been a boon for influenza B research. It has allowed for the easy manipulation and engineering of viruses with mutant or wild-type genomes to facilitate functional studies of any gene segment, as well as the recovery of virus for a vaccine seed stock. The first reverse genetics systems for influenza B, a 12-plasmid system for B/Beijing/1/87 and an 8-plasmid system for B/Yamagata/166/98, were published in 2002 (2, 52). Since this time, other reverse genetics viruses have been produced including B/Yamagata/1/73 and B/Lee/40 (127, 206, 207). Importantly, a reverse genetics system for B/Ann Arbor/1/66 cold-adapted, the licensed LAIV vaccine backbone, has also been generated, although this was done primarily to determine the role of each mutation present in the cold-adapted vaccine backbone (208).

Both the 8-plasmid and 12-plasmid reverse genetics systems rely on the RNA Pol I and RNA Pol II polymerases present in the host cell. Within a normal host cell, RNA Pol I transcribes ribosomal RNA (rRNA), which is not capped or polyadenylated, making RNA Pol I ideal for transcribing vRNA from plasmids (209). Similarly, the use of RNA Pol II, which transcribes pre-mRNA transcripts in a normal host cell, is ideal for the transcription of viral mRNA from plasmids, as RNA Pol II transcripts are capped and polyadenylated (210).

In both reverse genetics systems, all 8 influenza B gene segments were cloned into bidirectional plasmids containing Pol I and Pol II promoter sequences, allowing for the expression of vRNA and viral mRNA from each plasmid by host polymerases

upon transfection (2, 52). Plasmids are designed such that human Pol I and Pol II promoters as well as a corresponding t1 terminator (for Pol I) and a poly A signal (for Pol II) flank each gene segment (Fig. 1.3A and B). In the case of the 12-plasmid system, four expression plasmids each possessing only one promoter, Pol II, and one influenza B gene segment corresponding to one of the vRNP complex genes were also transfected (52). The expression plasmids ensure that host RNA Pol II transcribes the viral polymerase genes, enhancing the probability that the viral polymerase will be present to initiate viral transcription. Alternatively, the 8-plasmid system must rely solely on the transfected bidirectional polymerase plasmids for transcription of all gene segments (2). Plasmids are typically transfected into 293T/MDCK (Madin-Darby Canine Kidney) cell co-culture; 293T cells are readily transfectable and can be used to infect the MDCK cells, which are not as easily transfectable but propagate virus well (Fig. 1.3A).

Through the use of reverse genetics (RG), we have gained invaluable insight in areas such as viral protein function, host-virus interaction and novel vaccines. Although our knowledge of influenza B still lags behind that of influenza A, research progress has been expedited in the last 11 years due to the advent of a reliable reverse genetics system. Below is a segment-by-segment review of many of the most notable reverse genetics achievements in influenza B research as they pertain to vaccine development and antivirals.

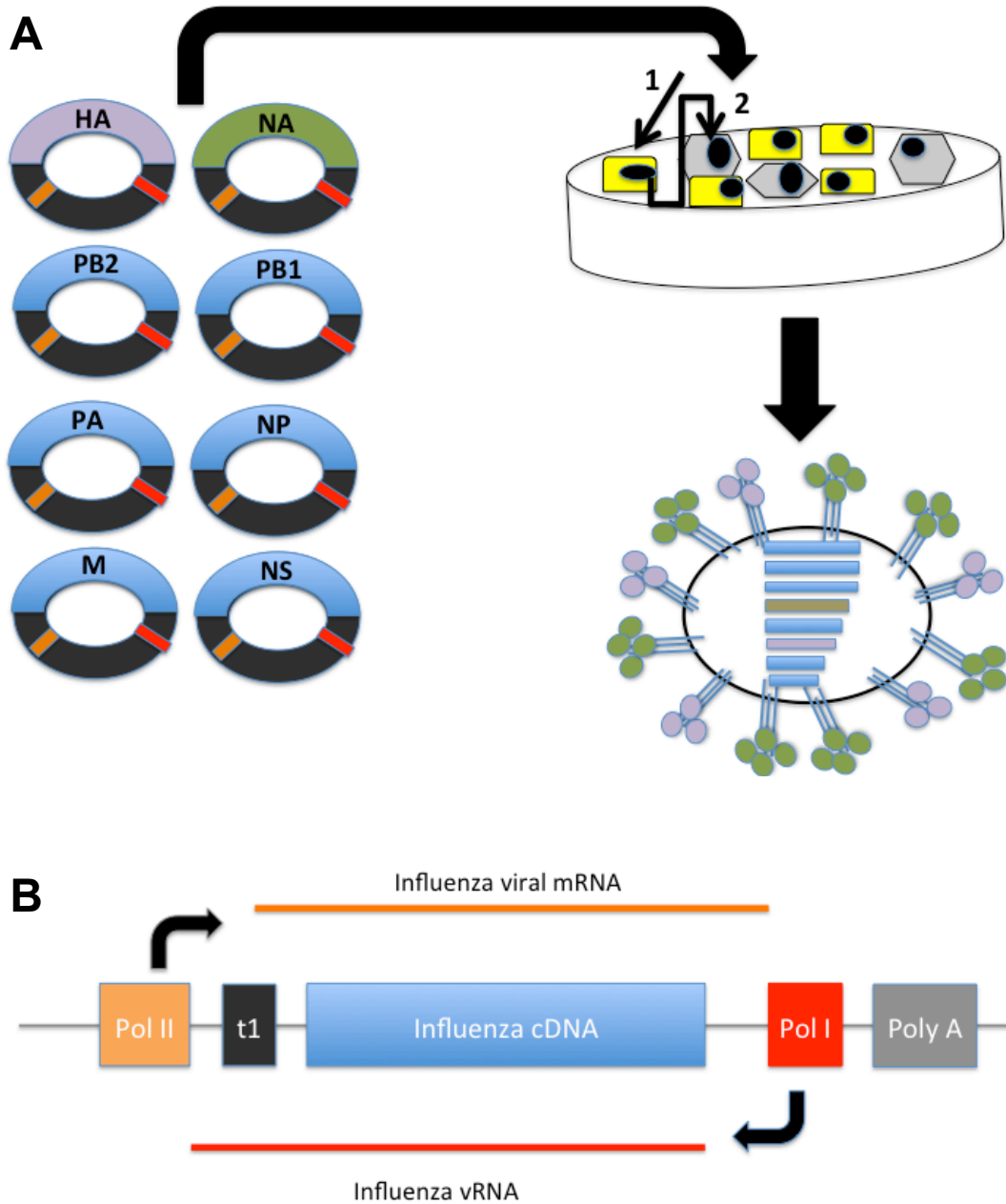


Figure 1.3. 8-plasmid reverse genetics. The transfection of 8 bidirectional plasmids in a 293T/MDCK cell co-culture is shown (A). The plasmids transfect the 293T cells (1), which produce virus that infects the MDCK cells (2). The MDCK cells propagate the infection. A schematic of a bidirectional plasmid is shown (B). Orange: Pol II promoter, Red: Pol I promoter, Yellow rectangle: 293T cells, Gray hexagon: MDCK cells.

1.6.1. HA receptor binding, egg-adapted mutations and the significance of the HA cytoplasmic tail

Not surprisingly, much research on influenza B has focused on the HA gene, as it encodes the primary antigenic protein. Although much was known about the HA of influenza B prior to the advent of reverse genetics, reverse genetics enabled several important discoveries. These include the determination of receptor binding sites responsible for receptor preference switching between alpha 2,6 and alpha 2,3 sialic acids as well as the sites responsible for increasing virus yield in eggs (211-214). As will be shown below, these studies are important for vaccine development.

Influenza vaccine candidates are typically grown in eggs. Viruses that do not initially grow well in eggs must be egg-adapted to improve vaccine yields; however, egg-adaptation generates mutations in the HA gene which can lead to antigenic drift, lowering vaccine efficacy (215). In order to determine which mutations enhance vaccine growth in eggs without altering antigenicity, numerous egg-adaptation studies have been carried out (211, 213). The first of these studies identified mutations associated with an egg-adapted B/Victoria/504/2000 and then introduced different combinations of these mutations into reverse genetics plasmids. The rescued viruses were assessed for virus growth in eggs and for antigenicity to the wild-type (WT) B/Victoria/504/2000 virus using hemagglutination inhibition (HI) assays (213). Several combinations (R162M/ D196Y and G141E/R162M/D196Y) of egg-adapted mutations were shown to enhance viral growth in eggs; however, only one mutation, R162M, enhanced viral growth without altering antigenicity (211). In an extension of

the egg-adaption studies, B/Victoria/504/2000 HA plasmid constructs carrying different combinations of the mutations identified to enhance growth in eggs, G141E, R162M and D196Y, were designed and evaluated to determine whether these mutations altered receptor binding preference for alpha 2,6 sialic acid (213). Interestingly, the G141E mutation was determined to be key in shifting sialic acid preference from 2,6 to 2,3. The generated RG virus carrying only G141E showed strong preference for alpha 2,3 sialic acids, while viruses carrying the R162M and D196Y mutations showed preference for alpha 2,6 sialic acid (213).

Glycosylation sites on receptor binding regions have been shown to affect antigenicity of influenza viruses; therefore, in order to maintain antigenicity of a virus through egg passaging, stable glycosylation sites are necessary (216-218). Research by Chen *et al.* identified stabilizing mutations that allow for the maintenance of glycosylation sites at the receptor binding regions of HA in influenza B while maintaining high growth in eggs (219). In this study, B/Victoria-like and B/Yamagata-like surfaces on the B/Ann Arbor/1/66 cold-adapted vaccine backbone were rescued by 8 plasmid reverse genetics to compare egg-adapted strains and MDCK cell-grown strains with the WT progenitor strains. The B/Ann Arbor/1/66 cold-adapted backbone was selected to simulate egg-adaptation during vaccine production (220, 221). Results showed that the glycosylation sites at 196/197 (B/Victoria-like and B/Yamagata-like viruses, respectively) present in progenitor strains were lost after egg-adaptation (219, 220, 222, 223). Despite this finding, a G141R mutation was found to stabilize the glycosylation sites at 196/197 without any antigenic alterations. Interestingly, this position is also responsible for controlling

receptor-binding preference, as described above. When the 141R mutation was incorporated into the HA segment of viruses previously shown to undergo antigenic drift after egg passaging, the presence of the 141R mutation prevented antigenic drift (219).

1.6.2. Antiviral resistance of NA and the role of NB

Segment 6 encodes two proteins, NA and NB, which are targets of viral inhibitors. As a sialidase, NA has been the target of antivirals known as neuraminidase (NA) inhibitors (82, 224). With the increasing use of these inhibitors, drug-resistance has become a concern, stimulating research on resistance markers (225). The NB ion channel, in contrast, is amantadine-susceptible; however, little is known about the significance of NB within the virus life cycle, although research is ongoing (226).

All NA inhibitors were similarly designed based on the crystal structure of NA as well as the structure of sialic acid, as sialic acid is itself a mild inhibitor of NA. Each inhibitor blocks the active site of NA, although by different means. Zanamivir was designed to bind the active site based on charge (227). The NA active site has a negatively charged region where it binds sialic acid, thus a molecule similar to sialic acid, but with a greater positive charge, was designed to bind more tightly to the NA active site (227).

Recently, the effectiveness of NA inhibitors outside the laboratory setting has been questioned, and the latest clinical trials suggest minimal benefit and negative

side effects (228, 229). With the frequent use of NA inhibitors such as zanamivir, oseltamivir and peramivir, the lack of effectiveness in clinical trials could be due to resistance mutations.

In order to determine molecular markers of influenza B NA inhibitor resistance, Jackson *et al.* used reverse genetics to introduce mutations into IBV and test susceptibility of mutant viruses to NA inhibitors (52). One of the first NA inhibitor resistance-associated mutations identified for influenza B was E116G (230, 231). By introducing the E116G mutation into NA, Jackson *et al.* showed that IBV shifted from being zanamivir-susceptible to zanamivir-resistant (52). The group also demonstrated that resistance markers identified in IAV were conserved in IBV. Each mutant virus was then evaluated for neuraminidase activity in the presence of neuraminidase inhibitors as well as viral growth, protein stability and protein expression. The results of these assays indicated that the NA inhibitor resistance mutations caused attenuation, by either decreasing NA stability or NA expression depending on the mutation (232).

While NB is sensitive to amantadine, an ion channel blocker, the utility of this sensitivity cannot be completely understood until more is known about the role of NB within the virus life cycle (226). Through the reverse genetics rescue of NB knockout viruses, researchers determined that, while required for efficient replication in mice, NB was not required for replication *in vitro* (in MDCK cells) (233). Thus, NB may not be as critical for influenza virus replication as BM2, which has been shown to be crucial for the production of infectious virus (103). By extension, amantadine treatment of IBV may not be an effective means of inhibiting virus replication.

1.6.3. Transcription of BM1 and BM2 and implications for vaccine development and experimentation

The manner in which IBV segment 7 encodes BM1 and BM2 has been the subject of extensive research, as it is done by a unique mechanism of translational regulation that could potentially be manipulated for vaccine development (47). In order to manipulate its unique translational mechanism and modify it for potential use as a vaccine, a clear understanding of how it works and the function of its protein products are required. Reverse genetics has been key in determining both the mechanism as well as protein functions of BM1 and BM2. This research may allow for the modification of segment 7 for the generation of experimental LAIV vaccine candidates and has already generated a tool to facilitate the evaluation of vaccine candidates and pathogenesis of IBV in mice (234).

As previously described, the M segment of influenza B encodes BM1 and BM2 by a stop-start translation termination-initiation pentanucleotide (UAAUG) mechanism in which the stop codon of BM1 overlaps the start codon of BM2 (47, 235). The region primarily responsible for the expression of BM2 is the 45-nucleotide sequence upstream of the stop-start region (or the terminal 45 nucleotides of the 3' end of BM1 mRNA) (235, 236). The importance of this region was determined by cloning a series of plasmids carrying various truncations in the coding region (mRNA sense) of the 3' end of BM1 and inserting *Gaussia* Luciferase (GLuc) in place of BM2. The precise region of the M gene responsible for BM2 expression was identified based on which truncations allowed for the highest GLuc expression (235).

Using a similar method, expression of foreign genes cloned in place of BM1 and BM2 was demonstrated, although expression of the foreign gene cloned in place of BM2 was dependent on the proportion of BM1 upstream of the stop-start signal. The most robust expression of the downstream foreign gene was achieved when BM1 was present in its entirety (235).

Using reverse genetics, BM2 was determined to be a requirement for viral replication and also necessary for incorporation of the vRNP complexes into the budding virion (127, 237). In both studies, a series of BM2 mutant plasmids were constructed including a full BM2 knockout, BM2 cytoplasmic tail mutants and various partial BM2 knockouts. The full BM2 knockout virus was not amplifiable, suggesting that BM2 is required for the generation of infectious virus (237). When BM2 knockout virus plasmids were transfected into cells stably expressing BM2, virus rescue was achieved. Further analysis of the growth of the BM2 mutant viruses showed that the cytoplasmic tail is specifically required for rescue (237). In a related study, the cytoplasmic tail was shown to be important for virus replication because it interacts with BM1 and BM1-vRNP complexes to promote assembly (103).

The translational control mechanisms and functional studies of BM2 have clear implications for vaccine development. First, the studies show that the stop-start translation mechanism can be utilized for the expression of foreign genes, suggesting that IBV could be used as a vector to carry immune-modulators to enhance the immune response to vaccination, or other genes. Indeed, the stop-start mechanism has been utilized in the NS segment of influenza A to express IL-2 in the context of an experimental LAIV vaccine candidate (238). Second, given the critical role that the

cytoplasmic tail plays in the production of infectious virus, it could be a viable candidate for modification to produce a LAIV vaccine. This has been demonstrated as an effective means of live-attenuation in the context of IAV, although M2 is expressed by a post-transcriptional splicing event, not a stop-start translation mechanism (239-241).

Manipulation of the M segment has also resulted in the generation of research tools. McCullers *et al.* identified a mutation in BM1 that enhances morbidity in mice infected with the BM1 mutant influenza B virus. Avirulent B/Memphis/12/97 was passaged in BALB/c mice until enhanced morbidity was observed (234). A mutation in BM1, 221S, was consistently found in the isolates associated with enhanced morbidity (234). Subsequently, various strains of reverse genetics viruses carrying the serine mutation at position 221 were rescued and used to infect mice and infected mice showed morbidity indistinguishable from the passaged virus (234). This finding is particularly important given that mice are not readily susceptible to influenza B (242, 243). The limited susceptibility makes the evaluation of vaccine candidates difficult, as a lethal dose of challenge virus is required to perform a stringent test of a vaccine candidate as well as clearly show protection or the lack of protection conferred by a vaccine. Incorporating the BM1 221S mutation into a challenge virus could enhance lethality in mice facilitating the evaluation of vaccine candidates.

1.6.4. BNS1 antagonism of the innate immune response

NS, segment 8, has been the focus of manipulation via reverse genetics primarily due to interest in the evasion of the innate immune response by BNS1 (50, 171, 172). Some of the primary functions and notable lack of functions related to BNS1 are: direct inhibition of ISG15, inability to inhibit host mRNA nuclear export, inability to activate phosphatidylinositol 3-kinase signaling (PI3K), inhibition of IFN stimulation, inhibition of PKR, inhibition of IRF-3 and interaction with nuclear speckle domains (50, 172, 194, 196, 244-247). The functions discovered via reverse genetics and their relevance to vaccine development are described below.

In order to determine whether or not BNS1 down-regulates the expression of IFN, Dauber *et al.* generated a BNS1 knockout (206). This virus was severely attenuated in tissue culture. When the IFN induction of the knockout virus was compared to WT, there was significantly more IFN induced in cells infected with the knockout compared to the WT (206). Although this study did not determine the mechanism by which BNS1 down-regulates IFN, it conclusively proved that BNS1 suppresses IFN expression.

In a study similar to the one described above, the BNS1 knockout was utilized to demonstrate the inhibition of IRF-3 nuclear translocation by the N-terminal and C-terminal regions of BNS1 (171). Cells were transfected with a green fluorescent protein (GFP)-IRF-3 fusion expression plasmid and then infected with either the BNS1 knockout or WT virus. Results showed that significantly more IRF-3 translocated to the nucleus when cells were infected with the knockout versus the WT

(171). Then, by separately knocking out the N-terminal and C-terminal regions of BNS1 to generate two expression plasmids and then transfecting these plasmids individually with the GFP-IRF-3 expression plasmid, the group showed that both the C-terminal and N-terminal regions of BNS1 are capable of inhibiting IRF-3 translocation (171).

In another study by Dauber *et al.*, the role of dsRNA binding by BNS1 in down-regulating IFN and inhibiting PKR activation was investigated. The group cloned a series of BNS1 truncation mutants including a full BNS1 knockout, a BNS1 C-terminal knockout and many BNS1 mutants containing point mutations (172). Each of the mutant viruses recovered differed in the ability to bind dsRNA. The study concluded that dsRNA binding is not essential for IRF-3 or IFN inhibition, as BNS1 mutants lacking the ability to bind dsRNA were still able to inhibit IRF-3 and IFN (172). Despite these findings, PKR inhibition was found to be dependent on dsRNA binding. Indeed, the N-terminal region and the degree to which it binds dsRNA were indispensable for PKR inhibition (172).

Given the critical role that BNS1 plays in antagonizing the host innate immune response, it is not surprising that BNS1 mutant viruses are attenuated. As the collection of data above suggests, the absence or decrease in BNS1 expression leaves the virus unable to evade the host immune response. Indeed, experimental vaccines based on a BNS1 truncation strategy have been shown to be effective (176, 248).

1.7. Introduction to LAIV Vaccines

Each fall, both KV and LAIV vaccines are manufactured to protect against the current circulating strains of influenza. The strains incorporated into the seasonal vaccines are selected each year, and selected strains are determined by surveillance through the WHO Global Influenza Surveillance and Response System, GISRS (25). The GISRS functions such that National Influenza Centers of the GISRS carry out surveillance of influenza viruses throughout the year on a national level. Together, these centers test over 600,000 clinical samples annually. The National Influenza Centers then send representative samples to WHO Collaborating Centers for characterization (35). Once characterization is complete, representatives from the Collaborating Centers and other branches of WHO make recommendations regarding which viruses to incorporate into the seasonal vaccines for both the Northern and Southern Hemispheres based on the data gathered by the Collaborating Centers (35). Vaccines are manufactured in trivalent and quadrivalent formulations necessitating the selection of 4 virus strains per hemisphere. The trivalent formulation carries 2 strains of influenza A and 1 strain of influenza B (of either the B/Yamagata or B/Victoria lineage) while the quadrivalent formulation carries 2 strains of influenza A and 2 strains of influenza B (both B/Yamagata and B/Victoria lineages) (24).

To generate a vaccine with a gene constellation consistent with the WHO recommendations, classical reassortment methods are commonly employed. This process involves co-infecting eggs with the appropriate influenza backbone virus and the currently circulating seasonal virulent virus (249). The influenza B KV backbone

virus is egg-adapted B/Lee/40, and the influenza B LAIV backbone is B/Ann Arbor/1/66 cold-adapted (36, 220). Classical reassortment methods are sometimes difficult with IBV, as it is a human virus and, depending on the strain, may not grow well in eggs. Before FDA approval of reverse genetics for vaccine seed stock preparation and in cases where reassortment through co-infection of eggs is not feasible, whole influenza B seasonal virus is adapted to eggs (215). In cases when co-infection and reassortment of eggs is possible, infection is followed by plaque isolation and genotyping to identify the desired virus isolate. This process is long, and reverse genetics could be employed to hasten production time of vaccines. Recently, many have called for such a switch to the reverse genetics system (249-252). Indeed, Medimmune, manufacturer of the licensed LAIV vaccine, received FDA approval for this technology in 2006 (253). The broad implementation of reverse genetics would allow for rescue of a vaccine seed virus by specifically transfecting DNA plasmids carrying the surface genes of the seasonal virulent virus along with the LAIV or KV backbone genes. No selection or genotyping would be required (254, 255). Today, though, classical reassortment methods are still widely used, although reverse genetics methods are utilized.

Aside from the difference in vaccine backbones distinguishing the KV vaccine from the LAIV vaccine, the KV formulation differs from the LAIV in its inactivation by formalin treatment and the immune response it generates. Traditionally, the KV vaccine has been administered in the form of an intramuscular injection, and given the route of administration and its non-replicative nature, the vaccine stimulates a humoral immune response through antibody production, primarily IgG, but does not

stimulate cell-mediated immunity (T cell memory) (256). Although it only stimulates a humoral immune response, the KV vaccine can be administered to a broad range of individuals and is recommended for individuals 6 months of age and older (24).

The LAIV backbone is replication-impaired due to mutations rather than a chemical treatment as is the case of the replication-incompetent KV vaccine. It is also distinct from the KV formulation in its route of administration and the immune response it generates. The mutations present in the influenza B LAIV vaccine were generated from the successive passaging of B/Ann Arbor/1/66 at progressively lower temperatures until the virus grew well at 25°C in Chicken Embryo Kidney cells (CEK) (220, 221, 223, 257, 258). In all, serial passaging generated 7 mutations, primarily located in the vRNP complex, and the resultant virus was dubbed B/Ann Arbor cold-adapted (ca) (208, 221, 259-262). In addition to being cold-adapted, it is also temperature sensitive, as it grows poorly, if at all, at 37°C, the temperature of the lower respiratory tract (257). Such cold-adaptation and temperature sensitivity restricts virus growth to the upper respiratory tract (33°C), allowing for safe immunization by preventing a lower respiratory tract infection while stimulating both humoral and cell-mediated immune responses (220, 221, 223, 257, 258, 263). While the LAIV vaccine stimulates a broader immune response and has been shown to be safe, it is only recommended for ages 2-49 (24). In addition to age limitations, it is not recommended for those who are ill, those who have pre-existing conditions (such as asthma), those who are immune-compromised or women who are pregnant.

The combination of both the LAIV and the KV vaccines provides coverage to most age groups, but each vaccine formulation has limitations and disadvantages

(24). Both vaccines are grown in eggs; although cell-grown vaccines are approved, they are not widely used, and thus vaccination of individuals with allergies to egg proteins remains an issue (24)(Hasan et al. 2013). Further, the KV vaccine has been reported to cause Vaccine Associated Enhanced Respiratory Disease (VAERD) which is a phenomenon that is generated by exposure to a virus post-vaccination containing an HA of the same type as the vaccine, but with antigenic drift, such that antibodies cross-react with the HA but cannot neutralize it (264-266). Finally, although studies have shown the LAIV vaccine to be safe in high-risk groups, inherent risk in vaccinating immune-compromised individuals with a replication-competent vaccine limits use of the LAIV formulation in those individuals who could most benefit from its more robust immune response (267, 268). For all of these reasons, researchers have developed numerous alternative LAIV strategies. While the majority of these strategies have been developed for influenza A, several influenza B strategies have also been developed. In addition to a discussion on the B/Ann Arbor ca vaccine backbone, two prominent experimental vaccine strategies are reviewed below.

1.7.1. Review of the B/Ann Arbor ca vaccine backbone

1.7.1.1. *In vitro* and *in vivo* characterization

Early studies with the B/Ann Arbor ca backbone showed that the virus is cold-adapted, temperature sensitive and attenuated. Cold-adaptation has been demonstrated by comparing virus plaque titers; titers at 25°C of the B/Ann Arbor/1/66 ca are high (example, 2×10^8 Plaque forming units (Pfu)/mL) while the WT virus does not form clear plaques at this temperature. The temperature sensitive phenotype has been confirmed at 37°C, as this is the viral growth shutoff temperature (263). Finally, the attenuation phenotype, defined as restricted growth in the lungs, was shown in ferrets. In ferrets, the B/Ann Arbor ca backbone has been shown to cause mild pathology in the upper respiratory tract and little to no pathology in the lower respiratory tract; thus, this virus is also attenuated (263).

These growth phenotypes are not only found in the wholly B/Ann Arbor ca virus, but are also found in reassortant viruses carrying different (recombinant) surface genes on the B/Ann Arbor ca backbone (263, 269). The ability of these phenotypes to be conferred to other viruses makes the backbone an ideal vaccine candidate, as the surface can be changed to match the WHO recommended strains without having to reformulate the entire vaccine. Another key feature of the B/Ann Arbor ca backbone growth phenotypes is that they are stable *in vivo* (270). To evaluate *in vivo* stability, a reassortant virus possessing the cold-adapted backbone was permitted to grow in the lower respiratory tract of immunosuppressed hamsters

for a prolonged period (6-15 days). Virus was then isolated and tested for temperature sensitivity and attenuated properties both *in vitro* and in immunocompetent hamsters, and both phenotypes were maintained (270).

Reverse genetics has allowed for careful study of the mutations present in the B/Ann Arbor ca backbone. These studies have resulted in the mapping of the temperature sensitive, cold-adapted and attenuated phenotypes to specific mutations (208, 259, 260). The mutations identified in the B/Ann Arbor ca backbone are PB2 630R and PA 431M as well as NP 114A, 410H and 509T. Mutations in BM1 have also been identified, 159Q and 183V (208, 259). Of these loci, 5 have been shown to confer the cold-adapted phenotype, and these include the three mutations in NP as well as the PA 431M and PB2 630R mutations (259). The temperature sensitive phenotype has been mapped to NP 114A, NP 410H, and PA 431M while the mutations in BM1 have been shown to enhance this phenotype (208, 260). Finally, the loci responsible for the attenuation phenotype are NP 114A, NP H410, PA 431M, M 159Q and M 183V (208).

1.7.1.2. Small-scale clinical trials: B/Ann Arbor ca monovalent vaccines

The first clinical trials to evaluate the safety and efficacy of the B/Ann Arbor ca backbone were done decades before it was licensed in 2003 (263, 267, 269, 271, 272). Monto *et al.* showed that the B/Ann Arbor ca backbone with a recombinant surface was safe in college age adults. In comparison to the placebo control group, the only identified symptom associated with vaccination with B/Ann Arbor ca was a sore

throat (263). Of the vaccinated group, 37.3% of these individuals had increased antibody titers to the virus that they were vaccinated against compared to pre-vaccination titers. Virus was detected in 8 vaccinees on day 2 post-vaccination with the B/Ann Arbor ca backbone. Following detection of shed virus, samples were evaluated, and shed virus was determined to have maintained its temperature sensitive properties demonstrating stability (263).

In another clinical trial, Keitel *et al.* showed that individuals vaccinated with a B/Ann Arbor ca backbone virus and recombinant surface genes (distinct from the surface described in Monto *et al.*) developed mild upper respiratory, cold-like symptoms (269). In this study, participants ages 18-35 were vaccinated with increasing doses of the cold-adapted vaccine. Cold-like symptoms were associated with high vaccination doses. Consistent with Monto *et al.*, some vaccinees did shed virus, although shedding was dose dependent. Additionally, 25% of vaccinated individuals were shown to have increased IgA responses against homologous virus compared to pre-vaccination titers. These data were compared to a group of volunteers who were similarly inoculated with increasing doses of the WT virus represented in the surface genes of the vaccine. The symptoms and viral shedding generated from inoculation with the WT virus were significantly higher than with the recombinant vaccine, although they were also dose-dependent (269).

Clinical trails with the B/Ann Arbor ca backbone have also been completed in children (271, 272). In one study, seropositive and seronegative infants and children ages 6 months to 9 years old showed a similar safety profile to that seen in adults (271). The vaccine was well-tolerated in both seropositive and seronegative

individuals, although there were differences in immunogenicity. A greater number of seronegative individuals experienced an increase in antibody titers post-vaccination than seropositive individuals. Differences in shedding among seropositive and seronegative individuals were also found, and although both groups shed virus, peak viral titers were lower in seropositive individuals than in seronegative (271). The shed virus was evaluated for temperature sensitivity and, consistent with other studies, it was shown to maintain its temperature sensitive phenotype. Importantly, despite viral shedding, this study found that the vaccine virus was not readily transmissible to naïve children who were in close contact with vaccinated individuals, evidenced by a lack of antibody titers and viral shedding detected in unvaccinated children who were in close contact with vaccinated children (271). Interestingly, seronegative children were shown to shed the vaccine virus for an average of 9 days, longer than both adults (6 days) and seropositive children (5 days) (271, 273). Another study in children ages 8 months to 14 years made similar findings (272). Additionally, this study quantified the amount of virus required to infect 50% of seronegative children at $10^{4.5}$ TCID₅₀, which was consistent with data from previous studies (272).

Finally, the B/Ann Arbor ca backbone has been tested in immunocompromised and elderly individuals. While these groups tolerate vaccination with the B/Ann Arbor ca backbone similarly to healthy individuals, the vaccine has shown less immunogenicity. Overall, the results have shown a poor immune response to vaccination in comparison to younger, healthy individuals (267). Although some antibody responses are generated in these individuals post-vaccination, the response was lower than in seronegative adults and children.

Interestingly, elderly individuals shed lower titer virus and were less likely to shed virus than younger, healthy individuals post-vaccination, suggesting that there is a lower rate of infectivity in elderly individuals which may be due to the immune history of older individuals, having likely been exposed to influenza virus infection a greater number of times than younger individuals (267).

1.7.1.3. Clinical trials and licensing

Large-scale clinical trials (typically including over 1,000 individuals per trial) were completed with the trivalent formulation of the LAIV vaccine to assess safety and efficacy in children and adults before it was licensed in 2003 (274-276). This formulation contains both the A/Ann Arbor and B/Ann Arbor ca backbones as well as surface genes corresponding to H1 and H3 strains of influenza A and one strain of influenza B (24). In a study of children 15-71 months of age, adverse vaccine side effects included mild respiratory tract infection and, in some cases, fever (274). Each of the vaccine components proved immunogenic in this age group. Consistent with the small-scale clinical trials described above, antibody responses post-vaccination were higher in seronegative individuals. Importantly, in a healthy adult challenge trial, the trivalent LAIV vaccine efficacy was compared to a trivalent inactivated vaccine. The estimated efficacy post-challenge in this study for all three components of the vaccine combined was 85% for the LAIV vaccine compared to 71% for the inactivated trivalent vaccine (277). Notably, in a working adult clinical trial, the trivalent LAIV vaccine was shown to decrease febrile illness, resulting in less

absenteeism from work among the vaccinated group (278). In total, 16 clinical trials were completed in ages ranging from 1-81, which lead to the licensing of the trivalent LAIV vaccine, and study cohorts included healthy and high-risk groups (275). Data obtained from these studies were consistent with the findings described in the smaller scale human studies (1.6.1.2).

Note: the following section is based on “Design of Alternative Live Attenuated Influenza Virus Vaccines”, a chapter written for *Current Opinions in Microbiology and Immunology* by Finch *et al.*

1.7.2. Modifying the NS Gene Segment

Considerable effort has been placed in modifying the influenza NS gene as a means of creating a safer alternative to the current LAIV vaccine strategy (40). The strategy relies on BNS1 antagonism of the innate immune response, as viruses containing BNS1 knockouts and truncations are attenuated (50, 171, 172, 206). Here, Influenza B BNS1 truncation mutants that have been shown to be efficacious vaccines in the mouse model are discussed (176, 177).

A series of Influenza B BNS1 truncated viruses have been generated and rescued via reverse genetics. A number of truncations were made in the C-terminus of BNS1: BNS1 1-14, BNS1 1-38, BNS1 B1-57 and BNS1 1-80 (Wressnigg *et al.* 2009). These viruses replicate well in Vero cells, which do not produce interferon and

are approved for vaccine production. While all of these truncated viruses are attenuated, the degree of attenuation corresponds to the length of the truncation; however, even BNS1 1-80 is insufficient to block IFN and induces an IgG response greater than that produced by the WT virus (Wressnigg et al. 2009). When mice were vaccinated with these mutants, they were fully protected after just one immunization (at 5×10^5 tissue culture infectious dose 50, TCID₅₀) against 5×10^5 TCID₅₀ homologous virus challenge. Viral titers of lung homogenates revealed that none of the mice immunized with a BNS1 mutant had detectable virus titers in the lungs after lethal challenge (177). In a similar study, BNS1 1-80 and BNS1 1-110 truncations were cloned, and the rescued viruses were used to vaccinate mice (176). Both viruses provided protection against homologous, 5×10^5 Pfu, challenge in mice (176).

The NS1 truncation vaccine strategy has been extensively studied in the context of influenza A and has shown efficacy in multiple animal models and in humans (248, 279-281). As both the NS1 and BNS1 truncation strategies revealed similar results in mice, it is likely that the BNS1 truncation strategy could be extended to other animal models and humans (279).

1.7.3. Modifications in the HA Cleavage Site

HA has been another target of manipulation for LAIV vaccine development, particularly at the monobasic cleavage site (40). As previously described, monobasic cleavage sites, like those found in influenza B, are cleaved by trypsin-like proteases present primarily in the upper respiratory tract of humans and many other mammals

(97). This contributes to the restriction of influenza B viruses to the upper respiratory tract, as trypsin-like proteases are located in this region (122, 282, 283). It follows then that altering the enzyme specificity of the cleavage site may be a means of attenuating the virus by restricting virus growth under specific conditions. Indeed, this has been shown to be an effective mean of generating a LAIV vaccine as is described below (284, 285).

Stech *et al.* modified the HA cleavage site of B/Lee/40 to recognize elastase, a porcine pancreatic enzyme. Two viruses were generated after mutating the cleavage site: B/Lee/40-Val (arginine to valine at position 361) and B/Lee/40-Ala (arginine to alanine at 361). In the presence of elastase, each vaccine candidate grew to WT levels in MDCK cells, although B/Lee/40-Val grew to slightly lower titers. Since B/Lee/40-Ala grew well *and* did not cause weight loss in mice, the vaccine study was completed using B/Lee/40-Ala. After lethal challenge of WT B/Lee/40 at 10^6 Pfu, no virus was detected in the lungs of mice immunized with at least 10^4 Pfu of B/Lee/40-Ala on day 3 post-challenge. Mice immunized with these doses maintained weight post-challenge and survived. In contrast, mice immunized with B/Lee/40-Ala formalin-treated KV vaccine had high viral titers detectable in the lungs on day 3 post-challenge, and weight loss was recorded (285).

This cleavage modification strategy presents major advantages. For instance, elastase vaccines can be grown to WT levels in approved cell lines while providing adequate protection with just one dose; however, this strategy is prone to reversion (285). Given its propensity for reversion, as the authors suggest, combining this

strategy with another, such as the B/Ann Arbor cold-adapted mutations, may be necessary (220, 222, 223, 257, 258).

1.7.4. Conclusions and Commentary: LAIV vaccines

While the currently licensed B/Ann Arbor ca backbone is safe, stable, immunogenic and effective, there are disadvantages and drawbacks to this strategy, particularly in coverage provided to high-risk groups. Although it has been shown to be safe in these groups, there is always a higher inherent risk in vaccinating these individuals. Additionally, the immune response in the elderly to the LAIV vaccine is poor, possibly as a result of the immune history of these individuals (267).

Despite a plethora of available experimental LAIV vaccine strategies, there are far fewer experimental vaccines available for IBV than are available for IAV. The elastase and the BNS1 truncation strategies are potentially viable candidates as alternative strategies to the B/Ann Arbor ca backbone; in fact, the influenza A NS1 truncation strategy has been shown to be efficacious and immunogenic in an aged mouse model and could be a potential alternative strategy for influenza B, as well (248). Nonetheless, there is still need for alternative influenza B vaccination strategies, which are safer and more efficacious. This dissertation will describe one such alternative.

1.8. Summary of Research Objectives

The primary goal of this dissertation was to develop an alternative LAIV vaccine strategy for influenza B that complements our lab's patented influenza A strategy using a contemporary influenza B virus. A contemporary influenza B virus was chosen for incorporation into an IBV vaccine strategy principally to provide better immune stimulation in elderly individuals. To this end, B/Brisbane/60/2008 was selected, and an RT-PCR system was designed to clone it. Initial attempts to develop a LAIV vaccine involving PB2 cap-binding mutants led to the identification of these mutations as virulence factors in mice; however, a subsequent attempt to develop an alternative LAIV vaccine for influenza B succeeded.

Two alternative LAIV B/Brisbane/60/2008 vaccines that are safe, immunogenic and confer full protection against lethal homologous challenge in mice were developed. Each vaccine virus contained the following mutations in PB1: K391E, E580G and S660A. Additionally, one virus also possessed an 8 amino acid HA tag at the C-terminus of PB1. The tag-less virus was named B/Brisbane/60/2008 *ts*, while the tagged virus was named B/Brisbane/60/2008 *att*. The reverse-genetics system, virulence factors and vaccines will aid in the future study of influenza B viruses as well as the future development of an alternative LAIV influenza quadrivalent vaccine using our lab's patented strategy.

1.8.1. Dissertation outline

- Development of a Contemporary B/Brisbane/60/2008 Reverse Genetics System
 - Two-step RT-PCR cloning strategy
 - Design of reporter system
 - *In vitro* characterization of RG-B/Brisbane/60/2008
 - *In vivo* characterization of RG-B/Brisbane/60/2008
 - Analysis of B/Brisbane/60/2008 relatedness to contemporary influenza B viruses
- Development of Alternative influenza B LAIV Vaccines: PB1/PB2 mutants
 - *In vitro* characterization of vaccine candidates
 - *In vivo* characterization of vaccine candidates
- Cap-binding Mutants as influenza B Virulence Factors in Mice
 - *In vitro* characterization of cap-binding mutants
 - *In vivo* characterization of cap-binding mutants
 - Pathogenesis of cap-binding mutants
- Development of an Alternative Influenza B LAIV Vaccines based on three amino acid mutations and an C-terminal HA tag in PB1
 - *In vitro* characterization of vaccine candidates
 - *In vivo* characterization of vaccine candidates
 - Vaccination and challenge of mice with vaccine candidates
 - Analysis of stability of vaccine candidates

- Conclusions and Future Directions

Chapter 2: Development of a Contemporary B/Brisbane/60/2008 Reverse Genetics System

2.1. Abstract

Although there are two influenza B HA antigenic lineages, both relevant to human disease, B/Victoria-like and B/Yamagata-like, there are no contemporary reverse genetics systems available for either lineage. Reverse genetics viruses B/Yamanashi/166/98, a B/Yamagata-like virus, and B/Lee/40, the first influenza B virus isolate, are widely used for both vaccine development and functional studies of the influenza B genome, but neither virus is closely related to contemporary strains of either lineage. Here, a “universal” RT primer set was designed for a 2-step RT-PCR approach to clone B/Brisbane/60/2008 in a strategy modeled after influenza A. Reverse genetics B/Brisbane/60/2008 (RG-B/Bris), a contemporary B/Victoria-like virus, was successfully cloned and rescued. This virus grew to similar viral titers as the WT and was virulent in mice. To our knowledge, this is the most contemporary reverse genetics system for the B/Victoria lineage. The RG-B/Bris strain was further explored as an alternative LAIV influenza B virus vaccine as described in subsequent chapters.

2.2. Introduction

Influenza B virus (IBV) belongs to the *Orthomyxoviridae* family of viruses and is one of three types of influenza viruses: A, B, and C. IBV has a negative-sense, single-stranded, segmented RNA genome (3). Its genome consists of 8 RNA segments and can be divided into backbone genes and surface genes (3, 44, 47, 48). Segments 1-3, 5, 7 and 8, which correspond to the PB1, PB2, PA, NP, M, and NS genes, respectively, are backbone genes that encode proteins present within the virion (39, 40). Segments 4, HA, and 6, NA, are surface genes that encode immunogenic surface proteins (39, 40, 73, 81, 162).

Although it has been isolated in seals and birds, IBV circulates annually as a primarily human pathogen, causing respiratory disease (18, 19, 21-23, 178). Infections occur throughout the year but peak during the winter months due to drier, colder conditions known to enhance transmission of influenza (30, 31). Individuals of all ages are susceptible to infection with symptoms including fever, muscle aches, anorexia and nasal discharge; nonetheless, the most severe cases in the U.S. have generally been reported in the young and elderly (4, 28). The same age-related severity has not been reported in other countries; however, this may be due to insufficient data (28).

IBV is generally less prevalent than influenza A virus (IAV); however, IBV still has a substantial impact on public health. Roughly every 3 years, an IBV is the dominant circulating influenza virus (32). Additionally, even in years when IBV has been less prevalent, it has caused a disproportionately greater impact on human

disease. For example, during the 2010-11 U.S. influenza season, IBV accounted for only 26% of all circulating influenza viruses, yet it accounted for 38% of all pediatric influenza-associated deaths (33). In fact, IBV has contributed heavily to influenza-associated mortality of all ages. For instance, 25% of all influenza-associated mortality in the U.S. from 1976/77-1998/99 was IBV-associated (28). Finally, IBV has a well-documented history of causing epidemics, despite having no history of causing pandemics (76, 180, 286, 287).

Influenza B strains cannot be categorized into subtypes, but instead, they are categorized based on antigenic lineage. There are two IBV antigenic lineages, B/Victoria/2/87-like (B/Victoria-like) and B/Yamagata/16/88-like (B/Yamagata-like), where B/Victoria/2/87 and B/Yamagata/16/88 are the prototypical strains of each lineage, respectively (75). These lineages were designated in the 1980s after strains of IBV with little to no cross-reactivity were detected (75, 77). Lineage designations are made based on sequence homology and antigenicity to the HA1 region of segment 4, hemagglutinin (HA), the major antigenic surface gene of IBV (40, 73, 75).

Prior to the 1980s, a monovalent IBV-component vaccine was sufficient to protect against most illness due to the circulation of antigenically similar viruses; however, with the divergence of IBVs into two distinct lineages, as described above, the production of IBV vaccines has become more complicated, particularly since the new millennium. For instance, B/Yamagata-like viruses dominated in the 1990s, but in the 2000s, B/Victoria-like viruses re-emerged (217). Since this time, B/Yamagata-like and B/Victoria-like viruses have co-circulated which has led to a trend of IBV infections amongst properly vaccinated individuals during years when there was

mismatch between the dominant circulating IBV strain and the vaccine strain (76). Recently, both B/Victoria-like and B/Yamagata-like HA antigenic lineages were incorporated into the seasonal influenza vaccine in an effort to provide better vaccine coverage (24, 77).

The specific virus strains selected for incorporation into the seasonal vaccines are recommended by the World Health Organization (WHO) Collaborating Centers based on surveillance of virus samples carried out by National Influenza Centers (35). As protection against the HA and, to a lesser extent, NA antigens is sufficient to provide neutralizing immunity, vaccines are manufactured with surface genes that correspond antigenically to the currently circulating IAV and IBV strains recommended for inclusion; however, the same backbone genes are incorporated into the seasonal vaccines each year (25, 37). Two primary formulations of the seasonal vaccine are manufactured, the killed virus (KV) and the live-attenuated influenza virus (LAIV) vaccines (24).

The WHO recommended vaccine virus gene constellation can be generated by either classical reassortment, involving the co-infection of eggs with either the LAIV backbone or the KV backbone virus and the wild-type (WT) recommended virus followed by genotyping, or by reverse genetics (249, 250). For cases in which the surface genes on the egg-adapted backbone do not yield high titer virus, the vaccine strain is passaged in eggs until high titer virus is achieved (215).

The KV vaccine is formalin-treated inactivated whole virus (25). Each year, the IBV-component is manufactured with a B/Lee/40 backbone, which was egg-adapted to achieve high growth in eggs for the purpose of vaccine production (37).

Once the vaccine strain stock is generated by the methods described above, it is treated with formalin, rendering it non-replicative, and as it is non-replicative vaccine, it generates a humoral immune response (170).

Although the IBV-component of the seasonal LAIV virus vaccine is produced in a manner similar to the KV vaccine, either by classical reassortment or reverse genetics, it is replication impaired at high temperatures, rather than replication incompetent (263). The vaccine backbone was generated by serially passaging B/Ann Arbor/1/66 virus at progressively lower temperatures in Chicken Embryonic Kidney (CEK) cells until it grew well at 25°C (220). The mutations generated through serial passage rendered the virus cold-adapted and temperature sensitive restricting growth to the low temperatures of the upper respiratory tract and preventing severe infection associated with replication in the lower respiratory tract (223, 263, 270).

Additionally, as a live-attenuated virus, the vaccine induces a broader immune response than the KV formulation, generating humoral and cell-mediated immunity as well as an enhanced innate immune response (170, 288).

While the efficacy of the trivalent KV seasonal vaccine, which contains 2 IAV strains and 1 IBV strain, is estimated to be about 60% for ages 18-65 (averaged over the course of 12 seasons) and the trivalent LAIV vaccine has enhanced coverage to about 90% for ages 6 months to 7 years (averaged over the course of 12 seasons), improvements in efficacy, safety and coverage can still be made (289). This is particularly true when one considers vaccine availability for the most at-risk populations. For instance, the elderly and those with pre-existing conditions are not permitted to receive the LAIV vaccine (24).

Importantly, an elderly person's immune system is not highly responsive to vaccination with the LAIV vaccine due to immunosenescence (290). Adjuvants and increased doses of HA have commonly been utilized, with some success, to enhance the immune response in this group (291). An alternative, though, to these methods could be the use of a different, more contemporary vaccine backbone.

Since an elderly person's immune system has been repeatedly exposed to the currently licensed vaccine backbone and it has been suggested that repeated exposure to the same virus strain provides a limited boost to the cellular and humoral immune response, a more contemporary backbone would likely provide greater stimulation of the immune system (292). An additional benefit to using a more contemporary backbone may also be increased heterologous immunity against currently circulating strains as heterologous protection is conferred by immunity against the backbone genes, and indeed, NP protein, encoded from segment 5, has been shown to be a major target of CD8⁺ T cells (293-297). Unfortunately, there are few, if any, reverse genetics (RG) viruses currently available for IBV with which to develop a more contemporary, more efficacious, safer vaccine.

In 2002, two reverse genetics systems were published for influenza B, an 8-plasmid and a 12-plasmid system, which described reverse genetics rescue of B/Yamanashi/166/98 and B/Beijing/1/87 viruses, respectively (2, 52). Since this time, other reverse genetics systems have been published for B/Lee/40, B/Ann Arbor/1/66 and B/Yamagata/1/73 (2, 52, 127, 206-208). All of these viruses are distantly related to IBV strains circulating today. In fact, B/Lee/40 is the first ever-isolated IBV strain (73). Despite the distant relationship of these viruses to currently circulating strains,

B/Lee/40 and B/Ann Arbor/1/66 backbones are incorporated into the seasonal influenza vaccine each year, as described above (37, 220).

Since there are no contemporary influenza B reverse genetics viruses available, the design of an alternative vaccine on a contemporary backbone required the cloning of a new virus. In this vein, this study sought to clone and characterize a reverse genetics plasmid set of B/Brisbane/60/2008, a B/Victoria-like virus, with the ultimate goal of developing an alternative LAIV vaccine based on a more contemporary strain. The data show the successful cloning and rescue of reverse genetics B/Brisbane/60/2008 (RG-B/Bris) via the design of a 2-step RT-PCR system modeled after that of influenza A (298, 299). Additionally, the results demonstrate that this virus grows to high titers and is virulent in mice, making it a suitable platform for the development of a vaccine candidate.

2.3. Materials and Methods

2.3.1. Maintenance of cells

Both Madin-Darby Canine Kidney cells (MDCK) and human 293T cells (293T) were maintained in Dulbecco's Modification of Eagle's Medium (DMEM) (Corning, Corning, NY) containing 10% Fetal Bovine Serum (FBS) (Sigma-Aldrich, St. Louis, MO), Antibiotic/Antimycotic (10mL/L, Sigma-Aldrich, St. Louis, MO), L-Glutamine (2mM, Sigma-Aldrich, St. Louis, MO) and HEPES Buffer (.025M, Sigma-Aldrich, St. Louis, MO). With each passage of the MDCK cells, the passage number was recorded. MDCK cells were not used beyond passage 60. Cells were maintained in T75 flasks (Greiner Bio-One, Monroe, North Carolina) in a CO₂ incubator at 37°C.

2.3.2. Cloning and sequencing of B/Brisbane/60/2008

All 8 genes of B/Brisbane/60/2008 (a gift from the CDC) were cloned into pDP2002, a bi-directional cloning vector (1). Segments 4, 5, 6 and 8 were cloned using a previously described strategy (2). To clone the remaining segments, reverse transcription (RT) primers were designed based on influenza B published UTRs described in Hoffman *et al.* and Jackson *et al.* (2, 52). Due to the inherent variability in influenza B UTRs, this resulted in 3 “universal” RT primers that are 11 nucleotides in length (corresponding to the 5' end of the cDNA) (Table 2.1). Each of these

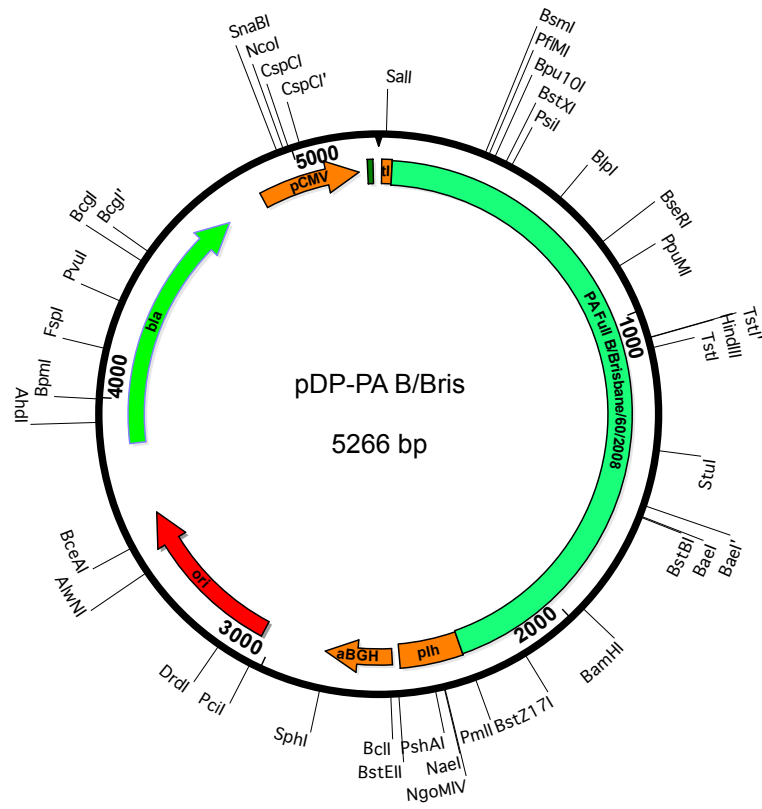
primers differs in the final 2 to 3 nucleotides. The first RT primer was designed to correspond to the UTR of segments 1, 2 and 3, the second RT primer was designed to correspond to the UTR of segments 5 and 7, and the final RT primer was designed to correspond to the UTR of segments 4, 6 and 8. Then, unique cloning primers were designed for each segment (Table 2.2). Each of the cloning primers was designed with AarI cut sites.

To begin cloning, AMV Reverse Transcriptase (Promega, Madison, WI), RNAsin (Promega, Madison, WI) and an RT primer were incorporated into a reverse transcription reaction according to the manufacturer's recommendations. Then, using cloning primers unique to each gene, cDNA was amplified by PCR. PCR was performed with Expand High Fidelity Polymerase (Roche, Indianapolis, IN) according to the manufacturer's recommendations, albeit with some modifications. The following parameters were employed: 95°C for 4 min (denaturation), 56°C for 30 sec (annealing), 72°C for 5-7 min (extension), 72°C for 10 min (final extension). The annealing and extension steps were repeated for 30 cycles. Segment 4 PCR was done with an extension of 5 min. PCR reactions for segments 1-3 were done with an extension of 7 min. After PCR amplification of each gene, an AarI digest (Thermo Scientific, Waltham, MA) was then performed to digest the amplified B/Bris gene, while a BsmBI digest (New England Biolabs, Ipswich, MA) was employed to digest the pDP2002 vector. Digested PCR products were ligated into pDP2002 using QuikLigase (New England Biolabs, Ipswich, MA).

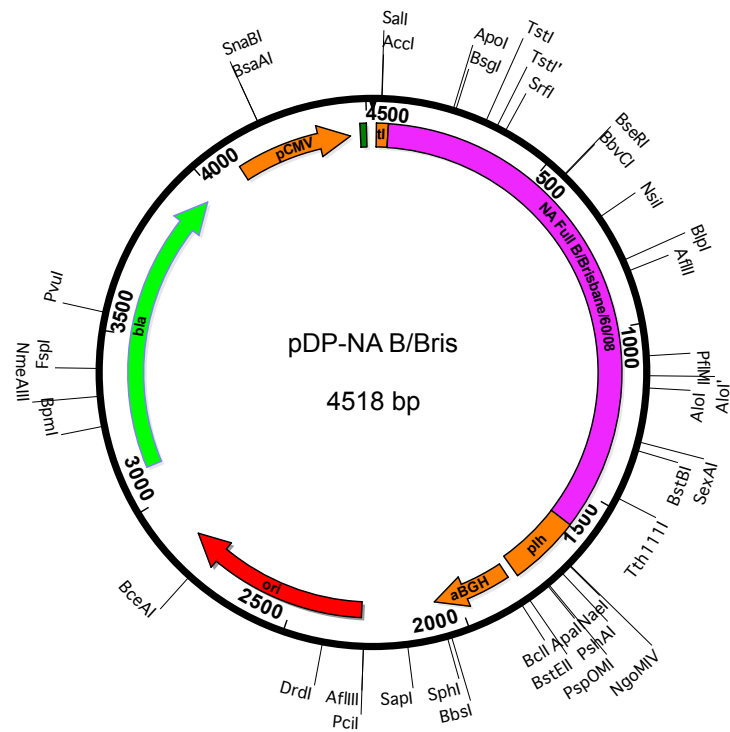
Each plasmid and WT vRNA segments were also sequenced by Sanger sequencing on a 3500xL Genetic Analyzer (Applied Biosystems, Foster City, CA)

using the BigDye Terminator v3.1 Cycle Sequencing Kit (Life Technologies, Carlsbad, CA) (Fig. 2.1).

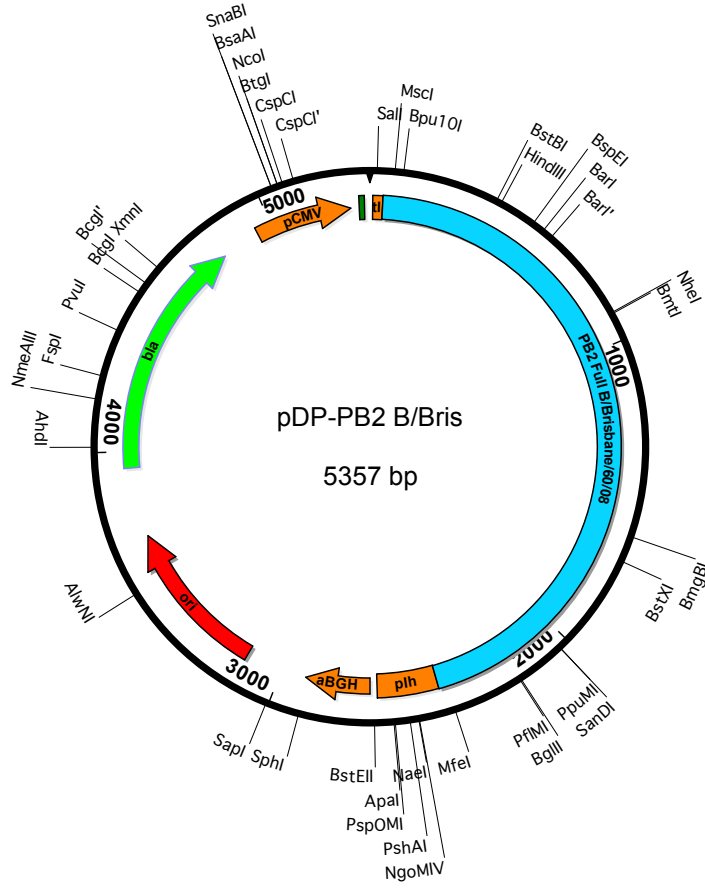
A



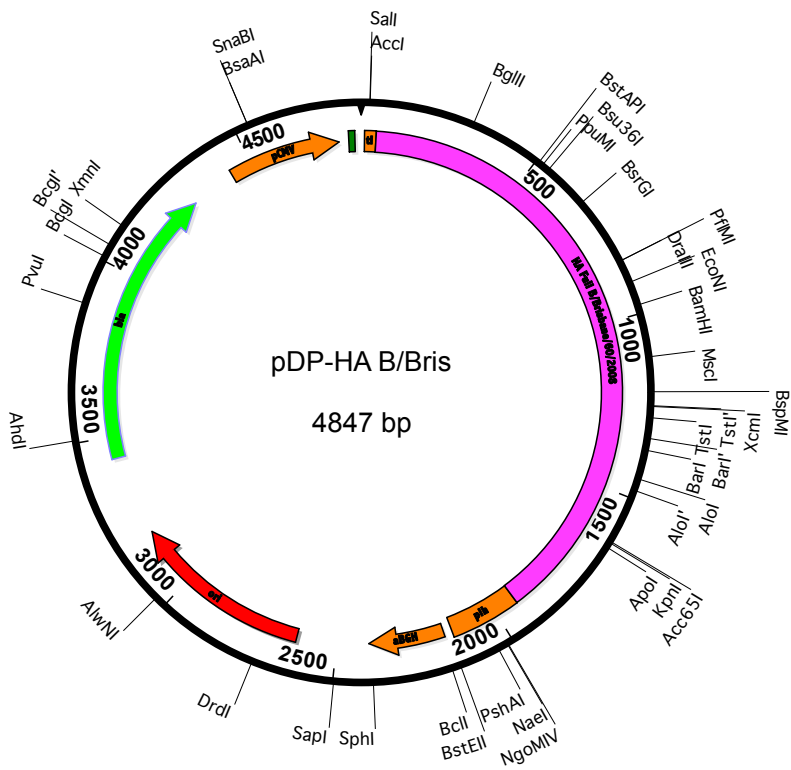
B



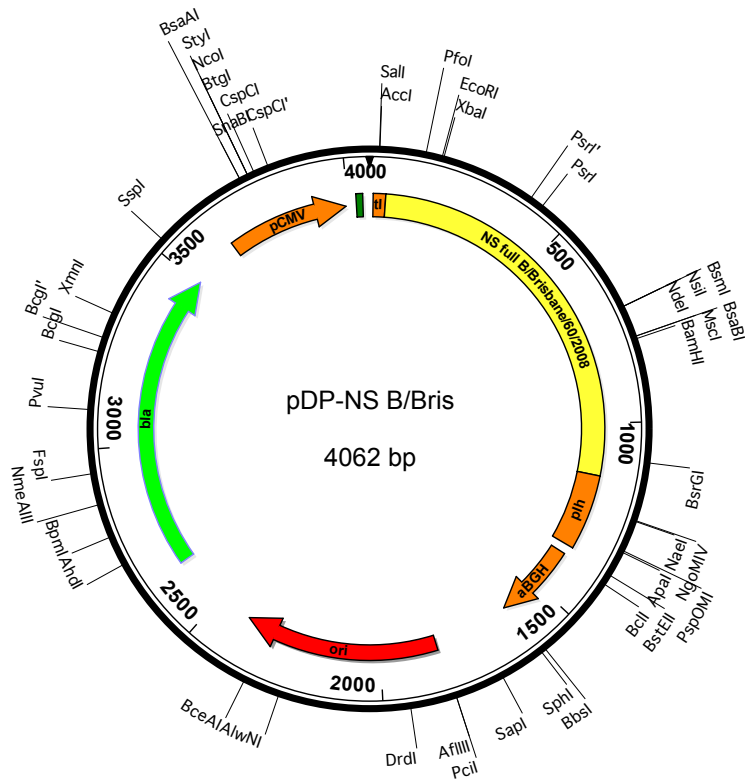
C



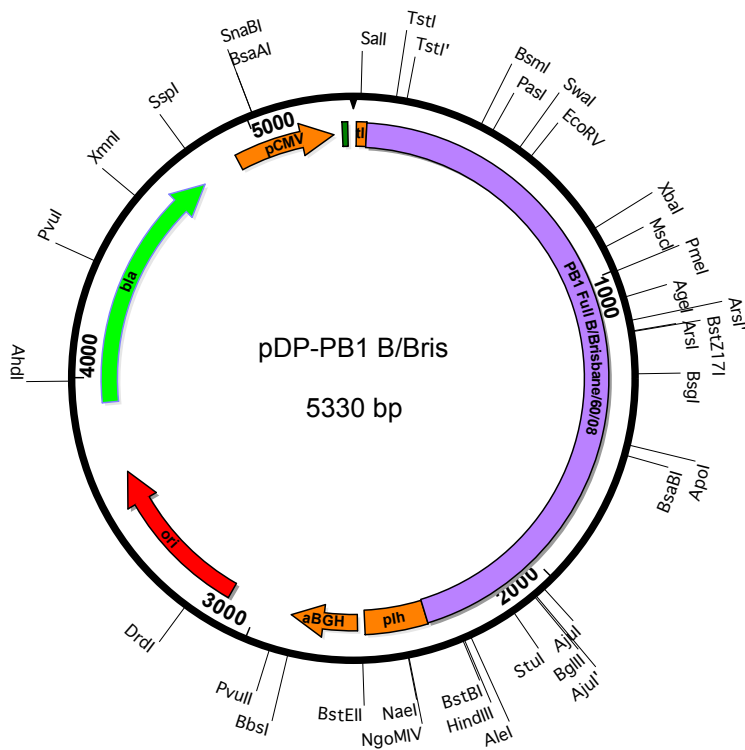
D



E



F



Primer Name	Sequence (5' to 3')	Gene Segment
B_uni11_Seg1,2,3	AGCAGAAGCGG	PB1, PB2, PA
B_uni11_Seg5,7	AGCAGAAGCAC	NP, M
B_uni11_Seg4,6,8	AGCAGAAGCAG	HA, NA, NS

Table 2.1. Universal primers for influenza B reverse transcription.

Each primer corresponds to either 2 or 3 gene segments. The primer sequence matches the 5' region of the cDNA. The first 9 nucleotides are identical in each primer.

Primer Name	Sequence (5' to 3')	Gene Segment
AarI_M_FluB_1F	TATTCACCTGCCTCAGGGAGCAGAA GCACGCAC	M
<i>AarI_M_FluB_1141R</i>	ATATCACCTGCCTCGTATTAGTAGA AACAAACGCACTTT	
AarI_PA_FluB_1F	TATTCACCTGCCTCAGGGAGCAGAA GCGGTGCG	PA
<i>AarI_PA_FluB_2245R</i>	ATATCACCTGCCTCGTATTAGTAGAA ACACGTGCATT	
AarI_PB1_FluB_1F	TATTCACCTGCCTCAGGGAGCAGAAG CGGAGC	PB1
<i>AarI_PB1_FluB_2368R</i>	ATATCACCTGCCTCGTATTAGTAGAA ACACGAGCCTT	
AarI_PB2_FluB_1F	TATTCACCTGCCTCAGGGAGCAGAAG CGGAGC	PB2
<i>AarI_PB2_FluB_2369R</i>	ATATCACCTGCCTCGTATTAGTAGAAA CACGAGCATT	

Table 2.2. Cloning primers for B/Brisbane/60/2008. Each primer contains an AarI cut site shown in bold. The sequences shown correspond to the cDNA. Sequences for only M, PA, PB1, and PB2 are shown. Reverse primers are shown in italics. The primers used for amplification of the remaining segments are described in Hoffman *et al.* (2).

2.3.3. Cloning of a *Gaussia* Luciferase reporter construct

An NP *Gaussia* Luciferase (GLuc) (template: pGLuc Basic, New England Biolabs, Ipswich, MA) reporter plasmid was engineered from pDP-NP B/Brisbane/60/2008 (B/Bris). NP 5' and 3' UTRs were designed to flank the GLuc open reading frame (ORF). Cloning was done via overlapping PCR. First, 3 PCR fragments were generated corresponding to the 5' NP UTR, the 3' NP UTR and the GLuc ORF. PCR primers used to amplify each fragment had overhangs such that overlapping PCR with these fragments generated a NP 5'-GLuc-NP 3' PCR product. This PCR product was cloned into pDP2002 using restriction sites present in the vector. Ligation was performed using QuikLigase (New England Biolabs, Ipswich, MA). The generated clone was dubbed, pDP-NP-GLuc-NP (Fig. 2.2).

Next, the pCMV (Pol II) promoter was removed. This was also done by overlapping PCR. The regions immediately upstream and immediately downstream of the pCMV sequence were amplified, generating 2 fragments. PCR primers were designed with overhangs such that overlapping PCR of these 2 fragments omitted pCMV. The resultant PCR product was digested with cut sites present in the pDP-NP-GLuc-NP vector. Ligation was performed with QuikLigase (New England Biolabs, Ipswich, MA). The final reporter clone was called, p Δ CMV-NP-GLuc-NP. Sanger sequencing performed using the BigDye Terminator v3.1 kit (Life Technologies, Carlsbad, CA) on a 3500xL Genetic Analyzer (Applied Biosystems, Foster City, CA) confirmed the absence of the pCMV promoter (Fig. 2.3).

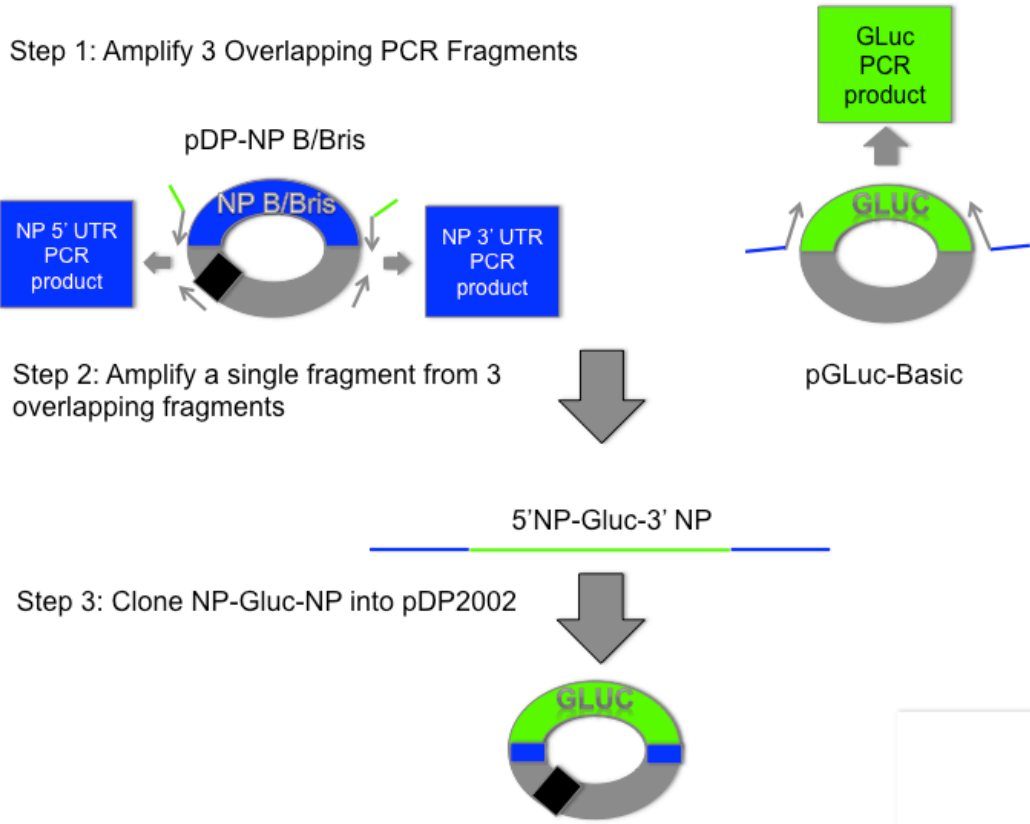


Figure 2.2. Cloning a GLuc Reporter: steps 1-3. Blue: NP B/Bris. Green: GLuc. Black: pCMV promoter. The primers used to amplify the UTR regions of NP had overhangs that corresponded to the GLuc ORF. Likewise, the primers used to amplify the GLuc ORF had overhangs that corresponded to either the 5' or 3' NP UTR.

Step 4: Remove pCMV promoter; Amplify 2 overlapping regions outside of pCMV

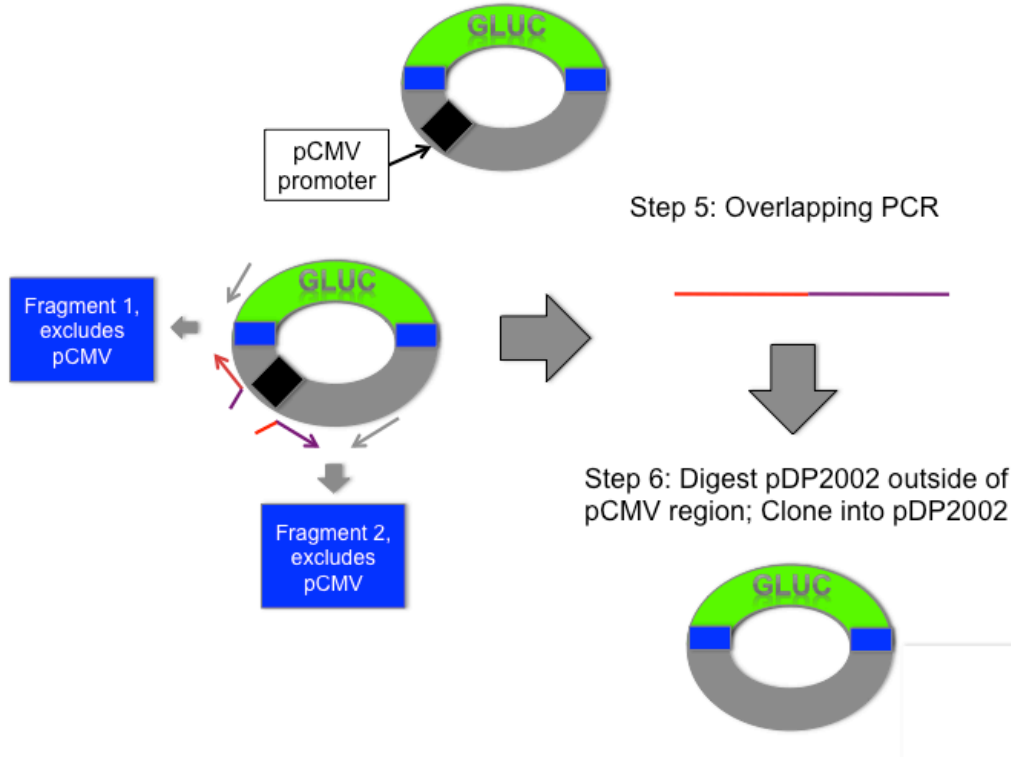


Figure 2.3. Cloning of a GLuc reporter: steps 4-6. Blue: NP B/Bris. Green: GLuc. Black: pCMV promoter. Regions immediately upstream and downstream of the pCMV promoter were amplified. The reverse primer of fragment 1 had an overhang that corresponded to fragment 2 (overhang is shown in red). Similarly, the forward primer for fragment 2 had an overhang that corresponded to fragment 1.

2.3.4. Virus rescue

The 8 plasmids described in 2.3.2, each carrying 1 of the 8 B/Bris genes, were transfected into a co-culture of 293T cells and MDCK cells. 1µg/mL of each plasmid was transfected into 8x10⁵ 293T cell/ 5x10⁵ MDCK cell co-culture in a 6-well plate (Corning, Corning, NY).

First, a master mix (master mix 1) containing all but one plasmid was mixed: 10µL of each plasmid (100ng/µL) was used per reaction and added to the master mix. 70µL of master mix 1 was aliquoted per reaction to each transfection reaction tube (1.5ml screwcap, USA Scientific, Orlando, FL) and mixed by vortexing. 10µL of EB buffer (QIAGEN, Valencia, CA) was added to the negative control. A positive control containing all reverse genetics B/Bris plasmids was also prepared. In all, each transfection reaction contained 80µL of plasmids (or plasmids and EB, in the case of the negative control).

Next, a second master mix was prepared containing [OPTI-MEM] I, FBS and Antibiotic/Antimycotic free, (Life Technologies, Carlsbad, CA) and Transit-LTI (Mirus Bio, Nutley, NJ). For every 1µg of plasmid, 2µL of Transit-LTI was used (16µL per one 8 plasmid transfection reaction) (Mirus Bio, Nutley, NJ). Transit-LTI and [OPTI-MEM] I, FBS and Antibiotic/Antimycotic free, (Life Technologies, Carlsbad, CA) were mixed up to 120µL per reaction (for each 8 plasmid reaction, 104µL [OPTI-MEM] I was added). Then, master mix 2 was vortexed, and 120µL was aliquoted to each plasmid mixture. Each reaction was vortexed again briefly. Reactions were then incubated at room temperature for 45 min. After 45 min, 800µL

of [OPTI-MEM] I (FBS free) (Life Technologies, Carlsbad, CA) containing 10mL/L Antibiotic/Antimycotic (Sigma-Aldrich, St. Louis, MO) was added slowly to each reaction.

Finally, media was aspirated from the 6-well plate co-cultures (Corning, Corning, NY) with a Pasteur pipette (Fisher, Hampton, NH). The 1mL of each transfection reaction was then overlaid on the cells. Each transfection reaction was carefully and slowly overlaid on the cells with a pipette, but was *not* mixed by pipetting. Cells were then placed at 33°C. After 24 h, the media was changed. Old media was carefully aspirated with a 1000µL pipette. Then, 2mL [OPTI-MEM] I (FBS free) (Life Technologies, Carlsbad, CA) containing 10mL/L Antibiotic/Antimycotic (Sigma-Aldrich, St. Louis, MO) and 1µg/mL of TPCK-trypsin (Worthington Biochemical, Lakewood, NJ) was gently overlaid on each well.

2.3.5. Virus stocks and titration

Following rescue of RG-B/Bris, transfection supernatant was collected 4-5 days post-transfection and spun down at 1000xg for 10 min at 4°C and then was passed onto MDCK cells. After 4 days, the supernatant was harvested, spun down at 1000xg for 10 min at 4°C and used to directly inoculate eggs. Eggs were also inoculated to grow a stock of WT B/Brisbane/60/2008.

To grow stocks, 10-fold serial dilutions of virus were prepared. Pipette tips were discarded between each dilution. Then, the allantoic cavities of specific

pathogen free (SPF) 9-day old hen eggs (B&E Eggs, York Springs, PA) were inoculated with 200 μ L. Three eggs were inoculated per dilution. Eggs were then incubated at 33°C for 72 h. After 3 days, allantoic fluid (AF) from each egg was harvested, and hemagglutination (HA) assays were performed to determine the HA titer of each egg.

To perform the HA assays, 100 μ L of undiluted AF was added to the first well in a V-bottom 96-well plate (Corning, Corning, NY). The remaining wells were filled with 50 μ L of PBS per well. Then, a series of 2-fold dilutions were made within the plate beginning at the first well (A1-A12). Finally, 0.5% cRBC (chicken Red Blood Cells, Lampire Biological Laboratories, Pipersville, PA) was added to each well. Plates were incubated at room temperature for 45 min, and HA titers were read. Virus positive wells were those that showed hemagglutination. The egg with the highest HA titer at the highest dilution was harvested. AF was spun down at 1,000 \times g for 10 min at 4°C, aliquoted and placed at -80°C. Each stock was then titrated by both egg infectious dose 50 (EID₅₀) and tissue culture infectious dose 50 (TCID₅₀) at 33°C.

TCID₅₀ titrations were performed using MDCK cells cultured in 96-well plates (Greiner Bio-One, Monroe, North Carolina). MDCK cells (25,000/well) that were seeded in 100 μ L of FBS free [OPTI-MEM] I (Life Technologies, Carlsbad, CA) containing 10mL/L Antibiotic/Antimycotic (Sigma-Aldrich, St. Louis, MO) and incubated overnight at 37°C. The following day in a new 96-well plate (Greiner Bio-One, Monroe, North Carolina), 10-fold serial dilutions were prepared. The 10-fold serial dilutions of virus were prepared in FBS free [OPTI-MEM] I supplemented with 1 μ g/mL TPCK-trypsin (Worthington Biochemical, Lakewood, NJ) by first filling the

plates with 216 μ L per well media and then adding 24 μ L of virus to the first well, a 1/10 dilution of virus (8 replicates for virus stocks and 4 replicates for virus samples). Next, dilutions were prepared beginning at the first well containing the 1/10 virus dilution. Dilutions of virus stocks were prepared out to 10^{-12} while dilutions of virus samples were prepared out to 10^{-6} . Tips were discarded between each dilution. After preparing the dilutions, media was removed from the MDCK cells. Then, cells were overlaid with 200 μ L of each dilution, being careful to transfer one column of dilutions at a time, beginning with the most dilute wells. The virus-overlaid cells were then incubated for 72 h at 33°C. After 72h, hemagglutination assays were performed. Wells that showed hemagglutination were considered virus positive, and the TCID₅₀ was determined by the Reed and Muench method (300).

Stock titration for the mouse study was done by EID₅₀ in 9-day old specific pathogen free (SPF) hen eggs (B&E Eggs, York Springs, PA). First, virus was serially diluted in 1.5mL tubes (USA Scientific, Orlando, FL), and tips were discarded between each dilution. After virus preparation, three eggs were inoculated per dilution (in the allantoic cavity), and each egg was inoculated with 200 μ L of virus dilution. Then, eggs were placed at either 33°C for 72 h post-inoculation. After 72 h, eggs were moved to 4°C overnight. The following day, each egg was harvested. Then, 100 μ L of allantoic fluid (AF) from each egg was placed in a 96-well V-bottom plate (Corning, Corning, NY). Empty wells were filled with 50 μ L of PBS, and AF was subsequently diluted to 2^{-3} . Then, a hemmagglutination assay (HA assay) was performed by aliquoting 50 μ L of 0.5% cRBC (Lampire Biological Laboratories, Pipersville, PA) to each well. Plates were incubated at room temperature for 45 min.

Eggs with HA assays showing hemagglutination in every well were considered virus positive. The EID₅₀ was determined by the Reed and Muench method (301).

2.3. 6. Virus rescue over time

Transfections were performed as described in 2.3.4 with some modifications. Assays were setup in 12-well plates (Corning, Corning, NY) that were seeded 1 day prior to transfection with a co-culture of 2.5×10^5 MDCK/ 4×10^5 293T cells/well. The following transfections were performed: RG-B/Bris with TPCK-trypsin, RG-B/BRis without TPCK-trypsin, and 7 plasmid RG-B/Bris with TPCK-trypsin (without pDP-HA B/Bris). Each transfection reaction contained $.5 \mu\text{g}/\text{mL}$ of each plasmid and was done at 35°C . Thus, instead of $80 \mu\text{L}$ of plasmid in a single reaction, $40 \mu\text{L}$ of plasmid ($100 \text{ng}/\mu\text{L}$) was used. The volume of Transit-LTI (Mirus Bio, Madison, WI) was similarly adjusted to compensate for the altered plasmid concentration. Thus, $8 \mu\text{L}$ Transit-LTI was incorporated. As before, the volume was added up to $200 \mu\text{L}$ with FBS free [OPTI-MEM] I (Life Technologies, Carlsbad, CA) containing Antibiotic/Antimycotic ($10 \text{mL}/\text{L}$, Sigma-Aldrich, St. Louis, MO). Transfection supernatant was collected at 6, 30, 54, 78, 102 h post-transfection. At each time point, $120 \mu\text{L}$ of supernatant was collected. After collection, media and TPCK-trypsin ($1 \mu\text{g}/\text{mL}$, Worthington Biochemical, Lakewood, NJ) were replenished with FBS free [OPTI-MEM] I containing Antibiotic/Antimycotic ($10 \text{mL}/\text{L}$, Sigma-Aldrich, St. Louis, MO). Samples were then titrated by TCID₅₀ as described in 2.3.5. Titers were calculated by the Reed and Muench method (301).

2.3.7. Mini-genome assays

Transfections were setup similar to those described in 2.3.4; however, there were some key differences. .5µg/mL of each plasmid was transfected into human 293T cells (1×10^6 /well) in a 12-well plate (Corning, Corning, NY). The total transfection volume was maintained at 1mL, although the volume of total plasmids per reaction was adjusted to 30µL instead of 80µL (5µL of 100ng/µL working stocks of each plasmid per reaction). [OPTI-MEM] I (Life Technologies, Carlsbad, CA) was mixed with 2µL/µg of Transit-LTI (Mirus Bio, Nutley, NJ) up to 200µL per reaction. In the case of the controls, 5µL of EB (QIAGEN, Valencia, CA) was added to the plasmid mixture to compensate for the omitted plasmid. After overlaying the transfection reaction on the 293T cells, cells were placed at 35°C. The media was not changed and TPCK-trypsin was not added post-transfection.

The transfected plasmids were those of the vRNP complex of B/Brisbane/60/2008 (pDP-PB2, pDP-PB1, pDP-PA, and pDP-NP), the *Gaussia* Luciferase reporter plasmid described in 2.3.3 and a Secreted Alkaline Phosphatase (SEAP) expression plasmid (pCMV-SEAP). The SEAP expression plasmid was included to control for transfection efficiency, as it is expressed under the control of pCMV, a Pol II promoter (i.e. only host RNA polymerase can generate SEAP expression). Two negative controls were included: a no reporter control (containing pCMV-SEAP and all 4 RNP plasmids) and a partial vRNP complex control (containing the reporter and 3 of 4 vRNP plasmids, no NP). Each transfection reaction was setup in triplicate and done at least twice.

Gaussia Luciferase (GLuc) expression was measured as an indirect indicator of polymerase activity. Since both SEAP and GLuc are secreted proteins, supernatant was collected at different time points (8, 16 and 24 h post-transfection) for analysis of GLuc activity. At every time point, 20 μ L of supernatant was collected, placed directly in a 96-well white micro-titer plate (Corning, Corning, NY) and stored at -20°C. At 24 h, additional supernatant was collected for SEAP quantification and stored at -20°C.

GLuc expression was quantified using a BioLux® *Gaussia* Luciferase Assay Kit (New England Biolabs, Ipswich, MA). Briefly, the Luciferase Substrate was prepared immediately prior to use by performing a 1/1000 dilution of the substrate into the Sample Buffer. Next, 50 μ L of diluted Luciferase Substrate in sample buffer was added to 20 μ L of sample in a flat-bottom 96-well white micro-titer plate (Corning, Corning, NY). Immediately after the addition of the substrate, the luminescence was measured over a 1- sec-integration time on a Victor X4 Luminescence Plate Reader (Perkin Elmer, Waltham, MA).

SEAP was measured utilizing the Phospha-Light System (Applied Biosystems, Foster City, CA) according to manufacturer recommendations. To perform this assay, Assay Buffer and Reaction Buffer were first equilibrated to room temperature. Then, a 1x dilution of 5x Dilution Buffer was prepared in water, preparing enough for 18.75 μ L /sample. To each sample of supernatant (6.75 μ L), 18.75 μ L of 1x Dilution Buffer was added and incubated at 65°C for 30 min. Next, samples were cooled on ice and then transferred to a 96-well flat-bottom white micro-titer plate (Corning, Corning, NY). Assay Buffer was then added to each sample, and

samples were incubated at room temperature for 5 min (25 μ L Assay Buffer/sample). During this incubation, reaction buffer, consisting of CSPD and Diluent (1:20 ratio), was prepared. After the incubation, 25 μ L of reaction buffer was added to each sample. Samples were incubated at room temperature for 20 min. SEAP activity was read in the Victor X4 Luminescence Plate Reader (PerkinElmer, Waltham, MA). GLuc activity was normalized with SEAP activity by dividing the raw GLuc activity at each time point by the raw SEAP activity, divided by 10,000, at 24 h [GLuc at x hpt/(SEAP at 24 hpt/10,000), where x is the number of hours post-transfection]. These values were graphed.

2.3.8. Growth kinetics

Growth kinetics assays were performed with virus stocks at 35°C with 0.01 multiplicity of infection, MOI, of virus. Roughly 24 h prior to infection, MDCK cells (5x10⁵/well) were seeded in a 6-well plate (Corning, Corning, NY) prepared with FBS free [OPTI-MEM] I (Life Technologies, Carlsbad, CA) containing 10mL/L Antibiotic/Antimycotic (Sigma-Aldrich, St. Louis, MO). The following morning, viruses were thawed and dilutions were prepared. Each well was infected with 1mL of 0.01 MOI of virus diluted in PBS. Plates were then moved to 4°C for 15 min to synchronize the infection. After 15 min, cells were moved to 37°C and incubated for 45 min to infect. After infecting the cells, each well was washed 3x with 1mL of sterile PBS, discarding tips between each well. Finally, [OPTI-MEM] I (FBS free) (Life Technologies, Carlsbad, CA) with 1 μ g/mL of TPCK-Trypsin (Worthington

Biochemical, Lakewood, NJ) was prepared. Then, 2mL of the media preparation was overlaid on each well. Again, tips were changed between each well. Plates were then placed at the appropriate temperature, 35°C. Viral supernatant was collected at 6, 12, 24, 48 and 72 h post-infection (hpi) (120µL/well), discarding tips between each well. After collecting each sample, the media was replenished with an equivalent volume of FBS free [OPTI-MEM] I (Life Technologies, Carlsbad, CA) and 1µg/µLTPCK-trypsin (Worthington Biochemical, Lakewood, NJ). When sample collection was complete, the samples were placed at -80°C to await titration by TCID₅₀. Each virus was assessed at least twice in triplicate.

2.3.9. Mouse Lethal Dose 50 (MLD₅₀)

RG-B/Bris MLD₅₀ studies were performed under BSL-2 conditions. First, serial dilutions from 10⁷-10⁵ EID₅₀/mL of the RG-B/Bris virus were prepared in PBS. Four mice were inoculated per virus dilution. Each mouse received 50µL of the virus inoculum intranasally, and all mice were weighed the day of inoculation and for 12 days post-inoculation. Mice that scored a 3 or greater for disease signs (described in Table 2.3) or mice that lost 20% or more of the starting weight were humanely euthanized. Euthanasia was performed by first anesthetizing the mice with the VetEquip Mobile Euthanasia System (VetEquip, Pleasanton, CA), which releases a mixture of isoflurane (Isoflo[®]) and oxygen (1 liter per min) into a chamber, and then performing cervical dislocation. The University of Maryland, College Park IACUC approved all mouse studies under protocol R-12-100.

Score	Physical Appearance	Body weight changes	Activity	Respiratory disease symptoms	Other disease symptoms (ex. Dehydration, Pinch Test)
0	Normal	Normal	Normal	Normal	Normal (<5% dehydration)
1	Lack of grooming	<10% light loss	Minor decrease in activity	Light nasal discharge	Diarrhea (>5% dehydration)
2	Rough coat	10-20%	Active only upon stimulation	Heavy nasal discharge/conjunctivitis	Heavy diarrhea (<10% dehydration)
3	Very rough coat	>20%	Inactive with stimulation	Mouth breathing/labored breathing	Neurological symptoms (>10% dehydration)

Table 2.3. Scoring explanations of signs and symptoms of disease in mice. This table describes how mice were scored. Any mouse scoring 3 or greater and/or showing weight loss of 20% or more was humanely euthanized.

2.3.10. Phylogenetic analysis of influenza B HA and NA

Sequences were gathered through nucleotide searches of full-length sequences using the Influenza Research Database (IRD, <http://www.fludb.org/brc/home.spg?decorator=influenza>). HA and NA sequences were collected internationally: Africa, Asia, Europe, North America and Oceania. Several sequences were gathered from each year from each country (of those available) in each region. Unfortunately, there were limited sequences available depending on the region and year. Thus, the phylogenetic tree is limited to the constraints of a limited dataset in certain regions, Africa in particular. After gathering the sequences from the IRD, sequences were downloaded by searching for accession numbers using the NCBI influenza database. Full-length coding regions were downloaded, and all duplicate sequences were removed. Then, sequences were aligned using Muscle with default parameters (302).

Next, phylogenetic inference was tested by distance and maximum likelihood. Trees were rooted using the maximum likelihood and 100 bootstrap replicates via RAxML v8.0.X (303) and under models of nucleotide substitution (GTR + Γ (HA, NA) and GTRCAT (HA, NA)).

Nucleotide BLASTs (Basic Logical Alignment Search Tool) were performed with each of the full-length RG-B/Brisbane/60/2008 genes to determine the sequences most closely related to the entire RG-B/Bris genome. BLASTs were performed by using NCBI Influenza Virus Resource database (http://www.ncbi.nlm.nih.gov/sutils/blast_table.cgi?taxid=11308&selectall). Four of

the top results showing the highest percentages of sequence identity were recorded.

Laboratory reassortant viruses were excluded.

2.4. Results

2.4.1. Polymerase activity shows that RG-Bris polymerase is functional

Mini-genome assays were performed to assess polymerase activity of the RG-B/Brisbane/60/2008 (RG-B/Bris) vRNP complex as well as confirm that the NP GLuc reporter plasmid functioned as desired. Bidirectional reverse genetic plasmids encoding the vRNP genes of B/Bris were transfected into 293T cells along with the GLuc vRNA reporter plasmid, and supernatant was harvested at time points up to 24 hpt. Finally, normalized GLuc expression was evaluated, and the results showed that the RG-B/Bris polymerase complex expressed GLuc above baseline, which was established by SEAP expression, confirming that the RG-B/Bris polymerase complex is functional. Additionally, all negative control complexes showed lower GLuc activity than the full polymerase complex after normalization by 2 logs and greater, consistent with the removal of the Pol II promoter from the reporter plasmid (Fig. 2.4).

2.4.2. Virus rescue over time shows RG-B/Bris rescues efficiently

To evaluate the efficiency of RG-B/Bris virus rescue, all 8 bi-directional RG-B/Bris plasmids were transfected into an MDCK/293T cell co-culture at 35°C. Supernatant was collected at several time points post-transfection and titrated by

TCID₅₀ to determine viral rescue titers over time. By 54 h post-transfection (hpt), rescue titers of the RG-B/Bris virus were near 10⁵ TCID₅₀/mL (Fig. 2.5). By 102 h post-transfection, virus titers were greater than 10⁶ TCID₅₀/mL (Fig. 2.5). As expected, RG-B/Bris does not rescue without TPCK-trypsin, an enzyme required to cleave HA and generate infectious virus (89). Thus, RG-B/Bris rescues efficiently and grows well in MDCK cells.

2.4.3. WT and RG-B/Bris grow to similar titers in tissue culture

Although all future work to be done in the development of a LAIV influenza B vaccine will be done with the reverse genetics virus, growth of the WT and RG-B/Brisbane/60/2008 viruses was compared *in vitro*. Growth kinetics assays were performed with 0.01 MOI of virus at 35°C, and time points were collected at 6, 12, 24, 48 and 72 h post-infection (hpi). The results showed that the WT and RG viruses replicate to similar titers, although at early time points (12 hpi) the WT virus may replicate better (Fig. 2.6). The difference seen at 12 hpi could be a result of a mutation, PB1 N635S, which was identified in the RG-B/Bris virus when compared to the WT virus, but no other mutations were identified.

2.4.4. RG-B/Bris is virulent in mice

An egg-grown stock of RG-B/Bris was generated to determine whether or not this virus is virulent in mice. To this end, 5-6 week old female DBA/2 mice were intranasally inoculated with 50 μ L of 10^7 , 10^6 or 10^5 EID₅₀ of virus, and signs of disease were monitored for 12 days post-inoculation (dpi). The results showed that at 10^7 and 10^6 EID₅₀ RG-B/Bris caused 100% mortality (data not shown, Fig 2.7, respectively). At 10^5 EID₅₀, only 1 of 4 mice succumbed to infection (Fig. 2.7). The results confirm that the RG-B/Bris virus is virulent and causes death in the DBA/2 mouse model, a finding that will facilitate future vaccine studies.

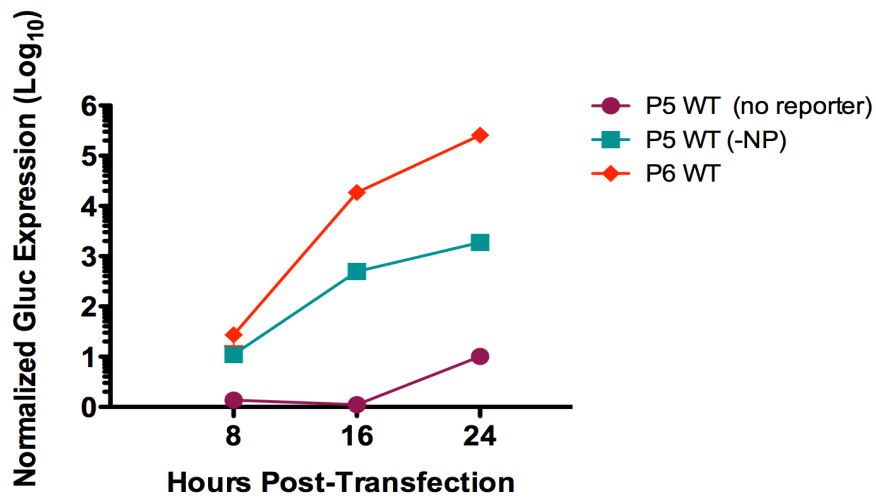


Figure 2.4. Polymerase activity of RG-B/Brisbane/60/2008 at 35°C. Plasmids were transfected. Supernatant was collected at 8, 16 and 24 hpt. Maroon: no reporter control. Teal: partial vRNP control. Red: 6-plasmid transfection including 4 vRNP plasmids, the GLuc reporter plasmid and a SEAP expression plasmid.

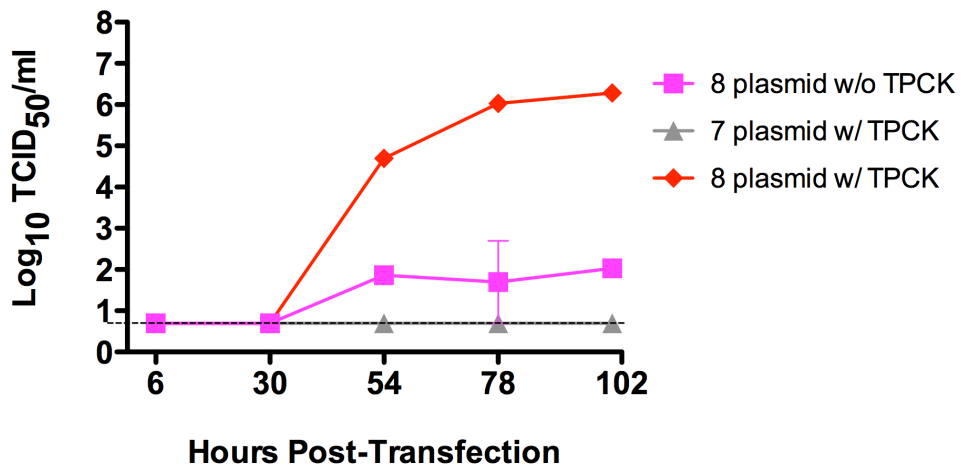


Figure 2.5. Virus rescue over time of RG-B/Brisbane/60/2008 at 35°C. Transfections were setup with and without TPCK-trypsin. Supernatant was collected at 6, 30, 54, 78 and 102 hpt. Pink: transfection of all 8 B/Brisbane/60/200 plasmids without TPCK. Gray: transfection of 7 plasmids, excluding the HA plasmid with TPCK. Red: transfection of all 8 plasmids with TPCK.

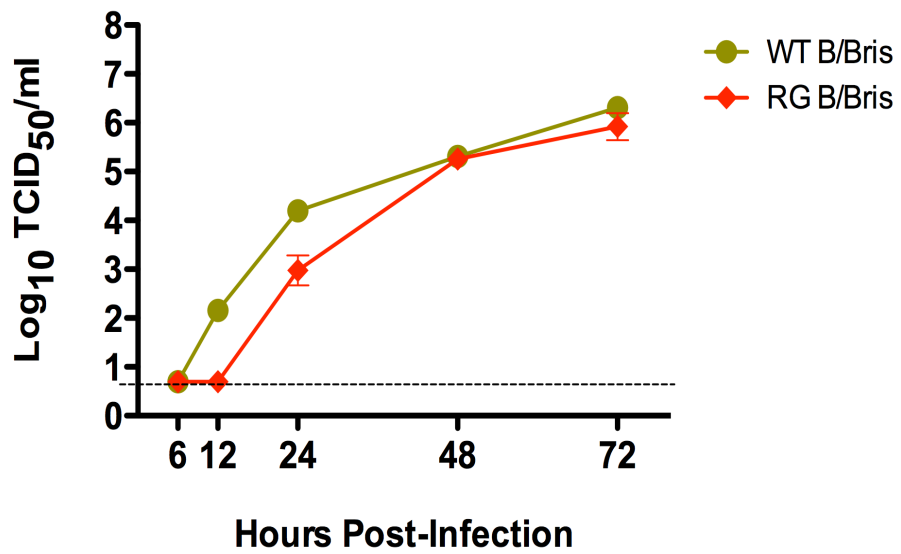


Figure 2.6. Growth kinetics of WT vs. RG-B/Brisbane/60/2008 viruses at 35°C. MDCK cells were infected with 0.01 MOI of each virus. Time points were collected at 6, 12, 24, 48 and 72hpi. Green: WT B/Brisbane/60/2008 virus. Red: RG-B/Brisbane/60/2008 virus.

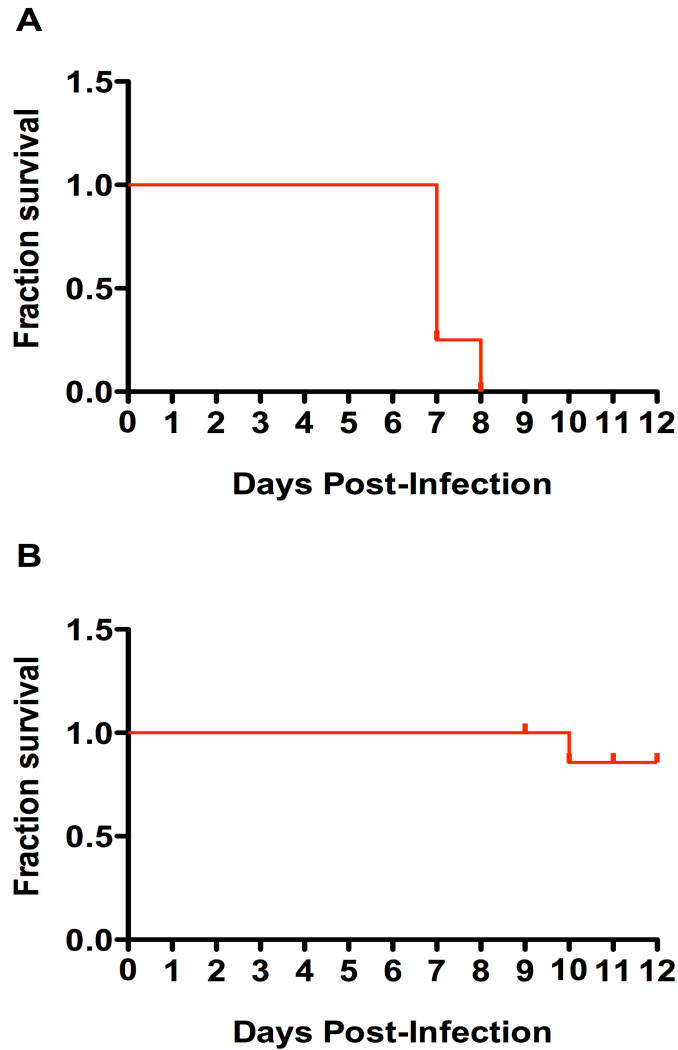


Figure 2.7. Survival of RG-B/Brisbane/60/2008 inoculated mice. Mice were inoculated with 50 μ L intranasally of RG-B/Brisbane/60/2008 at different doses. Results of the MLD₅₀ are shown. Red: RG-B/Brisbane/60/2008 inoculated mice. 10⁶ EID₅₀ inoculated mice (A). 10⁵ EID₅₀ inoculated mice (B).

2.4.5. Phylogenetic analysis of RG-B/Bris shows it is a member of the most recent B/Victoria-like virus clade

The B/Brisbane/60/2008 isolation date indicates that it is a contemporary virus, more contemporary than B/Lee/40 (B/Lee) and B/Yamanashi/166/98 (B/Yam), the most widely used reverse genetics IBV strains. The isolation date, however, does not indicate relative relatedness to current IBV strains. To determine the phylogenetic distance and relatedness between RG-B/Bris and other current IBV strains, phylogenetic analyses were performed. Specifically, phylogenetic analyses were performed on IBV HA and NA sequences available in the database using the maximum likelihood model.

The results confirm the distant relationship of B/Lee from all other isolates (Fig. 2.8A and B). Indeed, B/Lee/40 is the most appropriate root of both HA and NA phylogenetic trees, as it is related to all other viruses represented on the trees. Additionally, the highlighted regions of both the HA and NA phylogenetic trees comprise the sequences gathered from roughly the last decade (Fig. 2.8A and B). These highlighted regions clearly illustrate that RG-B/Bris shares a much closer relationship in the sequences of both HA and NA to the most contemporary strains of B/Victoria-like viruses than B/Yam does to the most contemporary B/Yamagata-like viruses. In fact, the trees show that sometime around the new millennium, the HA and NA sequences of both IBV lineages branched off into new clades of viruses. B/Yamanashi/166/98 does *not* belong to the newest clades of HA or NA B/Yamagata-like viruses, while RG-B/Bris belongs to the most recent clades of HA and NA of

B/Victoria-like viruses (Fig. 2.8A and B). As expected, RG-B/Bris HA and NA sequences are also very distantly related to B/Yamagata/16/88 and B/Victoria/2/87, the prototypical strains of the B/Yamagata-like and B/Victoria-like HA lineages.

BLASTs were performed with full-length RG-B/Bris genome sequences to determine the relatedness of its entire genome to other virus isolates. The top 4 most closely related sequences were recorded (Table 2.4). All gene segments are closely related to contemporary virus isolates with isolation dates of related viruses ranging from 2008-2011. Interestingly, several of the gene segments are closely related to viruses from countries other than Australia (the country of origin for B/Bris), emphasizing the role that human travel has on virus spread. This is true of the NS, NA, HA, PA and PB1 segments. Importantly, aside from offering further evidence that the RG-B/Bris surface genes are closely related to contemporary IBV strains, the results show that the backbone genes are closely related to modern IBV strains suggesting that RG-B/Bris could be used to generate cross-protection to modern IBV strains through the virus backbone (Table 2.4).

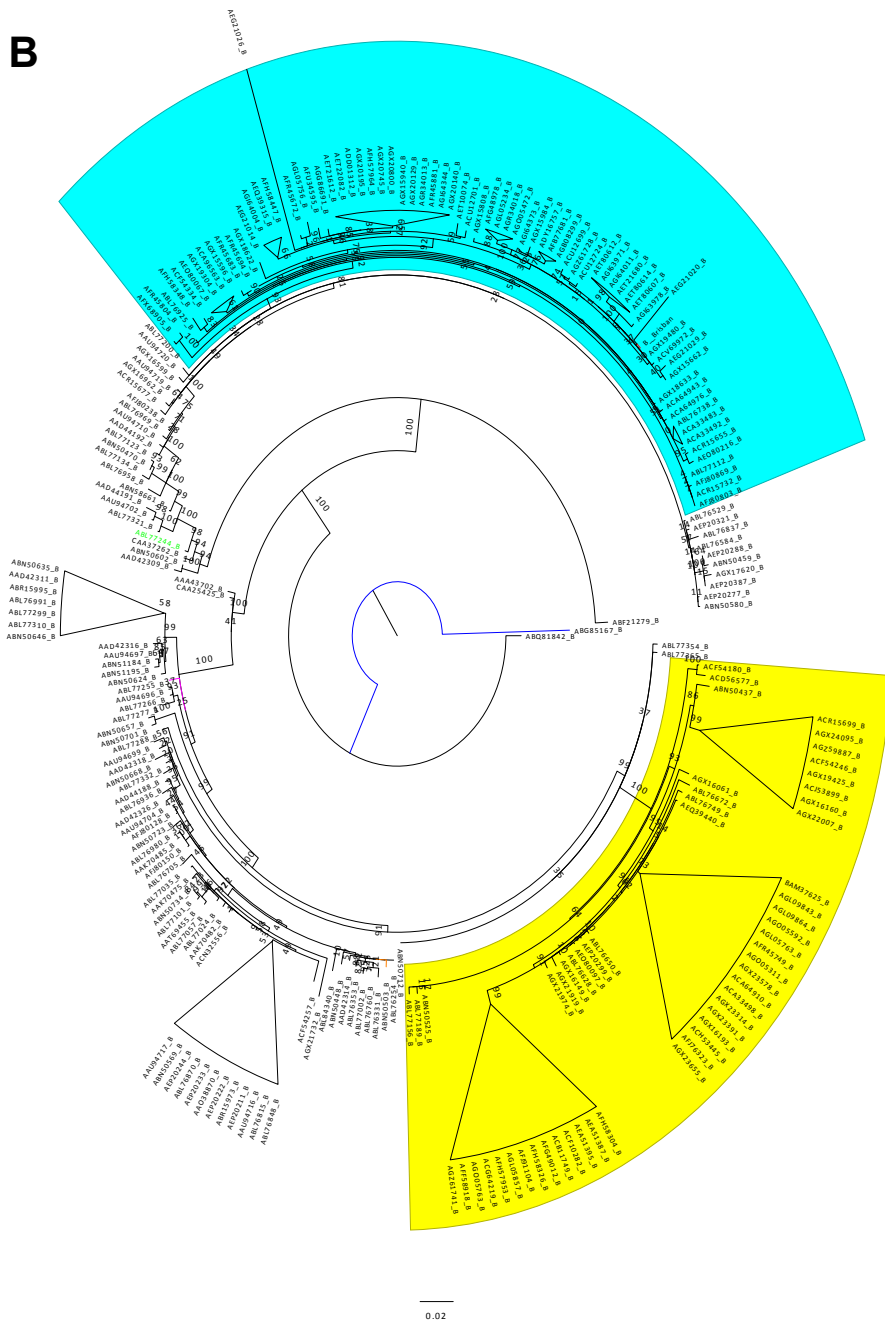


Figure 2.8. HA and NA phylogenetic trees. Each tree is rooted with B/Lee/40 shown in dark blue. HA (A) NA (B) Yellow highlighting: most contemporary clade of B/Yamagata-like viruses. Blue highlighting: most contemporary clade of B/Victoria-like viruses. Green: B/Victoria/2/87 Purple: B/Yamagata/16/88 Orange: B/Yamanashi/166/98. Tables of HA and NA accession numbers are located in the Appendices.

Gene Segment	Blast Results	% Identity	Accession#
BNS1/BNS2	B/Brisbane/60/2008	100	KC866606
	B/Wuhan/4/2009	99	CY110754
	B/Brisbane/60-6/2010	99	CY100421
	B/Bangladesh/5945/2009	99	CY100405
BM1/BM2	B/Brisbane/60/2008	100	KC866607
	B/Sydney/515/2011	99	CY153771
	B/Brisbane/30/2010	98	CY153771
	B/Brisbane/60/2008	98	CY115152
NA	B/Brisbane/60/2008	99	FJ766839
	B/Brisbane/60/2008	99	FJ766841
	B/Brisbane/33/2008	99	FJ766844
	B/Ontario/13040/2011	99	JN632582
NP	B/Brisbane/60/2008	99	KC866605
	B/Sydney/525/2009	99	CY153205
	B/Brisbane/122/2008	99	CY153189
	B/Victoria/2010/2008	99	CY153141
HA	B/Brisbane/60/2008	99	FJ766840
	B/Kenya/111/2011	99	JQ396206
	B/Kenya/109/2011	99	Q396205
	B/Kenya/107/2011	99	JQ396204
PA	B/Brisbane/60/2008	100	KC866602
	B/Thailand/CU-B2271/2010	99	JX512981
	B/Brisbane/102/2008	99	CY150020
	B/Brisbane/45/2008	98	CY149978
PB1	B/Brisbane/60/2008	99	KC866603
	B/Thailand/CU-B2271/2010	99	JX512979
	B/Thailand/CU-B2660/2010	99	JX513027
PB2	B/Brisbane/60/2008	98	CY115157
	B/Brisbane/60/2008	99	KC866604
	B/Brisbane/60/2008	99	CY115158
	B/Victoria/225/2008	99	CY153377
	B/Sydney/543/2008	99	CY153337

Note: excluded laboratory reassortant viruses

Table 2.4. Blast results for B/Brisbane/60/2008 plasmid sequences. Nucleotide blasts were performed with full-length plasmids sequences of each gene. The top 4 most closely related sequences are listed. Segments from top to bottom: 8, 7, 6, 5, 4, 3,1, and 2.

2.5. Discussion

This study showed the successful cloning and rescue of a contemporary reverse genetics virus, RG-B/Brisbane/60/2008 (RG-B/Bris), for the study of influenza B, particularly the future development of an alternative LAIV vaccine strategy. Cloning was done by a two-step RT-PCR system modeled after that of influenza A (298, 299). The strategy utilizes “universal” RT primers each of which share 9 nucleotides in common, accounting for the conservation of the IBV 5’ cDNA UTR region (51).

The results showed that RG-B/Bris rescues efficiently, grows to high titers and is virulent in mice. The virulence that RG-B/Bris displays in mice is particularly important for vaccine studies, as lethal challenge doses are required to stringently test vaccine candidates. Additionally, the results of the phylogenetic analyses performed demonstrated that RG-B/Bris is part of the most recent HA and NA clades of B/Victoria-like viruses.

In support of the findings which show that RG-B/Bris is more closely related to the most recent clade of B/Victoria-like viruses than currently available RG viruses and the currently licensed cold-adapted B/Ann Arbor/1/66 backbone in terms of isolation date and phylogenetic relatedness, the WHO has selected B/Brisbane/60/2008 as a vaccine candidate virus several times since its isolation (25, 37, 304). In fact, the B/Victoria-like virus selected for incorporated into the 2013-4 seasonal vaccine was B/Brisbane/60/2008-like. Given these facts and the findings presented above, RG-B/Bris is a viable candidate for a contemporary vaccine

backbone, as it still bears strong antigenic relatedness to currently circulating strains and, given the BLAST results, also a high percentage of sequence relatedness in the backbone to isolates as recent as 2011. A more contemporary vaccine backbone, as discussed in the introduction, could provide better immune stimulation in the elderly, as well as provide greater cross-protection due to the close relatedness of the virus backbone to circulating strains.

These findings clearly demonstrate a system (RG-B/Bris and the GLuc reporter plasmid) by which vaccine candidates will be able to designed, characterized and tested in the mouse model. Finally, given relatedness of RG-B/Bris to contemporary viruses, vaccine candidates designed on this backbone also have the potential to confer greater cross-protection in all vaccinated individuals and a better immune response in the elderly.

Chapter 3: Development of an Alternative Influenza B LAIV Vaccines: PB2/PB1 mutants

3.1. Abstract

Influenza B virus (IBV) causes significant respiratory disease in humans each year with symptoms ranging from fever, malaise, headaches, body aches and loss of appetite. Infections are not isolated to particular age groups, having been documented in all ages; however, in the U.S., the data suggests that severe infections are more common in infants, children and the elderly. The IBV-associated disease burden is great enough to warrant inclusion of IBV into both formulations of the seasonal influenza vaccine, killed virus (KV) and live-attenuated virus (LAIV). As the LAIV vaccine is known to induce a more robust immune response than KV vaccine, it is thought to confer better coverage. The LAIV vaccine platform carries mutations that map primarily to the vRNP complex and cause temperature sensitivity, cold-adaptation and attenuation. Among these mutations is a cap-binding mutation, PB2 N265S, which is part of the influenza A virus (IAV) component of the vaccine. IBV research has suggested that cap-binding mutations, specifically W359F and F406Y, may also be attenuating, as these mutations have been shown to decrease polymerase activity. Further, our lab has a patented strategy for an IAV vaccine platform in which the PB1 segment carries an HA tag at the C-terminus, and we have shown that this HA tag provides greater safety and stability to the other mutations present in the vaccine. This study describes an attempt to develop alternative LAIV IBV vaccines in

which the PB2 cap-binding mutations, W359F and F406Y, were separately combined with a C-terminal HA tag in PB1. The results show that this strategy is not suitable as a vaccine.

3.2. Introduction

Influenza B virus (IBV) belongs to the *Orthomyxoviridae* family of viruses, which is characterized by having a negative-sense, single-stranded, segmented RNA genome (3, 47, 48, 73). Its genome is comprised of 8 RNA segments, numbered 1-8, which encode a total of 11 proteins (3, 47, 48, 73). Each of these segments encodes at least 1 protein.

Segments 1-3 of IBV encode PB1, PB2 and PA, respectively (40). These proteins form a heterotrimeric polymerase complex, which binds to the vRNA for genomic replication and mRNA transcription (42). Host mRNA transcripts are bound through the 5' cap structures by PB2 and are then cleaved by PA, an endonuclease, to form a capped primer (61, 62, 135). This primer is then used by PB1 to initiate transcription of the viral mRNA (41, 58, 59). The polymerase complex also interacts with the nucleoprotein (NP), segment 5, to form the vRNP complex. NP coats each of the vRNA segments, stabilizing the RNA, and interacting with the polymerase complex that is bound to the 3' end of the vRNA in the virion (42, 57, 63, 64, 305). The remaining segments 4, 6, 7 and 8 encode the surface proteins HA and NA from segments 4 and 6, respectively, of which HA is the major antigenic protein, as well as ion channels, matrix protein, nuclear export protein and an antagonist of the innate immune response (40, 43-45, 47-49, 78, 81, 88, 103, 127, 166, 171, 196, 235, 237, 306-308).

IBV circulates in humans as a major respiratory pathogen with transmission peaking in the cold, dry conditions of the winter months; consequently, influenza B viruses are incorporated as components in the seasonal influenza vaccine each year (4, 28, 30, 31). The seasonal vaccine is manufactured in two formulations, killed virus (KV) and live-attenuated virus (LAIV); each confers protection to the same influenza virus strains and is typically grown in eggs (24, 170). Both have 2 influenza A virus (IAV) components and a least 1 IBV component which are updated as needed to ensure that they are good antigenic matches to the dominant circulating virus strains (24, 37). As the HA and, to a lesser extent, NA surface glycoproteins are generally sufficient to provide protection against infection, only these are updated while the internal genes for each vaccine component remain consistent (35, 81, 309).

Each year the IBV-component of the KV vaccine is produced with an egg-adapted B/Lee/40 backbone (35, 37). Once vaccine stocks are grown, the virus is formalin-treated, rendering the vaccine non-replicative (24). It is then administered via an intramuscular injection, generating an IgG antibody response post-vaccination (24, 170).

The IBV-component of the LAIV vaccine is replication impaired and contains cold-adapted internal genes from B/Ann Arbor/1/66 (B/Ann Arbor cold-adapted), which have high growth capacity in eggs and restricted growth in the lower respiratory tract (roughly 37°C) ensuring vaccine safety (208, 220, 257, 263, 310, 311). The B/Ann Arbor cold-adapted backbone is replication impaired due to mutations generated through the successive passaging of the virus at progressively lower temperatures (220). As a result of the intranasal route of administration and

virus replication in the upper respiratory tract, it generates IgG, IgA, T-cell and heightened innate immune responses to vaccination (170, 263, 269, 312).

The LAIV vaccine formulation, given the broadened immune response it generates in comparison to the KV virus formulation, is considered to be an improvement. Indeed, in a clinical trial comparing efficacy of the trivalent KV and LAIV vaccine formulations, the LAIV vaccine had 85% efficacy while the KV vaccine had only 71% efficacy (277). Despite the increased efficacy of the LAIV vaccine, the vaccine is only licensed for individuals ages 2-49 years old who have no pre-existing conditions, who are not immunocompromised and women who are not pregnant (24). The inherent risk involved in administering a live virus to groups with altered immune status has prevented licensing to these groups; however, in the elderly, studies have shown that the vaccine is safe but has limited efficacy likely due to immune history and immunosenescence (267).

An elderly person's immune system is not highly responsive to vaccination, particularly to the LAIV vaccine formulations, partly due to immunosenescence, which involves a shift towards Th2 T cell responses over Th1 and leads to a decrease in the cytolytic T cell (CD8+ T cell) response as well as a decrease in naïve T cells (among other changes) (290). As has been described, one of the benefits of the LAIV vaccine is that it generates a cell-mediated immune response, so it follows that a less efficient T cell response in the elderly would decrease LAIV vaccine effectiveness in this group. Efforts to boost the elderly immune response to vaccination have typically involved the use of adjuvants or increased doses of HA protein, but an alternative to these methods is a more contemporary vaccine backbone (24, 291).

Since an elderly person's immune system has likely been exposed to the vaccine backbones repeatedly over a long period of time and repeated vaccinations with the same vaccine has been shown to generate minimal boosting of the immune response, a contemporary backbone that has not been seen as frequently by the immune system would generate a more robust immune response (292, 312). Additionally, the T cell mediated immune response to vaccination is generated primarily against the backbone genes; therefore, using a more contemporary backbone would target the primary problem with vaccination of immunoscent individuals, T cell immunity (293, 296, 297, 313). A more contemporary vaccine backbone, though, is just one component of improving vaccine efficacy, and it must be combined with an attenuation strategy.

Our lab has developed an alternative vaccine strategy on an influenza A platform that includes the PB2 and PB1 mutations found in the IAV-component of the LAIV vaccine, the A/Ann Arbor cold-adapted (A/Ann Arbor/6/60 (H2N2) cold-adapted) backbone, and an HA tag at the C-terminus of PB1 such that the tag is expressed from the PB1 ORF (310, 311, 314). We have shown the addition of the HA tag yields a safer, more efficacious vaccine than a similarly constructed vaccine lacking the HA tag and that this vaccine can also serve as a Differentiating Infected from Vaccinated Animal (DIVA) vaccine (1, 314-316). Further, we have demonstrated this strategy to be effective in multiple animal models, such as swine, mouse, chicken and ferret against many IAV virus strains, providing good homologous and heterologous immunity (1, 314-316).

An important feature of the A/Ann Arbor cold-adapted backbone that we incorporated in our vaccine strategy is the PB2 cap-binding mutation, N265S, which has been shown to contribute to temperature sensitivity, growth restriction at 37°C, an important growth phenotype for vaccine safety (310, 311, 314). Accordingly, the mutation of other residues in the cap-binding region may prove effective targets for the development of future vaccines, both IAV and IBV. In fact, other cap-binding mutations have been described for IBV as potentially having attenuating effects. For instance, Wakai *et al.* showed that cap-binding mutations, W359F and F406Y, caused decreased polymerase activity at 37°C and 24 h post-transfection (hpt) in the context of B/Shanghai/361/2012 (61).

This study sought to design an IBV vaccine strategy that would complement our lab's IAV HA tag strategy described above. This was done in a contemporary backbone, RG-B/Brisbane/60/2008 (RG-B/Bris), with the aim of generating a vaccine that might better stimulate an immune response in the elderly. Here, the hypothesis that combining cap-binding mutations in PB2, W359F and F406Y, with the HA tag would result in a safe influenza B vaccine was tested. The W359F and F406Y mutations were cloned into separate plasmids to generate two PB2/PB1 vaccine candidates, each carrying a cap-binding mutation and the HA tag. The results show that this strategy, despite what appeared to be some attenuation *in vitro*, is untenable *in vivo*, disproving the hypothesis.

3.3. Materials and Methods

3.3.1. Cloning and confirmation of mutations

Cloning of the PB2 cap-binding mutant plasmids was done using the bidirectional pDP-PB2 plasmid described in chapters 2. In order to clone pDP-PB2_W359F and pDP-PB2_F406Y, site-directed mutagenesis was performed with the QuikChange II XL kit (Agilent, Santa Clara, CA). Site-directed mutagenesis primers were designed using the QuikChange Primer Design tool provided on the manufacturer's website (Agilent, Santa Clara, CA).

The HA tag was cloned into pDP-PB1 in-frame and at the C-terminus by inverse PCR, and cloning was modeled after the HA tag cloning procedure described in Song *et al.* (314). Primers were designed such that the original stop codon in PB1 was mutated to an alanine (A) and a new one was introduced following the HA tag. Additionally, the final amino acid, Isoleucine (I), in the WT PB1 sequence was repeated just before the mutated stop codon (A), thus the entire amino acid sequence introduced into PB1 was IAYPYDVDPDY, the final 8 amino acids being the HA tag (Fig. 3.1). The generated clone was named, pDP-PB1HA. PCR amplification was done using Pfu Ultra Polymerase AD (Agilent, Santa Clara, CA) following the cycling conditions described in the manufacturer's instructions. The HA tag and the PB2 cap-binding mutations were confirmed by Sanger Sequencing on a Genetic Analyzer 3500xL (Applied Biosystems, Foster City, CA) using the Big Dye

Terminator sequencing kit and protocol (Life Technologies, Carlsbad, CA). No undesired mutations were found.

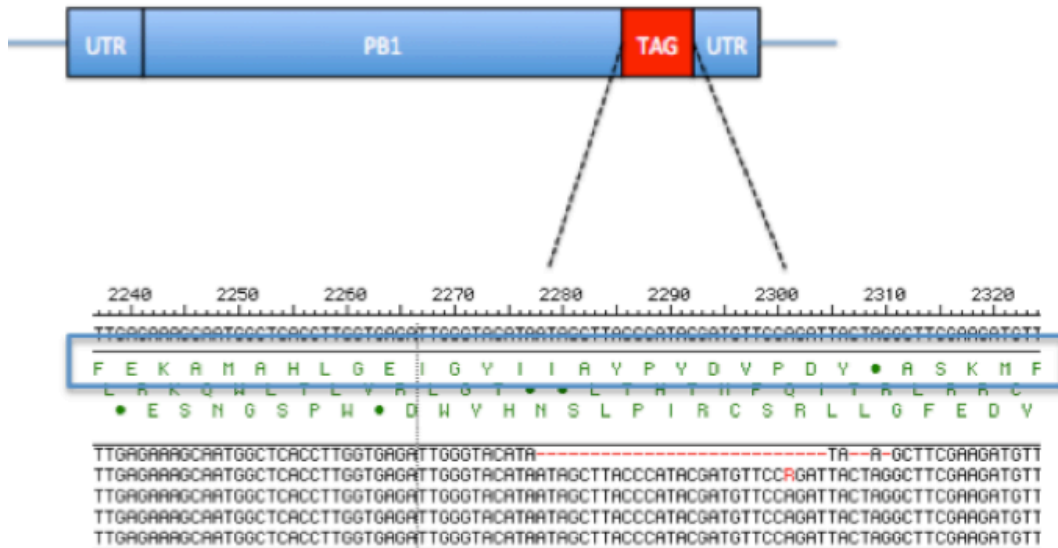


Figure 3.1. Diagram of the HA tag. The HA tag nucleotide and amino acid sequences are shown. Sequencing reads for pDP-PB1HA were compared to the pDP-PB1 B/Bris plasmid. The HA tag is: YPYDVPDY. Amino Acids occurring prior to the tag, I and A, were generated as a result of deliberately repeating the final amino acid is the PB1 sequence, I, and mutating the original stop codon, A. The correct ORF is identified in the blue box.

3.3.2. Virus rescue and stocks

Viruses were rescued using 8 plasmid reverse genetics as described in 2.3.4. Each PB2 mutant plasmid was paired with pDP-PB1HA, and two viruses were rescued, PB2_F406Y_PB1HA: B/Brisbane/60/2008 and PB2_W359F_PB1HA: B/Brisbane/60/2008. Briefly, 8 plasmids, 1µg each, corresponding to each virus were mixed. Then, FBS free [OPTI-MEM] I (Life Technologies, Carlsbad, CA) and Transit-LTI, 2µL/µg plasmid, (Mirus Bio, Madison, WI) were added up to 200µL. The reagents were mixed and incubated at room temperature for 45 min. Following incubation, 800µL FBS free [OPTI-MEM] I (Life Technologies, Carlsbad, CA) containing 10mL/L of Antibiotic/Antimycotic (Sigma-Aldrich, St. Louis, MO) was added gently to each tube and then overlaid on a 293T/MDCK cell (8×10^5 / 5×10^5) co-culture in a 6-well plate (Corning, Corning, NY). The cells were placed at 33°C overnight. The following day, the media was changed, FBS free [OPTI-MEM] I (Life Technologies, Carlsbad, CA) with TPCK (1µg/mL, Worthington Biochemicals, Lakewood, NJ) and 10mL/L of Antibiotic/Antimycotic (Sigma-Aldrich, St. Louis, MO).

After virus rescue, supernatant was serially diluted and used to inoculate T75 flasks (Greiner Bio-One, Monroe, NC) seeded with MDCK cells at 33°C. After 4-5 days at 33°C, tissue culture supernatant was harvested, and the flask with the highest HA titer at the highest dilution was used to inoculate eggs. Serial dilutions were made to inoculate 9-day old SPF hen eggs (B&E Eggs, York Springs, PA). Three eggs were inoculated per dilution, and 200µL of diluted supernatant was used to inoculate each egg. Eggs were then placed at 33°C and allowed to grow for 72 h at which time they

were placed at 4°C. The following day AF was harvested from the eggs, and HA assays were performed as described in 2.3.5. The AF with the highest HA titer at the highest dilution was harvested.

3.3.3. Virus titrations

Virus titrations were done by tissue culture infectious dose 50 (TCID₅₀) and egg infectious dose 50 (EID₅₀). Calculations for growth kinetics assays were done based on TCID₅₀. Both TCID₅₀ and EID₅₀ protocols were carried out in the same manner as described in 2.3.5. Titers were calculated by the Reed and Muench method (301).

3.3.4. Mini-genome assays

Polymerase assays and transfections were carried out as described in 2.3.7; however, three distinct polymerase complexes were evaluated. The first complex tested was generated by transfecting pDP-NP and pDP-PA with pDP-PB2_F406Y and pDP-PB1HA. Separately, pDP-NP and pDP-PA, pDP-PB2_W359F and pDP-PB1HA plasmids were also transfected. Both PB2/PB1 polymerase mutant complexes were compared to the wholly WT RG-B/Bris polymerase complex. The *Gaussia* Luciferase (Gluc) reporter plasmid (described in 2.3.3) and secreted alkaline phosphatase expression (SEAP) plasmids were transfected with each set of plasmids

described above. Two negative controls were included: a no reporter control (containing pCMV-SEAP and all 4 RNP plasmids) and a partial vRNP complex control (containing the reporter and 3 of 4 vRNP plasmids, no NP). Assays were performed at 33, 35, 37 and 39°C. Time points were collected at 6, 12, 24, 48 and 72 h post-transfection (hpt).

3.3.5. Growth kinetics

Growth kinetics assays were carried out as described in 2.3.8.

PB2_F406Y_PB1HA: B/Brisbane/60/2008, PB2_W359F_PB1HA:

B/Brisbane/60/2008 and WT RG-B/Bris viruses were evaluated. These assays were completed by infecting MDCK cells with 0.01 MOI of each virus at all temperatures previously described: 33, 35, 37 and 39°C. Time points were collected at 6, 12, 24, 48 and 72 h post-infection (hpi). After each sample was collected, the media was replenished, and the samples were placed at -80°C to await titration by TCID₅₀. TCID₅₀ titers were determined by the Reed and Muench method (301).

3.3.6. Western blot

MDCK cells were infected with 2 MOI (based on virus titers by TCID₅₀) of each virus: mock [FBS free [OPTI-MEM] I (Life Technologies, Carlsbad, CA)], WT RG-B/Bris, PB2_F406Y_PB1HA: B/Bris, PB2_W359F_PB1HA: B/Bris, and

1malH7:WF10att (positive control virus, described in Song *et al.*) (317). Prior to infection, 1 well of MDCK cells was trypsinized and counted to determine the cell number per well that would then be incorporated into the calculation of MOI. Each well was infected with 500 μ L of 2 MOI virus. After overlaying MDCK cells with virus, cells were placed at 37°C for 1 h. Next, 1mL of serum-free [OPTI-MEM] I (Life Technologies, Carlsbad, CA) with of 1 μ g/mL TPCK-trypsin (Worthington Biochemical, Lakewood, NJ) was added to each well. The infected cells were then placed at 33°C for 24 h. At 24 h post-infection, tissue culture supernatant was aspirated and 150 μ L of Laemilli Buffer (Bio-Rad, Berkley, CA) and β -ME were added (10:1 ratio, Laemilli Buffer to β -ME) to each well, while gently swirling the pipette tip. Then, each sample was immediately heated for 10 min at 95°C to complete protein denaturation. Finally, all samples were placed at -20°C.

In order to perform the western blot, a gradient SDS-PAGE gel (Bio-Rad, Berkley, CA) loaded with 5 μ L of protein ladder (Fermentas, Hanover, MD) and 25 μ L of each sample was placed in a Mini-Protean Tetra Cell electrophoresis chamber (Bio-Rad, Berkley, CA) and run for 1 h at 130V. The gel was then removed from the electrophoresis chamber and placed on nitrocellulose paper (Bio-Rad, Berkley, CA) and blotting paper in transfer buffer. Then, the nitrocellulose paper, blotting paper and gel were placed into a semi-dry transfer chamber at 22V for 1 h (Bio-Rad, Berkley, CA). After transfer, the nitrocellulose paper was blocked for 2 h at room temperature on a rocker with 5mL of molecular grade non-fat dry milk (NFDM) (Bio-Rad, Berkley, CA) [(1g) dissolved in 5mL of TTBS (a mixture of Tris-buffered saline and Tween 20)]. After blocking, the nitrocellulose paper was washed 3X with TTBS.

Each wash was 5 min in length at room temperature on a rocker. Finally, a 1:2000 dilution of anti-HA-tag primary antibody (Cell Signaling Technologies, Beverly, MA) was prepared in 5mL of TTBS with 1g of dissolved NFDM and allowed to incubate on a rocker at 4°C overnight.

The following day, the nitrocellulose paper was again washed with TTBS as described above. Then, goat anti-mouse secondary antibody (Southern Biotech, Birmingham, AL) was diluted 1:50000 in 5mL NFDM and TTBS and incubated at room temperature on a rocker for 1 h and 30 min. The nitrocellulose paper was again washed 3x with TTBS. Finally, Clarity Western ECL Substrate (Bio-Rad, Berkley, CA) chemiluminescent substrate was applied to the nitrocellulose paper according to the supplied protocol, and the film was developed after a 10-min exposure to the nitrocellulose paper in an exposure cassette.

3.3.7. Mouse study

A mouse study to test vaccine candidate safety was carried out by inoculating 5-6 week old female DBA/2 mice intranasally with 50µL of 10^6 EID₅₀ of virus. Virus groups included: PB2_F406Y_PB1HA: B/Bris, PB2_W359F_PB1HA: B/Bris, and PBS. Four mice were inoculated per group. Weight loss and disease signs were monitored (for 9 days and 12 days post-inoculation, respectively). The mouse study was approved under University of Maryland approved protocol, R-12-100. Any mouse that lost 20% of its starting weight or more or scored a 3 or more in signs of disease was humanely euthanized as described in 2.3.9.

3.3.8. Experimental replication and statistical analyses

All data analyses were performed using GraphPad Prism Software Version 6.00 (GraphPad Software Inc., San Diego, CA), and all *in vitro* assays were performed a minimum of two times in triplicate. For multiple comparisons, two-way ANOVA was performed followed by a post-hoc Bonferroni test; $p < 0.05$ was considered significant.

3.4. Results

3.4.1. Similar GLuc expression of PB2/PB1 mutants compared to WT

To begin the characterization of the PB2/PB1 mutant viruses, polymerase assays were performed. The polymerase genes of these complexes and the WT complex were transfected with the GLuc reporter (described in Chapter 2) in 293T cells, and experiments were setup at 33, 35, 37 and 39°C. Both PB2/PB1 mutant polymerase complexes were found to express GLuc at levels similar to WT at 33 and 35°C (Fig. 3.2A and B). At 37°C, however, expression of GLuc from both PB2/PB1 mutant polymerase complexes was found to be impaired compared to the WT complex, although the difference, at least for the PB2_F406Y_PB1HA: B/Bris complex, is only roughly 10 fold at late time points (Fig. 3.2C). After normalization, GLuc expression of all polymerase complexes tested was nearly undetectable at 39°C, as expected, given that influenza B is not known to replicate at such high temperatures (data not shown)(318). In all, these assays do not suggest any difference between the polymerase activity of PB2_W359F_PB1HA: B/Bris and PB2_F406Y_PB1HA: B/Bris, but the data does suggest that the PB2/PB1 mutant complexes may display some temperature sensitivity at 37°C.

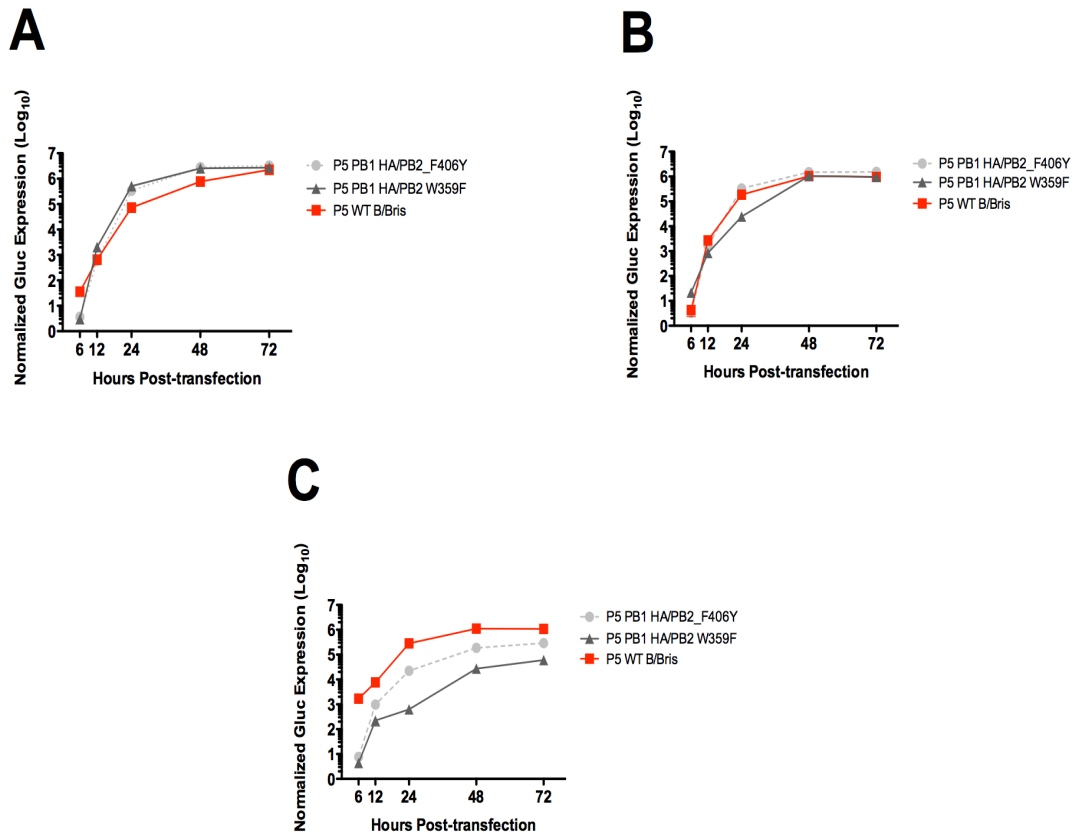


Figure 3.2. Polymerase activity of PB2/PB1 mutant complexes. GLuc expression normalized with SEAP is shown for the following polymerase complexes: PB2_F406Y_PB1HA: B/Bris, PB2_W359F_PB1HA: B/Bris and WT. Assays were completed at 33, 35 and 37°C (A, B, and C, respectively). Red: WT. Dashed gray: PB2_F406Y_PB1HA: B/Bris. Dark gray: PB2_W359F_PB1HA: B/Bris. Time points were collected at 6, 12, 24, 48 and 72hpt. GLuc activity was measured using a Bioluminescence Assay Kit (New England Biolabs, Ipswich, MA).

3.4.2. Growth curves of PB2/PB1 mutant viruses are similar to WT

Growth kinetics of the PB2/PB1 mutant viruses was compared to that of the WT RG-B/Bris virus. MDCK cells were infected at 0.01 MOI, and assays were performed at 33, 35, 37 and 39°C. As with the polymerase assays, time points were collected at 6, 12, 24, 48 and 72 hpi. Finally, samples were titrated by TCID₅₀ to determine the growth curves of each virus.

The results indicate that the PB2/PB1 mutant viruses replicate to titers similar to WT at 33 and 35°C, although at 35°C, the PB2_F406Y_PB1HA: B/Bris virus grows to significantly lower titers than the WT (Fig. 3.3A and B). In contrast, at 37°C, the PB2/PB1 mutant viruses grow to significantly lower levels than the WT at 24 and 48 hpi, but by 72 hpi, there is no difference (Fig. 3.3C). At 39°C, all viruses were similarly undetectable (data not shown). Overall, the results suggest that the PB2/PB1 mutant viruses may be attenuated in comparison to the WT virus at 37°C, at least at early time points (Fig. 3.3B)

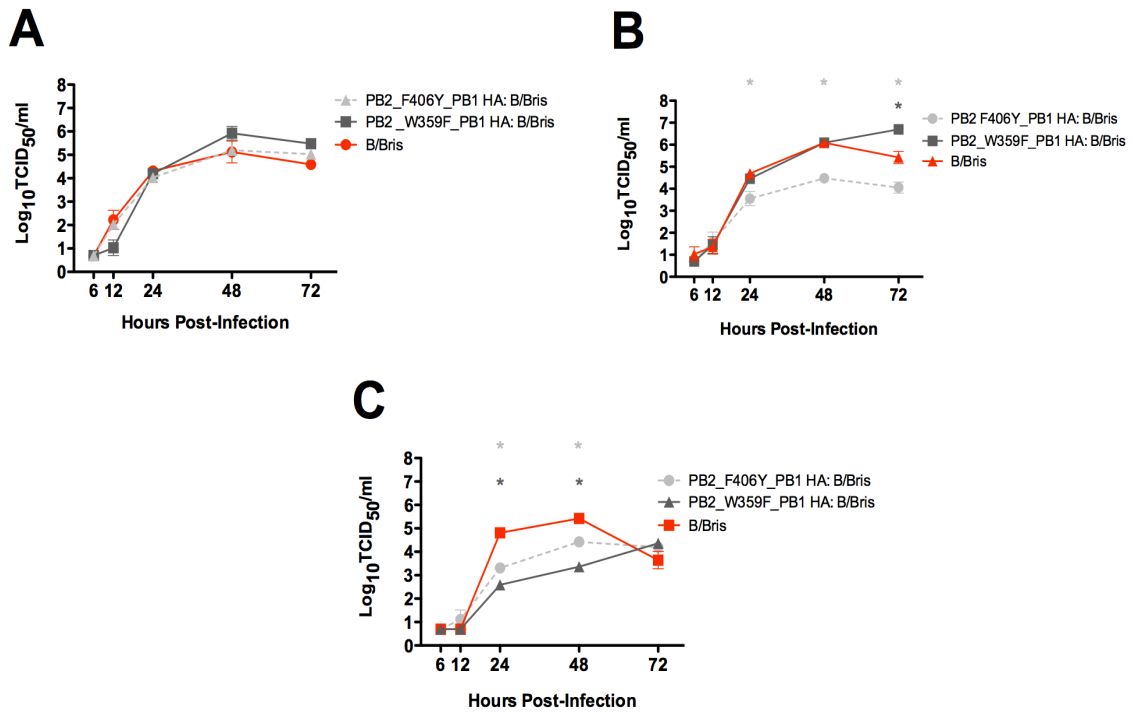


Figure 3.3. Growth kinetics of PB2/PB1 mutant viruses. Growth curves for the PB2_F406Y_PB1HA: B/Bris and PB2_W359F_PB1HA: B/Bris viruses are shown at 33, 35 and 37°C (A, B, and C, respectively). Red: WT. Dashed gray: PB2_F406Y_PB1HA: B/Bris. Dark gray: PB2_W359F_PB1HA: B/Bris. 0.01MOI of each virus was used for infection. Time points were collected at 6, 12, 24, 48 and 72hpi. Titrations were done by TCID₅₀. Asterisk indicates p<0.05, each PB2/PB1 mutant was compared to WT separately.



Figure 3.4. Expression of HA tag from PB2/PB1 mutant viruses. Using a mouse anti-HA-tag primary antibody, a western blot was performed to determine HA tag protein expression by both PB2_W359F_PB1HA: B/Bris, PB2_F406_PB1HA: B/Bris and 1malH7: WF10att. MDCK cells were infected with 2MOI of each virus at 33°C. After 24 h, supernatant was aspirated, and samples were prepared for western blot. Exposure time: 10 min. Lane 1: mock infected. Lane 2: WT RG B/Bris infected. Lane 3: PB2_W359F_PB1HA: B/Bris infected. Lane 4: PB2_F406Y_PB1HA: B/Bris infected. Lane 5: positive control, 1malH7:WF10att infected.

3.4.3. PB2/PB1 mutant viruses express the HA tag from the PB1 ORF

To complete the *in vitro* characterization of the PB2/PB1 mutant viruses, HA tag expression from the PB1 ORF was evaluated. A western blot was performed by first infecting MDCK cells with 2 MOI of the mutant viruses, the WT and a positive IAV control and then collecting a time point at 24 h post-infection (hpi). Following sample collection, a western blot was performed with an anti-HA tag primary antibody.

The western blot results showed clear expression of the HA tag from both of the PB2/PB1 mutant viruses as well as the IAV positive control, consistent with the design of the pDP-PB1HA plasmid used to generate the mutant viruses. Both PB2/PB1 mutant virus PB1 proteins ran lower than that of the IAV control, as IBV PB1 encodes a shorter protein than influenza A (Fig. 3.4). As expected, no HA tag was detected in the mock or WT RG-B/Bris infected samples, although there was some non-specific binding likely due to the long exposure time.

3.4.4. PB2/PB1 mutant viruses are lethal in mice at 10^6 EID₅₀

Safety of the PB2/PB1 mutant viruses was evaluated in mice by inoculating female DBA/2 mice with 50µL intranasally of PB2_W359F_PB1HA: B/Bris, PB2_F406Y_PB1HA: B/Bris and PBS at 10^6 EID₅₀, a standard vaccination dose. The results showed that the PB2/PB1 mutant viruses were lethal in mice at this dose (Fig. 3.5). Although 2 mice in the PB2_W359F_PB1HA: B/Bris group survived, these

mice did not lose weight (data note shown); therefore, it is unclear whether or not these mice ever developed an infection.

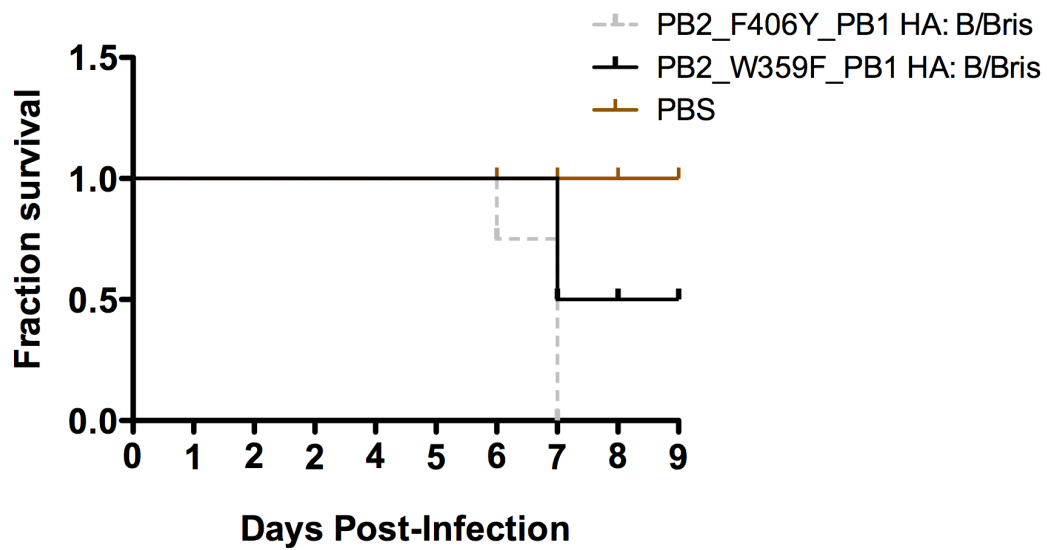


Figure 3.5. Survival of PB2/PB1 mutant inoculated mice at 10^6 EID₅₀. Mice were inoculated with 50 μ L of 10^6 EID₅₀/mL of virus or PBS, depending on the group. Dashed gray: PB2_F406Y_PB1HA: B/Bris. Dark gray: PB2_W359F_PB1HA: B/Bris. Brown: PBS.

3.5. Discussion

This study described the development of two experimental LAIV vaccine candidates designed on an IBV platform in which both viruses generated contained a PB2 cap-binding mutation, either F406Y or W359F, and an HA epitope tag at the C-terminus of PB1. These modifications showed some indications of attenuation *in vitro* at 37°C as the GLuc expression exhibited by the polymerase complexes and the viral titers at early time points post-infection were lower than WT. Given that temperature sensitivity at 37°C is a key growth phenotype of the licensed LAIV influenza vaccine which contributes to restriction of LAIV vaccine replication to the upper respiratory tract and helps to ensure vaccine safety, the PB2_W359F_PB1HA: B/Bris and PB2_F406Y_PB1HA: B/Bris viruses were tested for safety in mice at a standard vaccine dose of 10⁶ EID₅₀; however, contrary to the attenuation that the *in vitro* data seemed to suggest, both of these PB2/PB1 mutant viruses were lethal *in vivo* (220, 260, 263).

The mortality caused by the PB2/PB1 mutant viruses was surprising for several reasons aside from simply the *in vitro* data. First, previous work with our HA tag in the context of IAV indicated that the tag enhances safety, efficacy and stability (314). Second, the PB2 F406Y and W359F cap-binding mutations had been previously shown to decrease polymerase activity compared to WT in the context of B/Shanghai/361/2002 (61). Third, a PB2 cap-binding mutation is included in the IAV-component of the LAIV vaccine, suggesting that the cap-binding region is a viable target for attenuation (220, 310). In all, this information suggests that the HA

tag and the cap-binding mutations would cause attenuation, but instead, the results show that the PB2/PB1 mutant viruses are, at best, as virulent as the WT virus (based on the MLD₅₀ of the WT virus established in Chapter 2).

While cap-binding mutations, as has been described above, have been known to cause attenuation, the idea of cap-binding mutants and other mutations in PB2 being virulence factors in specific hosts is not unprecedented (310, 319). For instance, a mutation at 357 (H to N) in PB2, which is analogous to position 359 of IBV, in the context of IAV pH1N1 is an established virulence factor in mice (320). Aside from the cap-binding mutation, other PB2 residues associated with mammalian host adaptation and virulence in IAV are 81, 199, 355, 627, 647, 667, 671 and 701 (321-325). Indeed, the role of PB2 in IAV adaptation to mammalian hosts is well established, and considering the conservation of PB2 structure, sequence and function between IAV and IBV, it is conceivable that some PB2 IBV residues have implications for host adaptation as well as enhanced virulence (61, 326).

The lethality of these PB2/PB1 mutant viruses necessitated a re-evaluation of potential vaccine strategies and a closer analysis of our successful IAV vaccine strategy in order to develop an effective IBV vaccine in mice. Additionally, the data presented here and other findings discussed above suggest that the PB2 F406Y and W359F mutations may be virulence factors in the context of RG-B/Bris. Thus, the next chapter sought to characterize these cap-binding mutations.

Chapter 4: PB2 Cap-binding Mutants as Influenza B Virulence Factors in Mice

4.1. Abstract

Influenza A virus (IAV) and Influenza B virus (IBV) have a similar host mRNA cap-snatching mechanism which is a key and unique feature of the viral life cycle utilized during viral transcription, so it follows that any perturbation of this complex activity would likely result in attenuation of the virus. Indeed, a cap-binding mutation in IAV is included in the licensed seasonal live-attenuated virus (LAIV) vaccine. Additionally, IBV cap-binding mutations, PB2 F406Y and W359F, have been shown to decrease polymerase activity in B/Shanghai/361/2002. This study sought to characterize these cap-binding mutations in the context of B/Brisbane/60/2008 as potential virulence factors based on findings described in Chapter 3. The data presented here show that in the context of B/Brisbane/60/2008, cap-binding mutations, PB2 W359F and F406Y, were more virulent, as evidenced by increased weight loss and mortality in DBA/2 mice compared to wild-type (WT) RG-B/Brisbane/60/2008 (RG-B/Bris). The results suggest that this increased virulence may at least be partially due to improved growth and polymerase activity of the cap-binding mutants at 37°C early in infection. As IBV is not readily infectious in mice and the IBV cap-binding region is conserved, these mutations could serve as tools for future studies of IBV pathogenesis and vaccine efficacy in mice and possibly other animal models.

4.2. Introduction

Influenza B virus (IBV), a significant human respiratory virus, is part of the *Orthomyxoviridae* virus family which also includes influenza A virus (IAV) and influenza C virus (3, 28, 76, 180, 286, 287). The IBV genome consists of 8 segments of single-stranded, negative-sense RNA, where each segment encodes at least 1 protein (3).

Of the 8 IBV RNA segments, 4 are associated with the viral ribonucleoprotein complex (vRNP), which is comprised of the RNA dependent RNA polymerase complex proteins (RdRp) and the nucleoprotein, NP, bound to vRNA (57). Segments 1-3 encode the PB1, PB2 and PA polymerase proteins, respectively, forming the RdRp (42). NP, encoded from segment 5, stabilizes each vRNA segment and interacts with the viral RdRp, which is bound to each segment (42, 65, 327). The interactions of the RdRp and NP proteins are required for the panhandle structure of the vRNA to be maintained, a necessary structure for successful transcription and replication (42, 57, 327). Upon entry of the vRNP into the host cell nucleus, the RdRp functions synergistically to snatch the 5' pre-mRNA cap of host mRNA in order to initiate viral mRNA transcription (61, 328). First, the PB2 protein binds the host pre-mRNA cap (60, 61). Then, PA, which encodes a 5' to 3' endonuclease, cleaves the cap (62, 135, 329, 330). Finally, PB1 initiates viral mRNA transcription using the 5' pre-mRNA cap as a primer (41, 58).

The remaining gene segments, segments 4, 6, 7 and 8, code for hemagglutinin (HA) and neuraminidase (NA) surface proteins, M and NS proteins, respectively. HA

serves as the major antigenic protein and is responsible for binding the host cell receptor, alpha 2,6 sialic acid (203, 306, 309, 331). Although NA is a surface protein and does have antigenic properties, its primary function is as a sialidase that cleaves the sialic acid moiety off the host cell, releasing the mature virion during budding (78, 81, 82). Segment 6 also encodes NB protein, an ion channel protein (44, 45). Segment 7 encodes BM1, which serves as a matrix protein, while BM2, translated by a stop-start mechanism following the BM1 open-reading frame (ORF), functions as an ion channel protein. The IBV ion channels are involved in acidification of the virion after entry; however, BM2 is also involved in viral assembly and packaging (103, 332). Finally, segment 8 encodes BNS1 and BNS2 by a post-transcriptional splicing event. BNS1, non-structural protein 1, is involved in inhibiting the host innate immune response, while BNS2 serves as a nuclear export protein (49, 50, 308).

Cap snatching is an essential feature of the influenza virus life cycle, as described above, so it is not surprising that IAV and IBV cap-binding mutants have been shown to cause attenuation. For example, the IAV-component of the live-attenuated licensed seasonal vaccine contains a cap-binding mutation at position 265, asparagine to serine, in PB2 contributing to virus temperature sensitivity and attenuation (220, 221, 223, 310). In addition, many cap-binding mutations introduced into B/Shanghai/361/2002 have been shown to decrease polymerase activity compared to the wild-type (WT) polymerase complex in 293T cells (61). Wakai *et al.* identified various mutations at positions 359 and 406 of the PB2 B/Shanghai/361/2002 polymerase gene including W359H, W359F and F406Y that affected polymerase expression at 24 hpt and 37°C. The W359H and W359F

mutations showed severe decreases in activity at 24 hpt when compared to WT, whereas the F406Y mutant complex showed a moderate decrease in activity compared to WT (61). Contrary to these findings, other reports suggest that some cap-binding mutants may be virulence factors *in vivo* depending on the virus strain into which the mutations are introduced. For instance, H357N in PB2 of influenza A pH1N1 has been shown to increase virulence and mortality in BALB/c mice as compared to the virus carrying the WT PB2 (320).

IBV strains are known to infect many genetic strains of mice, both with and without adaptation; nonetheless, productive infection of mice with IBV has been difficult due to reduced susceptibility (243). Susceptibility of mice to influenza is a complex issue. One factor is the role of Mx1 gene, an IFN regulated gene, which has been shown to dramatically decrease susceptibility to influenza; however, most inbred mice possess a defective Mx1 gene (243, 333, 334). Another factor is the distribution of alpha 2,6 sialic acid receptors recognized by IBV, as alpha 2,3 sialic acid receptors are more abundant in mouse airways than alpha 2,6 (243, 331).

Despite factors hindering mouse susceptibility to IBV, some IBV strains are known to infect mice without prior adaptation, and B/Lee/40 and B/Victoria/16/88 are examples (242). These IBV strains have been shown to naturally infect DBA/2 and C57BL/6 mice, but for other IBV strains, adaptation has been shown to effectively increase susceptibility of mice (242). For example, with the introduction of a mutation in BM1, N221S, B/Yamagata/166/98 has been shown to infect BALB/c mice (234). Susceptibility of mice to IBV appears to be highly variable depending on the virus strain as well as the genetic background of the mouse (242).

Given the findings described in Wakai *et al.* showing PB2 cap-binding mutants with decreased polymerase activity in the context of B/Shanghai/361/2002 and the findings described in Chapter 3, this study sought to characterize cap-binding mutants of WT RG-B/Brisbane/60/2008 (WT RG-B/Bris), PB2 F406Y and PB2 W359F, speculating that these mutations were the reason the PB2/PB1 viruses described Chapter 3 were lethal (61). It was hypothesized that the F406Y and W359F PB2 mutations would result in increased virulence *in vivo* but not *in vitro*, as both showed decreased polymerase activity at 24 hpt and 37°C in the context of B/Shanghai/361/2002 and the data presented in Chapter 3 show insignificant differences between viruses carrying these mutations and the WT (61). Here, the results show that the introduction of these cap-binding mutants into the PB2 of RG-B/Bris increased both virulence and mortality in DBA/2 mice as compared to WT. The *in vitro* and *in vivo* data suggests this increased virulence may be, at least in part, due to enhanced replication of the PB2 F406Y and PB2 W359F mutant viruses at 37°C compared to WT early during infection. Given these findings, these cap-binding mutations may be useful as tools to study pathogenesis and to test vaccine efficacy in mice.

4.3. Materials and Methods

4.3.1. Cloning of cap-binding mutants by site-directed mutagenesis, virus rescue, and stocks

All 8 plasmids of RG-B/Brisbane/60/2008 (RG-B/Bris) described in Chapter 2 were used in these studies; however, only the PB2 plasmid was modified. The cap-binding mutants, PB2 F406Y and PB2 W359F, were cloned through site-directed mutagenesis using the QuickChange II XL kit (Agilent, Santa Clara, CA) and the pDP-PB2 B/Bris plasmid as a template. Primers were designed using the QuickChange® Primer Design Program (Agilent, Santa Clara, CA). The cloning procedure was performed as per the manufacturer's recommendations, and two constructs were generated, pDP-PB2_F406Y and pDP-PB2_W359F. Each plasmid was subject to Sanger sequencing using methods described in Chapter 2 to the confirm sequences.

Two viruses, PB2_F406Y: B/Bris and PB2_W359F: B/Bris, were rescued by 8-plasmid reverse genetics in which 7 RG-B/Bris plasmids and 1 mutant PB2 plasmid containing a mutation at either position 359 or 406 were transfected. Transfections were performed as described in 2.3.4. Briefly, 1 µg of each plasmid was mixed with Transit-LTI, 2 µL/µg plasmid (Mirus, Madison, WI), and [OPTI-MEM] (Life Technologies, Carlsbad, CA) up to 200 µL. The solution was vortexed and incubated at room temperature for 45 min. After a 45-min incubation, 800 µL of [OPTI-MEM] was added gently. A 293T/MDCK cell ($8 \times 10^5 / 5 \times 10^5$ cells per well) co-culture was

then overlaid with the transfection solution, and cells were placed at 33°C overnight. The following day, the media was changed, 2mL of [OPTI-MEM] and TPCK-trypsin, 1µg/mL (Worthington, Lakewood, NJ). Stocks were grown in MDCK cells in T75 flasks (Greiner Bio-One, Monroe, NC) as described in 3.3.2. Whole genome sequencing was performed to ensure that virus stocks contained only the desired mutations. Sanger sequencing was carried out using the Big Dye Terminator kit (BigDye® Terminator v3.1 Cycle Sequencing Kit, Life Technologies) and run on 3500xL Genetic Analyzer (Applied Biosystems, Foster City, CA).

4.3.2. Titrations

To titrate stock viruses, cell culture supernatants, and tissue homogenates, TCID₅₀ titrations were performed using MDCK cells cultured in 96-well plates (Greiner Bio-One, Monroe, NC). Titrations were performed as described in 2.3.5. Briefly, MDCK cells (25,000/well) were seeded in 100µL of [OPTI-MEM] (Life Technologies, Carlsbad, CA) and incubated overnight at 37°C. Subsequently, 10-fold serial dilutions of virus samples were prepared in [OPTI-MEM] supplemented with 1µg/mL TPCK-trypsin (Worthington, Lakewood, NJ). After removing the media from the MDCK cells, 200µL of each dilution was overlaid on multiple wells per dilution. The virus-overlaid cells were then incubated for 3 days at 33°C. After incubation, HA assays were performed as described in 2.3.4. Briefly, 50µL of virus supernatant was removed from each well and added to a 96 well v-bottom plate

(Corning, Corning, NY). Next, 50 μ L of 0.5% chicken red blood cells (cRBC) in PBS was added to each well, and the plates were incubated for 45 min at room temperature. Finally, hemagglutination was recorded, and the 50% infectious dose titer was determined by the Reed and Muench method (300).

4.3.3. Mini-genome assays

Polymerase assays were performed using a mini-genome assay as described in 2.3.7 with some modifications. Briefly, assays were performed in 12-well plates (Corning, Corning, NY) with 0.5 μ g of the GLuc reporter plasmid, each RG-B/Bris vRNP plasmid and a secreted alkaline phosphatase (SEAP) expression plasmid. All 6 plasmids were transfected in 293T cells (1x10⁶ cells/well) with 2 μ L/ μ g plasmid of Transit-LTI (Mirus, Madison, WI). Negative controls were also included: a no reporter control (polymerase genes only) and a no PB1 control (contained polymerase genes and reporter but lacked PB1). Following transfection, supernatant was collected at 6, 12, 24, 48 and 72 h post-transfection (hpt), and an additional sample was collected at 24 hpt for SEAP analysis. This procedure was carried out at 33, 35, 37 and 39°C. SEAP assays were performed using the Tropix Phospha-Light SEAP Reporter Gene Assay System kit (Life Technologies, Carlsbad, CA) and protocol. GLuc expression was quantified using a BioLux® *Gaussia* Luciferase Assay Kit (New England Biolabs, Ipswich, MA). The luminescence for GLuc and SEAP assays was measured over a 1 sec integration time on a Victor X4 Luminescence Plate Reader (Perkin Elmer, Waltham, MA).

4.3.4. Growth kinetics

Growth kinetics were performed in MDCK cells in 6-well plates using an MOI of 0.01 based on virus titers by TCID₅₀ as described in 2.3.8 with some modifications. Time points were collected at 6, 12, 24, 48 and 72 h post-infection (hpi), and for each time point, 120µL of supernatant was collected on ice and frozen at -80°C until titration. After sample collection, the media was replenished by adding [OPTI-MEM] (Life Technologies, Carlsbad, CA) containing 1µg/mL of TPCK-trypsin (Worthington, Lakewood, NJ)]. The same procedure was followed at each temperature, 33°C, 35°C, 37°C and 39°C. Then, samples were titrated by TCID₅₀, and the viral titer was determined by the Reed and Muench method (301).

4.3.5. Mouse studies

Six-week old female DBA/2 mice were purchased from Charles River, Frederick, MD. Animal experiments were performed under BSL-2 conditions under the approval of the University of Maryland Institutional Animal Care and Use Committee protocols R-12-100 and R-13-65. On day 0, mice were weighed and then inoculated with 50µL of 10⁵ EID₅₀/mL of virus intranasally. There were four groups of mice: PB2_F406Y: B/Bris, PB2_W359F: B/Bris, WT RG-B/Bris and PBS. In each group, there were ten mice, except for the PBS in which there were only 4 mice, inoculated to be monitored for weight loss and disease signs. For each virus group, 9

additional mice were inoculated for tissue collection, but for the PBS group, only 3 additional mice were inoculated for tissue collection. Mice were monitored throughout the experiment for weight loss and clinical signs until 12 days post-infection (dpi) and mice exhibiting 20% weight loss or greater and/or a scoring of 3 or more for clinical signs (described in 2.3.9) were humanely euthanized. On days 3, 5 and 7 post-inoculation, 3 mice per virus group and 1 PBS mouse were humanely euthanized and necropsied.

4.3.6. Tissues

The right lung lobe and nasal turbinates were harvested for titration while the left lung lobe was collected in 10% formalin for histopathology. Tissues were homogenized using a QIAgen tissue lyser at 50Hz for 4 min and then clarified by centrifugation at 4°C for 10 min at 1,000xg (QIAgen, Valencia, CA).

Formalin fixed lung samples were embedded, sectioned and subjected to hematoxylin and eosin (H&E) staining. Tissue from days 3, 5 and 7 days post-infection (dpi) were analyzed by a board certified veterinary pathologist. Scoring of the bronchi/bronchioles, pulmonary vasculature, alveoli and overall/extent lung was performed. Tissue damage was scored on a scale of 0-4, 0 being normal and 4 being severe. A total score/extent lung score of 4 indicates the involvement of the entire lung lobe.

Following the *in vivo* mouse studies and titrations of lung tissue, RNA was

extracted from lung homogenate supernatant of 1 mouse per virus group on peak titer days. RNA extractions were performed using the QIAgen RNeasy mini-kit, following the provided protocol (QIAgen, Valencia, CA), and cDNA was prepared by the 2-step RT-PCR protocol described 2.3.2. Full-length sequence was obtained for the PB2 gene of each mouse sample for sequencing. The PB2 F406Y and W359F mutations were confirmed by Sanger sequencing, and no unwanted mutations were detected.

4.3.7. Statistical analyses

All data analyses were performed using GraphPad Prism Software Version 6.00 (GraphPad Software Inc., San Diego, CA). All assays were performed a minimum of two times in triplicate. For multiple comparisons, two-way ANOVA was performed followed by a post-hoc Bonferroni test; $p < 0.05$ was considered significant.

4.4. Results

4.4.1. Polymerase assays and growth kinetics of cap-binding mutants show trend towards increased activity and replication at 37°C

Polymerase activity of the PB2 cap-binding mutants was assessed by performing mini-genome assays at 33, 35, 37 and 39°C. Samples were collected out to 72 hpt. Although normalized GLuc expression of the cap-binding mutant complexes was generally higher than the WT, these differences are not significant as all were less than 1 log; therefore, these assays showed that the PB2_F406Y and PB2_W359F polymerase complexes express similar levels of GLuc as the WT polymerase complex at all temperatures (Fig. 4.1A-C). Interestingly, at 37°C, the PB2_W359F cap-binding mutant had higher GLuc expression compared to the WT, although, again, the difference was less than 1 log (Fig. 4.1A-C). Despite the fact that the difference in PB2_W359F polymerase expression was not significant compared to WT, it was in contrast to the findings in Wakai *et al.*, which showed decreased polymerase activity of this mutation in comparison to WT in the context of B/Shanghai/361/2002. The PB2_F406Y complex showed nearly identical GLuc expression to the WT at 37°C, and like the results for PB2_W359F, this finding contrasted the results in Wakai *et al.* which showed a mild decrease in polymerase activity with the introduction of this mutation in the B/Shanghai/361/2002 polymerase complex (Fig. 4.1C) (61). Finally, at 39°C, normalized polymerase activity of all complexes was similarly low, as expected (data not shown).

Viral replication of the cap-binding mutants relative to the WT RG-B/Bris virus was evaluated next by performing growth kinetics. As with luciferase activity, viral growth kinetics were evaluated at 33, 35, 37 and 39°C. Supernatant was collected up to 72 hpi and titrated by TCID₅₀ to determine viral titers. At 33 and 35°C, the WT virus grew to significantly higher titers compared to both the cap-binding mutant viruses at late time points (Fig. 4.2A and B). Similar to the polymerase assays, the PB2_F406Y and PB2_W359F viruses showed slightly enhanced growth when compared to the WT RG-B/Bris virus at 37°C over the range of time points measured; however, the difference in viral titers between the PB2_W359F and WT RG-B/Bris virus was insignificant (Fig. 4C). At 39°C, virus growth was below the detectable limit for all three viruses (data not shown). Overall, though, viral titers were similar among all viruses at all temperatures.

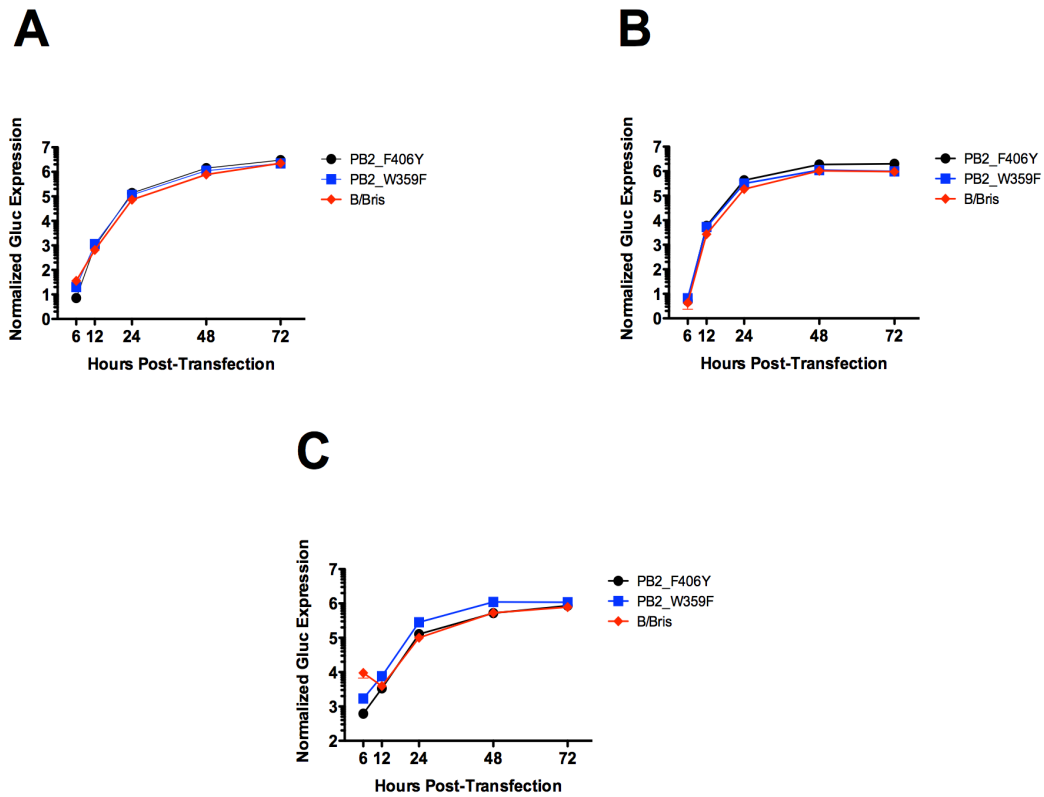


Figure 4.1. Mini-genome assays of B/Brisbane/60/2008 cap-binding mutants.

Plasmids carrying the influenza polymerase genes as well as *Gussia* Luciferase and secreted alkaline phosphatase (SEAP) were used to transfect 293T cells. Assays were completed at 33°C (A), 35°C (B), and 37°C (C). Luciferase activity was normalized to SEAP activity at 24hpt. Supernatant was collected at 6, 12, 24, 48 and 72hpt to assay for GLuc activity. The blue line represents the polymerase complex carrying the PB2_W359F mutation. The black line represents the polymerase complex carrying the PB2_F406Y mutation. The red line represents the WT B/Brisbane polymerase complex.

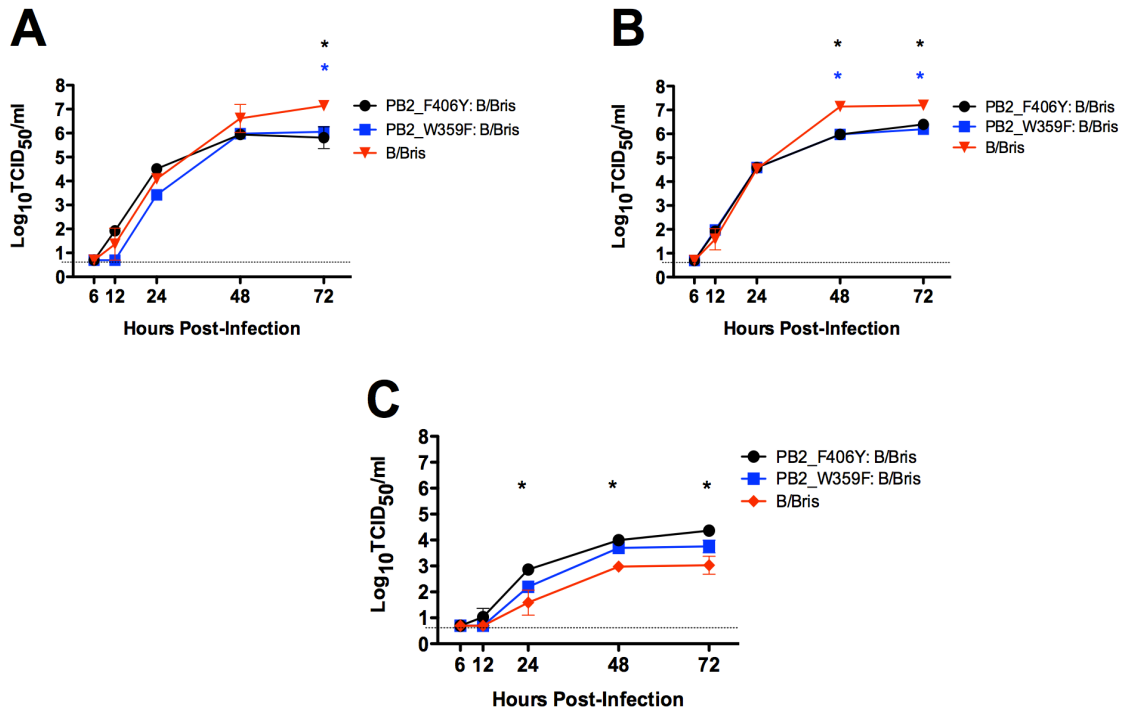


Figure 4.2. Viral growth kinetics of B/Brisbane/60/2008 cap-binding mutants. MDCK cells were infected with 0.01 MOI of each virus. Growth kinetics were assessed at 33°C (A), 35°C (B), and 37°C (C). Supernatant was collected at 6, 12, 24, 48 and 72hpi. Virus titers of collected supernatant were determined by TCID₅₀. Red: WT RG-B/Bris, Black: PB2_F406Y: B/Bris, Blue: PB2_W359F: B/Bris. Asterisk indicates p<0.05, each PB2 mutant was compared to WT separately.

4.4.2. Increased weight loss and mortality with cap-binding mutant viruses in DBA/2 mice

To determine whether the cap-binding mutations confer some advantage to the WT RG-B/Bris virus *in vivo*, DBA/2 mice were inoculated with 10^5 EID₅₀/mL of virus and monitored for weight loss and clinical signs (242). The results showed a significant increase in weight loss with the introduction of the F406Y and W359F PB2 cap-binding mutations, and similar weight loss was seen in both cap-binding mutant virus inoculated mice groups compared to the WT (Fig. 4.3A). While weight loss in the WT RG-B/Bris group began on the same day as the weight loss in the cap-binding mutant virus groups, overall weight loss seen in the WT inoculated mice was less severe, averaging roughly 10% of the starting weight (Fig. 4.3A).

The contrast in survival rate of mice inoculated with the PB2 cap-binding mutant and WT viruses reflected the differences seen in weight loss. Most mice in the PB2_F406Y and PB2_W359F groups either succumbed to infection or had to be euthanized based on weight loss by 8 dpi, although all mice in both groups had to be euthanized or succumbed to infection, while only 3 mice in the WT RG-B/Bris group developed severe disease requiring euthanasia (Fig. 4.3B). Notably, these deaths occurred late during the time course of infection (Fig. 4.3B). The majority of mice in the WT group began to recover on day 9 post-inoculation (Fig. 4.3A).

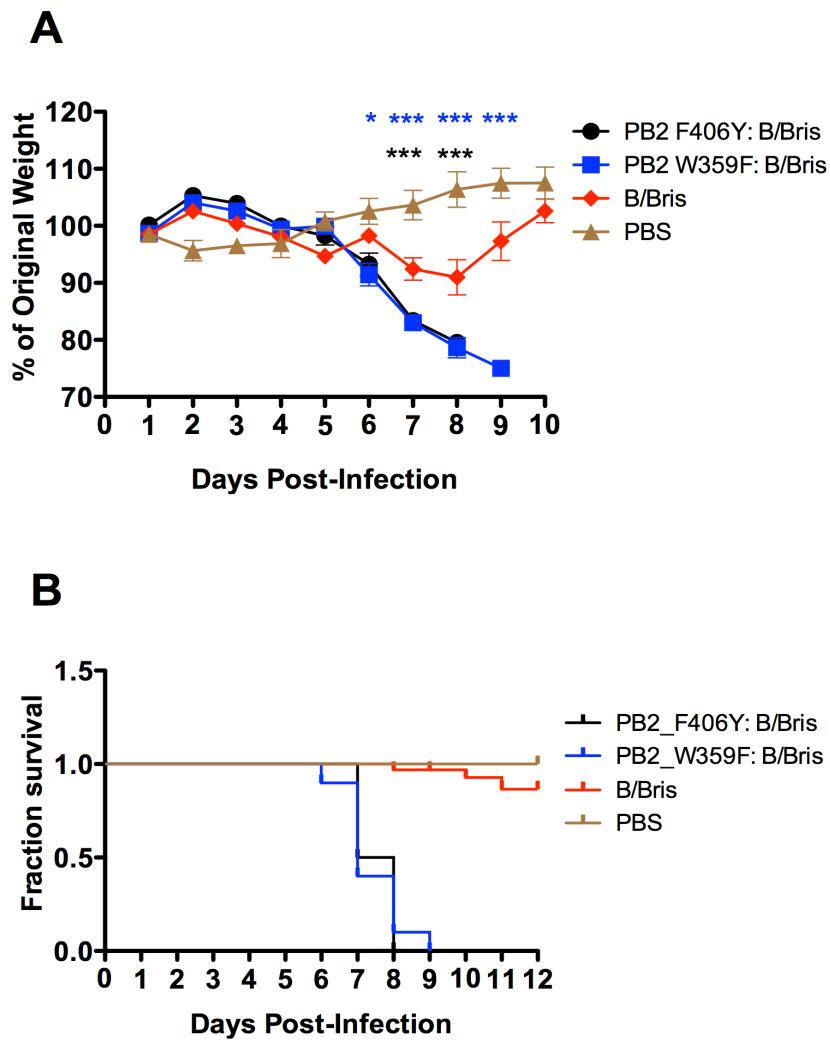


Figure 4.3. Weight loss and survival of cap-binding mutant infected mice. Each group was inoculated with 50 μ L intranasally of 10^5 EID₅₀/mL of virus, either a B/Bris cap-binding mutant virus or the WT RG-B/Bris virus. Mice were weighed and monitored daily for 12 days post-infection. Weight loss (A) Survival (B). The asterisk indicates significance, and the color of the asterisk indicates which virus group lost significantly more weight in comparison to WT. P-values of <0.05 were considered significant. $p < 0.05$ (*), $p < .001$ (***) $n=10$ per group. Red: WT RG-B/Bris. Black: PB2_F406Y: B/Bris. Blue: PB2_W359F: B/Bris. Brown: PBS.

4.4.3. Pulmonary virus titers early during infection trend toward increased replication of cap-binding mutants

Next, the relationship of the observed morbidity and mortality with viral titers in the lungs and nasal turbinates was assessed. On days 3, 5 and 7 post-inoculation, lung and nasal turbinates from 3 mice/group were harvested, and each sample was titrated by TCID₅₀. Results revealed that lung titers on days 5 and 7 post-inoculation were similar among all virus groups. On day 3, lung titers were greater in the PB2_F406Y and PB2_W359F inoculated mice; nevertheless, with only 3 samples per group and an outlier in the PB2 F406Y group, significance cannot be determined (Fig. 4.4A-C). Virus titers in the nasal turbinates (NT) were evaluated next, and the results suggest that the WT RG-B/Bris virus grows to similar titers in the nasal cavity as the PB2 mutant viruses. WT RG-B/Bris nasal turbinate titers, however, dropped off gradually, while NT titers in both PB2 F406Y and PB2 W359F mutant groups dropped off more rapidly, although more samples would be needed to confirm this trend (Fig. 4.4D-F).

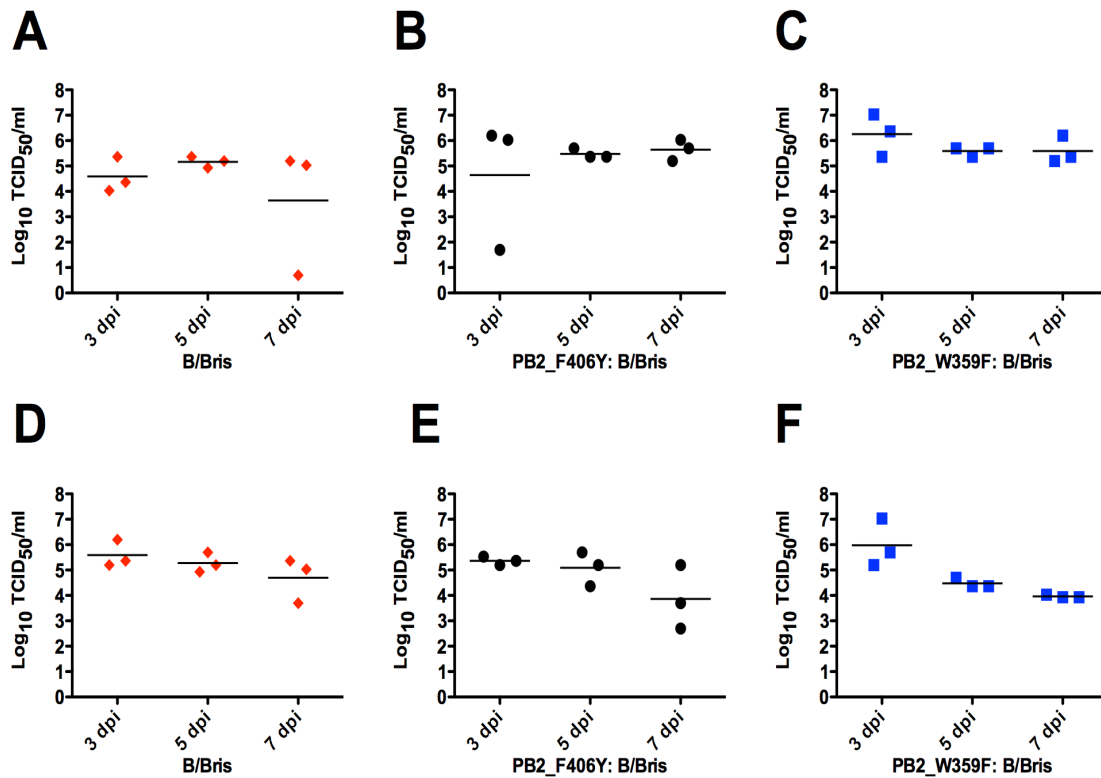


Figure 4.4. Tissue titers of cap-binding mutant infected mice. Each group was inoculated with 50 μ L intranasally of 10⁵ EID₅₀/mL of either a B/Bris cap-binding mutant virus or WT RG-B/Bris. Three DBA/2 mice per group were sacrificed on days 3, 5 and 7 post-infection. Lung and nasal turbinates were collected for tissue titration. The left lung lobe was harvested from each mouse for tissue while the remaining lobes were homogenized in 500 μ L of PBS for tissue titration (A-C). The nasal turbinates were harvested from each mouse and homogenized in 500 μ L of PBS for titration (D-F). Virus titers were determined by TCID₅₀. n=3 per group. Red: WT RG-B/Bris. Black: PB2_F406Y: B/Bris. Blue: PB2_W359F: B/Bris.

4.4.4. PB2 cap-binding mutant viruses show enhanced lung pathology

Tissue pathology in the left lung lobe of mice from each group on days 3, 5 and 7 post-inoculation was assessed. The results showed that severe pathology associated with the WT virus progressed/developed more slowly in comparison to the progression/development of pathology in the PB2 mutant groups. This was evident in the severity scores of both the total (extent) tissue pathology and the pulmonary vascular pathology on 3 and 5 dpi when severity scores were higher in mice inoculated with cap-binding mutant viruses than mice inoculated with WT virus (Fig. 4.5B and D). By day 7, virus-related tissue pathology scores were similar among mice in all virus groups (Fig. 4.5A-D). Representative images of histopathology from each group further support these overall findings. On day 3 post-inoculation, the WT virus inoculated group is nearly indistinguishable from the PBS group. On day 5, the pathology observed in the WT image is clearly more severe but reduced relative to both the PB2_F406Y and PB2_W359F inoculated groups. By day 7, virus-associated pathology is nearly indistinguishable among all virus groups (Fig. 4.6).

Most of the severe pathology observed in the virus-infected tissues was observed in the pulmonary vascular regions. The pathology seen in the vasculature consisted primarily of vasculitis as evidenced by perivascular cuffing, the accumulation of a dense mass of lymphocytes around the blood vessel. Infection of this region is associated with acute lung injury in both mice and humans, as this region is involved in gas exchange, and any damage to it would contribute to respiratory distress and hypoxemia (335-338).

Less severe pathology was observed in the alveolar and bronchiolar tissues, although severity scores were higher in the alveolar than the bronchiolar tissues. The majority of necrosis and inflammation was seen in the alveoli. Normal to mild pathology was seen in the bronchi, and severity scores were similar amongst all virus groups. In all, similar manifestations of pathology were seen in mouse tissue from all virus groups; however, they differed in severity.

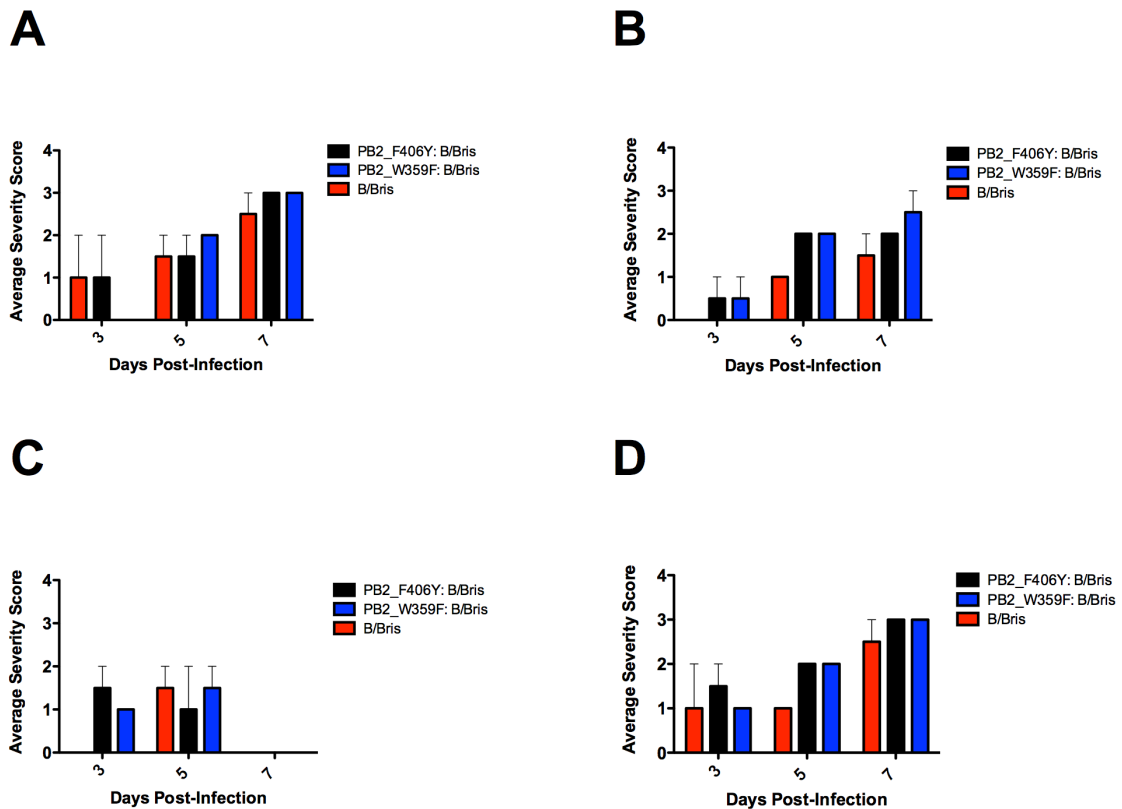


Figure 4.5. Lung pathology of cap-binding mutant infected mice. Tissue pathology was assessed for 2 mice per virus group. Each group was inoculated with 50 μ L intranasally of 10⁵ EID₅₀/mL of either a B/Bris cap-binding mutant virus or WT RG-B/Bris. Tissue pathology was analyzed in the right lung lobe of each mouse on days 3, 5 and 7 dpi. Aveoli pathology (A), vascular pathology (B), bronchi pathology (C) and extent pathology (D) Red: WT RG-B/Bris. Black: PB2_F406Y: B/Bris. Blue: PB2_W359F: B/Bris.

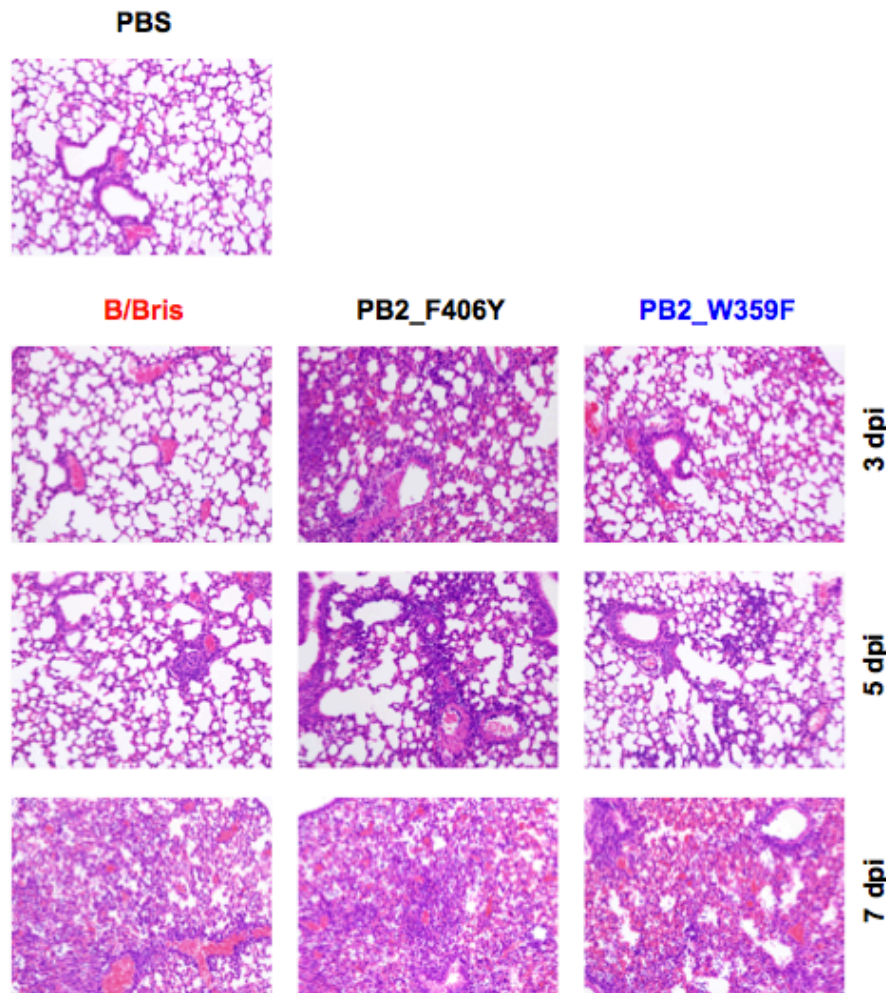


Figure 4.6. Representative images of lung pathology of cap-binding mutant infected mice. Top left image: PBS negative control. First row of images, from left to right: PB2_F406Y, PB2_W359F and WT RG-B/Bris on 3 dpi. Second row of images, from left to right: WT RG-B/Bris, PB2_F406Y and PB2_W359F on 5 dpi. Third row of images, from left to right: WT-RG B/Bris, PB2_F406Y and PB2_W359F on 7 dpi.

4.5. Discussion

Here, PB2 cap-binding mutations, F406Y and W359F, originally described in B/Shanghai/361/2002 were characterized in the context of WT RG-B/Brisbane/60/2008 to determine if the PB2 cap-binding mutations would be virulence factors *in vivo* but attenuated *in vitro* (61). In order to characterize these mutations, polymerase assays, growth kinetics and *in vivo* analyses of survival and pathology in a DBA/2 mouse model were performed.

The *in vitro* data generated in this study showed few differences between the cap-binding mutant viruses and the WT virus, although the results did suggest that the cap-binding mutants may replicate to higher titers at 37°C. In contrast, the *in vivo* results showed some clear differences between the PB2 cap-binding mutant viruses and the WT virus indicating that the PB2 cap-binding mutants are virulence factors in mice. Viral titers in the lungs and nasal turbinates were similar among all virus groups; however, at 3dpi, lung titers were higher in both PB2 mutant infected mouse groups than in the WT infected group. Additionally, the pathology scores and images suggested that the development of severe pathology was slower in the WT virus infected group than the development of pathology seen in both PB2 cap-binding virus infected groups. The survival data, however, is the most compelling evidence of enhanced virulence of the cap-binding mutant viruses. Overall, 100% of the mice in both PB2_F406Y and PB2_W359F virus groups either succumbed to infection or had to be euthanized, while the same outcome occurred in only 30% of the mice in the WT virus group. Thus, both of the cap-binding mutant viruses were more pathogenic

and more virulent in the DBA/2 mouse model while expressing similar levels of GLuc and replicating to similar titers as the WT *in vitro*.

As previously noted, Wakai *et al.* showed decreased polymerase activity of these cap-binding mutants at 24 h and 37°C in the context of B/Shanghai/361/2002 indicating that the mutations may be attenuated in mice as the body temperature of a mouse is 37°C (61). The results presented here, which show no decrease in polymerase activity of the cap-binding mutants compared to WT at 37°C and enhanced virulence of the cap-binding mutants in mice, are contrary to these findings, but they are consistent with the virulence seen in mice inoculated with the PB2/PB1 mutant viruses in Chapter 3.

There are several potential explanations for the discrepancy between the findings in Wakai *et al.* and those presented here including phylogenetic differences between B/Brisbane/60/2008 and B/Shanghai/361/2002 as well as potential temporal differences between the behaviors of these viruses. Influenza B viruses are subdivided into two HA antigenic lineages, B/Victoria and B/Yamagata, which differ from one another based on antigenicity and sequence (75). B/Brisbane/60/2008 is a B/Victoria-like virus, while B/Shanghai/361/2002 is a B/Yamagata-like virus. These lineages are known to have different preferences for sialic acid receptors (alpha 2,3 versus alpha 2,6) as well as dissimilarities in susceptibility of mice; therefore, given these known distinctions in behavior, it is also conceivable that the PB2_F406Y and PB2_W359F mutations could behave disparately in each lineage (234, 242, 331). Importantly, it is also possible that, had the polymerase assays with B/Shanghai/361/2002 been carried out to later time points, the decrease in polymerase activity of the cap-binding

mutants relative to WT would have proven to be only temporal.

Although this study did not seek to identify a mechanism of the enhanced morbidity and mortality associated with the PB2_F406Y and PB2_W359F mutations, one possibility is that these mutations may alter polymerase interactions with mouse host factors, as the overall growth differences are relatively small but the difference in mortality is comparatively large. In influenza A, PB2 is known to be a major determinant of host range. For example, PB2 E627K is a marker of mammalian adaptation and has been shown to enhance replication in mammalian cells without altering tissue tropism (321, 339, 340). Given the strong degree of structural and sequence homology between the PB2 of IAV and IBV, it is conceivable that the influenza B cap-binding mutants described here could have similar effects, thus future studies on tissue tropism would address this question (61, 326).

To conclude, the findings presented here are consistent with other studies that have shown IBV adaptation in mice involves the backbone genes of the virus rather than the surface genes (234, 341). They are also consistent with another study, which showed that an IAV PB2 cap-binding mutant virus with a mutation at amino acid residue 357, analogous to position 359 of IBV, was more virulent in mice than the WT (320). Finally, these mutations are potential tools for the study of IBV pathogenesis and vaccine efficacy in mice. Since many IBV strains are not naturally virulent in mice, IBV studies have traditionally been performed in immunodeficient mice or with mouse-adapted viruses, but with the incorporation of the PB2 F406Y or PB2_W359F, studies could more easily be performed in mouse models, although the degree to which these mutations affect virulence could be strain dependent (234, 342,

343).

Chapter 5: Development of Alternative Influenza B LAIV Vaccines based on three amino acid mutations and an C-terminal HA tag in PB1.

5.1. Abstract

Influenza B virus (IBV) is a major cause of human respiratory illness and is such a significant cause of human disease that it is incorporated into the seasonal influenza vaccine. Traditionally, one strain of IBV was incorporated into a trivalent vaccine, which also contained two strains of influenza A virus (IAV); however, beginning in the early 2000s, this composition was sometimes associated with antigenic mismatch due to co-circulation of IBV HA antigenic lineages, B/Yamagata-like and B/Victoria-like, and the lack of cross-reactivity between them. In response, a quadrivalent vaccine was developed which incorporates both HA antigenic lineages of IBV as well as two strains of IAV. While this has improved vaccine coverage against IBV, additional improvements could be made in both vaccine safety and efficacy. Previously, we showed that the incorporation of 391E, 581G, 661T and a C-terminal HA tag in PB1 in addition to a 265S mutation in PB2 of A/guinea fowl/Hong Kong/WF10/99 (H9N2) and A/turkey/Ohio/313053/2004 (H3N2) viruses enhanced vaccine stability, safety and efficacy over similar but tag-less vaccine formulations. The study described here details efforts to develop a complementary strategy for IBV. The results show that an IBV carrying mutations in PB1 (K391E, E580G, S660A and a C-terminal HA tag) is safe and immunogenic in mice. Importantly, the findings

demonstrate for the first time that a subset of mutations analogous to those found in the A/Ann Arbor cold-adapted licensed vaccine backbone can attenuate IBV and prove that 3 mutations rather than the licensed 7 found in the B/Ann Arbor cold-adapted vaccine backbone are sufficient to attenuate IBV.

5.2. Introduction

Influenza B virus (IBV) is part of the *Orthomyxoviridae* family of viruses, which also includes influenza A virus (IAV) and influenza C virus (3). IBV is an enveloped, negative-sense, single-stranded RNA virus with a segmented genome (3). Each of the 8 RNA segments of its genome encodes 1 or 2 proteins, and the entire genome encodes a total of 11 proteins (44, 47, 48).

Segments 1-3, 5, 7, and 8 comprise the virus backbone. Segments 1-3 and 5 encode proteins that form the viral ribonucleoprotein complex (vRNP). The vRNP complex is comprised of the polymerase proteins, PB1, PB2 and PA, encoded from segments 1-3, respectively, as well as NP, a nucleoprotein, encoded from segment 5 and bound to each vRNA segment (41, 42, 58, 60). The polymerase proteins work together to initiate viral mRNA, cRNA and vRNA transcription. To initiate viral mRNA transcription, the PB2 protein binds the host 5' mRNA cap (61, 329). Then, PA cleaves the cap, and PB1, which contains the polymerase active site, initiates transcription of the viral genome (41, 42, 58, 59, 62, 344). The remaining backbone segments, 5 and 7, encode a variety of proteins including an innate immune response antagonist, a nuclear export protein, a matrix protein and an ion channel protein (47-50, 69, 101, 126, 172, 194, 197, 198, 206, 235, 244, 245, 308, 345).

Segments 4 and 6 encode surface proteins HA and NA, respectively, although HA is the major antigenic protein. In addition to being antigenic surface proteins, HA binds the host cell receptor, sialic acid, and NA is a neuraminidase responsible for cleaving sialic acid from the surface of the host cell to allow for release of newly budded virions from the cell (63, 82, 186). Segment 6 also encodes NB via an

alternate open reading frame (ORF), but unlike NA, NB is an ion channel that likely facilitates the acidification of the virion after endocytosis (44, 45, 85, 207).

IBV causes respiratory disease in humans, is considered a major human pathogen and has a well-documented history of causing epidemics; however, IBV infections are seasonal, as infections peak in the winter due to the drier, colder conditions (30, 76, 180, 286, 287). Although IBV infects all age groups, infections are particularly severe in the very young and the elderly. For instance, from 2004-2011 (excluding the 2009 pandemic), 22-44% of all pediatric influenza-related deaths in the U.S. were IBV-related (28). From 1979/80-2000/01, hospitalization rates for persons of all ages due to IBV-related illness occurred at a rate of 83.4/100,000 cases (4). Interestingly, influenza B hospitalization rates during this period were higher than seasonal influenza A H1N1 but lower than influenza A H3N2 (4).

Each year, seasonal influenza vaccines are manufactured to confer protection against circulating strains of influenza A and B; nonetheless, the same backbone genes are always incorporated into the seasonal vaccine, while the surface genes are updated as needed to match circulating strains since immunity is associated primarily with the HA and NA surface proteins (35, 81, 309). Traditionally, the seasonal vaccine possessed three strains of influenza viruses, two IAV strains (an H1 and an H3) and one IBV strain; however, new for the 2013-14 influenza season, quadrivalent vaccines carrying two strains of IAV and two strains of IBV were made available (24, 25, 37). The reason for the addition of a second strain of IBV is a result of the co-circulation of influenza B HA-antigenic lineages which emerged in the 1980s and

have little cross-reactivity in that immunity to one lineage does not protect against exposure to the other (75, 76, 217, 346).

Influenza vaccines come in two main platforms: killed virus (KV) and live-attenuated (LAIV) (24). KV vaccines are grown and are then inactivated with formalin, a process that renders the component viruses non-replicative (24, 249). In contrast, the licensed LAIV vaccine contains a series of cold-adapted mutations that were identified by passing A/Ann Arbor/6/60 (H2N2) and B/Ann Arbor/1/66 viruses at progressively lower temperatures until these viruses grew well at 25°C, far below the optimum growth temperature of a wild-type (WT) virus of either type (220, 223, 257, 319). Over the course of these passages, each virus accumulated a series of mutations enabling growth at lower temperatures. The mutations identified in both A/Ann Arbor/6/60 (H2N2) (A/Ann Arbor) and B/Ann Arbor/1/66 (B/Ann Arbor) are located primarily in the vRNP complex. The A/Ann Arbor mutations are PB2 265S, PB1 391E, PB1 581G, PB1 661T and NP 34G, while the B/Ann Arbor mutations are PB2 630R, PA 341M, NP 114A, NP 410H, NP 509T, M1 159Q and M1 183V (208, 220, 222, 223, 257-259, 311, 319). The cold-adapted backbones of both of these viruses are incorporated into the LAIV seasonal vaccine each year as the presence of these mutations restricts virus replication of the vaccine to the upper respiratory tract, preventing severe vaccine-related influenza infection and ensuring vaccine safety (263).

Live-attenuated vaccines have been shown to confer better coverage than KV vaccines due to the stimulation of a humoral (primarily IgG and IgA) and a T-cell mediated immune response (virus specific CD4⁺ and CD8⁺ T cells), instead of

simply the humoral (IgG) response associated with KV vaccines (347-349). In addition to an adaptive response, LAIV vaccines have also been shown to heighten the innate immune response, inducing increased IFN (170, 288, 350). Despite the enhanced protection conferred by LAIV vaccination, improvement is still needed, as LAIV vaccines can only be administered to healthy individuals of a select age group, ages 2-49 years old (24). Thus, the most at-risk populations, the very young, the elderly and those with pre-existing conditions, do not have access to the most immunogenic vaccine because of the potential risk that a replicative vaccine carries in those with altered immune status.

Aside from the health and age-related restrictions associated with the LAIV vaccine, the outdated LAIV vaccine backbones present other limitations. These backbones potentially limit the amount of cross-protection elicited by the vaccine since cross-protection has been associated with an immune response to internal genes; however, they also limit the robustness of the immune response in individuals who have been repeatedly exposed, like elderly individuals (290, 292, 294-297). Elderly persons have been shown to respond less well to the LAIV vaccine than younger healthy individuals in part due to immune history and immunosenescence, so a possible resolution to this problem could be the use of a more contemporary vaccine backbone (267, 351). The limitations of the currently licensed LAIV vaccine based on A/Ann Arbor/6/60 (H2N2) and B/Ann Arbor/1/66 cold-adapted (ca) backbones have led to a concerted research effort to improve upon the current strategy in order to develop a more efficacious vaccine that can safely be administered to all, in particular at-risk populations (220, 223, 257).

A variety of strategies have been employed to develop alternative experimental LAIV influenza vaccines. Such strategies include, but are not limited to, whole and partial gene knockouts, the insertion of foreign sequences, and the manipulation of the HA cleavage site (176, 177, 239, 240, 248, 284, 352-355). Extensive work has been done on NS, M, NA and PB2 partial and full knockout vaccines, and while such vaccines have proven effective, there are drawbacks (239, 240, 248, 352-354). For instance, the full knockout vaccines must be grown in cell lines which are not FDA approved that stably express the missing gene in order to achieve the level of growth required of a vaccine strain (354). The manipulated HA cleavage site strategy, which has been shown to limit virus growth to the presence of elastase, grows to high titers in approved cell lines but has shown some signs of instability *in vitro* (284, 355). Finally, while some of these strategies such as the elastase cleavage site have been shown to be effective in the context of IBV, most of these strategies have only been tested in the context of IAV (176, 248, 355).

Our lab has developed an alternative IAV strategy, which incorporates the PB2 and PB1 mutations found in the A/Ann Arbor cold-adapted backbone (311, 319, 356). Additionally, our strategy involves an in-frame introduction of an 8-amino acid HA tag derived from H3 at the C-terminus of PB1 (314). We have demonstrated safety and efficacy of our strategy *in ovo* as well as in mouse, chicken, ferret and swine models; furthermore, we have shown that it grows to high titers in approved cell lines and eggs (1, 314-316, 357). When compared to similar viruses differing only in the presence of the HA tag, the tagged virus has been proven to confer better protection than the traditional mutations alone (1, 314-316, 357). Finally, our lab has

shown that this strategy is a viable DIVA (Differentiating Infected from Vaccinated Animals) vaccine strategy, as the HA tag can be detected by RT-PCR and western blot (314). Indeed, our strategy has many advantages over other experimental vaccines including high growth titers, a DIVA vaccine element, enhanced stability and similarity to the currently licensed strategy, a fact that would likely expedite the FDA approval process.

In order to develop a quadrivalent vaccine with our strategy that could better stimulate the immune response in immunosenescent individuals, we required a contemporary complementary IBV backbone. To this end, this study asked whether modifications in PB1 analogous to those found in our IAV strategy would be sufficient to attenuate B/Brisbane/60/2008 as our previous data suggested that the mutations primarily responsible for the temperature sensitive phenotype of our IAV strategy are located in PB1 (314). Thus, the following mutations were cloned into PB1 of the reverse genetics B/Brisbane/60/2008 (RG-B/Bris) system: K391E, E580G, and S660A. The subsequently rescued virus was called B/Brisbane/60/2008 *ts* (B/Bris *ts*). Another virus carrying these mutations as well as an HA tag at the C-terminus of PB1 was also generated and labeled B/Brisbane/60/2008 *att*. Here, the results show that both the B/Brisbane/60/2008 *ts* and *att* viruses are safe and immunogenic in the DBA/2 mouse model; however, B/Brisbane/60/2008 *ts* is unstable after just two passages in eggs. B/Brisbane/60/2008 *att* (B/Bris *att*), in contrast, is both stable and immunogenic, yet despite differences in stability, both viruses conferred protection against lethal challenge.

5.3. Materials and Methods

5.3.1. Cloning and confirmation of mutations

Previously described bi-directional reverse genetics B/Brisbane/60/2008 (RG-B/Bris) plasmids were used to clone the B/Brisbane/60/2008 *ts* and *att* constructs. First, four overlapping PCR fragments were generated. To generate the fragments, PCR using pDP-PB1 B/Bris as the template was performed with site-directed mutagenesis primers designed with the QuikChange Primer Design tool to generate forward and reverse primers for each mutation, K391E, E580G and S660A, (Agilent, Santa Clara, CA) and PB1 AarI cloning primers (described in 2.3.2). Then, overlapping PCR was performed to join all four fragments to obtain full-length PB1 carrying all three mutations (PB1 *ts*). All PCR reactions were performed with Pfu Ultra Polymerase AD (Agilent, Santa Clara, CA) according to manufacturer recommendations. The full-length fragment was then digested with AarI (Agilent, Santa Clara, CA) while the pDP2002 vector was digested with BsmB1. Then, PB1 *ts* was ligated into pDP2002 using Quick Ligase (New England Biolabs, Ipswich, MA). Following the same procedure but using pDP-PB1HA (described in Chapter 3) as the template, pDP-PB1 *att* was also cloned. Both clones were sequenced using Sanger Sequencing on a Genetic Analyzer 3500xl (Applied Biosystems, Foster City, CA) following the Big Dye Terminator v3.1 kit and sequencing protocol (Life Technologies, Carlsbad, CA). All mutations were confirmed through sequencing and no undesired mutations were identified.

5.3.2. Virus rescue and stocks

Virus rescue was done via 8-plasmid reverse genetics as described in 2.3.4. Each of the PB1 mutant clones, pDP-PB1 *ts* and pDP-PB1 *att*, was paired with the corresponding 7 WT RG-B/Bris plasmids. Briefly, 1µg of each (10µL per plasmid at concentrations of 100ng/µL each) was mixed with 2µL/µg plasmid of Transit-LTI transfection reagent (Mirus Bio, Madison, WI) and serum free [OPTI-MEM] I (Life Technologies, Carlsbad, CA) up to 200µL. Following a 45-min incubation at room temperature, 800µL of serum free [OPTI-MEM] I (Life Technologies, Carlsbad, CA) was carefully added to each reaction. This solution was then overlaid on a co-culture of 293T/MDCK cells ($8 \times 10^5 / 5 \times 10^5$ cells/well) in a 6-well plate (Corning, Corning, NY). Plates were then placed at 33°C, and 24 h later, the media was changed, serum-free [OPTI-MEM] I with 1µg/mL TPCK-trypsin (Worthington Biochemicals, Lakewood, NJ) containing Antibiotic/Antimycotic (10mL/L, Sigma-Aldrich, St. Louis, MO). Following virus rescue, tissue culture supernatant was used to infect 9-day old specific pathogen free (SPF) hen eggs to grow virus stocks (33°C). All virus stocks were sequenced by Sanger Sequencing on a Genetic Analyzer 3500xl (Applied Biosystems, Foster City, CA) following the Big Dye Terminator v3.1 kit and sequencing protocol (Life Technologies, Carlsbad, CA) to confirm that the desired mutations were present in both the B/Bris *att* and B/Bris *ts* stocks.

5.3.3. Virus titrations

Virus stocks were titrated by both tissue culture infectious dose 50 (TICD₅₀) and egg infectious dose 50 (EID₅₀) (done in 9-day old SPF hen eggs, B&E Eggs, York Springs, PA). Animal samples were titrated by TCID₅₀, and EID₅₀ titers were used for the mouse safety and vaccine studies. Titrations were performed according to the protocol described in 2.3.5 at 33°C. Viral titers were determined by the Reed and Muench method (300).

5.3.4. Mini-genome assays

In order to assess polymerase activity, WT RG-B/Bris, B/Bris *ts* and B/Bris *att* polymerase complexes were transfected with the previously described NP *Gaussia* Luciferase (GLuc) reporter plasmid (described in Chapter 2) as well as a pCMV-SEAP (secreted alkaline phosphatase) plasmid to control for transfection efficiency. Additionally, a no reporter control and a partial vRNP complex control that excluded pDP-PB2 B/Bris were included. Transfections were setup in 12-well plates (Corning, Corning, NY) as described in 2.3.7, and each polymerase complex was tested in triplicate at 33, 35, 37 and 39°C. At 6, 12, 24, 48 and 72 h post-transfection (hpt), tissue culture supernatant was collected in white high-binding 96-well microtiter plates (Corning, Corning, NY). At 24 hpt, additional supernatant was collected for analysis of SEAP activity.

GLuc activity was assessed using the Bioluminescence *Gaussia* Luciferase Assay Kit (New England Biolabs, Ipswich, MA) following the provided protocol, and expression was measured on a Victor x3 Multilabel Plate Reader (PerkinElmer, Waltham, MA). SEAP activity was assayed using Phospha-light SEAP Reporter Gene Assay System (Life Technologies, Carlsbad, CA) following the provided protocol. Then, like the GLuc measurements, SEAP activity was measured on a Victor x3 Multilabel Plate Reader (PerkinElmer, Waltham, MA). In order to normalize for transfection efficiency, calculations were performed as described in 2.3.7.

5.3.5. Growth kinetics

Growth kinetics for the WT RG-B/Bris, B/Bris *att*, and B/Bris *ts* viruses were evaluated at 33, 35, 37, and 39°C and 0.01 MOI. Assays were performed following the protocol described in 2.3.8. Briefly, each virus was tested in triplicate at each temperature in a 6-well plate (Corning, Corning, NY) seeded with 5×10^5 MDCK cells. Viruses were diluted to 0.01 MOI in serum free [OPTI-MEM] I (Life Technologies, Carlsbad, CA). Each well was infected with 1mL of virus. The plates were then placed at 4°C for 15 min to synchronize infection time. Next, the cells were placed at 37°C for 45 min to infect. At each time point, 6, 12, 24, 48 and 72 h post-infection (hpi), 120µL of tissue culture supernatant was collected per well. The media was replenished after each sample was collected. After collection, all samples were placed at -80°C. Finally, the virus titer for each sample was determined by TCID₅₀ using the Reed and Muench method and graphed (301).

5.3.6. Western blot

Prior to western blotting, MDCK cells were infected with 1 MOI of each virus: mock (serum free [OPTI-MEM] I, Life Technologies, Carlsbad, CA), WT RG-B/Bris, B/Bris *ts*, B/Bris *att*, and 7malH7:WF10att described in Song *et al.* (317). To do this, 1 well of MDCK cells was first trypsinized and counted to determine the number of cells to be incorporated into the calculation of MOI. Then, each well was infected with 500 μ L of 1 MOI of each virus for 1-h at 37°C. Following incubation, the media was changed: 1mL of serum-free [OPTI-MEM] I (Life Technologies, Carlsbad, CA) with 1 μ g/mL of TPCK-trypsin (Worthington Biochemicals, Lakewood, NJ). The infected cells were then placed at 33°C for 20 h. At 20 hpi, tissue culture supernatant was aspirated, and 150 μ L of Laemilli Buffer (Bio-Rad, Berkeley, CA) and β -ME was added (10:1 ratio) to each well and swirled gently before collection. Then, each sample was heated for 7 min at 95°C to complete protein denaturation. Finally, samples were placed at -20°C.

In order to perform the western blot, a gradient (4-20%) SDS-PAGE gel (Bio-Rad, Berkeley, CA) carrying 5 μ L of protein ladder (Fermentas, Hanover, MD) and 25 μ L of each sample was electrophoresed in a Mini-Protean Tetra Cell eletrophoresis chamber (Bio-Rad, Berkeley, CA) for 1 h at 130V. The gel was then removed from the electrophoresis chamber and placed with nitrocellulose paper (Bio-Rad, Berkeley, CA) and blotting paper (Bio-Rad, Berkeley, CA) into transfer buffer. This was then placed into a semi-dry transfer chamber (Bio-Rad, Berkeley, CA) at 16V for 1 h. The nitrocellulose paper was then blocked for 2 h at room temperature on a rocker with

5mL of molecular grade non-fat dry milk (NFDM) (Bio-Rad, Berkeley, CA).

Following blocking, the nitrocellulose paper was washed with TTBS. Each wash was 5 min in length at room temperature on a rocker. In total, the nitrocellulose paper was washed 3 times. Finally, a 1:1000 dilution of mouse anti-HA-tag primary antibody (Cell Signaling Technologies, Danvers, MA) was prepared in 5mL of NFDM and TTBS (1g NFDM dissolved in 5mL TTBS) and allowed to incubate on a rocker at 4°C overnight.

The following day, the nitrocellulose paper was again washed with TTBS as described above. Then, goat anti-mouse secondary antibody (Southern Biotech, Birmingham, AL) was diluted 1:3000 in a 5mL NFDM/TTBS solution and incubated at room temperature on a rocker for 1 h. Next; the nitrocellulose paper was again washed 3 times with TTBS. Finally, Clarity Western ECL Substrate (Bio-Rad, Berkeley, CA), a chemiluminescent substrate, was applied to the nitrocellulose paper according to the supplied protocol, and the film was developed after a 30 sec exposure to the nitrocellulose paper in an exposure cassette.

In order to control for overall protein expression, GAPDH expression was evaluated. First, stripping buffer (Thermo Scientific, Waltham, MA) was applied to the nitrocellulose membrane after development. Next, the membrane was washed with TTBS as described above. After washing, anti-GAPDH mouse primary antibody diluted in a 5mL NFDM/TTBS solution to a ratio of 1:3000 (Santa Cruz Biotech, Dallas, Texas) was applied to the membrane and allowed to incubate on a rocker for 2 h at room temperature. The nitrocellulose paper was washed again following incubation with the primary antibody. Then, the secondary antibody was applied

(using the same procedure as described above). After incubation with the secondary antibody, the nitrocellulose paper was washed 3 times, and the chemiluminescent substrate was applied (as described previously). Finally, the film was developed after a 15 sec exposure to the nitrocellulose paper.

5.3.7. Assessing stability of vaccine candidates

B/Bris *ts* and *att* viruses were passaged 10 times in 9-day-old SPF hen eggs (B&E Eggs, York Springs, PA). Serial dilutions were made of each virus prior to inoculating eggs. For every dilution, the allantoic cavities of 3 eggs were inoculated (200 μ L per egg). Following inoculation, eggs were placed at 33°C for 72 h. After 72 h, the eggs were moved to 4°C to kill the embryos. The following day, HA assays were performed on the allantoic fluid (AF) of each egg, and the egg with the highest HA titer at the highest dilution was harvested, spun down at 1,000xg for 10 min at 4°C and frozen at -80°C until further passaging. After 10 passages, the PB1 segment of each virus was sequenced as described below to determine whether or not the mutations were still present. To sequence the PB1 gene, RNA was extracted from AF using the QIAgen RNeasy mini-kit, following the provided protocol (QIAgen, Valencia, CA). Then, cDNA was prepared by the 2-step RT-PCR protocol described in 2.3.2.

Additionally, supernatant from nasal turbinates from day 3 post-vaccination, the peak titer day, was sequenced. RNA was extracted and cDNA was prepared as described above. Once again, full length PB1 of both B/Bris *att* and *ts* vaccinated

mice was sequenced. All sequencing was done by Sanger Sequencing using a Big Dye Terminator v3.1 kit and the corresponding sequencing protocol (Life Technologies, Carlsbad, CA) and then run on a Genetic Analyzer 3500xl (Applied Biosystems, Foster City, CA).

5.3.8. Vaccine safety studies

In order to assess the safety and immunogenicity of each vaccine candidate prior to the vaccine study, 5-6 week old female DBA/2 mice (Charles River, Frederick, MD), 4 mice/group, were inoculated with 50 μ L intranasally of 10^7 , 10^6 and 10^5 EID₅₀/mL of B/Bris *att*, B/Bris *ts* or WT RG-B/Bris virus. Weight loss and signs of disease were monitored for 12 days post-inoculation (dpi), but mice were kept for 3 weeks post-inoculation. After 3 weeks, immunogenicity was assessed at 10^6 EID₅₀, as this dose was the designated vaccination dose. To assess immunogenicity, mice were exsanguinated via the mandibular vein, and blood was collected in 1.5mL tubes (USA Scientific, Orlando, FL) and left overnight at 4°C. The following day, the blood was spun down at 1,000xg for 10 min, and all sera was collected and frozen at -20°C. Then, immunogenicity was assessed by determining the hemagglutination inhibition titers (HI or HAI) against an egg grown stock of WT B/Brisbane/60/2008. The safety studies were performed with the approval of the University of Maryland, College Park IACUC (R-12-100) in BSL-2 containment. Mice that lost 20% or more of the starting weight or scored a 3 or higher in disease signs described in 2.3.9 were humanely euthanized.

5.3.9. Vaccine study

The vaccine study was performed with 4 groups of 5-6 week old female DBA/2 mice (Charles River, Frederick, MD). The group names were assigned based on which vaccine virus was used for vaccination and whether or not the group was challenged (C, challenged; NC, not challenged), thus the groups were B/Bris *ts*/ C, B/Bris *att*/ C, PBS/ C, and PBS/ NC. Each group contained 8 mice to be monitored throughout the study for weight loss and disease signs as well as additional mice to be used for tissue harvest post-vaccination and post-challenge. Each group was vaccinated intranasally with 50 μ L of 1×10^6 EID₅₀/mL of the appropriate vaccine or PBS. Weight loss and disease signs were monitored for days 1-12 post-vaccination. On days 1, 3 and 5 post-vaccination, 4 mice were euthanized per group (except the PBS groups in which only 3 mice/day were euthanized) for collection of trachea, nasal turbinates and lung tissues. On day 20 post-vaccination, all remaining mice were bled 10% of their body weight for serology, and on day 21 post-vaccination, all mice were challenged with 100 MLD₅₀ of PB2_F406Y: B/Bris virus (described in Chapter 4). Post-challenge, mice were monitored for weight loss and disease signs for 14 days. On days 3 and 5 post-challenge, 4 mice per group (except the PBS challenge group, 3 mice/day) were euthanized for tissue collection. Finally, three weeks post-challenge, all remaining mice were euthanized and exsanguinated for serology. The University of Maryland, College Park IACUC approved this study under protocol R-13-65. Once again, any mouse that lost 20% or more of its starting weight or scored a 3 or higher in disease signs was humanely euthanized.

To process the tissues, the left lung lobe and trachea were preserved in 10% formalin for pathology while the remaining lung and nasal turbinates were homogenized in 500 μ L PBS per sample at 50Hz for 4 min using a QIAgen Tissue Lyser LT (QIAgen, Valencia, CA). Homogenized tissues were then spun down at 1,000xg for 10 min before being frozen at -80°C to await titration. All tissue titrations were performed by TCID₅₀ at 33°C as described in 2.3.5. Tissue titers for the nasal turbinate and trachea post-vaccination and post-challenge for each group were determined by the Reed and Muench method and graphed (301).

5.3.10. Tissues for pathology

Post-challenge tissues were sent to Histoserv, Inc. (Germantown, MD) for sectioning, staining and analysis (as described in Chapter 4). Two samples per group from days 3 and 5 post-challenge were scored by a board certified veterinary pathologist, who examined the bronchi/bronchioles, pulmonary vasculature, alveoli and overall/extent lung regions as well as trachea from each sample. Tissue damage was scored on a scale of 0-4, where 0 is normal and 4 indicates severe lesions. A total score/extent lung score of 4 signifies the involvement of the entire lung lobe. In addition to tissue scoring, representative images of pathology were taken at 200x magnification.

5.3.11. Hemagglutination Inhibition assays

In order to determine whether or not the vaccine candidates were immunogenic, hemagglutination inhibitions assays (HI or HAI) were performed as part of the safety and vaccine studies. Roughly 18 h prior to performing HI assays, 50 μ L of each serum sample was added to 3 volumes of receptor destroying enzyme (RDE) (Fisher Scientific, Pittsburgh, PA) and incubated in a 37°C water bath to destroy non-specific inhibitors of hemagglutination. The following day, the sera were removed from the water bath, and 6 volumes of physiological saline (.85% NaCl) was mixed with each sample to yield a 1:10 dilution of serum per sample. Samples were then placed in a 56°C water bath for 30 min to inactivate the RDE. Following inactivation, 96-well v-bottom plates (Corning, Corning, NY) were filled with 25 μ L per well of PBS (wells B1-H1), and 50 μ L of serum was added to the first well (A1). The serum was then diluted down serially from A1-H1, transferring 25 μ L with each dilution. This process was repeated for each serum sample. Then, WT B/Brisbane/60/2008 was diluted to 4HAU (hemagglutination assay units) in PBS. Following confirmation of the HA titer by HA assay on the virus dilution, 25 μ L per well of the virus was overlaid on the diluted sera, and the plate was gently shaken and allowed to incubate for 15 min at room temperature. After 15 min, 0.5% cRBC (50 μ L/well) was overlaid on the sera and virus in the 96-well plate. Finally, after a 45-min incubation at room temperature, hemagglutination inhibition (HI) was recorded to determine the HI titer of each sample. Each assay was run with a PBS negative control, a serum negative control and a serum positive control.

5.3.12. Statistical analyses

All data analyses were performed using GraphPad Prism Software Version 6.00 (GraphPad Software Inc., San Diego, CA). All *in vitro* assays were performed a minimum of two times in triplicate. For multiple comparisons, two-way ANOVA was performed followed by a post-hoc Bonferroni test; $p < 0.05$ was considered significant.

5.4. Results

5.4.1. B/Bris *ts* and B/Bris *att* polymerase complexes have the highest GLuc expression at low temperatures

Characterization of the B/Bris *ts* and B/Bris *att* vaccine candidates began by measuring GLuc expression of the polymerase complexes. These assays were aimed at determining whether the mutations incorporated in these complexes would result in a temperature sensitive phenotype consistent with LAIV vaccines, restriction at 37°C. To this end, the vRNP plasmids (pDP-PB2, pDP-PB1, pDP-PA and pDP-NP B/Bris) and the GLuc reporter plasmid were transfected in 293T cells. Transfections were done at 33, 35, 37 and 39°C, and samples were collected at 6, 12, 24, 48 and 72 h post-transfection (hpt) (Fig. 5.1A-F).

Interestingly, the results showed that at 33°C both the B/Bris *ts* and *att* complexes display GLuc expression similar to that of WT, both in raw and normalized data (Fig. 5.1A and B). An increase of 2 degrees, however, resulted in a decrease in the luciferase expression from both the B/Bris *ts* and *att* polymerase complexes as compared to WT (Fig. 5.1C and D). At 35 and 37°C, the B/Bris *ts* and *att* complexes have roughly 1-2 logs lower raw GLuc expression than the WT and normalized activity is roughly 1 log lower (Fig. 5.1C- F). This is particularly noteworthy at 35°C, as GLuc expression of the WT polymerase complex is similar to the expression at 33°C even after normalization (Fig. 5.1C and D). At 37°C after normalization, WT GLuc expression is detectable but at reduced levels compared to

WT normalized expression at 33 and 35°C (Fig. 5.1F), and at 39°C after normalization, all polymerase activity is similar (data not shown).

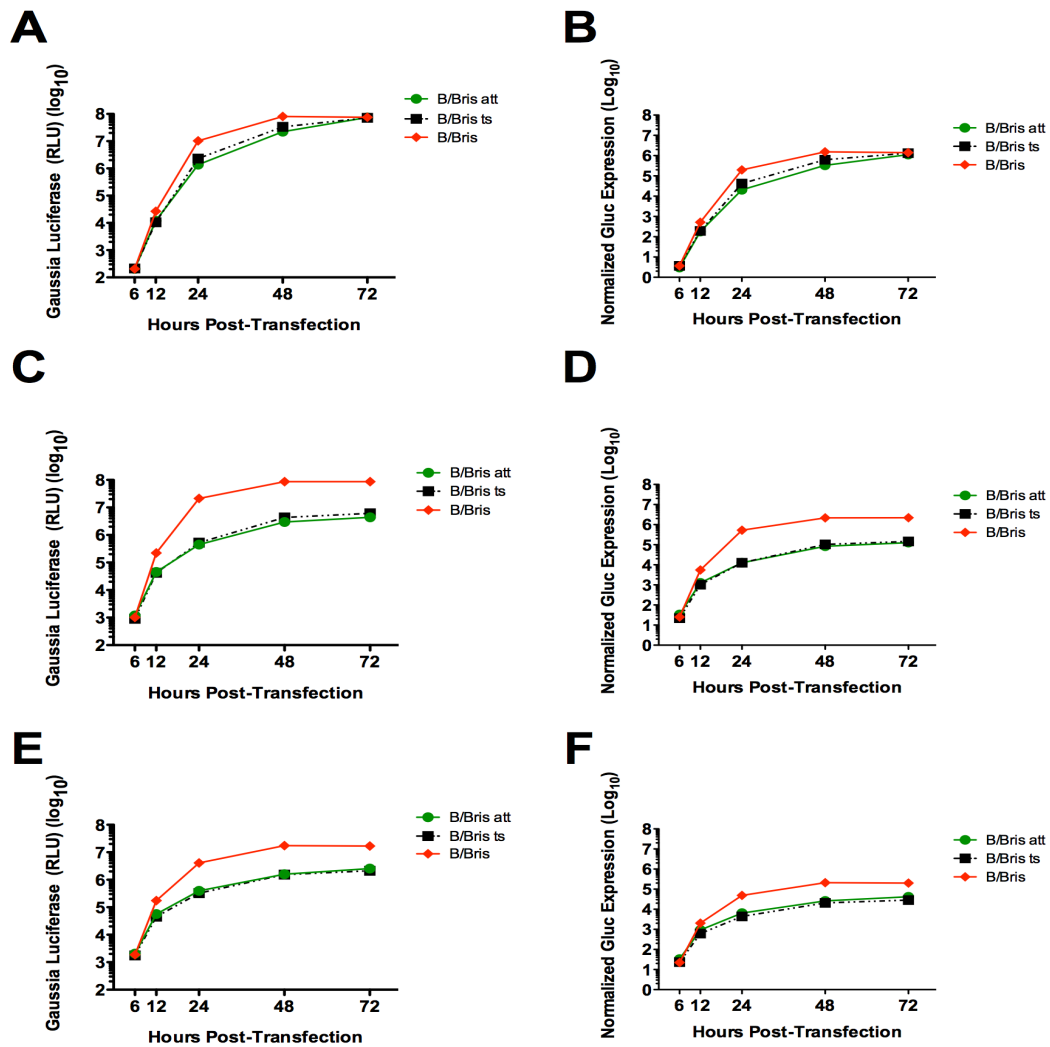


Figure 5.1. Mini-genome assay results for B/Bris *att* and *ts* polymerase complexes. Assays were carried out at 33°C (A and B), 35°C (C and D) and 37°C (E and F). Supernatant was collected at 6, 12, 24, 48 and 72hpt. Left panels: raw GLuc Expression. Right panels: normalized GLuc expression. Red: WT. Green: B/Bris *att*. Black dashes: B/Bris *ts*.

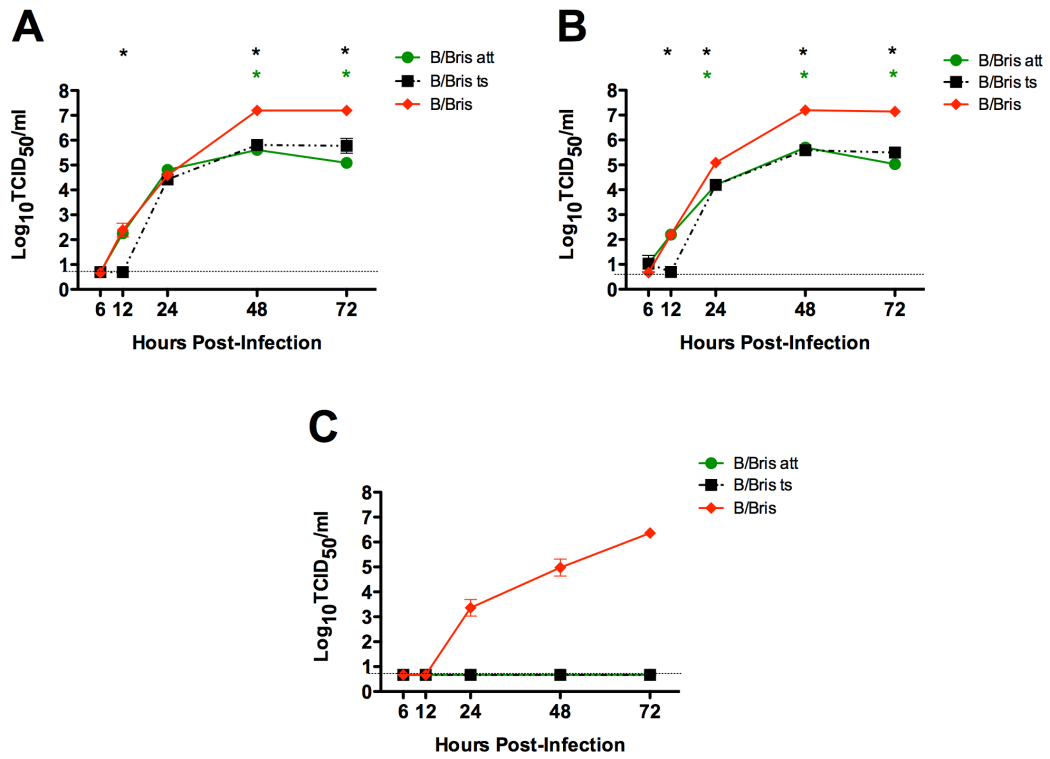


Figure 5.2. Growth kinetics assay results for B/Bris *att* and *ts* vaccine candidates. Assays were carried out at 33°C (A), 35°C (B) and 37°C (C). Supernatant was collected at 6, 12, 24, 48 and 72hpi. Samples were titrated by TCID₅₀. Red: WT, Green: B/Bris *att*, Black dashes: B/Bris *ts*. Asterisk indicates $p < 0.05$, the color of the asterisk indicates that the corresponding virus is significantly different from WT.

5.4.2. B/Bris *ts* and *att* viral titers are undetectable at 37 and 39°C

Next, growth kinetics of the B/Bris *ts* and *att* viruses were evaluated. MDCK cells were infected with 1mL of 0.01 MOI virus, and assays were performed at 33, 35, 37 and 39°C. As with the polymerase assays, time points were collected at 6, 12, 24, 48 and 72 h post-infection (hpi). Following completion of each assay, viral titers were determined by TCID₅₀.

Overall, the results are consistent with the polymerase activity. At 33°C, the B/Bris *ts* and *att* viruses grew to similar titers as the WT, although at late time points the WT grew to significantly higher titers (Fig. 5.2A). Interestingly, in contrast to the mini-genome assay results, B/Bris *ts* and *att* viruses also grew to similar titers at 35°C; however, at the 24, 48, and 72 h time points, the WT virus grew to significantly higher titers than both vaccine candidates (Fig. 5.2B). At 37°C, neither the B/Bris *ts* nor the *att* viruses grew to detectable viral titers, while the WT virus grew to low but detectable titers, reaching roughly 10⁵ TCID₅₀ by 48 hpi (Fig. 5.2C). None of the B/Bris viruses grew to detectable titers at 39°C, consistent with the polymerase data (data not shown). In all, viral growth of the B/Bris *ts* and *att* viruses was restricted to low temperatures.

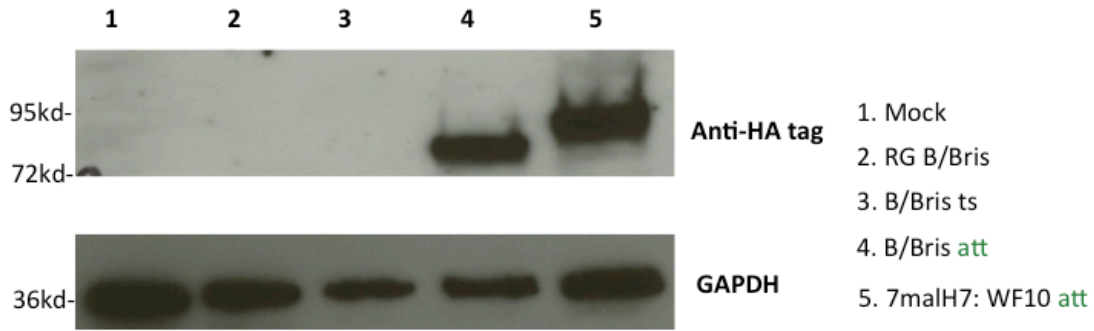


Figure 5.3. B/Bris att expression of HA tag. Using a mouse anti-HA-tag primary antibody, a western blot was performed to detect PB1HA proteins expressed by B/Bris att and the positive control virus, 1malH7: WF10att, lanes 4 and 5 respectively. To control for overall protein expression, another western blot was done to assess GAPDH expression. Negative controls included a mock infected well, lane 1, WT RG-B/Bris, lane 2, and B/Bris ts, lane 3. MDCK cells were infected with 1MOI of each virus at 33°C. After 20 h, supernatant was aspirated, and samples were prepared for western blotting. The anti-HA tag film was developed after a 30 sec exposure while the anti-GAPDH film was developed after a 1 sec exposure time.

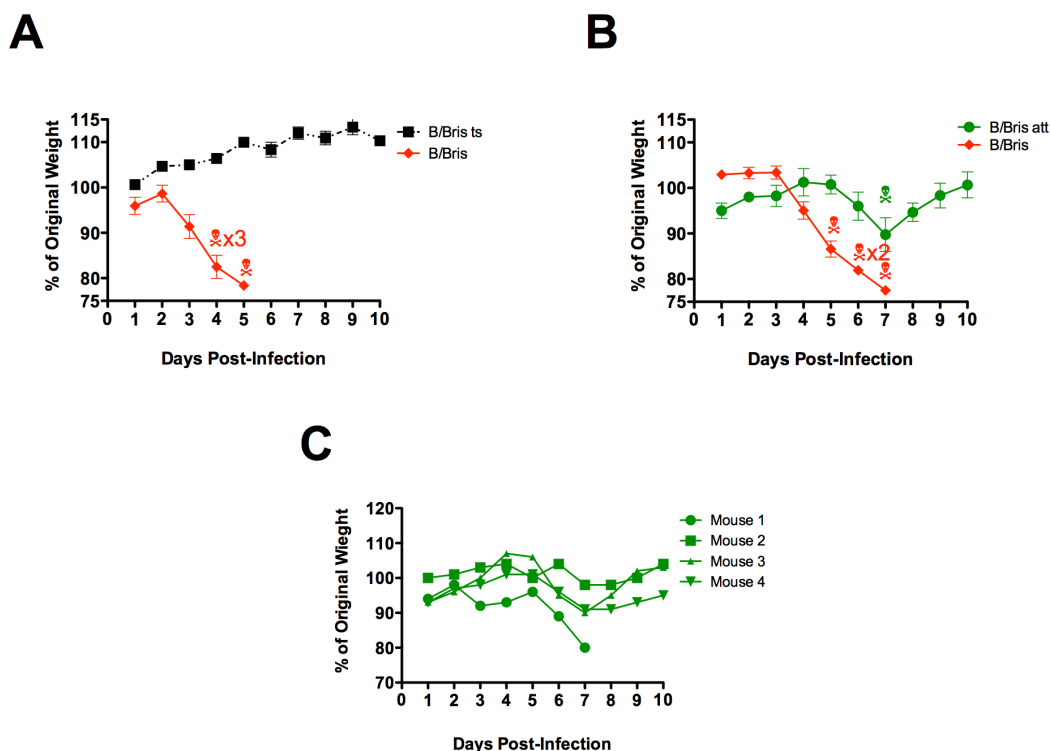


Figure 5.4. Vaccine safety studies: weight loss of B/Bris *ts* and B/Bris *att* inoculated mice. Mice were inoculated intranasally with 50 μ L of 10⁷ EID₅₀ of each virus and monitored for weight loss and signs of disease for 12 days post-inoculation. The skull and cross bones indicate a dead/ethanized mouse. B/Bris *ts* safety study (A) B/Bris *att* safety study (B) Individual weight loss of B/Bris *att* mice (C). Red: WT RG-B/Bris. Green: B/Bris *att*. Black dashes: B/Bris *ts*. Note that B/Bris *ts* and *att* safety studies were performed independently. Each group, n=4

B/Bris <i>att</i>	HI Titer	B/Bris <i>ts</i>	HI Titer
Mouse 1	160-320	Mouse 1	80-160
Mouse 2	160	Mouse 2	40
Mouse 3	40	Mouse 3	40
Mouse 4	40	Mouse 4	20
Mouse 5	80		

Table 5.1. B/Bris *att* and *ts* inoculated mice HI titers (21dpi). Mice were inoculated with 50 μ L of 10⁶ EID₅₀ virus. HI assays were performed against WT B/Brisbane/60/2008. Results are shown. Note that there was an extra mouse for the B/Bris *att* experiment at 10⁶. It is included here.

5.4.3. B/Bris *att* expresses the HA tag

To complete the *in vitro* characterization of the vaccine candidates, a western blot was performed to determine whether the B/Bris *att* virus expresses the HA tag from the PB1 ORF. First, MDCK cells were infected with 1 MOI of each virus: B/Bris *ts*, B/Bris *att*, WT RG-B/Bris and 1malH7: WF10 *att* (IAV positive control), and mock (314). After infection, the cells were placed at 33°C for 20 h.

The western blot clearly shows that the B/Bris *att* virus, not the B/Bris *ts* virus, expresses an HA tag from PB1. Notably, the B/Bris PB1 *att* protein ran lower than the IAV 1malH7: WF10 *att* positive control virus, as influenza B PB1 protein is smaller than that of influenza A (Fig. 5.3). Additionally, although it may appear as though protein expression from 1malH7:WF10 *att* virus was stronger than that of B/Bris *att*, this is not likely the case. Given the expression of GAPDH, this difference is more likely a result of greater overall protein expression in the 1malH7: WF10 *att* infected well (Fig. 5.3).

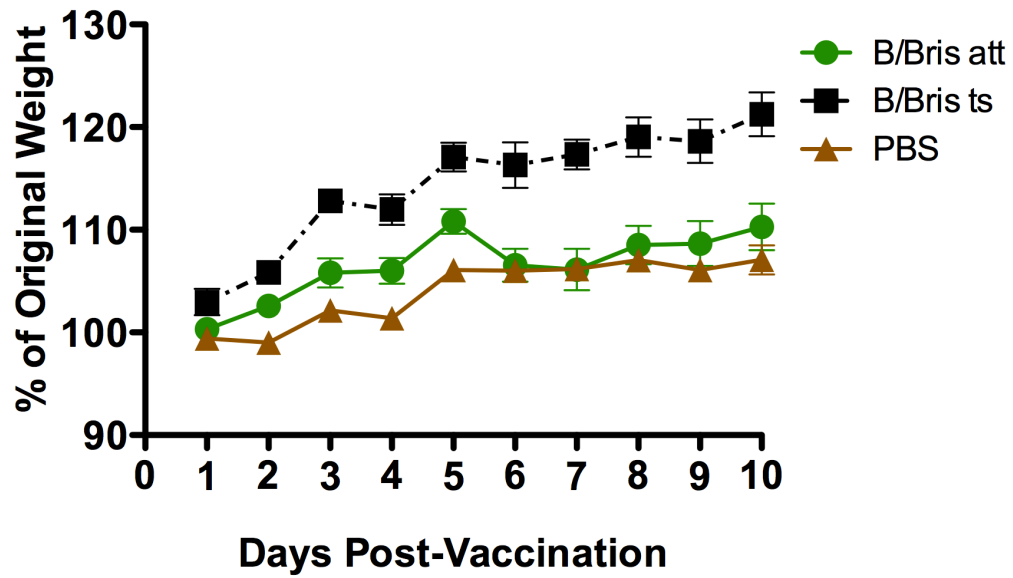


Figure 5.5. Weight loss post-vaccination. Mice were inoculated with 50 μ L intranasally of a vaccine candidate at a dose of 10^6 EID₅₀/mL or with PBS. Weight changes are shown. Brown: PBS, Green: B/Bris *att*. Black dashes: B/Bris *ts*. Each group, n=8

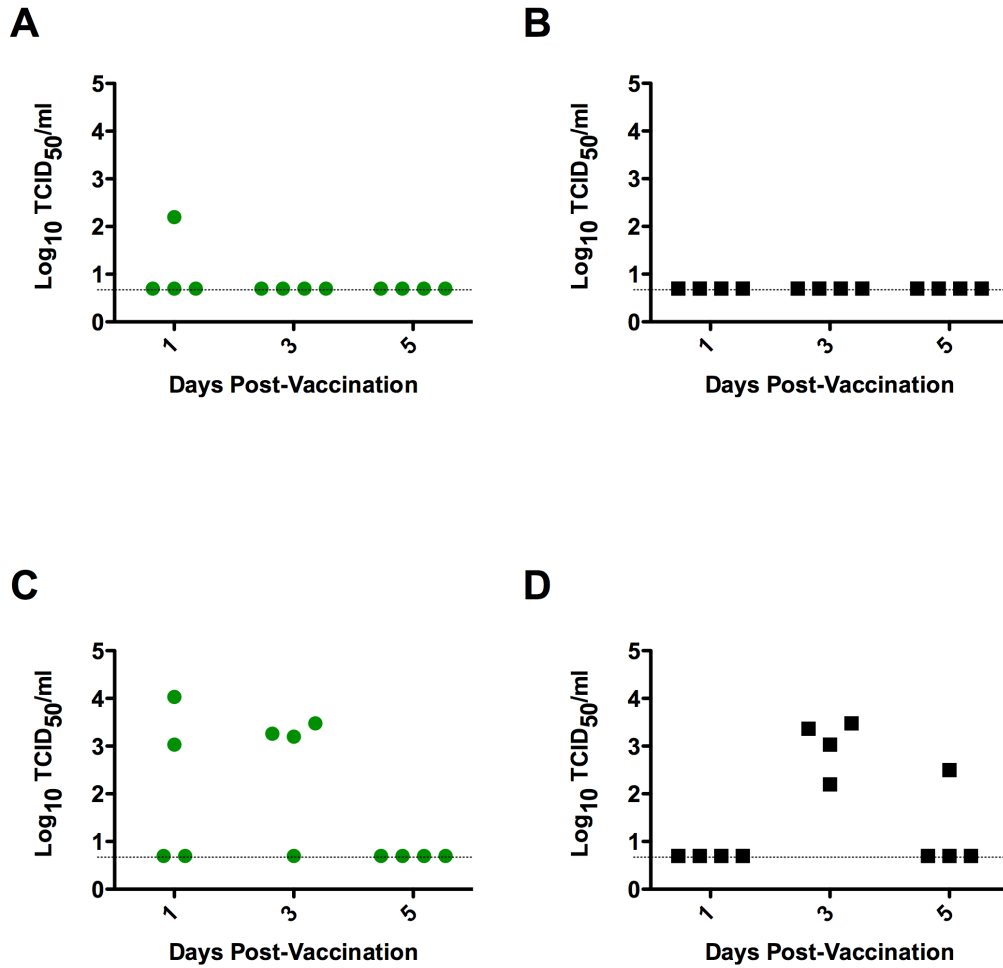


Figure 5.6. Post-vaccination tissue titers. Nasal turbinates and lung tissues were harvested on days 1, 3 and 5 post-vaccination. Tissue was homogenized in PBS and titrated by TCID₅₀. Results are shown. B/Bris *att* lung titers (A) B/Bris *ts* lung titers (B) B/Bris *att* nasal turbinates titers (C) B/Bris *ts* nasal turbinates titers (D). Green: B/Bris *att*. Black dashes: B/Bris *ts*. Each group, n=4

5.4.4. Vaccine safety studies show B/Bris *ts* and *att* viruses are safe and immunogenic in mice

Prior to a vaccine study, the B/Bris *ts* and *att* viruses were evaluated for safety and immunogenicity in female 5-6 week old DBA/2 mice. Mice were inoculated intranasally with 50 μ L of 10⁷, 10⁶, or 10⁵ EID₅₀ of the B/Bris *att*, B/Bris *ts* or WT RG-B/Bris virus. Weight loss and signs of disease were monitored for 12 days post-inoculation. On day 21, mice were exsanguinated for serology.

Both vaccine candidates were safe at all doses, while all WT inoculated mice in the 10⁷ and 10⁶ EID₅₀ dosage groups either succumbed to infection or had to be humanely euthanized (Fig. 5.4, data not shown, respectively). It should be noted, however, that one mouse in the B/Bris *att* 10⁷ EID₅₀ inoculated group had to be euthanized due to weight loss late during the time course of infection (Fig. 5.4B). Also noteworthy, though, is that this mouse was the only mouse in its group to lose significant weight (Fig 5.4C). Importantly, at 10⁶ EID₅₀, the vaccine dose, neither vaccine candidate caused weight loss or death.

To evaluate the immunogenicity of these vaccine candidates, HI titers were assessed against WT B/Brisbane/60/2008 on day 21 sera from the 10⁶ EID₅₀ dosage groups. Nearly all B/Bris *att* and *ts* mouse sera had HI titers of greater than or equal to 40, suggesting that nearly all mice developed an antibody response equivalent to or greater than the standard correlate of protection (Table 5.1).

5.4.5. Vaccine study: no weight loss post-vaccination

To assess efficacy of the vaccine candidates, 5-6 week old female DBA/2 mice were vaccinated with 50 μ L intranasally of 10⁶ EID₅₀ of either the B/Bris *att* virus, the B/Bris *ts* virus or PBS. Each mouse was monitored for weight loss and signs of disease for 12 days post-vaccination. Consistent with the safety studies, none of the *att* or *ts* vaccinated mice showed any weight loss post-vaccination nor did any of the mice show signs of disease. Finally, all weight changes were comparable to those seen in the PBS group (Fig. 5.5).

5.4.6. B/Bris *att* and *ts* vaccine replication is restricted to growth in nasal turbinates

Viral tropism of the vaccine viruses was established in mice post-vaccination to determine if either the B/Bris *att* or *ts* viruses replicated in the lungs. On days 1, 3 and 5 post-vaccination, nasal turbinates and lung tissues were harvested from 4 mice in each vaccine group and 3 mice in each PBS group. Tissues were then homogenized, clarified and titrated by TCID₅₀.

The results showed that neither the B/Bris *att* nor *ts* vaccine viruses replicated in mouse lung, although 1 B/Bris *att* vaccinated mouse had a low but detectable viral titer in the lung on day 1 post-vaccination (Fig. 5.6A and B). These findings are consistent with the polymerase assay and growth kinetics results, which found little to

no activity or growth at 37°C. In contrast, viral titers of both B/Bris *att* and *ts* vaccinated mice were detected in the nasal turbinates, also consistent with both the polymerase assays and growth kinetics at 33°C (Fig. 5.6C and D).

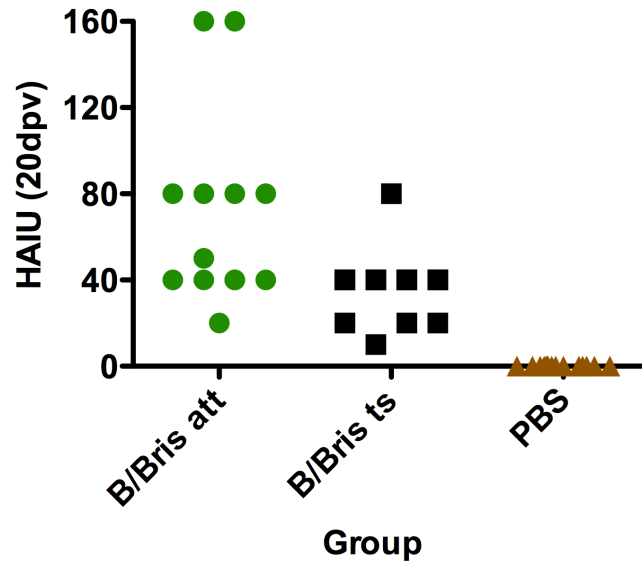


Figure 5.7. HI titers 20 days post-vaccination. Mice were bled 10% of their body weight on day 20 post-vaccination. HI assays were performed to determine pre-challenge HI titers. Brown: PBS. Green: B/Bris *att*. Black: B/Bris *ts*. Sera from 11 mice per group were assessed.

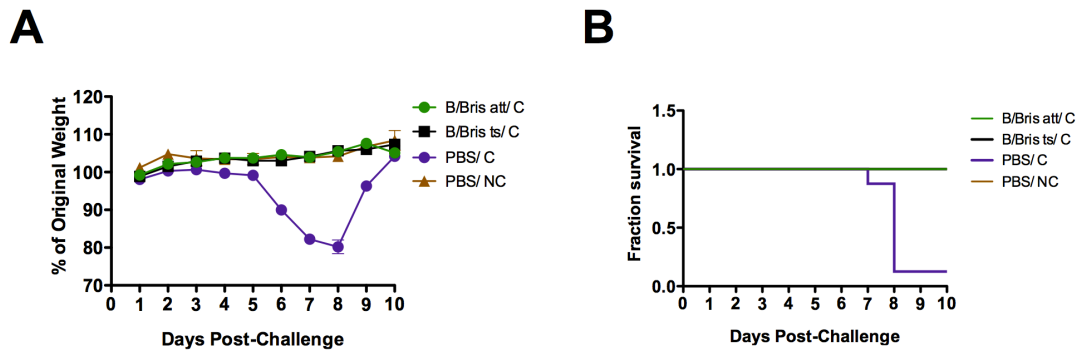


Figure 5.8. Weight loss and survival post-challenge. Mice were challenged with 100 MLD₅₀ of the challenge virus. A) Weight loss B) Survival. Brown: PBS/ NC. Purple: PBS/ C. Green: B/Bris *att*/ C. Black dashes: B/Bris *ts*/ C. Each group, n=8.

5.4.7. Pre-challenge HI assays reveal detectable HI titers in B/Bris *att* and *ts* vaccinated mice

In order to assess pre-challenge HI titers, all mice were bled on day 20 post-vaccination, and HI assays were then performed against WT B/Bris. The HI assay results were consistent with the HI results from the safety studies. Additionally, there was a trend towards higher HI titers in the B/Bris *att* vaccinated mice as compared to the B/Bris *ts* vaccinated mice (Fig. 5.7). Interestingly, some B/Bris *att* and *ts* vaccinated mice showed no seroconversion. There were insufficient mouse sera to perform HI assays on all mice bled; however, sera from the majority of mice (11/14) from each group were assessed, and equal numbers of samples were acquired for the B/Bris *att* and *ts* vaccinated groups.

5.4.8. No weight loss in B/Bris *att* or *ts* vaccinated mice post-challenge

All vaccinated and mock-vaccinated mice were challenged with 100 MLD₅₀ of a homologous B/Bris virus except for 1 group that was mock-challenged with PBS. Nearly all mock-vaccinated and challenged mice (PBS/ C) either succumbed to infection or had to be humanely euthanized by day 8 post-challenge, while all B/Bris *att* and B/Bris *ts* vaccinated mice survived challenge (Fig. 5.8B). Not only was no weight loss seen in any of the vaccinated mice, but also, change in weight over time

for the B/Bris *att* and *ts* vaccinated groups post-challenge was indistinguishable from the mock-vaccinated/mock-challenge mice (PBS/NC) (Fig. 5.8A).

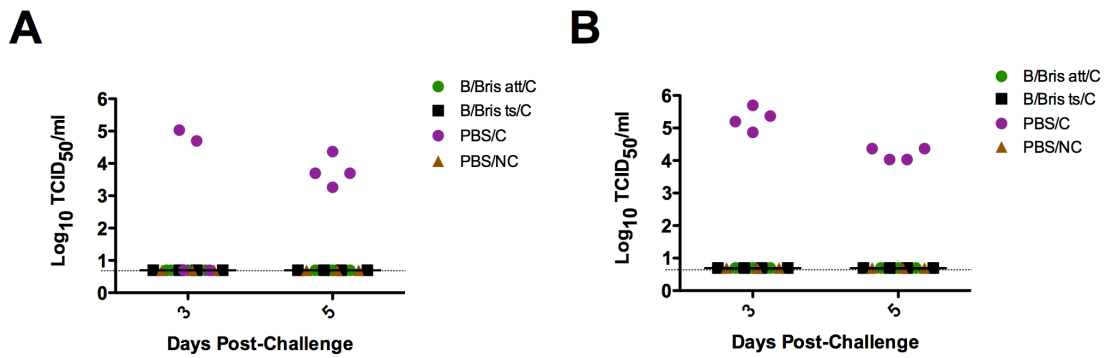


Figure 5.9. Post-challenge tissue titers. Nasal turbinates and lungs were homogenized in PBS and titrated by TCID₅₀. Results are shown. Lung titers (A) Nasal turbinate titers (B). Brown: PBS/ NC. Purple: PBS/ C. Green: B/Bris *att*/ C. Black: B/Bris *ts*/ C. Each group, n=4; PBS/ NC, n=3

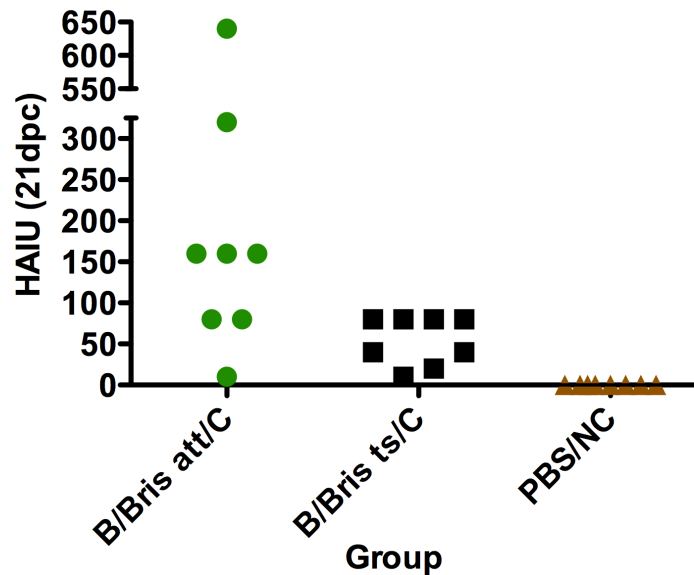


Figure 5.10. Post-challenge HI titers. Mice were exsanguinated on day 21 post-challenge. HI assays were performed to determine post-challenge HI titers. Brown: PBS/ NC. Purple: PBS/ C. Green: B/Bris *att*/ C. Black: B/Bris *ts*/ C. Each group, n=8

5.4.9. No virus detected in tissues of B/Bris *att* or *ts* vaccinated mice post-challenge, suggests sterilizing immunity

Lung and nasal turbinates were harvested from the B/Bris *att*/C, B/Bris *ts*/C, PBS/C and PBS/NC groups on days 3 and 5 post-challenge and titrated by TCID₅₀. No virus was detected in the B/Bris *att* or *ts* vaccinated mice on days 3 or 5 post-challenge in either the lungs or the nasal turbinates, thus titers were indistinguishable from the PBS/NC group. In contrast, virus was detected in both the lungs and nasal turbinates of the PBS/C mice on days 3 and 5 post-challenge (Fig. 5.9). These results suggest sterilizing immunity in all vaccinated mice.

5.4.10. Increased HI titers in vaccinated mice post-challenge

In order to determine post-challenge HI titers of all remaining mice, mice were exsanguinated on day 21 post-challenge, and HI assays were performed on all sera against WT B/Bris. As anticipated, PBS/ NC had no detectable HI titers against B/Bris whereas HI titers were detected in B/Bris *att*/ C and *ts*/ C mice sera. Similar to the post-vaccination HI results, there was a trend towards higher HI titers in the B/Bris *att* vaccinated mice in comparison to the B/Bris *ts* vaccinated group. Overall, HI titers of all vaccinated mice were higher than those found pre-challenge, suggesting that all mice were properly challenged (Fig. 5.10). Finally, the only surviving mouse from the PBS/ C group had an HI titer of 320.

5.4.11. Increased pulmonary pathology in PBS/C group post-challenge

Post-challenge tissue pathology was assessed by a board certified pathologist. Bronchiole, alveolar, vascular, total/extent lung and tracheal tissues were scored on a scale of 0-4 where a score of 4 indicated severe pathology. Overall, tissue pathology was similarly mild amongst the PBS/NC, B/Bris *att*/C and B/Bris *ts*/C groups. All PBS/NC tissue evaluated had a total/extent lung score of 1 on days 3 and 5 post-challenge while nearly all vaccinated mice had a total lung score of 2 on the same days. The most severe pathology in the vaccinated mice was in the bronchioles (bronchiole score of 2 for nearly all mice) in which minimal epithelial lesions were observed. Mice of all groups, including PBS/C, scored either 0 or 1 in tracheal and vascular pathology; however, one B/Bris *ts* vaccinated mouse did have a vascular score of 3 (Table 5.2).

The PBS/C mouse tissues showed more severe pathology than the vaccinated and mock-vaccinated groups. For instance, PBS/C mice had total lung scores of 3 on days 3 and 5 post-challenge, and the most severe pathology was found in the alveolar tissue. This tissue of mice in this group showed some necrosis, thickening of the alveolar walls and the presence inflammatory cells (Table 5.2).

Finally, representative images of pulmonary pathology for each group on each day post-challenge were taken (Fig. 5.11). Consistent with the pathology scores, pathology in all B/Bris *att*/C, B/Bris *ts*/C and PBS/NC images are similar, but

pathology in the PBS/C group, particularly on day 5 post-challenge, is visibly more severe than in the other groups.

Mouse	dpc	Extent	Bronchioles	Aveoli	Vascular	Trachea
B/Bris <i>ts</i> /C	3	2	2	2	3	1
B/Bris <i>ts</i> /C	3	2	2	1	2	1
B/Bris <i>ts</i> /C	5	1	1	0	1	0
B/Bris <i>ts</i> /C	5	2	2	2	1	1
B/Bris <i>att</i> /C	3	2	2	1	2	0
B/Bris <i>att</i> /C	3	2	2	2	1	1
B/Bris <i>att</i> /C	5	2	2	2	1	0
B/Bris <i>att</i> /C	5	2	2	2	1	1
PBS/C	3	3	2	3	1	1
PBS/C	3	3	2	3	2	1
PBS/C	5	1	1	0	1	1
PBS/C	5	3	2	3	2	1
PBS/NC	3	1	1	1	1	0
PBS/NC	5	1	1	1	1	0

Table 5.2. Tissue pathology post-challenge. Scores were assigned from 0-4, 4 being severe pathology. Scores for days 3 and 5 post-challenge are shown. Days post-challenge: dpc. Scores from 2 mice per group per day are shown, except for the PBS/NC group (1 mouse/day shown).

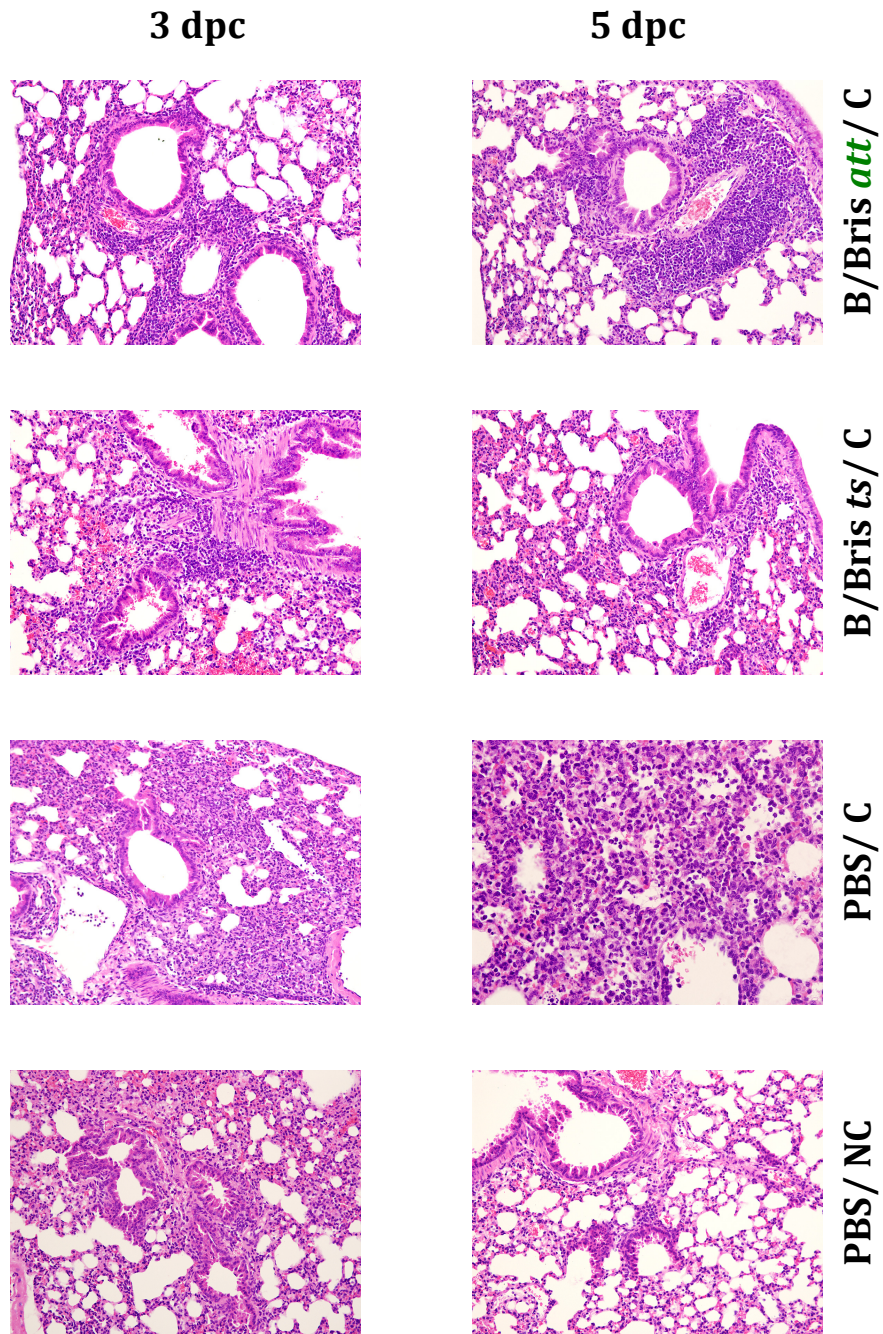


Figure 5.11. Post-challenge representative pulmonary pathology images. Representative images are shown for each group on days 3 and 5 post-challenge. Right column: 3 dpc. Left column: 5dpc. All images are 200x magnification.

5.4.12. Enhanced stability of B/Bris *att* virus over the B/Bris *ts* virus

To assess the stability of the vaccine candidates, the B/Bris *att* and *ts* virus vaccines were passaged 10 times in eggs. After 10 passages, PB1 was sequenced to determine which mutations were present and whether any other mutations arose. Results showed that by egg passage 2 the K391E mutation reverted in the B/Bris *ts* vaccine, although no additional mutations were identified in subsequent passages. In stark contrast to these results, the B/Bris *att* mutations remained stable throughout all 10-egg passages; nonetheless, an additional mutation at position 48 (E to K) was identified in egg passages 9 and 10. This E48K mutation will have to be investigated to determine if it affects safety.

In addition to testing the stability of the vaccine viruses in eggs, RNA extracted from B/Bris *att* and *ts* vaccinated mice nasal turbinates from day 3 post-vaccination was sequenced. Consistent with the egg passage results, PB1 of B/Bris *ts* was unstable at position 391. Indeed, there was a mixed base causing a mixed amino acid, both K and E, at position 391. Once again, the B/Bris *att* virus was stable as all three mutations and the HA tag were confirmed present. No additional mutations were found in either virus extracted from nasal turbinates.

5.5. Discussion

This study described the development of two IBV vaccine candidates carrying PB1 mutations (K391E, E580G and S660A), B/Bris *att* and B/Bris *ts*, which differ only in the presence of an HA tag at the C-terminus of PB1 in B/Bris *att*. The data suggests that both vaccines are temperature sensitive, cold-adapted and attenuated. The temperature sensitive phenotype was evident in the absence of normalized GLuc expression and viral growth of B/Bris *att* and *ts* at 37°C while the high GLuc expression and growth of the B/Bris *att* and *ts* viruses at 33°C demonstrated that each is cold-adapted. Finally, the absence of B/Bris *att* and *ts* viral replication in the lungs of mice suggests that both viruses are attenuated. These growth characteristics are consistent with those of the currently licensed B/Ann Arbor cold-adapted backbone and are ideal for a safe LAIV vaccine (208, 259, 260, 263).

Consistent with the temperature sensitive, cold-adapted and attenuated growth characteristics displayed by B/Bris *att* and *ts*, both vaccine candidates were safe in mice, causing virtually no weight loss even at a high dose of 10^7 EID₅₀, and each virus was restricted to growth in the nasal turbinates. Upon a 100 MLD₅₀ challenge, all vaccinated mice showed sterilizing immunity to the challenge virus as no virus was detected in the lungs or nasal turbinates of vaccinated mice on either of the days assayed; furthermore, no weight loss was seen in any vaccinated mice post-challenge. In contrast, all but 1 mouse of the mock-vaccinated/challenge group (PBS/C) succumbed to infection; however, the surviving mouse saw nearly 20% weight loss post-challenge.

Although the B/Bris *att* and *ts* vaccine candidates behaved similarly both *in vitro* and *in vivo*, there were differences in stability and immunogenicity; furthermore, given that the B/Bris *att* and *ts* viruses differ only in the presence of the HA tag, it is the likely cause of the dissimilarities that were observed. Previously, our lab showed that an HA tag in the context of IAV enhances stability, safety and efficacy of viruses carrying the PB2 and PB1 mutations found in A/Ann Arbor cold-adapted backbone, and similar to these findings, the B/Bris *att* and *ts* egg passage experiment demonstrated that the HA tag enhances stability of the PB1 mutations *in ovo* (1, 315-317). No changes were seen in the B/Bris *att* PB1 segment through 8 passages in eggs, although a spurious mutation, E48K, was identified by passage 9; however, all the desired mutations were maintained (K391E, E580G, S660A and HA tag). In contrast, the B/Bris *ts* virus, absent an HA tag, was unstable after just 2 passages in eggs. Similar findings were made in sequencing virus from the nasal turbinates of vaccinated mice. Additionally, the HI results post-vaccination and post-challenge suggest that the presence of the HA tag may enhance immunogenicity of the vaccine. In each case, HI titers tended to be higher in the B/Bris *att* vaccinated mice, but notably, both the B/Bris *att* and *ts* vaccines were immunogenic.

The variation in stability between the B/Bris *att* and *ts* viruses offers some insight into which mutations are primarily responsible for attenuation. Despite the instability of the B/Bris *ts* vaccine *in vivo*, no weight loss, disease signs or viral replication in the lungs were observed which suggests that the stable E580G and S660A mutations were sufficient to attenuate the virus and prevent replication at 37°C, the temperature of the mouse lower respiratory tract (358). Interestingly, the

temperature sensitive phenotype of the A/Ann Arbor cold-adapted backbone is determined primarily by the PB1 mutations, K391E and E581G, although A661T also contributes, yet the data presented here suggest that the K391E mutation may not be critical for attenuation of WT RG-B/Bris (310).

This study shows that 3 mutations, rather than the licensed 7 mutations found in the B/Ann Arbor cold-adapted backbone, are sufficient to attenuate WT RG-B/Bris in the context of the mouse model. Importantly, the 3 mutations incorporated into the B/Bris *att* and *ts* vaccines (K391E, E580G and S660A) are analogous to a subset of the mutations present in the A/Ann Arbor cold-adapted backbone (310, 314, 356). Further studies must be done to evaluate the IgA and IgG responses to the B/Bris *att* vaccine as they relate to cross-protection in adult and aged mice. Aged mice could also be used to evaluate the efficacy of administering an alternative LAIV vaccine on a contemporary backbone, B/Bris *att*, after repeated exposure to the B/Ann Arbor backbone. This would give insight into the potential of enhancing the vaccine response in the elderly by using a more contemporary backbone. Finally, another possibility for future study is adapting the B/Bris *att* vaccine to other species such as chickens to be used as a DIVA vaccine.

Chapter 6: Conclusions and Future Directions

6.1. Conclusions

The work described here sought to develop an alternative reverse genetics based live-attenuated (LAIV) influenza B virus (IBV) vaccine. To do this, a contemporary IBV isolate, B/Brisbane/60/2008 was cloned. In the process of developing the vaccine, a novel cloning strategy for IBV was developed and virulence factors of B/Brisbane/60/2008 were identified.

The impetus for developing an alternative LAIV IBV vaccine based on a contemporary IBV isolate was three fold. Firstly, our lab required an IBV strategy, which complemented our alternative LAIV influenza A virus (IAV) vaccine in order to develop a quadrivalent vaccine (1, 315-317, 357). Secondly, there is a need for LAIV vaccines that enhance the immune response in immunosenescent individuals who have repeatedly been exposed to the currently licensed LAIV vaccine backbones which were originally isolated roughly 50 years ago (220, 223, 258, 290, 292, 294, 295). Finally, vaccination of poultry against IAV is a significant problem as it is difficult to distinguish infected from vaccinated animals and administering standard IAV LAIV vaccines, which are considered to be the most efficacious, risks reassortment of the LAIV vaccine with virulent circulating strains; therefore, another strategy that could serve as a DIVA (Differentiating Infected from Vaccinated Animals) vaccine without risk of recombination is essential.

This dissertation describes several firsts in the field. For instance, to our knowledge, the wild-type (WT) reverse genetics (RG) B/Brisbane/60/2008 is the most modern B/Victoria-like reverse-genetics virus available, and the manner in which it was cloned, 2-step RT-PCR, is a novel cloning strategy for IBV. This dissertation also contains the first description of PB2 cap-binding mutants F406Y and W359F as virulence factors in mice. Finally, the B/Brisbane/60/2008 *att* vaccine strategy marks the first time that mutations analogous to those found in A/Ann Arbor cold-adapted have been shown to attenuate IBV; furthermore, this vaccine strategy shows that only 3 mutations rather than the licensed 7 mutations present in the IBV-component of the LAIV seasonal vaccine are necessary to attenuate IBV (208, 220, 310).

6.1.2. Chapter 2 conclusions: A contemporary reverse genetics system for B/Brisbane/60/2008 grows to high titers and is virulent in mice

Chapter 2 described a reverse genetics RG-B/Brisbane/60/2008 (RG-B/Bris) virus generated by a 2-step RT-PCR system. In this 2-step system, “universal” reverse transcription primers are used to target specific segments of the IBV genome, and then, cloning primers are used to amplify individual segments. After generating RG-B/Bris using this system, the virus was characterized. The results showed that this virus rescues efficiently, grows to high titers, behaves similarly to the WT B/Brisbane/60/2008 virus and is virulent in mice. Finally, phylogenetic analysis of RG-B/Bris demonstrated that it is a contemporary virus closely related and in the

same clade as all recent B/Victoria-like IBV sequences. The cloning of this reverse genetics virus permitted the development of a contemporary LAIV IBV platform vaccine that grows titers suitable for vaccine production and is testable in an animal model.

6.1.3. Chapter 3 conclusions: PB2/PB1 mutant vaccine strategy is lethal in mice

Chapter 3 describes a first attempt to develop an alternative IBV vaccine strategy that would complement our lab's influenza A virus (IAV) HA tag strategy. In this study, 2 vaccine candidates, each carrying an HA tag at the C-terminus of PB1 and a cap-binding mutation in PB2, were designed. While each of these vaccine candidates appeared to show signs of attenuation *in vitro* in comparison to the WT RG-B/Bris, both were lethal at the desired vaccine dose of 10^6 EID₅₀ in a DBA/2 mouse model. This was surprising given that cap-binding mutations have previously been shown to be attenuating and that the HA tag has been proven to enhance safety and efficacy in the context of our IAV strategy. The mortality seen in mice caused by the PB2/PB1 mutants precipitated the characterization of the PB2 cap-binding mutants described in Chapter 4.

6.1.4. Chapter 4 conclusions: PB2_F406Y and PB2_W359F are virulence factors of B/Brisbane/60/2008

Chapter 4 sought to characterize PB2 F406Y and W359F cap-binding mutations in the context of WT RG-B/Bris. The results showed that each of these mutations had enhanced virulence and pathogenicity in comparison to WT RG-B/Bris in a DBA/2 mouse model. The cap-binding mutant viruses were shown to enhance virulence and pathogenicity early in infection in comparison to the WT virus, showing pathology as early as day 3 post-infection. Although there is some evidence that these viruses replicate better at 37°C, the enhanced virulence is likely related to host factors; however, more research is required to determine if this is the cause. Regardless of the means by which enhanced disease is achieved, these mutations present tools to facilitate the study of pathogenesis and vaccine efficacy in mice.

6.1.5. Chapter 5 conclusions: B/Bris *att* is stable, safe and immunogenic in mice

Chapter 5 describes the evaluation of two vaccine candidates, B/Bris *att* and *ts*, for safety, efficacy and immunogenicity in a DBA/2 mouse model. B/Bris *att* and B/Bris *ts* differ only in the presence of an HA tag at the C-terminus of PB1; each virus contains 3 amino acids mutations in PB1 analogous to those present in the PB1 segment of the A/Ann Arbor cold-adapted backbone and our A/turkey/Ohio/2004 (H3N2) and A/guinea fowl/Hong Kong/WF10/99 (H9N2) *att* backbones. *In vitro*

growth kinetics assays confirmed that both vaccine candidates grow to high titers at low temperatures (33°C) but are temperature sensitive at high temperatures (37°C). Additionally, both vaccine candidates were safe, immunogenic and efficacious against a 100 MLD₅₀ homologous challenge, and both induced sterilizing immunity. Despite the similar safety and efficacy findings, these viruses differed in stability and immunogenicity. B/Bris *att* was stable up to 10 passages in eggs and tended to generate greater serum immunity, while the B/Bris *ts* vaccine was unstable after just 2 egg passages and tended to generate lower serum immunity compared to B/Bris *att*. The results clearly indicate that 3 mutations analogous to those found in the IAV-component of the licensed LAIV vaccine rather than the 7 licensed IBV-component LAIV mutations are sufficient to attenuate IBV.

6.2. Future Directions

6.2.1. Determine efficacy of the B/Bris *att* backbone in the context of a quadrivalent vaccine

Future work with the B/Bris *att* backbone must be done in the context of a quadrivalent vaccine which would incorporate our Ty/04 *att* influenza A platform carrying H1 and H3 surface genes as well as our B/Bris *att* platform carrying representative HAs from B/Yamagata-like and B/Victoria-like HA antigenic lineages. Given the phylogenetic analyses discussed in Chapter 2 of HA and NA IBV isolates which clearly show two NA lineages diverging with the HA antigenic lineages, NA segments corresponding to each lineage should also be incorporated to prevent IBV infection post-vaccination as a result of reassortment of the NA segment. This should first be done in a mouse model, and challenge viruses should include both homologous and heterologous challenges in order to test cross-protection of each strain represented in the vaccine.

6.2.2. Assess IgG, IgA and innate responses to vaccination

In addition to evaluating the efficacy of the B/Bris and Ty/04 *att* backbones in the context of a quadrivalent vaccine, IgG, IgA and innate responses to vaccination should be assessed. Analysis of the immune response is particularly important because the vaccine is live-attenuated and generates a more complex immune

response than KV formulations. This would most easily be done in a mouse model and should also be compared to a formalin-treated KV version of the quadrivalent vaccine. Additionally, IgA antibodies should be further evaluated for cross-reactivity with a panel of H1, H3, B/Victoria-like and B/Yamagata-like viruses, as IgA has been shown to be involved in cross-reactivity and heterologous protection (359).

6.2.3. Evaluate the B/Bris *att* backbone in a quadrivalent vaccine for ferrets

After analyzing the immune response and cross-protection of the quadrivalent vaccine in the mouse model, the vaccine must then be evaluated in the ferret model, as ferrets are the best model for human influenza illness available and allow for the study of transmission. Cross-protection should be evaluated in a ferret study in a manner similar to the mouse studies in 6.2.1 and 6.2.2 with homologous and heterologous challenges using contemporary IAV and IBV strains. Naïve ferrets should be co-housed with vaccinated ferrets immediately following vaccination, and viral shedding should also be assessed by nasal washing all ferrets in the days post-vaccination. Nasal washes should be titrated to ascertain if virus was shed, and the naïve ferrets should be bled for serology three weeks post-vaccination of their cage-mate. In this manner, one could determine whether there is risk of spread of the vaccine viruses post-vaccination in addition to determining whether the vaccines are efficacious and cross-reactive against a panel of contemporary viruses.

6.2.4. Analyze the immune response conferred by the B/Bris *att* vaccine in an aged mouse model

The B/Bris *att* vaccine must also be evaluated in an aged mouse model to provide justification for the use of a more contemporary vaccine backbone as an alternative to adjuvants in immunosenescent individuals. This study must be carried out over a long period of time, possibly a year or more, to be done thoroughly as the immune history of an elderly individual must be simulated through repeated ‘seasonal’ vaccinations with the B/Ann Arbor cold-adapted backbone. Then, once mice reach the appropriate age (18 months), they should be vaccinated with B/Bris *att* or B/Ann Arbor cold-adapted. IgA, IgG and T cell responses after vaccination in the now 18-month-old mice must be measured, and cross-reactivity of IgA and IgG with a panel of currently circulating influenza B viruses should also be analyzed to determine whether B/Bris *att* has enhanced heterologous reactivity in comparison to the B/Ann Arbor cold-adapted backbone. Differences in T cell responses between these groups should be closely evaluated since immunosenescence is associated with changing T cell immunity and it is important to discern whether B/Bris *att* induces a more robust T cell response. Finally, each group should be challenged with homologous and heterologous challenge viruses to assess whether there is enhanced protection in the B/Bris *att* vaccinated group compared to the B/Ann Arbor vaccinated group.

6.2.5. Adapt B/Bris *att* to birds for use as a DIVA vaccine

Adapting B/Bris *att* to birds would provide a vaccine vector for use in avian species that would carry no risk of becoming incorporated into the pool of circulating avian viruses, even if attenuating mutations were to revert, and would also function as a DIVA vaccine. IAV has been shown to be capable of tolerating the incorporation of IBV surface genes in cases where the IAV packaging signals have been maintained (360). Thus, provided the IBV packaging signals are maintained in HA and NA of B/Bris *att*, it is likely that IAV avian surface genes such as those from highly lethal avian H5N1 could be incorporated into B/Bris *att*, and then the B/Bris *att*-IAV virus could be adapted to birds such as chickens through serially passaging. Vaccinated chickens could then be distinguished from non-vaccinated via a standard RT-PCR assay to detect the PB1HA sequence.

Appendices

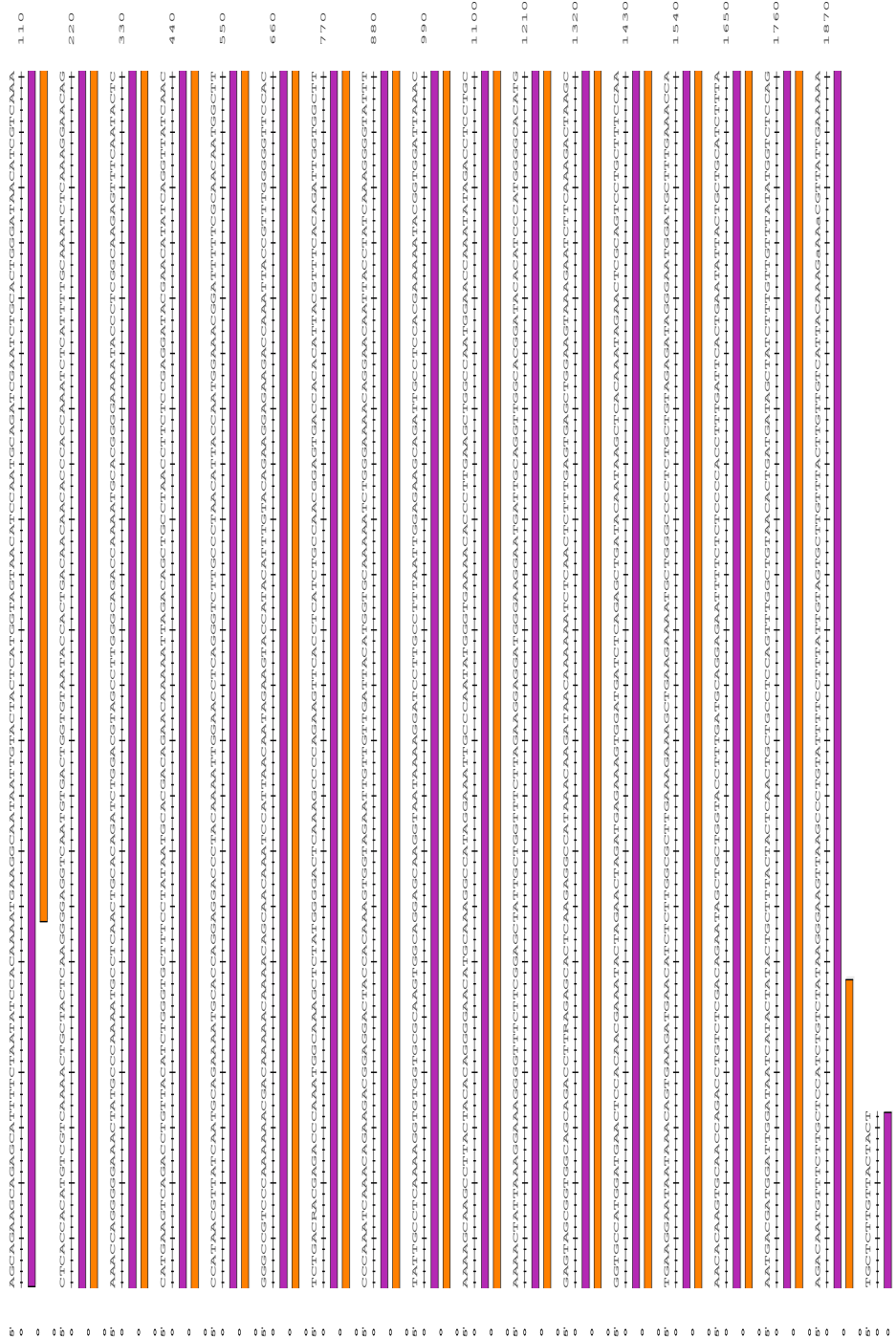
Reagents List

- 1 1.5 ml self-standing screw cap tube, mixed color caps, USA Scientific, Orlando, FL, 1415-9799
- 2 AarI, Thermo Scientific, ER1581
- 3 AMV Reverse Transcriptase, Promega, Madison, WI, M5101
- 4 Antibiotic/Antimycotic, Sigma-Aldrich, St. Louis, MO, A5955
- 5 Anti-HA tag mouse monoclonal antibody (6E2), Cell Signaling Technologies, Beverly, MA, 2367S
- 6 Anti-GAPDH mouse monoclonal antibody (65C), SantaCruz Biotech, Dallas, TX, sc-32233
- 7 BioLux® Gaussia Luciferase Assay Kit, New England Biolabs, Ipswich, MA, E3300
- 8 BigDye Terminator v3.1 Sequencing Kit, Applied Biosystems, Foster City, CA, 4337455
- 9 Blotting Grade Blocker, Bio-Rad, Berkeley, CA, 170-6404EDU
- 10 BsmBI, New England Biolabs, Ipswich, MA, R0580S
- 11 Chicken Blood in Alsevers, Lampire Biological Laboratories, Pipersville, PA
- 12 Clarity Western ECL Substrate, Bio-Rad, Berkeley, CA, 170-5060
- 13 Disposable Glass Pasteur Pipets, Fisher, Hampton, NH, 13-678-20D
- 14 Dulbecco's Modification of Eagle's Medium (DMEM), Corning, Corning, NY, 10-013-CM

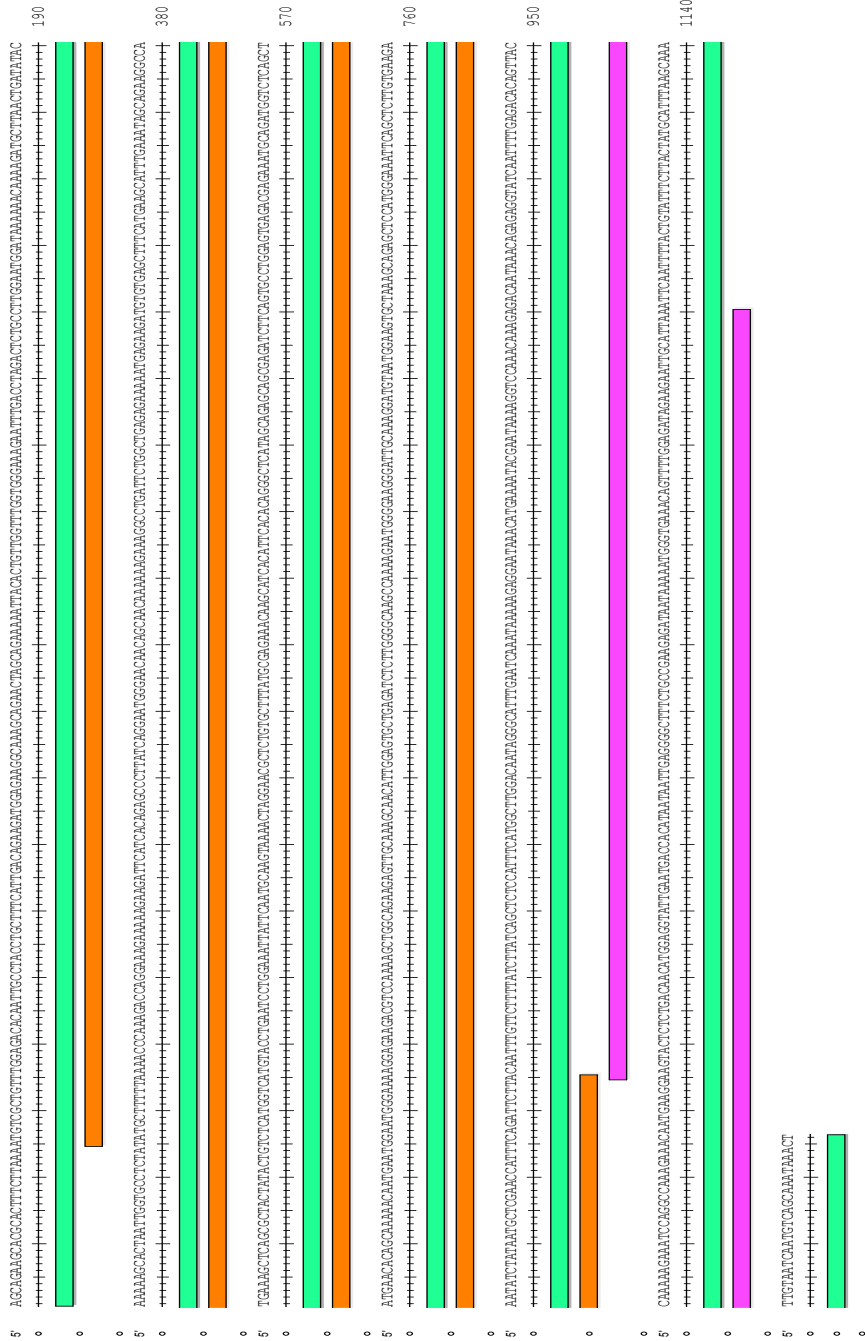
- 15 EB Buffer, QIAgen, Valencia, CA, 19086
- 16 Expand High Fidelity PCR System, Roche, Indianapolis, IN, 11732641001
- 17 Fetal Bovine Serum (FBS), heat inactivated, Sigma-Aldrich, St. Louis, MO, F4135
- 18 FLSK 75CM W/MEMBRN CP 100/CS, Greiner Bio-One, Monroe, NC, 658175
- 19 Goat anti-mouse secondary antibody, Southern Biotech, Birmingham, AL, 1010-05
- 20 HEPES Buffer, Sigma-Aldrich, St. Louis, MO, H0887
- 21 Laemilli Buffer, Bio-Rad, Berkeley, CA, 161-0737
- 22 L-Glutamine, Sigma-Aldrich, St. Louis, MO, G7513
- 23 Mini-PROTEAN® TGX™ Gel (4-20%), Bio-Rad, Berkeley, CA, 456-1093
- 24 OPTI-MEM I Reduced Serum Media, Life Technologies, Carlsbad, CA, 31985-070
- 25 PfuUltra High Fidelity DNA Polymerase Alternative Detergent, Agilent, Santa Clara, CA, 600385
- 26 Plate 6-Well TC 50/CS, Corning, Corning, NY, 3516
- 27 Plate 12-Well TC 6.9ML 50/CS, Corning, Corning, NY, 3513
- 28 Plate 96-Well FLT BTM .365 50/CS, Greiner Bio-One, Monroe, NC, 658175
- 29 PLT MICR 96WL V-BTM PVC 100/CS, Corning, Corning, NY 2897
- 30 Page Ruler Plus Prestained Protein Ladder, Fermentas, SM1819
- 31 Phospha-light SEAP Reporter Gene Assay System, Life Technologies, Carlsbad, CA, T1016
- 32 Receptor Destroying Enzyme (RDE), Fisher, Hampton, NH, 9553641

- 33 Restore Plus Western Blot Stripping Buffer, Thermo Scientific, Waltham, MA,
46430
- 34 RNeasy Mini-kit, QIAgen, Valencia, CA, 74106
- 35 RNasin Ribonuclease Inhibitor, Promega, Madison, WI, N2511
- 36 Seal-Rite 1.5 ml microcentrifuge tube, natural, USA Scientific, Orlando, FL,
1615-5500
- 37 Specific pathogen free hen eggs, B&E Eggs, York Springs, PA
- 38 Supported Nitrocellulose Membrane, Bio-Rad, Berkely, CA, 162-0097
- 39 Trypsin, TPCCK treated- Irradiated, Worthington Biochemical, Lakewood, NJ,
TRTVMF
- 40 Tungsten Carbide Beads (300mm), QIAgen, Valencia, CA, 69997
- 41 QuickChange II XL Site-Directed Mutagenesis kit, Agilent, Santa Clara, CA,
200521
- 42 Quick Ligation kit, New England Biolabs, Ipswich, MA, M2200S

B/Brisbane/60/2008 Plasmid Sequences



HA B/Brisbane/60/2008
 Purple: full-length; orange: ORF



M B/Brisbane/60/2008

Green: full-length; Orange: BM1; Pink: BM2

Accession #	Virus Name
ACF10282	(B/California/01/2008)
AFH58326	(B/England/145/2008)
AGZ61741	(B/Finland/282/2009)
ACG64219	(B/Indiana/08/2008)
AGL05857	(B/Iowa/01/2012)
AEA51387	(B/Kol/1013/2007)
AEA51395	(B/Kol/N-140/2009)
AFJ91104	(B/Malaysia/1919534/2008)
AGO05763	(B/New Hampshire/02/2013)
AFF58918	(B/Riyadh/02/2010)
AFG49012	(B/Ulaanbaatar/1798/2008)
AFH57953	(B/Wisconsin/01/2010)
ACB11749	(B/Wisconsin/04/2008)
AGX23314	(B/Brisbane/4/2006)
AEO80097	(B/California/NHRC0001/2004)
AGX23578	(B/Christchurch/18/2007)
ABL76628	(B/Houston/B720/2004)
ABL76650	(B/Houston/B756/2005)
ACA64910	(B/Mississippi/UR060031/2007)
ACA33498	(B/New Jersey/01/2008)
AEP20299	(B/Texas/NHRC0001/2005)
AGX23391	(B/Waikato/1/2006)
ABN50646	(B/Alaska/03/1992)
ABL76991	(B/Ann Arbor/1994)
ABN50525	(B/Argentina/132/2001)
AGX21919	(B/Auckland/1/2004)
ABN50624	(B/Bangkok/163/1990)
AFH58304	(B/Bangladesh/3333/2007)
AGX24095	(B/Brisbane/29/2007)
ACJ53899	(B/Cheongju/411/2008)
AGX22007	(B/Christchurch/33/2004)
ABL77310	(B/Connecticut/07/1993)
ABN50635	(B/Cordoba/2979/1991)
ABL76749	(B/Egypt/2040/2004)
ACF54246	(B/Florida/4/2006)
ABN50437	(B/Georgia/09/2005)
BAM37625	(B/Hokkaido/FO/2012)
ABL77288	(B/Hong Kong/03/1992)
ABL77266	(B/Hong Kong/22/1989)
AAD42316	(B/Houston/1/91)
ABL76672	(B/Houston/B846/2005)

ABN50701	(B/Johannesburg/06/1994)
ACH53445	(B/Kentucky/02/2006)
ABR15995	(B/Lisbon/02/1994)
AFJ76323	(B/Malaysia/1710547/2007)
ACR15699	(B/Managua/4705.02/2008)
AAD42311	(B/Memphis/18/95)
ABL77156	(B/Moscow/16/2002)
AAU94697	(B/Nashville/45/91)
ABN50657	(B/New York/24/1993)
ABN51184	(B/New York/39/1991)
ABL77299	(B/Oita/15/1992)
AAU94696	(B/Panama/45/90)
ABL77277	(B/Singapore/04/1991)
ABN50712	(B/Singapore/11/1994)
AGX16061	(B/Sydney/3/2004)
AGX23655	(B/Sydney/502/2007)
AGX19425	(B/Sydney/55/2008)
ACD56577	(B/Taiwan/125/2004)
ABN51195	(B/Texas/14/1991)
AGX16193	(B/Townsville/2/2005)
ABL77189	(B/Ulan-Ude/6/2003)
AGX21974	(B/Victoria/109/2004)
AGX16160	(B/Victoria/503/2005)
AGX16149	(B/Waikato/1/2005)
AGZ59887	(B/Wellington/7/2008)
ABL77255	(B/Yamagata/16/1988)
ABL76705	(B/Alaska/12/1996)
ABL76848	(B/Alaska/16/2000)
ABL77035	(B/Argentina/3640/1999)
ABN50668	(B/Bangkok/141/1994)
ABL84340	(B/Brazil/975/2000)
ABL77365	(B/California/01/1995)
AEP20321	(B/California/NHRC0004/2003)
AEP20387	(B/California/NHRC0006/2006)
ABL76870	(B/Canada/16188/2000)
ABN50569	(B/Chile/3162/2002)
ABL76760	(B/Florida/02/1998)
ABL77002	(B/Georgia/04/1998)
ABL76837	(B/Hawaii/11/2004)
AAK70482	(B/Hong Kong/157/99)
AAO38870	(B/Hong Kong/548/2000)
AAU94704	(B/Houston/2/96)
ABL76353	(B/Houston/B15/1999)
ABL76254	(B/Houston/B56/1997)

ABL76584	(B/Houston/B84/2003)
ABN50459	(B/Illinois/13/2005)
ABN50723	(B/Indiana/01/1995)
AFJ80128	(B/Malaysia/06535/1995)
AFJ80150	(B/Malaysia/10928/1996)
ACR15732	(B/Malaysia/2506/2004)
AFJ80803	(B/Malaysia/30589/2005)
AFJ80869	(B/Malaysia/33808/2006)
AAD42314	(B/Memphis/12/97)
AAU94716	(B/Memphis/3/01)
ABL76815	(B/Mexico/84/2000)
ABL77332	(B/Mie/01/1993)
AEP20233	(B/Missouri/NHRC0001/2001)
AEP20277	(B/Missouri/NHRC0001/2003)
AAU94699	(B/Nanchang/195/94)
AAD44188	(B/Nanchang/26/93)
AAD42326	(B/Nashville/3/96)
AAU94717	(B/Nebraska/1/01)
ACN32556	(B/New York/347/1999)
AAA43702	(B/Oregon/5/80)
ABL77024	(B/Paris/549/1999)
ABN50734	(B/Romania/318/1998)
ABL76936	(B/Russia/22/1995)
ABL77057	(B/Shizuoka/480/2000)
AAD42318	(B/Sichuan/8/92)
CAA25425	(B/Singapore/222/79)
ABL76980	(B/Singapore/31/1998)
ABN50448	(B/Singapore/35/1998)
ABN50580	(B/South Carolina/04/2003)
AEP20211	(B/South Carolina/NHRC0001/2000)
AEP20222	(B/South Carolina/NHRC0001/2001)
AEP20288	(B/South Carolina/NHRC0001/2004)
AEP20244	(B/South Carolina/NHRC0002/2001)
AAK70485	(B/Switzerland/4291/97)
AGX21732	(B/Sydney/200/2002)
ACF54257	(B/Taiwan/45/2001)
ABR15973	(B/Temple/B1190/2001)
ABL76529	(B/Temple/B21/2003)
ABL76331	(B/Temple/B9/1999)
AAT69455	(B/Victoria/504/2000)
ABL77101	(B/Victoria/504/2000)
AAK70475	Influenza B virus (B/Vienna/1/99)
AGX17620	(B/Waikato/6/2005)
ABL77354	(B/Wellington/01/1994)

ABN50503	(B/Yamanashi/166/1998)
ABL77134	(B/Akita/27/2001)
ACA33483	(B/Alaska/01/2007)
AGI64373	(B/Alaska/01/2011)
AGX16962	(B/Auckland/16/2002)
AGX19480	(B/Auckland/23/2008)
AFH58447	(B/Bangladesh/5945/2009)
CAA37262	(B/Beijing/1/1987)
AGX20129	(B/Brisbane/1/2010)
AGX20745	(B/Brisbane/13/2011)
AGX16599	(B/Brisbane/2/2002)
AGX15662	(B/Brisbane/33/2008)
AGI63978	(B/California/01/2011)
AFX68905	(B/Cambodia/V0112324/2011)
AGI64011	(B/Colorado/01/2011)
ABN58661	(B/Czechoslovakia/69/1990)
AGL05756	(B/Delaware/01/2012)
ADY16757	(B/Denmark/11/2011)
AGI64004	(B/Florida/02/2011)
ACU12701	(B/Florida/04/2009)
AFH58348	(B/Fujian-Gulou/1272/2008)
AET80614	(B/Georgia/01/2011)
AET21680	(B/Georgia/02/2010)
ABN50470	(B/Hawaii/10/2001)
ABL77321	(B/Hong Kong/02/1993)
ABL77123	(B/Hong Kong/167/2002)
AFH57964	(B/Hong Kong/259/2010)
ABL77112	(B/Hong Kong/310/2004)
ABL76958	(B/Hong Kong/70/1996)
ACA96563	(B/Illinois/UR06-0016/2007)
AET21612	(B/Iowa/01/2010)
AFB77681	(B/Kenya/104/2011)
AEG21020	(B/Kol/1373/2008)
AEG21029	(B/Kol/273/2010)
AEG21014	(B/Kol/515/2006)
AEG21026	(B/Kol/N-2121/2010)
AAU94719	(B/Los Angeles/1/02)
AFJ80238	(B/Malaysia/15048/1998)
AEQ39315	(B/Managua/3323.01/2010)
AET22082	(B/Massachusetts/01/2010)
AAD42309	(B/Memphis/3/89)
AAU94720	(B/Memphis/7/03)
AGI64344	(B/Michigan/01/2011)
AET80612	(B/Minnesota/01/2011)

ACA64976	(B/Mississippi/UR06-0340/2007)
AAU94702	(B/Nanchang/3/95)
AAD44192	(B/Nanchang/5/97)
AAD44191	(B/Nanchang/6/96)
AAU94710	(B/Nanchang/6/98)
AGG86691	(B/Nanjing/1521/2011)
AGI63971	(B/Nebraska/01/2011)
ABL76925	(B/Nepal/1331/2005)
ACA33492	(B/New Jersey/02/2007)
AGL05234	(B/New Mexico/01/2012)
AGR34013	(B/Novosibirsk/05/2011)
AGR34018	(B/Novosibirsk/74/2012)
AET80607	(B/Ohio/01/2011)
ABL76969	(B/Osaka/547/1997)
ABL77200	(B/Paraguay/636/2003)
AET10074	(B/Sao Paulo/09-949/2011)
AGB08299	(B/Sao Paulo/10977/2012)
AFG48978	(B/Selenge/1099/2012)
AGX20800	(B/South Auckland/3/2011)
AEO80067	(B/South Carolina/NHRC0001/2006)
ABL76738	(B/St. Petersburg/14/2006)
AGX15808	(B/Sydney/1/2009)
AGX20195	(B/Sydney/202/2010)
AGX15940	(B/Sydney/47/2011)
AEO80216	(B/Taiwan/14/2007)
ACR15655	(B/Taiwan/202/2005)
ACR15677	(B/Taiwan/2643/2002)
ACF54334	(B/Taiwan/70690/2006)
ACU12699	(B/Tennessee/03/2009)
ACA64943	(B/Tennessee/UR06-0263/2007)
AGO05472	(B/Texas/02/2013)
AGZ61728	(B/Texas/23/2009)
ABN50602	(B/Texas/37/1988)
AFR45694	(B/Thailand/CU-243/2006)
AFR45683	(B/Thailand/CU-364/2008)
AFR45881	(B/Thailand/CU-B2372/2010)
AFR45804	(B/Thailand/CU-B4585/2011)
AFR45672	(B/Thailand/CU-H1400/2010)
ADD01312	(B/Ulaanbaatar/289/2010)
ABL77244	(B/Victoria/02/1987)
AGX19304	(B/Victoria/210/2007)
AGX18633	(B/Victoria/307/2006)
AGX20140	(B/Victoria/503/2010)
ACU12724	(B/Virginia/02/2009)

AGX15984	(B/Waikato/7/2011)
ACV69972	(B/Washington/01/2009)
AGX18622	(B/Wellington/1/2006)
AGX15596	(B/Wellington/85/2006)
AFU34595	(B/Wuhan/4/2009)
ABF21279	(B/Ann Arbor/1/1986)
BG85167	(B/Lee/40)
ABQ81842	(B/Russia/69)

Table 2. HA Accession numbers for phylogenetic tree. Accession numbers and corresponding virus names are listed for the HA phylogenetic tree presented in chapter 2, figure 2.8.

Accession #	Virus Name
AGO05311	(B/Alabama/01/2013)
AGX21919	(B/Auckland/1/2004)
AFH58304	(B/Bangladesh/3333/2007)
AGX24095	(B/Brisbane/29/2007)
AGX23314	(B/Brisbane/4/2006)
ACF10282	(B/California/01/2008)
AGO05592	(B/California/01/2013)
AEO80097	(B/California/NHRC0001/2004)
AEQ39440	(B/California/NHRC0006/2005)
ACJ53899	(B/Cheongju/411/2008)
AGX23578	(B/Christchurch/18/2007)
AGX22007	(B/Christchurch/33/2004)
ABL76749	(B/Egypt/2040/2004)
AFH58326	(B/England/145/2008)
AGZ61741	(B/Finland/282/2009)
AGL09843	(B/Florida/3277/2013)
ACF54246	(B/Florida/4/2006)
ABN50437	(B/Georgia/09/2005)
BAM37625	(B/Hokkaido/FO/2012)
ABL76628	(B/Houston/B720/2004)
ABL76650	(B/Houston/B756/2005)
ABL76672	(B/Houston/B846/2005)
ACG64219	(B/Indiana/08/2008)
AGL05857	(B/Iowa/01/2012)
ACF54180	(B/Jilin/20/2003)
ACH53445	(B/Kentucky/02/2006)
AEA51387	(B/Kol/1013/2007)
AEA51395	(B/Kol/N-140/2009)
AFJ76323	(B/Malaysia/1710547/2007)
AFJ91104	(B/Malaysia/1919534/2008)
ACR15699	(B/Managua/4705.02/2008)
ACA64910	(B/Mississippi/UR06-0031/2007)
AGL05763	(B/New Hampshire/01/2012)
AGO05763	(B/New Hampshire/02/2013)
ACA33498	(B/New Jersey/01/2008)
AGL09864	(B/Oklahoma/3298/2013)
AFF58918	(B/Riyadh/02/2010)
AGX16061	(B/Sydney/3/2004)
AGX23655	(B/Sydney/502/2007)
AGX19425	(B/Sydney/55/2008)
ACD56577	(B/Taiwan/125/2004)
AEP20299	(B/Texas/NHRC0001/2005)
AFR45749	(B/Thailand/CU-B6078/2012)

AGX16193	(B/Townsville/2/2005)
AFG49012	(B/Ulaanbaatar/1798/2008)
AGX21974	(B/Victoria/109/2004)
AGX16160	(B/Victoria/503/2005)
AGX16149	(B/Waikato/1/2005)
AGX23391	(B/Waikato/1/2006)
AGZ59887	(B/Wellington/7/2008)
AFH57953	(B/Wisconsin/01/2010)
ACB11749	(B/Wisconsin/04/2008)
ABL77134	(B/Akita/27/2001)
ABN50646	(B/Alaska/03/1992)
ABL76991	(B/Ann Arbor/1994)
ABN50525	(B/Argentina/132/2001)
AGX16962	(B/Auckland/16/2002)
ABN50624	(B/Bangkok/163/1990)
CAA37262	(B/Beijing/1/1987)
AGX16599	(B/Brisbane/2/2002)
AFX68905	(B/Cambodia/V0112324/2011)
ABL77310	(B/Connecticut/07/1993)
ABN50635	(B/Cordoba/2979/1991)
ABN58661	(B/Czechoslovakia/69/1990)
AFH58348	(B/Fujian-Gulou/1272/2008)
ABN50470	(B/Hawaii/10/2001)
ABL77321	(B/Hong Kong/02/1993)
ABL77288	(B/Hong Kong/03/1992)
ABL77123	(B/Hong Kong/167/2002)
ABL77266	(B/Hong Kong/22/1989)
ABL76958	(B/Hong Kong/70/1996)
AAD42316	(B/Houston/1/91)
ABN50701	(B/Johannesburg/06/1994)
ABR15995	(B/Lisbon/02/1994)
AAU94719	(B/Los Angeles/1/02)
AFJ80238	(B/Malaysia/15048/1998)
AAD42311	(B/Memphis/18/95)
AAD42309	(B/Memphis/3/89)
AAU94720	(B/Memphis/7/03)
ABL77156	(B/Moscow/16/2002)
AAU94702	(B/Nanchang/3/95)
AAD44192	(B/Nanchang/5/97)
AAD44191	(B/Nanchang/6/96)
AAU94710	(B/Nanchang/6/98)
AAU94697	(B/Nashville/45/91)
ABL76925	(B/Nepal/1331/2005)
ABN50657	(B/New York/24/1993)

ABN51184	(B/New York/39/1991)
ABL77299	(B/Oita/15/1992)
AAA43702	(B/Oregon/5/80)
ABL76969	(B/Osaka/547/1997)
AAU94696	(B/Panama/45/90)
ABL77200	(B/Paraguay/636/2003)
ABL77277	(B/Singapore/04/1991)
ABN50712	(B/Singapore/11/1994)
CAA25425	(B/Singapore/222/79)
ACR15677	(B/Taiwan/2643/2002)
ABN51195	(B/Texas/14/1991)
ABN50602	(B/Texas/37/1988)
AFR45804	(B/Thailand/CU-B4585/2011)
ABL77189	(B/Ulan-Ude/6/2003)
ABL77244	(B/Victoria/02/1987)
ABL77255	(B/Yamagata/16/1988)
ABL76705	(B/Alaska/12/1996)
ABL76848	(B/Alaska/16/2000)
ABF21279	(B/Ann Arbor/1/1986)
ABL77035	(B/Argentina/3640/1999)
ABN50668	(B/Bangkok/141/1994)
ABL84340	(B/Brazil/975/2000)
ABL77365	(B/California/01/1995)
AEP20387	(B/California/NHRC0006/2006)
ABL76870	(B/Canada/16188/2000)
ABN50569	(B/Chile/3162/2002)
ABL76760	(B/Florida/02/1998)
ABL77002	(B/Georgia/04/1998)
AAK70482	(B/Hong Kong/157/99)
AAO38870	(B/Hong Kong/548/2000)
AAU94704	(B/Houston/2/96)
ABL76353	(B/Houston/B15/1999)
ABL76254	(B/Houston/B56/1997)
ABN50723	(B/Indiana/01/1995)
ABG85167	(B/Lee/40)
AFJ80128	(B/Malaysia/06535/1995)
AFJ80150	(B/Malaysia/10928/1996)
AAD42314	(B/Memphis/12/97)
AAU94716	(B/Memphis/3/01)
ABL76815	(B/Mexico/84/2000)
ABL77332	(B/Mie/01/1993)
AEP20233	(B/Missouri/NHRC0001/2001)
AEP20277	(B/Missouri/NHRC0001/2003)
AAU94699	(B/Nanchang/195/94)

AAD44188	(B/Nanchang/26/93)
AAD42326	(B/Nashville/3/96)
AAU94717	(B/Nebraska/1/01)
ACN32556	(B/New York/347/1999)
ABL77024	(B/Paris/549/1999)
ABN50734	(B/Romania/318/1998)
ABL76936	(B/Russia/22/1995)
ABQ81842	(B/Russia/69)
ABL77057	(B/Shizuoka/480/2000)
AAD42318	(B/Sichuan/8/92)
ABL76980	(B/Singapore/31/1998)
ABN50448	(B/Singapore/35/1998)
ABN50580	(B/South Carolina/04/2003)
AEP20211	(B/South Carolina/NHRC0001/2000)
AEP20222	(B/South Carolina/NHRC0001/2001)
AEP20244	(B/South Carolina/NHRC0002/2001)
AAK70485	(B/Switzerland/4291/97)
AGX21732	(B/Sydney/200/2002)
ACF54257	(B/Taiwan/45/2001)
ABR15973	(B/Temple/B1190/2001)
ABL76331	(B/Temple/B9/1999)
AAT69455	(B/Victoria/504/2000)
ABL77101	(B/Victoria/504/2000)
AAK70475	(B/Vienna/1/99)
ABL77354	(B/Wellington/01/1994)
ABN50503	(B/Yamanashi/166/1998)
ACA33483	(B/Alaska/01/2007)
AGI64373	(B/Alaska/01/2011)
AGX19480	(B/Auckland/23/2008)
AFH58447	(B/Bangladesh/5945/2009)
AGX20129	(B/Brisbane/1/2010)
AGX20745	(B/Brisbane/13/2011)
AGX15662	(B/Brisbane/33/2008)
AGI63978	(B/California/01/2011)
AEP20321	(B/California/NHRC0004/2003)
AGI64011	(B/Colorado/01/2011)
AGL05756	(B/Delaware/01/2012)
ADY16757	(B/Denmark/11/2011)
AGI64004	(B/Florida/02/2011)
ACU12701	(B/Florida/04/2009)
AET80614	(B/Georgia/01/2011)
AET21680	(B/Georgia/02/2010)
ABL76837	(B/Hawaii/11/2004)
AFH57964	(B/Hong Kong/259/2010)

ABL77112	(B/Hong Kong/310/2004)
ABL76584	(B/Houston/B84/2003)
ABN50459	(B/Illinois/13/2005)
ACA96563	(B/Illinois/UR06-0016/2007)
AET21612	(B/Iowa/01/2010)
AFB77681	(B/Kenya/104/2011)
AEG21020	(B/Kol/1373/2008)
AEG21029	(B/Kol/273/2010)
AEG21014	(B/Kol/515/2006)
AEG21026	(B/Kol/N-2121/2010)
ACR15732	(B/Malaysia/2506/2004)
AFJ80803	(B/Malaysia/30589/2005)
AFJ80869	(B/Malaysia/33808/2006)
AEQ39315	(B/Managua/3323.01/2010)
AET22082	(B/Massachusetts/01/2010)
AGI64344	(B/Michigan/01/2011)
AET80612	(B/Minnesota/01/2011)
ACA64976	(B/Mississippi/UR06-0340/2007)
AGG86691	(B/Nanjing/1521/2011)
AGI63971	(B/Nebraska/01/2011)
ACA33492	(B/New Jersey/02/2007)
AGL05234	(B/New Mexico/01/2012)
AGR34013	(B/Novosibirsk/05/2011)
AGR34018	(B/Novosibirsk/74/2012)
AET80607	(B/Ohio/01/2011)
AET10074	(B/Sao Paulo/09-949/2011)
AGB08299	(B/Sao Paulo/10977/2012)
AFG48978	(B/Selenge/1099/2012)
AGX20800	(B/South Auckland/3/2011)
AEP20288	(B/South Carolina/NHRC0001/2004)
AEO80067	(B/South Carolina/NHRC0001/2006)
ABL76738	(B/St. Petersburg/14/2006)
AGX15808	(B/Sydney/1/2009)
AGX20195	(B/Sydney/202/2010)
AGX15940	(B/Sydney/47/2011)
AEO80216	(B/Taiwan/14/2007)
ACR15655	(B/Taiwan/202/2005)
ACF54334	(B/Taiwan/70690/2006)
ABL76529	(B/Temple/B21/2003)
ACU12699	(B/Tennessee/03/2009)
ACA64943	(B/Tennessee/UR06-0263/2007)
AGO05472	(B/Texas/02/2013)
AGZ61728	(B/Texas/23/2009)
AFR45694	(B/Thailand/CU-243/2006)

AFR45683	(B/Thailand/CU-364/2008)
AFR45881	(B/Thailand/CU-B2372/2010)
AFR45672	(B/Thailand/CU-H1400/2010)
ADD01312	(B/Ulaanbaatar/289/2010)
AGX19304	(B/Victoria/210/2007)
AGX18633	(B/Victoria/307/2006)
AGX20140	(B/Victoria/503/2010)
ACU12724	(B/Virginia/02/2009)
AGX17620	(B/Waikato/6/2005)
AGX15984	(B/Waikato/7/2011)
ACV69972	(B/Washington/01/2009)
AGX18622	(B/Wellington/1/2006)
AGX15596	(B/Wellington/85/2006)
AFU34595	(B/Wuhan/4/2009)

Table 2. NA Accession numbers for phylogenetic tree. Accession numbers and corresponding virus names are listed for the NA phylogenetic tree presented in chapter 2, figure 2.8.

Bibliography

1. Pena L, Vincent AL, Ye J, Ciacci-Zanella JR, Angel M, Lorusso A, et al. Modifications in the polymerase genes of a swine-like triple-reassortant influenza virus to generate live attenuated vaccines against 2009 pandemic H1N1 viruses. *J Virol.* 2011;85(1):456-69.
2. Hoffmann E, Mahmood K, Yang CF, Webster RG, Greenberg HB, Kemble G. Rescue of influenza B virus from eight plasmids. *Proc Natl Acad Sci U S A.* 2002;99(17):11411-6.
3. Ritchey MB, Palese P, Kilbourne ED. RNAs of influenza A, B, and C viruses. *J Virol.* 1976;18(2):738-44.
4. Thompson WW, Shay DK, Weintraub E, Brammer L, Bridges CB, Cox NJ, et al. Influenza-associated hospitalizations in the United States. *JAMA.* 2004;292(11):1333-40.
5. Baltimore D. Expression of animal virus genomes. *Bacteriological reviews.* 1971;35(3):235-41.
6. Falk K, Namork E, Rimstad E, Mjaaland S, Dannevig BH. Characterization of infectious salmon anemia virus, an orthomyxo-like virus isolated from Atlantic salmon (*Salmo salar* L.). *J Virol.* 1997;71(12):9016-23.
7. Freedman-Faulstich EZ, Fuller FJ. Nucleotide sequence of the tick-borne, orthomyxo-like Dhori/Indian/1313/61 virus envelope gene. *Virology.* 1990;175(1):10-8.
8. Kuno G, Chang GJ, Tsuchiya KR, Miller BR. Phylogeny of Thogoto virus. *Virus genes.* 2001;23(2):211-4.
9. Presti RM, Zhao G, Beatty WL, Mihindikulasuriya KA, da Rosa AP, Popov VL, et al. Quarantfil, Johnston Atoll, and Lake Chad viruses are novel members of the family Orthomyxoviridae. *J Virol.* 2009;83(22):11599-606.
10. Mjaaland S, Rimstad E, Falk K, Dannevig BH. Genomic characterization of the virus causing infectious salmon anemia in Atlantic salmon (*Salmo salar* L.): an orthomyxo-like virus in a teleost. *J Virol.* 1997;71(10):7681-6.
11. Calvo C, García-García ML, Centeno M, Pérez-Breña P, Casas I. Influenza C virus infection in children, Spain. *Emerg Infect Dis.* 2006;12(10):1621-2.

12. Calvo C, García-García ML, Borrell B, Pozo F, Casas I. Prospective study of influenza C in hospitalized children. *Pediatr Infect Dis J*. 2013;32(8):916-9.
13. Matsuzaki Y, Katsushima N, Nagai Y, Shoji M, Itagaki T, Sakamoto M, et al. Clinical features of influenza C virus infection in children. *J Infect Dis*. 2006;193(9):1229-35.
14. Taubenberger JK, Kash JC. Influenza virus evolution, host adaptation, and pandemic formation. *Cell host & microbe*. 2010;7(6):440-51.
15. Tong S, Li Y, Rivaller P, Conrardy C, Castillo DA, Chen LM, et al. A distinct lineage of influenza A virus from bats. *Proc Natl Acad Sci U S A*. 2012;109(11):4269-74.
16. Tong S, Zhu X, Li Y, Shi M, Zhang J, Bourgeois M, et al. New world bats harbor diverse influenza A viruses. *PLoS pathogens*. 2013;9(10):e1003657.
17. Brown IH, Harris PA, Alexander DJ. Serological studies of influenza viruses in pigs in Great Britain 1991-2. *Epidemiol Infect*. 1995;114(3):511-20.
18. Osterhaus AD, Rimmelzwaan GF, Martina BE, Bestebroer TM, Fouchier RA. Influenza B virus in seals. *Science*. 2000;288(5468):1051-3.
19. Bodewes R, Morick D, de Mutsert G, Osinga N, Bestebroer T, van der Vliet S, et al. Recurring influenza B virus infections in seals. *Emerg Infect Dis*. 2013;19(3):511-2.
20. Bodewes R, van de Bildt MW, van Elk CE, Bunschoek PE, van de Vijver DA, Smits SL, et al. No Serological Evidence that Harbour Porpoises Are Additional Hosts of Influenza B Viruses. *PLoS One*. 2014;9(2):e89058.
21. Ohishi K, Ninomiya A, Kida H, Park CH, Maruyama T, Arai T, et al. Serological evidence of transmission of human influenza A and B viruses to Caspian seals (*Phoca caspica*). *Microbiology and immunology*. 2002;46(9):639-44.
22. Blanc A, Ruchansky D, Clara M, Achaval F, Le Bas A, Arbiza J. Serologic evidence of influenza A and B viruses in South American fur seals (*Arctocephalus australis*). *J Wildl Dis*. 2009;45(2):519-21.
23. Romváry J, Mészáros J, Barb K. Susceptibility of birds to type-B influenza virus. *Acta Microbiol Acad Sci Hung*. 1980;27(4):279-87.
24. CDC. Key Facts About Seasonal Flu Vaccine: Centers for Disease Control and Prevention, National Center for Immunization and Respiratory Diseases (NCIRD); 2013 [updated 11/7/2013; cited 2014 2/26/2014]. Available from: <http://www.cdc.gov/flu/protect/keyfacts.htm>.

25. CDC. Selecting Viruses for the Seasonal Influenza Vaccine: Centers for Disease Control and Prevention; 2014 [updated 2/21/2014; cited 2014 3/18/2014]. Available from: <http://www.cdc.gov/flu/about/season/vaccine-selection.htm>.
26. Suzuki Y, Nei M. Origin and evolution of influenza virus hemagglutinin genes. *Molecular biology and evolution*. 2002;19(4):501-9.
27. Webster RG, Bean WJ, Gorman OT, Chambers TM, Kawaoka Y. Evolution and ecology of influenza A viruses. *Microbiological reviews*. 1992;56(1):152-79.
28. Paul Glezen W, Schmier JK, Kuehn CM, Ryan KJ, Oxford J. The burden of influenza B: a structured literature review. *Am J Public Health*. 2013;103(3):e43-51.
29. Wie SH, So BH, Song JY, Cheong HJ, Seo YB, Choi SH, et al. A comparison of the clinical and epidemiological characteristics of adult patients with laboratory-confirmed influenza A or B during the 2011-2012 influenza season in Korea: a multi-center study. *PLoS One*. 2013;8(5):e62685.
30. Lowen AC, Mubareka S, Steel J, Palese P. Influenza virus transmission is dependent on relative humidity and temperature. *PLoS pathogens*. 2007;3(10):1470-6.
31. Pica N, Chou YY, Bouvier NM, Palese P. Transmission of influenza B viruses in the Guinea pig. *J Virol*. 2012;86(8):4279-87.
32. Lin YP, Gregory V, Bennett M, Hay A. Recent changes among human influenza viruses. *Virus Res*. 2004;103(1-2):47-52.
33. McCullers JA, Hayden FG. Fatal influenza B infections: time to reexamine influenza research priorities. *J Infect Dis*. 2012;205(6):870-2.
34. McCullers JA, Wang GC, He S, Webster RG. Reassortment and insertion-deletion are strategies for the evolution of influenza B viruses in nature. *J Virol*. 1999;73(9):7343-8.
35. WHO. Influenza vaccine viruses and reagents: World Health Organization; 2014 [cited 2014 4/14/2014]. Available from: <http://www.who.int/influenza/vaccines/virus/en/>.
36. Recommended composition of influenza virus vaccines for use in the 2014 southern hemisphere influenza season: World Health Organization (WHO); 2013 [updated 10/11/2013; cited 2014 3/26/2014]. Available from: http://www.who.int/influenza/vaccines/virus/recommendations/201309_recommendation.pdf?ua=1.

37. WHO. Recommended composition of influenza virus vaccines for use in the 2014 southern hemisphere influenza season: World Health Organization; [updated 10/11/ 2013; cited 2014 3/26/ 2014]. Available from: http://www.who.int/influenza/vaccines/virus/recommendations/201309_recommendation.pdf?ua=1.
38. Palese P, Shaw ML. Orthomyxoviridae: The Viruses and Their Replication. In: Knipe DM, Howley PM, editors. *Fields Virology*. 2. 5 ed: Lippincott Williams and Wilkins; 2007. p. 1647-89.
39. Desselberger U, Palese P. Molecular weights of RNA segments of influenza A and B viruses. *Virology*. 1978;88(2):394-9.
40. Racaniello VR, Palese P. Influenza B virus genome: assignment of viral polypeptides to RNA segments. *J Virol*. 1979;29(1):361-73.
41. Kobayashi M, Toyoda T, Ishihama A. Influenza virus PB1 protein is the minimal and essential subunit of RNA polymerase. *Arch Virol*. 1996;141(3-4):525-39.
42. Jambrina E, Barcena J, Uez O, Portela A. The three subunits of the polymerase and the nucleoprotein of influenza B virus are the minimum set of viral proteins required for expression of a model RNA template. *Virology*. 1997;235(2):209-17.
43. Kathan RH, Winzler RJ, Johnson CA. Preparation of an inhibitor of viral hemagglutination from human erythrocytes. *The Journal of experimental medicine*. 1961;113:37-45.
44. Shaw MW, Choppin PW, Lamb RA. A previously unrecognized influenza B virus glycoprotein from a bicistronic mRNA that also encodes the viral neuraminidase. *Proc Natl Acad Sci U S A*. 1983;80(16):4879-83.
45. Sunstrom NA, Premkumar LS, Premkumar A, Ewart G, Cox GB, Gage PW. Ion channels formed by NB, an influenza B virus protein. *J Membr Biol*. 1996;150(2):127-32.
46. Briedis DJ, Tobin M. Influenza B virus genome: complete nucleotide sequence of the influenza B/lee/40 virus genome RNA segment 5 encoding the nucleoprotein and comparison with the B/Singapore/222/79 nucleoprotein. *Virology*. 1984;133(2):448-55.
47. Horvath CM, Williams MA, Lamb RA. Eukaryotic coupled translation of tandem cistrons: identification of the influenza B virus BM2 polypeptide. *EMBO J*. 1990;9(8):2639-47.

48. Briedis DJ, Lamb RA. Influenza B virus genome: sequences and structural organization of RNA segment 8 and the mRNAs coding for the NS1 and NS2 proteins. *J Virol.* 1982;42(1):186-93.
49. Paragas J, Talon J, O'Neill RE, Anderson DK, García-Sastre A, Palese P. Influenza B and C virus NEP (NS2) proteins possess nuclear export activities. *J Virol.* 2001;75(16):7375-83.
50. Yuan W, Krug RM. Influenza B virus NS1 protein inhibits conjugation of the interferon (IFN)-induced ubiquitin-like ISG15 protein. *EMBO J.* 2001;20(3):362-71.
51. Desselberger U, Racaniello VR, Zazra JJ, Palese P. The 3' and 5'-terminal sequences of influenza A, B and C virus RNA segments are highly conserved and show partial inverted complementarity. *Gene.* 1980;8(3):315-28.
52. Jackson D, Cadman A, Zurcher T, Barclay WS. A reverse genetics approach for recovery of recombinant influenza B viruses entirely from cDNA. *J Virol.* 2002;76(22):11744-7.
53. Stoeckle MY, Shaw MW, Choppin PW. Segment-specific and common nucleotide sequences in the noncoding regions of influenza B virus genome RNAs. *Proc Natl Acad Sci U S A.* 1987;84(9):2703-7.
54. Lee YS, Seong BL. Nucleotides in the panhandle structure of the influenza B virus virion RNA are involved in the specificity between influenza A and B viruses. *J Gen Virol.* 1998;79 (Pt 4):673-81.
55. Lee YS, Seong BL. Mutational analysis of influenza B virus RNA transcription in vitro. *J Virol.* 1996;70(2):1232-6.
56. Flick R, Neumann G, Hoffmann E, Neumeier E, Hobom G. Promoter elements in the influenza vRNA terminal structure. *RNA (New York, NY).* 1996;2(10):1046-57.
57. Baudin F, Bach C, Cusack S, Ruigrok RW. Structure of influenza virus RNP. I. Influenza virus nucleoprotein melts secondary structure in panhandle RNA and exposes the bases to the solvent. *EMBO J.* 1994;13(13):3158-65.
58. Kemdirim S, Palefsky J, Briedis DJ. Influenza B virus PB1 protein; nucleotide sequence of the genome RNA segment predicts a high degree of structural homology with the corresponding influenza A virus polymerase protein. *Virology.* 1986;152(1):126-35.
59. Nakagawa Y, Oda K, Nakada S. The PB1 subunit alone can catalyze cRNA synthesis, and the PA subunit in addition to the PB1 subunit is required for viral RNA synthesis in replication of the influenza virus genome. *J Virol.* 1996;70(9):6390-4.

60. Guilligay D, Tarendeau F, Resa-Infante P, Coloma R, Crepin T, Sehr P, et al. The structural basis for cap binding by influenza virus polymerase subunit PB2. *Nature structural & molecular biology*. 2008;15(5):500-6.
61. Wakai C, Iwama M, Mizumoto K, Nagata K. Recognition of cap structure by influenza B virus RNA polymerase is less dependent on the methyl residue than recognition by influenza A virus polymerase. *J Virol*. 2011;85(15):7504-12.
62. Dias A, Bouvier D, Crépin T, McCarthy AA, Hart DJ, Baudin F, et al. The cap-snatching endonuclease of influenza virus polymerase resides in the PA subunit. *Nature*. 2009;458(7240):914-8.
63. Almond JW, Haymerle HA, Felsenreich VD, Reeve P. The structural and infected cell polypeptides of influenza B virus. *J Gen Virol*. 1979;45(3):611-21.
64. Compans RW, Caliguiri LA. Isolation and properties of an RNA polymerase from influenza virus-infected cells. *J Virol*. 1973;11(3):441-8.
65. Pons MW, Schulze IT, Hirst GK, Hauser R. Isolation and characterization of the ribonucleoprotein of influenza virus. *Virology*. 1969;39(2):250-9.
66. Pons MW. Isolation of influenza virus ribonucleoprotein from infected cells. Demonstration of the presence of negative-stranded RNA in viral RNP. *Virology*. 1971;46(1):149-60.
67. Watanabe K, Handa H, Mizumoto K, Nagata K. Mechanism for inhibition of influenza virus RNA polymerase activity by matrix protein. *J Virol*. 1996;70(1):241-7.
68. Cao S, Jiang J, Li J, Li Y, Yang L, Wang S, et al. Characterization of The Nucleocytoplasmic Shuttle of The Matrix Protein of Influenza B Virus. *J Virol*. 2014.
69. Mould JA, Paterson RG, Takeda M, Ohigashi Y, Venkataraman P, Lamb RA, et al. Influenza B virus BM2 protein has ion channel activity that conducts protons across membranes. *Dev Cell*. 2003;5(1):175-84.
70. Paterson RG, Takeda M, Ohigashi Y, Pinto LH, Lamb RA. Influenza B virus BM2 protein is an oligomeric integral membrane protein expressed at the cell surface. *Virology*. 2003;306(1):7-17.
71. Hale BG, Steel J, Medina RA, Manicassamy B, Ye J, Hickman D, et al. Inefficient control of host gene expression by the 2009 pandemic H1N1 influenza A virus NS1 protein. *J Virol*. 84(14):6909-22.

72. Dela-Moss LI, Moss WN, Turner DH. Identification of conserved RNA secondary structures at influenza B and C splice sites reveals similarities and differences between influenza A, B, and C. *BMC research notes*. 2014;7:22.
73. Francis T, Jr. A New Type of Virus from Epidemic Influenza. *Science*. 1940;92(2392):405-8.
74. Wang YF, Chang CF, Chi CY, Wang HC, Wang JR, Su IJ. Characterization of glycan binding specificities of influenza B viruses with correlation with hemagglutinin genotypes and clinical features. *J Med Virol*. 2012;84(4):679-85.
75. Rota PA, Wallis TR, Harmon MW, Rota JS, Kendal AP, Nerome K. Cocirculation of two distinct evolutionary lineages of influenza type B virus since 1983. *Virology*. 1990;175(1):59-68.
76. Win MK, Chow A, Chen M, Lau YF, Ooi EE, Leo YS. Influenza B outbreak among influenza-vaccinated welfare home residents in Singapore. *Ann Acad Med Singapore*. 2010;39(6):448-52.
77. Ambrose CS, Levin MJ. The rationale for quadrivalent influenza vaccines. *Hum Vaccin Immunother*. 2012;8(1):81-8.
78. Padgett BL, Walker DL. Enzymatic Variants of Influenza Virus. Iii. Function of Neuraminidase in the Viral Growth Cycle. *Journal of bacteriology*. 1964;87:363-9.
79. Shaw MW, Lamb RA, Erickson BW, Briedis DJ, Choppin PW. Complete nucleotide sequence of the neuraminidase gene of influenza B virus. *Proc Natl Acad Sci U S A*. 1982;79(22):6817-21.
80. Hoyle L. The multiplication of influenza viruses in the fertile egg: A Report to the Medical Research Council. *The Journal of hygiene*. 1950;48(3):277-97.
81. Curry RL, Brown JD, Baker FA, Hobson D. Serological studies with purified neuraminidase antigens of influenza B viruses. *The Journal of hygiene*. 1974;72(2):197-204.
82. Yamamoto-Goshima F, Maeno K. Approach to the involvement of influenza B neuraminidase in the cleavage of HA by host cell protease using low pH-induced cell fusion reaction. *Microbiology and immunology*. 1994;38(10):819-22.
83. Shaw MW, Choppin PW. Studies on the synthesis of the influenza V virus NB glycoprotein. *Virology*. 1984;139(1):178-84.
84. Betakova T, Nermut MV, Hay AJ. The NB protein is an integral component of the membrane of influenza B virus. *J Gen Virol*. 1996;77 (Pt 11):2689-94.

85. Betakova T, Kollerova E. pH modulating activity of ion channels of influenza A, B, and C viruses. *Acta virologica*. 2006;50(3):187-93.
86. White J, Kartenbeck J, Helenius A. Membrane fusion activity of influenza virus. *EMBO J*. 1982;1(2):217-22.
87. Nakamura K, Kitame F, Homma M. A comparison of proteins among various influenza B virus strains by one-dimensional peptide mapping. *J Gen Virol*. 1981;56(Pt 2):315-23.
88. Skehel JJ, Waterfield MD. Studies on the primary structure of the influenza virus hemagglutinin. *Proc Natl Acad Sci U S A*. 1975;72(1):93-7.
89. Lazarowitz SG, Compans RW, Choppin PW. Proteolytic cleavage of the hemagglutinin polypeptide of influenza virus. Function of the uncleaved polypeptide HA. *Virology*. 1973;52(1):199-212.
90. Zambon MC. The pathogenesis of influenza in humans. *Reviews in medical virology*. 2001;11(4):227-41.
91. Rott R, Klenk HD, Nagai Y, Tashiro M. Influenza viruses, cell enzymes, and pathogenicity. *American journal of respiratory and critical care medicine*. 1995;152(4 Pt 2):S16-9.
92. Wang Q, Tian X, Chen X, Ma J. Structural basis for receptor specificity of influenza B virus hemagglutinin. *Proc Natl Acad Sci U S A*. 2007;104(43):16874-9.
93. Shinya K, Ebina M, Yamada S, Ono M, Kasai N, Kawaoka Y. Avian flu: influenza virus receptors in the human airway. *Nature*. 2006;440(7083):435-6.
94. Gurevitz M, Schulze IT, Swierkosz EM, Arens MQ, Schwarz KB. Effect of influenza B virus on nutrient transport in cultured epithelial cells. *Laboratory investigation; a journal of technical methods and pathology*. 1987;57(6):657-64.
95. Ni F, Chen X, Shen J, Wang Q. Structural insights into the membrane fusion mechanism mediated by influenza virus hemagglutinin. *Biochemistry*. 2014;53(5):846-54.
96. Wang H, Jiang C. Influenza A virus H5N1 entry into host cells is through clathrin-dependent endocytosis. *Science in China*. 2009;52(5):464-9.
97. Skehel JJ, Wiley DC. Receptor binding and membrane fusion in virus entry: the influenza hemagglutinin. *Annu Rev Biochem*. 2000;69:531-69.

98. Root CN, Wills EG, McNair LL, Whittaker GR. Entry of influenza viruses into cells is inhibited by a highly specific protein kinase C inhibitor. *J Gen Virol.* 2000;81(Pt 11):2697-705.
99. Sieczkarski SB, Brown HA, Whittaker GR. Role of protein kinase C betaII in influenza virus entry via late endosomes. *J Virol.* 2003;77(1):460-9.
100. Bullough PA, Hughson FM, Skehel JJ, Wiley DC. Structure of influenza haemagglutinin at the pH of membrane fusion. *Nature.* 1994;371(6492):37-43.
101. Cross TA. Flu BM2 structure and function. *Nature structural & molecular biology.* 2009;16(12):1207-9.
102. Bui M, Whittaker G, Helenius A. Effect of M1 protein and low pH on nuclear transport of influenza virus ribonucleoproteins. *J Virol.* 1996;70(12):8391-401.
103. Imai M, Kawasaki K, Odagiri T. Cytoplasmic domain of influenza B virus BM2 protein plays critical roles in production of infectious virus. *J Virol.* 2008;82(2):728-39.
104. Wanitchang A, Narkpuk J, Jongkaewwattana A. Nuclear import of influenza B virus nucleoprotein: involvement of an N-terminal nuclear localization signal and a cleavage-protection motif. *Virology.* 2013;443(1):59-68.
105. Deng Q, Wang D, Xiang X, Gao X, Hardwidge PR, Kaushik R, et al. Nuclear localization of influenza B polymerase proteins and their binary complexes. *Virus Res.* 2011;156(1-2):49-53.
106. Melen K, Fagerlund R, Franke J, Kohler M, Kinnunen L, Julkunen I. Importin alpha nuclear localization signal binding sites for STAT1, STAT2, and influenza A virus nucleoprotein. *The Journal of biological chemistry.* 2003;278(30):28193-200.
107. Boulo S, Akarsu H, Ruigrok RW, Baudin F. Nuclear traffic of influenza virus proteins and ribonucleoprotein complexes. *Virus Res.* 2007;124(1-2):12-21.
108. Robertson JS, Schubert M, Lazzarini RA. Polyadenylation sites for influenza virus mRNA. *J Virol.* 1981;38(1):157-63.
109. Resa-Infante P, Jorba N, Coloma R, Ortin J. The influenza virus RNA synthesis machine: advances in its structure and function. *RNA Biol.* 2011;8(2):207-15.
110. Beaton AR, Krug RM. Transcription antitermination during influenza viral template RNA synthesis requires the nucleocapsid protein and the absence of a 5' capped end. *Proc Natl Acad Sci U S A.* 1986;83(17):6282-6.

111. Hay AJ, Lomniczi B, Bellamy AR, Skehel JJ. Transcription of the influenza virus genome. *Virology*. 1977;83(2):337-55.
112. Deng T, Vreede FT, Brownlee GG. Different de novo initiation strategies are used by influenza virus RNA polymerase on its cRNA and viral RNA promoters during viral RNA replication. *J Virol*. 2006;80(5):2337-48.
113. Crow M, Deng T, Addley M, Brownlee GG. Mutational analysis of the influenza virus cRNA promoter and identification of nucleotides critical for replication. *J Virol*. 2004;78(12):6263-70.
114. Azzeh M, Flick R, Hobom G. Functional analysis of the influenza A virus cRNA promoter and construction of an ambisense transcription system. *Virology*. 2001;289(2):400-10.
115. Shapiro GI, Gurney T, Jr., Krug RM. Influenza virus gene expression: control mechanisms at early and late times of infection and nuclear-cytoplasmic transport of virus-specific RNAs. *J Virol*. 1987;61(3):764-73.
116. Imai M, Watanabe S, Odagiri T. Influenza B virus NS2, a nuclear export protein, directly associates with the viral ribonucleoprotein complex. *Arch Virol*. 2003;148(10):1873-84.
117. Ludwig S, Wolff T, Ehrhardt C, Wurzer WJ, Reinhardt J, Planz O, et al. MEK inhibition impairs influenza B virus propagation without emergence of resistant variants. *FEBS letters*. 2004;561(1-3):37-43.
118. Demers AJ, Ran Z, Deng Q, Wang D, Edman B, Lu W, et al. Palmitoylation Is Required for Intracellular Trafficking of Influenza B Virus NB Protein and Efficient Influenza B Growth In Vitro. *J Gen Virol*. 2014.
119. Watanabe S, Imai M, Ohara Y, Odagiri T. Influenza B virus BM2 protein is transported through the trans-Golgi network as an integral membrane protein. *J Virol*. 2003;77(19):10630-7.
120. Luo C, Nobusawa E, Nakajima K. Analysis of the desialidation process of the haemagglutinin protein of influenza B virus: the host-dependent desialidation step. *J Gen Virol*. 2002;83(Pt 7):1729-34.
121. Griffiths G, Pfeiffer S, Simons K, Matlin K. Exit of newly synthesized membrane proteins from the trans cisterna of the Golgi complex to the plasma membrane. *The Journal of cell biology*. 1985;101(3):949-64.
122. Bertram S, Glowacka I, Blazejewska P, Soilleux E, Allen P, Danisch S, et al. TMPRSS2 and TMPRSS4 facilitate trypsin-independent spread of influenza virus in Caco-2 cells. *J Virol*. 2010;84(19):10016-25.

123. Bottcher-Friebertshauer E, Freuer C, Sielaff F, Schmidt S, Eickmann M, Uhlenendorff J, et al. Cleavage of influenza virus hemagglutinin by airway proteases TMPRSS2 and HAT differs in subcellular localization and susceptibility to protease inhibitors. *J Virol.* 2010;84(11):5605-14.
124. Baron J, Tarnow C, Mayoli-Nussle D, Schilling E, Meyer D, Hammami M, et al. Matriptase, HAT, and TMPRSS2 activate the hemagglutinin of H9N2 influenza A viruses. *J Virol.* 2013;87(3):1811-20.
125. Rossman JS, Lamb RA. Influenza virus assembly and budding. *Virology.* 2011;411(2):229-36.
126. Wang J, Pielak RM, McClintock MA, Chou JJ. Solution structure and functional analysis of the influenza B proton channel. *Nature structural & molecular biology.* 2009;16(12):1267-71.
127. Imai M, Watanabe S, Ninomiya A, Obuchi M, Odagiri T. Influenza B virus BM2 protein is a crucial component for incorporation of viral ribonucleoprotein complex into virions during virus assembly. *J Virol.* 2004;78(20):11007-15.
128. Imai M, Watanabe T, Hatta M, Das SC, Ozawa M, Shinya K, et al. Experimental adaptation of an influenza H5 HA confers respiratory droplet transmission to a reassortant H5 HA/H1N1 virus in ferrets. *Nature.* 2012;486(7403):420-8.
129. Imai M, Watanabe S, Kawaoka Y. The cytoplasmic tail domain of influenza B virus hemagglutinin is important for its incorporation into virions but is not essential for virus replication in cell culture in the presence of compensatory mutations. *J Virol.* 2012;86(21):11633-44.
130. Zheng H, Palese P, Garcia-Sastre A. Nonconserved nucleotides at the 3' and 5' ends of an influenza A virus RNA play an important role in viral RNA replication. *Virology.* 1996;217(1):242-51.
131. Liang Y, Huang T, Ly H, Parslow TG, Liang Y. Mutational analyses of packaging signals in influenza virus PA, PB1, and PB2 genomic RNA segments. *J Virol.* 2008;82(1):229-36.
132. Watanabe T, Watanabe S, Noda T, Fujii Y, Kawaoka Y. Exploitation of nucleic acid packaging signals to generate a novel influenza virus-based vector stably expressing two foreign genes. *J Virol.* 2003;77(19):10575-83.
133. Luytjes W, Krystal M, Enami M, Parvin JD, Palese P. Amplification, expression, and packaging of foreign gene by influenza virus. *Cell.* 1989;59(6):1107-13.

134. Noda T, Sugita Y, Aoyama K, Hirase A, Kawakami E, Miyazawa A, et al. Three-dimensional analysis of ribonucleoprotein complexes in influenza A virus. *Nat Commun.* 2012;3:639.
135. Akoto-Amanfu E, Sivasubramanian N, Nayak DP. Primary structure of the polymerase acidic (PA) gene of an influenza B virus (B/Sing/222/79). *Virology.* 1987;159(1):147-53.
136. Yamamoto-Goshima F, Maeno K, Morishita T, Ueda M, Fujita Y, Nakajima K, et al. Role of neuraminidase in the morphogenesis of influenza B virus. *J Virol.* 1994;68(2):1250-4.
137. Chen BJ, Takeda M, Lamb RA. Influenza virus hemagglutinin (H3 subtype) requires palmitoylation of its cytoplasmic tail for assembly: M1 proteins of two subtypes differ in their ability to support assembly. *J Virol.* 2005;79(21):13673-84.
138. Chen BJ, Leser GP, Morita E, Lamb RA. Influenza virus hemagglutinin and neuraminidase, but not the matrix protein, are required for assembly and budding of plasmid-derived virus-like particles. *J Virol.* 2007;81(13):7111-23.
139. Bourmakina SV, García-Sastre A. Reverse genetics studies on the filamentous morphology of influenza A virus. *J Gen Virol.* 2003;84(Pt 3):517-27.
140. Pampin M, Simonin Y, Blondel B, Percherancier Y, Chelbi-Alix MK. Cross talk between PML and p53 during poliovirus infection: implications for antiviral defense. *J Virol.* 2006;80(17):8582-92.
141. Kumar H, Kawai T, Akira S. Pathogen recognition by the innate immune system. *International reviews of immunology.* 2011;30(1):16-34.
142. Schenten D, Medzhitov R. The control of adaptive immune responses by the innate immune system. *Advances in immunology.* 2011;109:87-124.
143. Pang IK, Iwasaki A. Inflammasomes as mediators of immunity against influenza virus. *Trends in immunology.* 2011;32(1):34-41.
144. Alexopoulou L, Holt AC, Medzhitov R, Flavell RA. Recognition of double-stranded RNA and activation of NF-kappaB by Toll-like receptor 3. *Nature.* 2001;413(6857):732-8.
145. Heil F, Hemmi H, Hochrein H, Ampenberger F, Kirschning C, Akira S, et al. Species-specific recognition of single-stranded RNA via toll-like receptor 7 and 8. *Science.* 2004;303(5663):1526-9.
146. Lund JM, Alexopoulou L, Sato A, Karow M, Adams NC, Gale NW, et al.

Recognition of single-stranded RNA viruses by Toll-like receptor 7. *Proc Natl Acad Sci U S A*. 2004;101(15):5598-603.

147. Holzinger D, Jorns C, Stertz S, Boisson-Dupuis S, Thimme R, Weidmann M, et al. Induction of MxA gene expression by influenza A virus requires type I or type III interferon signaling. *J Virol*. 2007;81(14):7776-85.

148. Haller O, Kochs G. Interferon-induced mx proteins: dynamin-like GTPases with antiviral activity. *Traffic*. 2002;3(10):710-7.

149. Haller O, Frese M, Kochs G. Mx proteins: mediators of innate resistance to RNA viruses. *Rev Sci Tech*. 1998;17(1):220-30.

150. Kim HM, Lee YW, Lee KJ, Kim HS, Cho SW, van Rooijen N, et al. Alveolar macrophages are indispensable for controlling influenza viruses in lungs of pigs. *J Virol*. 2008;82(9):4265-74.

151. Tumpey TM, Garcia-Sastre A, Taubenberger JK, Palese P, Swayne DE, Pantin-Jackwood MJ, et al. Pathogenicity of influenza viruses with genes from the 1918 pandemic virus: functional roles of alveolar macrophages and neutrophils in limiting virus replication and mortality in mice. *J Virol*. 2005;79(23):14933-44.

152. Jayasekera JP, Vinuesa CG, Karupiah G, King NJ. Enhanced antiviral antibody secretion and attenuated immunopathology during influenza virus infection in nitric oxide synthase-2-deficient mice. *J Gen Virol*. 2006;87(Pt 11):3361-71.

153. Lin KL, Suzuki Y, Nakano H, Ramsburg E, Gunn MD. CCR2+ monocyte-derived dendritic cells and exudate macrophages produce influenza-induced pulmonary immune pathology and mortality. *J Immunol*. 2008;180(4):2562-72.

154. Peper RL, Van Campen H. Tumor necrosis factor as a mediator of inflammation in influenza A viral pneumonia. *Microbial pathogenesis*. 1995;19(3):175-83.

155. Ben-Sasson SZ, Hu-Li J, Quiel J, Cauchetaux S, Ratner M, Shapira I, et al. IL-1 acts directly on CD4 T cells to enhance their antigen-driven expansion and differentiation. *Proc Natl Acad Sci U S A*. 2009;106(17):7119-24.

156. Acosta-Rodriguez EV, Napolitani G, Lanzavecchia A, Sallusto F. Interleukins 1beta and 6 but not transforming growth factor-beta are essential for the differentiation of interleukin 17-producing human T helper cells. *Nature immunology*. 2007;8(9):942-9.

157. Zhang N, Bevan MJ. CD8(+) T cells: foot soldiers of the immune system. *Immunity*. 2011;35(2):161-8.

158. Soghoian DZ, Streeck H. Cytolytic CD4(+) T cells in viral immunity. *Expert review of vaccines*. 2010;9(12):1453-63.
159. Lucey DR, Clerici M, Shearer GM. Type 1 and type 2 cytokine dysregulation in human infectious, neoplastic, and inflammatory diseases. *Clinical microbiology reviews*. 1996;9(4):532-62.
160. Lamb JR, Woody JN, Hartzman RJ, Eckels DD. In vitro influenza virus-specific antibody production in man: antigen-specific and HLA-restricted induction of helper activity mediated by cloned human T lymphocytes. *J Immunol*. 1982;129(4):1465-70.
161. Mazanec MB, Coudret CL, Fletcher DR. Intracellular neutralization of influenza virus by immunoglobulin A anti-hemagglutinin monoclonal antibodies. *J Virol*. 1995;69(2):1339-43.
162. Rothbarth PH, Groen J, Bohnen AM, de Groot R, Osterhaus AD. Influenza virus serology--a comparative study. *Journal of virological methods*. 1999;78(1-2):163-9.
163. Murphy BR, Nelson DL, Wright PF, Tierney EL, Phelan MA, Chanock RM. Secretory and systemic immunological response in children infected with live attenuated influenza A virus vaccines. *Infection and immunity*. 1982;36(3):1102-8.
164. Fernandez Gonzalez S, Jayasekera JP, Carroll MC. Complement and natural antibody are required in the long-term memory response to influenza virus. *Vaccine*. 2008;26 Suppl 8:186-93.
165. Jayasekera JP, Moseman EA, Carroll MC. Natural antibody and complement mediate neutralization of influenza virus in the absence of prior immunity. *J Virol*. 2007;81(7):3487-94.
166. Potter CW, Oxford JS. Determinants of immunity to influenza infection in man. *British medical bulletin*. 1979;35(1):69-75.
167. Mancini N, Solfrosi L, Clementi N, De Marco D, Clementi M, Burioni R. A potential role for monoclonal antibodies in prophylactic and therapeutic treatment of influenza. *Antiviral research*. 2011;92(1):15-26.
168. Gerhard W. The role of the antibody response in influenza virus infection. *Current topics in microbiology and immunology*. 2001;260:171-90.
169. Kreijtz JH, Fouchier RA, Rimmelzwaan GF. Immune responses to influenza virus infection. *Virus Res*. 2011;162(1-2):19-30.

170. Nakaya HI, Wrammert J, Lee EK, Racioppi L, Marie-Kunze S, Haining WN, et al. Systems biology of vaccination for seasonal influenza in humans. *Nature immunology*. 2011;12(8):786-95.
171. Donelan NR, Dauber B, Wang X, Basler CF, Wolff T, Garcia-Sastre A. The N- and C-terminal domains of the NS1 protein of influenza B virus can independently inhibit IRF-3 and beta interferon promoter activation. *J Virol*. 2004;78(21):11574-82.
172. Dauber B, Schneider J, Wolff T. Double-stranded RNA binding of influenza B virus nonstructural NS1 protein inhibits protein kinase R but is not essential to antagonize production of alpha/beta interferon. *J Virol*. 2006;80(23):11667-77.
173. Wang W, Krug RM. The RNA-binding and effector domains of the viral NS1 protein are conserved to different extents among influenza A and B viruses. *Virology*. 1996;223(1):41-50.
174. Sadler AJ, Williams BR. Structure and function of the protein kinase R. *Current topics in microbiology and immunology*. 2007;316:253-92.
175. Hiscott J, Pitha P, Genin P, Nguyen H, Heylbroeck C, Mamane Y, et al. Triggering the interferon response: the role of IRF-3 transcription factor. *J Interferon Cytokine Res*. 1999;19(1):1-13.
176. Hai R, Martinez-Sobrido L, Fraser KA, Ayllon J, Garcia-Sastre A, Palese P. Influenza B virus NS1-truncated mutants: live-attenuated vaccine approach. *J Virol*. 2008;82(21):10580-90.
177. Wressnigg N, Shurygina AP, Wolff T, Redlberger-Fritz M, Popow-Kraupp T, Muster T, et al. Influenza B mutant viruses with truncated NS1 proteins grow efficiently in Vero cells and are immunogenic in mice. *J Gen Virol*. 2009;90(Pt 2):366-74.
178. Ramis AJ, van Riel D, van de Bildt MW, Osterhaus A, Kuiken T. Influenza A and B virus attachment to respiratory tract in marine mammals. *Emerg Infect Dis*. 2012;18(5):817-20.
179. de Silva UC, Tanaka H, Nakamura S, Goto N, Yasunaga T. A comprehensive analysis of reassortment in influenza A virus. *Biology open*. 2012;1(4):385-90.
180. Jian JW, Lai CT, Kuo CY, Kuo SH, Hsu LC, Chen PJ, et al. Genetic analysis and evaluation of the reassortment of influenza B viruses isolated in Taiwan during the 2004-2005 and 2006-2007 epidemics. *Virus Res*. 2008;131(2):243-9.
181. Chen R, Holmes EC. The evolutionary dynamics of human influenza B virus. *Journal of molecular evolution*. 2008;66(6):655-63.

182. Tsai HP, Wang HC, Kiang D, Huang SW, Kuo PH, Liu CC, et al. Increasing appearance of reassortant influenza B virus in Taiwan from 2002 to 2005. *J Clin Microbiol.* 2006;44(8):2705-13.
183. Xu X, Lindstrom SE, Shaw MW, Smith CB, Hall HE, Mungall BA, et al. Reassortment and evolution of current human influenza A and B viruses. *Virus Res.* 2004;103(1-2):55-60.
184. Luo C, Morishita T, Satou K, Tateno Y, Nakajima K, Nobusawa E. Evolutionary pattern of influenza B viruses based on the HA and NS genes during 1940 to 1999: origin of the NS genes after 1997. *Arch Virol.* 1999;144(10):1881-91.
185. Hiromoto Y, Saito T, Lindstrom SE, Li Y, Nerome R, Sugita S, et al. Phylogenetic analysis of the three polymerase genes (PB1, PB2 and PA) of influenza B virus. *J Gen Virol.* 2000;81(Pt 4):929-37.
186. Ghate AA, Air GM. Influenza type B neuraminidase can replace the function of type A neuraminidase. *Virology.* 1999;264(2):265-77.
187. Kaverin NV, Varich NL, Sklyanskaya EI, Amvrosieva TV, Petrik J, Vovk TC. Studies on heterotypic interference between influenza A and B viruses: a differential inhibition of the synthesis of viral proteins and RNAs. *J Gen Virol.* 1983;64 (Pt 10):2139-46.
188. Tanaka T, Urabe M, Goto H, Tobita K. Isolation and preliminary characterization of a highly cytolytic influenza B virus variant with an aberrant NS gene. *Virology.* 1984;135(2):515-23.
189. Nobusawa E, Sato K. Comparison of the mutation rates of human influenza A and B viruses. *J Virol.* 2006;80(7):3675-8.
190. Air GM, Gibbs AJ, Laver WG, Webster RG. Evolutionary changes in influenza B are not primarily governed by antibody selection. *Proc Natl Acad Sci U S A.* 1990;87(10):3884-8.
191. Yamashita M, Krystal M, Fitch WM, Palese P. Influenza B virus evolution: co-circulating lineages and comparison of evolutionary pattern with those of influenza A and C viruses. *Virology.* 1988;163(1):112-22.
192. Fitch WM, Leiter JM, Li XQ, Palese P. Positive Darwinian evolution in human influenza A viruses. *Proc Natl Acad Sci U S A.* 1991;88(10):4270-4.
193. Ina Y, Gojobori T. Statistical analysis of nucleotide sequences of the hemagglutinin gene of human influenza A viruses. *Proc Natl Acad Sci U S A.* 1994;91(18):8388-92.

194. Sridharan H, Zhao C, Krug RM. Species specificity of the NS1 protein of influenza B virus: NS1 binds only human and non-human primate ubiquitin-like ISG15 proteins. *The Journal of biological chemistry*. 2010;285(11):7852-6.
195. Versteeg GA, Hale BG, van Boheemen S, Wolff T, Lenschow DJ, García-Sastre A. Species-specific antagonism of host ISGylation by the influenza B virus NS1 protein. *J Virol*. 2010;84(10):5423-30.
196. Yuan W, Aramini JM, Montelione GT, Krug RM. Structural basis for ubiquitin-like ISG 15 protein binding to the NS1 protein of influenza B virus: a protein-protein interaction function that is not shared by the corresponding N-terminal domain of the NS1 protein of influenza A virus. *Virology*. 2002;304(2):291-301.
197. Okumura A, Lu G, Pitha-Rowe I, Pitha PM. Innate antiviral response targets HIV-1 release by the induction of ubiquitin-like protein ISG15. *Proc Natl Acad Sci U S A*. 2006;103(5):1440-5.
198. Lenschow DJ, Giannakopoulos NV, Gunn LJ, Johnston C, O'Guin AK, Schmidt RE, et al. Identification of interferon-stimulated gene 15 as an antiviral molecule during Sindbis virus infection in vivo. *J Virol*. 2005;79(22):13974-83.
199. Guan Z, Liu D, Mi S, Zhang J, Ye Q, Wang M, et al. Interaction of Hsp40 with influenza virus M2 protein: implications for PKR signaling pathway. *Protein & cell*. 2010;1(10):944-55.
200. Karpala AJ, Stewart C, McKay J, Lowenthal JW, Bean AG. Characterization of chicken Mda5 activity: regulation of IFN-beta in the absence of RIG-I functionality. *J Immunol*. 2011;186(9):5397-405.
201. Barber MR, Aldridge JR, Jr., Webster RG, Magor KE. Association of RIG-I with innate immunity of ducks to influenza. *Proc Natl Acad Sci U S A*. 2010;107(13):5913-8.
202. Rajsbaum R, Albrecht RA, Wang MK, Maharaj NP, Versteeg GA, Nistal-Villan E, et al. Species-specific inhibition of RIG-I ubiquitination and IFN induction by the influenza A virus NS1 protein. *PLoS pathogens*. 2012;8(11):e1003059.
203. Matrosovich MN, Gambaryan AS, Tuzikov AB, Byramova NE, Mochalova LV, Golbraikh AA, et al. Probing of the receptor-binding sites of the H1 and H3 influenza A and influenza B virus hemagglutinins by synthetic and natural sialosides. *Virology*. 1993;196(1):111-21.
204. Ni F, Mbawuike IN, Kondrashkina E, Wang Q. The roles of hemagglutinin Phe-95 in receptor binding and pathogenicity of influenza B virus. *Virology*. 2014;450-451:71-83.

205. Bradley KC, Galloway SE, Lasanajak Y, Song X, Heimbarg-Molinaro J, Yu H, et al. Analysis of influenza virus hemagglutinin receptor binding mutants with limited receptor recognition properties and conditional replication characteristics. *J Virol*. 2011;85(23):12387-98.
206. Dauber B, Heins G, Wolff T. The influenza B virus nonstructural NS1 protein is essential for efficient viral growth and antagonizes beta interferon induction. *J Virol*. 2004;78(4):1865-72.
207. Hatta M, Kawaoka Y. The NB Protein of influenza B virus is not necessary for virus replication in vitro. *Journal of Virology*. 2003;77(10):6050-4.
208. Hoffmann E, Mahmood K, Chen Z, Yang CF, Spaete J, Greenberg HB, et al. Multiple gene segments control the temperature sensitivity and attenuation phenotypes of ca B/Ann Arbor/1/66. *J Virol*. 2005;79(17):11014-21.
209. Russell J, Zomerdijk JC. The RNA polymerase I transcription machinery. *Biochemical Society symposium*. 2006(73):203-16.
210. Sims RJ, 3rd, Mandal SS, Reinberg D. Recent highlights of RNA-polymerase-II-mediated transcription. *Current opinion in cell biology*. 2004;16(3):263-71.
211. Lugovtsev VY, Vodeiko GM, Strupczewski CM, Ye Z, Levandowski RA. Generation of the influenza B viruses with improved growth phenotype by substitution of specific amino acids of hemagglutinin. *Virology*. 2007;365(2):315-23.
212. Imai M, Kawaoka Y. The role of receptor binding specificity in interspecies transmission of influenza viruses. *Curr Opin Virol*. 2012;2(2):160-7.
213. Lugovtsev VY, Smith DF, Weir JP. Changes of the receptor-binding properties of influenza B virus B/Victoria/504/2000 during adaptation in chicken eggs. *Virology*. 2009;394(2):218-26.
214. Chen Z, Aspelund A, Jin H. Stabilizing the glycosylation pattern of influenza B hemagglutinin following adaptation to growth in eggs. *Vaccine*. 2008;26(3):361-71.
215. Palese P. Making better influenza virus vaccines? *Emerg Infect Dis*. 2006;12(1):61-5.
216. Robertson JS, Naeve CW, Webster RG, Bootman JS, Newman R, Schild GC. Alterations in the hemagglutinin associated with adaptation of influenza B virus to growth in eggs. *Virology*. 1985;143(1):166-74.

217. Shaw MW, Xu X, Li Y, Normand S, Ueki RT, Kunimoto GY, et al. Reappearance and global spread of variants of influenza B/Victoria/2/87 lineage viruses in the 2000-2001 and 2001-2002 seasons. *Virology*. 2002;303(1):1-8.
218. Saito T, Nakaya Y, Suzuki T, Ito R, Saito H, Takao S, et al. Antigenic alteration of influenza B virus associated with loss of a glycosylation site due to host-cell adaptation. *J Med Virol*. 2004;74(2):336-43.
219. Chen BJ, Leser GP, Jackson D, Lamb RA. The influenza virus M2 protein cytoplasmic tail interacts with the M1 protein and influences virus assembly at the site of virus budding. *J Virol*. 2008;82(20):10059-70.
220. Maassab HF. Adaptation and growth characteristics of influenza virus at 25 degrees c. *Nature*. 1967;213(5076):612-4.
221. Maassab HF, Bryant ML. The development of live attenuated cold-adapted influenza virus vaccine for humans. *Reviews in medical virology*. 1999;9(4):237-44.
222. DeBorde DC, Naeve CW, Herlocher ML, Maassab HF. Nucleotide sequences of the PA and PB1 genes of B/Ann Arbor/1/66 virus: comparison with genes of B/Lee/40 and type A influenza viruses. *Virus Res*. 1987;8(1):33-41.
223. Alexandrova GI, Maassab HF, Kendal AP, Medvedeva TE, Egorov AY, Klimov AI, et al. Laboratory properties of cold-adapted influenza B live vaccine strains developed in the US and USSR, and their B/Ann Arbor/1/86 cold-adapted reassortant vaccine candidates. *Vaccine*. 1990;8(1):61-4.
224. Cabezas JA, Milicua M, Bernal CS, Villar E, Perez N, Hannoun C. Kinetic studies on the sialidase of three influenza B and three influenza A virus strains. *Glycoconjugate journal*. 1989;6(2):219-27.
225. Whitley RJ, Boucher CA, Lina B, Nguyen-Van-Tam JS, Osterhaus A, Schutten M, et al. Global assessment of resistance to neuraminidase inhibitors, 2008-2011: the Influenza Resistance Information Study (IRIS). *Clinical infectious diseases : an official publication of the Infectious Diseases Society of America*. 2013;56(9):1197-205.
226. Fischer WB, Pitkeathly M, Sansom MS. Amantadine blocks channel activity of the transmembrane segment of the NB protein from influenza B. *European biophysics journal : EBJ*. 2001;30(6):416-20.
227. Elspeth Garman GL. The Structure, Function, and Inhibition of Influenza Virus Neuraminidase. In: Fischer W, editor. *Viral Membrane Proteins: Structure, Function, and Drug Design*. New York: Kluwer Academic / Plenum Publishers; 2005. p. 247-67.

228. Jefferson T, Jones M, Doshi P, Spencer EA, Onakpoya I, Heneghan CJ. Oseltamivir for influenza in adults and children: systematic review of clinical study reports and summary of regulatory comments. *BMJ*. 2014;348.
229. Heneghan CJ, Onakpoya I, Thompson M, Spencer EA, Jones M, Jefferson T. Zanamivir for influenza in adults and children: systematic review of clinical study reports and summary of regulatory comments. *BMJ*. 2014;348.
230. Barnett JM, Cadman A, Burrell FM, Madar SH, Lewis AP, Tisdale M, et al. In vitro selection and characterisation of influenza B/Beijing/1/87 isolates with altered susceptibility to zanamivir. *Virology*. 1999;265(2):286-95.
231. Staschke KA, Colacino JM, Baxter AJ, Air GM, Bansal A, Hornback WJ, et al. Molecular basis for the resistance of influenza viruses to 4-guanidino-Neu5Ac2en. *Virology*. 1995;214(2):642-6.
232. Jackson D, Barclay W, Zürcher T. Characterization of recombinant influenza B viruses with key neuraminidase inhibitor resistance mutations. *J Antimicrob Chemother*. 2005;55(2):162-9.
233. Hatta M, Kawaoka Y. The NB protein of influenza B virus is not necessary for virus replication in vitro. *J Virol*. 2003;77(10):6050-4.
234. McCullers JA, Hoffmann E, Huber VC, Nickerson AD. A single amino acid change in the C-terminal domain of the matrix protein M1 of influenza B virus confers mouse adaptation and virulence. *Virology*. 2005;336(2):318-26.
235. Hatta M, Kohlmeier CK, Hatta Y, Ozawa M, Kawaoka Y. Region required for protein expression from the stop-start pentanucleotide in the M gene of influenza B virus. *J Virol*. 2009;83(11):5939-42.
236. Powell ML, Napthine S, Jackson RJ, Brierley I, Brown TD. Characterization of the termination-reinitiation strategy employed in the expression of influenza B virus BM2 protein. *RNA (New York, NY)*. 2008;14(11):2394-406.
237. Hatta M, Goto H, Kawaoka Y. Influenza B virus requires BM2 protein for replication. *J Virol*. 2004;78(11):5576-83.
238. Kittel C, Ferko B, Kurz M, Voglauer R, Sereinig S, Romanova J, et al. Generation of an influenza A virus vector expressing biologically active human interleukin-2 from the NS gene segment. *J Virol*. 2005;79(16):10672-7.
239. Watanabe T, Watanabe S, Kim JH, Hatta M, Kawaoka Y. Novel approach to the development of effective H5N1 influenza A virus vaccines: use of M2 cytoplasmic tail mutants. *J Virol*. 2008;82(5):2486-92.

240. Watanabe S, Watanabe T, Kawaoka Y. Influenza A virus lacking M2 protein as a live attenuated vaccine. *J Virol.* 2009;83(11):5947-50.
241. Lamb RA, Lai CJ, Choppin PW. Sequences of mRNAs derived from genome RNA segment 7 of influenza virus: colinear and interrupted mRNAs code for overlapping proteins. *Proc Natl Acad Sci U S A.* 1981;78(7):4170-4.
242. Pica N, Iyer A, Ramos I, Bouvier NM, Fernandez-Sesma A, García-Sastre A, et al. The DBA.2 mouse is susceptible to disease following infection with a broad, but limited, range of influenza A and B viruses. *J Virol.* 2011;85(23):12825-9.
243. Bouvier NM, Lowen AC. Animal Models for Influenza Virus Pathogenesis and Transmission. *Viruses.* 2010;2(8):1530-63.
244. Li L, Wang D, Jiang Y, Sun J, Zhang S, Chen Y, et al. Crystal structure of human ISG15 protein in complex with influenza B virus NS1B. *The Journal of biological chemistry.* 2011;286(35):30258-62.
245. Guan R, Ma LC, Leonard PG, Amer BR, Sridharan H, Zhao C, et al. Structural basis for the sequence-specific recognition of human ISG15 by the NS1 protein of influenza B virus. *Proc Natl Acad Sci U S A.* 2011;108(33):13468-73.
246. Ehrhardt C, Wolff T, Ludwig S. Activation of phosphatidylinositol 3-kinase signaling by the nonstructural NS1 protein is not conserved among type A and B influenza viruses. *J Virol.* 2007;81(21):12097-100.
247. Schneider J, Dauber B, Melén K, Julkunen I, Wolff T. Analysis of influenza B Virus NS1 protein trafficking reveals a novel interaction with nuclear speckle domains. *J Virol.* 2009;83(2):701-11.
248. Pica N, Langlois RA, Krammer F, Margine I, Palese P. NS1-truncated live attenuated virus vaccine provides robust protection to aged mice from viral challenge. *J Virol.* 2012;86(19):10293-301.
249. Gerdil C. The annual production cycle for influenza vaccine. *Vaccine.* 2003;21(16):1776-9.
250. Webby RJ, Perez DR, Coleman JS, Guan Y, Knight JH, Govorkova EA, et al. Responsiveness to a pandemic alert: use of reverse genetics for rapid development of influenza vaccines. *Lancet.* 2004;363(9415):1099-103.
251. Gack MU, Albrecht RA, Urano T, Inn KS, Huang IC, Carnero E, et al. Influenza A virus NS1 targets the ubiquitin ligase TRIM25 to evade recognition by the host viral RNA sensor RIG-I. *Cell host & microbe.* 2009;5(5):439-49.

252. Bardiya N, Bae JH. Influenza vaccines: recent advances in production technologies. *Applied microbiology and biotechnology*. 2005;67(3):299-305.
253. Roumeliotis G. Medimmune cleared to offer Flumist the reverse-genetics treatment. *William Reed Business Media SAS*; 2006.
254. Lipatov AS, Govorkova EA, Webby RJ, Ozaki H, Peiris M, Guan Y, et al. Influenza: emergence and control. *J Virol*. 2004;78(17):8951-9.
255. Jung EJ, Lee KH, Seong BL. Reverse genetic platform for inactivated and live-attenuated influenza vaccine. *Exp Mol Med*. 2010;42(2):116-21.
256. Beyer WE, Palache AM, de Jong JC, Osterhaus AD. Cold-adapted live influenza vaccine versus inactivated vaccine: systemic vaccine reactions, local and systemic antibody response, and vaccine efficacy. A meta-analysis. *Vaccine*. 2002;20(9-10):1340-53.
257. Maassab HF, Francis T, Jr., Davenport FM, Hennessy AV, Minuse E, Anderson G. Laboratory and clinical characteristics of attenuated strains of influenza virus. *Bull World Health Organ*. 1969;41(3):589-94.
258. DeBorde DC, Donabedian AM, Herlocher ML, Naeve CW, Maassab HF. Sequence comparison of wild-type and cold-adapted B/Ann Arbor/1/66 influenza virus genes. *Virology*. 1988;163(2):429-43.
259. Chen Z, Aspelund A, Kemble G, Jin H. Genetic mapping of the cold-adapted phenotype of B/Ann Arbor/1/66, the master donor virus for live attenuated influenza vaccines (FluMist). *Virology*. 2006;345(2):416-23.
260. Chen Z, Aspelund A, Kemble G, Jin H. Molecular studies of temperature-sensitive replication of the cold-adapted B/Ann Arbor/1/66, the master donor virus for live attenuated influenza FluMist vaccines. *Virology*. 2008;380(2):354-62.
261. Kiseleva IV, Voeten JT, Teley LC, Larionova NV, Drieszen-van der Crujisen SK, Basten SM, et al. PB2 and PA genes control the expression of the temperature-sensitive phenotype of cold-adapted B/USSR/60/69 influenza master donor virus. *J Gen Virol*. 2010;91(Pt 4):931-7.
262. He W, Wang W, Han H, Wang L, Zhang G, Gao B. Molecular basis of live-attenuated influenza virus. *PLoS One*. 2013;8(3):e60413.
263. Monto AS, Miller FD, Maassab HF. Evaluation of an attenuated, cold-recombinant influenza B virus vaccine. *J Infect Dis*. 1982;145(1):57-64.
264. Falchi A, Arena C, Andreoletti L, Jacques J, Leveque N, Blanchon T, et al. Dual infections by influenza A/H3N2 and B viruses and by influenza A/H3N2 and

A/H1N1 viruses during winter 2007, Corsica Island, France. *J Clin Virol.* 2008;41(2):148-51.

265. Gauger PC, Vincent AL, Loving CL, Henningson JN, Lager KM, Janke BH, et al. Kinetics of lung lesion development and pro-inflammatory cytokine response in pigs with vaccine-associated enhanced respiratory disease induced by challenge with pandemic (2009) A/H1N1 influenza virus. *Vet Pathol.* 2012;49(6):900-12.

266. Khurana S, Loving CL, Manischewitz J, King LR, Gauger PC, Henningson J, et al. Vaccine-induced anti-HA2 antibodies promote virus fusion and enhance influenza virus respiratory disease. *Sci Transl Med.* 2013;5(200):200ra114.

267. Treanor J, Dumyati G, O'Brien D, Riley MA, Riley G, Erb S, et al. Evaluation of cold-adapted, reassortant influenza B virus vaccines in elderly and chronically ill adults. *J Infect Dis.* 1994;169(2):402-7.

268. Monto AS, Maassab HF. Use of influenza vaccine in non-high risk populations. *Developments in biological standardization.* 1977;39:329-35.

269. Keitel WA, Couch RB, Cate TR, Six HR, Baxter BD. Cold recombinant influenza B/Texas/1/84 vaccine virus (CRB 87): attenuation, immunogenicity, and efficacy against homotypic challenge. *J Infect Dis.* 1990;161(1):22-6.

270. Snyder MH, London WT, Maassab HF, Murphy BR. Attenuation and phenotypic stability of influenza B/Texas/1/84 cold-adapted reassortant virus: studies in hamsters and chimpanzees. *J Infect Dis.* 1989;160(4):604-10.

271. Edwards KM, King JC, Steinhoff MC, Thompson J, Clements ML, Wright PF, et al. Safety and immunogenicity of live attenuated cold-adapted influenza B/Ann Arbor/1/86 reassortant virus vaccine in infants and children. *J Infect Dis.* 1991;163(4):740-5.

272. Anderson EL, Newman FK, Maassab HF, Belshe RB. Evaluation of a cold-adapted influenza B/Texas/84 reassortant virus (CRB-87) vaccine in young children. *J Clin Microbiol.* 1992;30(9):2230-4.

273. Clements ML, Snyder MH, Sears SD, Maassab HF, Murphy BR. Evaluation of the infectivity, immunogenicity, and efficacy of live cold-adapted influenza B/Ann Arbor/1/86 reassortant virus vaccine in adult volunteers. *J Infect Dis.* 1990;161(5):869-77.

274. Belshe RB, Mendelman PM, Treanor J, King J, Gruber WC, Piedra P, et al. The efficacy of live attenuated, cold-adapted, trivalent, intranasal influenzavirus vaccine in children. *N Engl J Med.* 1998;338(20):1405-12.

275. Mendelman PM, Cordova J, Cho I. Safety, efficacy and effectiveness of the influenza virus vaccine, trivalent, types A and B, live, cold-adapted (CAIV-T) in healthy children and healthy adults. *Vaccine*. 2001;19(17-19):2221-6.
276. Halloran ME, Longini IM, Jr., Gaglani MJ, Piedra PA, Chu H, Herschler GB, et al. Estimating efficacy of trivalent, cold-adapted, influenza virus vaccine (CAIV-T) against influenza A (H1N1) and B using surveillance cultures. *American journal of epidemiology*. 2003;158(4):305-11.
277. Treanor JJ, Kotloff K, Betts RF, Belshe R, Newman F, Iacuzio D, et al. Evaluation of trivalent, live, cold-adapted (CAIV-T) and inactivated (TIV) influenza vaccines in prevention of virus infection and illness following challenge of adults with wild-type influenza A (H1N1), A (H3N2), and B viruses. *Vaccine*. 1999;18(9-10):899-906.
278. Nichol KL, Mendelman PM, Mallon KP, Jackson LA, Gorse GJ, Belshe RB, et al. Effectiveness of live, attenuated intranasal influenza virus vaccine in healthy, working adults: a randomized controlled trial. *JAMA*. 1999;282(2):137-44.
279. Steel J, Lowen AC, Pena L, Angel M, Solórzano A, Albrecht R, et al. Live attenuated influenza viruses containing NS1 truncations as vaccine candidates against H5N1 highly pathogenic avian influenza. *J Virol*. 2009;83(4):1742-53.
280. Quinlivan M, Zamarin D, Garcia-Sastre A, Cullinane A, Chambers T, Palese P. Attenuation of equine influenza viruses through truncations of the NS1 protein. *J Virol*. 2005;79(13):8431-9.
281. Morokutti A, Muster T, Ferko B. Intranasal vaccination with a replication-deficient influenza virus induces heterosubtypic neutralising mucosal IgA antibodies in humans. *Vaccine*. 2014.
282. Hatesuer B, Bertram S, Mehnert N, Bahgat MM, Nelson PS, Pohlman S, et al. Tmprss2 is essential for influenza H1N1 virus pathogenesis in mice. *PLoS pathogens*. 2013;9(12):e1003774.
283. Tyrrell DA, Horsfall FL, Jr. Disruption of influenza virus; properties of degradation products of the virus particle. *The Journal of experimental medicine*. 1954;99(4):321-42.
284. Stech J, Garn H, Wegmann M, Wagner R, Klenk HD. A new approach to an influenza live vaccine: modification of the cleavage site of hemagglutinin. *Nat Med*. 2005;11(6):683-9.
285. Stech J, Garn H, Herwig A, Stech O, Dauber B, Wolff T, et al. Influenza B virus with modified hemagglutinin cleavage site as a novel attenuated live vaccine. *J Infect Dis*. 2011;204(10):1483-90.

286. Daum LT, Canas LC, Klimov AI, Shaw MW, Gibbons RV, Shrestha SK, et al. Molecular analysis of isolates from influenza B outbreaks in the U.S. and Nepal, 2005. *Arch Virol.* 2006;151(9):1863-74.
287. Camilloni B, Neri M, Lepri E, Basileo M, Sigismondi N, Puzelli S, et al. An influenza B outbreak during the 2007/2008 winter among appropriately immunized elderly people living in a nursing home. *Vaccine.* 2010;28(47):7536-41.
288. Lanthier PA, Huston GE, Moquin A, Eaton SM, Szaba FM, Kummer LW, et al. Live attenuated influenza vaccine (LAIV) impacts innate and adaptive immune responses. *Vaccine.* 2011;29(44):7849-56.
289. Osterholm M, Kelley N, Sommer A, Belongia E. Efficacy and Effectiveness of influenza vaccines: a systematic review and meta-analysis. *The Lancet.* 2011;12(1):36-44.
290. McElhaney JE. The unmet need in the elderly: designing new influenza vaccines for older adults. *Vaccine.* 2005;23 Suppl 1:S10-25.
291. Lang PO, Samaras D, Samaras N, Govind S, Aspinall R. Influenza vaccination in the face of immune exhaustion: is herd immunity effective for protecting the elderly? *Influenza research and treatment.* 2011;2011:419216.
292. Keynan Y, Card CM, Ball BT, Li Y, Plummer FA, Fowke KR. Cellular immune responses to recurring influenza strains have limited boosting ability and limited cross-reactivity to other strains. *Clinical microbiology and infection : the official publication of the European Society of Clinical Microbiology and Infectious Diseases.* 2010;16(8):1179-86.
293. Grant E, Wu C, Chan KF, Eckle S, Bharadwaj M, Zou QM, et al. Nucleoprotein of influenza A virus is a major target of immunodominant CD8+ T-cell responses. *Immunology and cell biology.* 2013;91(2):184-94.
294. He F, Prabakaran M, Rajesh Kumar S, Tan Y, Kwang J. Monovalent H5 vaccine based on epitope-chimeric HA provides broad cross-clade protection against variant H5N1 viruses in mice. *Antiviral research.* 2014.
295. Xu K, Ling ZY, Sun L, Xu Y, Bian C, He Y, et al. Broad humoral and cellular immunity elicited by a bivalent DNA vaccine encoding HA and NP genes from an H5N1 virus. *Viral immunology.* 2011;24(1):45-56.
296. Lee LY, Ha do LA, Simmons C, de Jong MD, Chau NV, Schumacher R, et al. Memory T cells established by seasonal human influenza A infection cross-react with avian influenza A (H5N1) in healthy individuals. *The Journal of clinical investigation.* 2008;118(10):3478-90.

297. Terajima M, Babon JA, Co MD, Ennis FA. Cross-reactive human B cell and T cell epitopes between influenza A and B viruses. *Virology*. 2013;10:244.
298. Hoffmann E, Neumann G, Kawaoka Y, Hobom G, Webster RG. A DNA transfection system for generation of influenza A virus from eight plasmids. *Proc Natl Acad Sci U S A*. 2000;97(11):6108-13.
299. Hoffmann E, Stech J, Guan Y, Webster RG, Perez DR. Universal primer set for the full-length amplification of all influenza A viruses. *Arch Virol*. 2001;146(12):2275-89.
300. Reed L, Muench H. A simple method of estimating fifty percent endpoints. *American journal of hygiene*. 1938;27:493-7.
301. Reed IJ, Muench H. A simple method for estimating fifty percent endpoints. *American journal of hygiene*. 1938;27(3):493-7.
302. Edgar RC. MUSCLE: multiple sequence alignment with high accuracy and high throughput. *Nucleic acids research*. 2004;32(5):1792-7.
303. Stamatakis A. RAxML version 8: a tool for phylogenetic analysis and post-analysis of large phylogenies. *Bioinformatics*. 2014.
304. WHO. Summary of status of development and availability of influenza candidate vaccine viruses and potency testing reagents: World Health Organization (WHO); 2011 [updated 1/26/2011]. Available from: http://www.who.int/influenza/vaccines/virus/candidates_reagents/summary_b_cvv_reagents_2011_01_26.pdf?ua=1.
305. Zhu W, Zhou J, Qin K, Du N, Liu L, Yu Z, et al. A reporter system for assaying influenza virus RNP functionality based on secreted Gaussia luciferase activity. *Virology*. 2008;381:29-34.
306. Goodeve A, Potter CW, Clark A, Jennings R, Schild GC, Yetts R. A graded-dose study of inactivated, surface antigen influenza B vaccine in volunteers: reactogenicity, antibody response and protection to challenge virus infection. *The Journal of hygiene*. 1983;90(1):107-15.
307. Odagiri T, Hong J, Ohara Y. The BM2 protein of influenza B virus is synthesized in the late phase of infection and incorporated into virions as a subviral component. *J Gen Virol*. 1999;80 (Pt 10):2573-81.
308. O'Neill RE, Talon J, Palese P. The influenza virus NEP (NS2 protein) mediates the nuclear export of viral ribonucleoproteins. *EMBO J*. 1998;17(1):288-96.

309. Kuo YC, Oxford JS, Schild GC. Immunological studies with the HA1 and HA2 polypeptides of influenza A virus haemagglutinin. *Experimental cell biology*. 1978;46(6):338-54.
310. Jin H, Lu B, Zhou H, Ma C, Zhao J, Yang CF, et al. Multiple amino acid residues confer temperature sensitivity to human influenza virus vaccine strains (FluMist) derived from cold-adapted A/Ann Arbor/6/60. *Virology*. 2003;306(1):18-24.
311. Chan W, Zhou H, Kemble G, Jin H. The cold adapted and temperature sensitive influenza A/Ann Arbor/6/60 virus, the master donor virus for live attenuated influenza vaccines, has multiple defects in replication at the restrictive temperature. *Virology*. 2008;380(2):304-11.
312. He XS, Holmes TH, Zhang C, Mahmood K, Kemble GW, Lewis DB, et al. Cellular immune responses in children and adults receiving inactivated or live attenuated influenza vaccines. *J Virol*. 2006;80(23):11756-66.
313. Thomas PG, Keating R, Hulse-Post DJ, Doherty PC. Cell-mediated protection in influenza infection. *Emerg Infect Dis*. 2006;12(1):48-54.
314. Song H, Nieto GR, Perez DR. A new generation of modified live-attenuated avian influenza viruses using a two-strategy combination as potential vaccine candidates. *J Virol*. 2007;81(17):9238-48.
315. Hickman D, Hossain MJ, Song H, Araya Y, Solórzano A, Perez DR. An avian live attenuated master backbone for potential use in epidemic and pandemic influenza vaccines. *J Gen Virol*. 2008;89(Pt 11):2682-90.
316. Solórzano A, Ye J, Pérez DR. Alternative live-attenuated influenza vaccines based on modifications in the polymerase genes protect against epidemic and pandemic flu. *J Virol*. 2010;84(9):4587-96.
317. Song H, Nieto GR, Perez DR. A new generation of modified live-attenuated avian influenza viruses using a two-strategy combination as potential vaccine candidates. *J Virol*. 2007;81(17):9238-48.
318. Reeve P, Pibermann M, Gerendas B. Studies with some influenza B viruses in cell cultures, hamsters and hamster tracheal organ cultures. *Medical microbiology and immunology*. 1981;169(3):179-86.
319. Snyder MH, Betts RF, DeBorde D, Tierney EL, Clements ML, Herrington D, et al. Four viral genes independently contribute to attenuation of live influenza A/Ann Arbor/6/60 (H2N2) cold-adapted reassortant virus vaccines. *J Virol*. 1988;62(2):488-95.

320. Zhu W, Zhu Y, Qin K, Yu Z, Gao R, Yu H, et al. Mutations in polymerase genes enhanced the virulence of 2009 pandemic H1N1 influenza virus in mice. *PLoS One*. 2012;7(3):e33383.
321. de Jong RM, Stockhofe-Zurwieden N, Verheij ES, de Boer-Luijtz EA, Ruiter SJ, de Leeuw OS, et al. Rapid emergence of a virulent PB2 E627K variant during adaptation of highly pathogenic avian influenza H7N7 virus to mice. *Virol J*. 2013;10:276.
322. Yao Y, Mingay LJ, McCauley JW, Barclay WS. Sequences in influenza A virus PB2 protein that determine productive infection for an avian influenza virus in mouse and human cell lines. *J Virol*. 2001;75(11):5410-5.
323. Hiromoto Y, Yamazaki Y, Fukushima T, Saito T, Lindstrom SE, Omoe K, et al. Evolutionary characterization of the six internal genes of H5N1 human influenza A virus. *J Gen Virol*. 2000;81(Pt 5):1293-303.
324. Katz JM, Lu X, Tumpey TM, Smith CB, Shaw MW, Subbarao K. Molecular correlates of influenza A H5N1 virus pathogenesis in mice. *J Virol*. 2000;74(22):10807-10.
325. Sutton TC, Finch C, Shao H, Angel M, Chen H, Capua I, et al. Airborne Transmission of Highly Pathogenic H7N1 Influenza in Ferrets. *J Virol*. 2014.
326. Schreier E, Petzold DR, Michel S, Dittmann S. Evolution of influenza polymerase: nucleotide sequence of the PB2 gene of A/Chile/1/83 (H1 N1). *Arch Virol*. 1988;103(3-4):179-87.
327. Klumpp K, Ruigrok RW, Baudin F. Roles of the influenza virus polymerase and nucleoprotein in forming a functional RNP structure. *EMBO J*. 1997;16(6):1248-57.
328. Plotch SJ, Bouloy M, Ulmanen I, Krug RM. A unique cap(m7GpppXm)-dependent influenza virion endonuclease cleaves capped RNAs to generate the primers that initiate viral RNA transcription. *Cell*. 1981;23(3):847-58.
329. Blaas D, Patzelt E, Kuechler E. Identification of the cap binding protein of influenza virus. *Nucleic acids research*. 1982;10(15):4803-12.
330. Sugiyama K, Obayashi E, Kawaguchi A, Suzuki Y, Tame JR, Nagata K, et al. Structural insight into the essential PB1-PB2 subunit contact of the influenza virus RNA polymerase. *EMBO J*. 2009;28(12):1803-11.
331. Wang YF, Chang CF, Chi CY, Wang HC, Wang JR, Su IJ. Characterization of glycan binding specificities of influenza B viruses with correlation with hemagglutinin genotypes and clinical features. *J Med Virol*. 2012;84(4):679-85.

332. Iwatsuki-Horimoto K, Horimoto T, Noda T, Kiso M, Maeda J, Watanabe S, et al. The cytoplasmic tail of the influenza A virus M2 protein plays a role in viral assembly. *J Virol*. 2006;80(11):5233-40.
333. Staeheli P, Haller O, Boll W, Lindenmann J, Weissmann C. Mx protein: constitutive expression in 3T3 cells transformed with cloned Mx cDNA confers selective resistance to influenza virus. *Cell*. 1986;44(1):147-58.
334. Tumpey TM, Szretter KJ, Van Hoeven N, Katz JM, Kochs G, Haller O, et al. The Mx1 gene protects mice against the pandemic 1918 and highly lethal human H5N1 influenza viruses. *J Virol*. 2007;81(19):10818-21.
335. Armstrong SM, Wang C, Tigdi J, Si X, Dumpit C, Charles S, et al. Influenza infects lung microvascular endothelium leading to microvascular leak: role of apoptosis and claudin-5. *PLoS One*. 2012;7(10):e47323.
336. Harms PW, Schmidt LA, Smith LB, Newton DW, Pletneva MA, Walters LL, et al. Autopsy findings in eight patients with fatal H1N1 influenza. *Am J Clin Pathol*. 2010;134(1):27-35.
337. Zeng H, Pappas C, Belser JA, Houser KV, Zhong W, Wadford DA, et al. Human pulmonary microvascular endothelial cells support productive replication of highly pathogenic avian influenza viruses: possible involvement in the pathogenesis of human H5N1 virus infection. *J Virol*. 2012;86(2):667-78.
338. Fauci ASB, Eugene. Kasper, Dennis L. Hauser, Stephen L. Longo, Dan L. Jameson, J. Larry. Loscalzo, Joseph. Shanahan, James. Englis, Mariapaz Ramos., editor. *Harrison's Manual of Medicine*. 17 ed: McGraw-Hill; 2009.
339. Subbarao EK, London W, Murphy BR. A single amino acid in the PB2 gene of influenza A virus is a determinant of host range. *J Virol*. 1993;67(4):1761-4.
340. Shinya K, Hamm S, Hatta M, Ito H, Ito T, Kawaoka Y. PB2 amino acid at position 627 affects replicative efficiency, but not cell tropism, of Hong Kong H5N1 influenza A viruses in mice. *Virology*. 2004;320(2):258-66.
341. Hirst GK. Studies on the Mechanism of Adaptation of Influenza Virus to Mice. *The Journal of experimental medicine*. 1947;86(5):357-66.
342. Dreyfus C, Laursen NS, Kwaks T, Zuijdgheest D, Khayat R, Ekiert DC, et al. Highly conserved protective epitopes on influenza B viruses. *Science*. 2012;337(6100):1343-8.
343. Lai C, Struckhoff JJ, Schneider J, Martinez-Sobrido L, Wolff T, Garcia-Sastre A, et al. Mice lacking the ISG15 E1 enzyme Ube1L demonstrate increased

- susceptibility to both mouse-adapted and non-mouse-adapted influenza B virus infection. *J Virol.* 2009;83(2):1147-51.
344. Fodor E, Crow M, Mingay LJ, Deng T, Sharps J, Fechter P, et al. A single amino acid mutation in the PA subunit of the influenza virus RNA polymerase inhibits endonucleolytic cleavage of capped RNAs. *J Virol.* 2002;76(18):8989-9001.
345. Martin K, Helenius A. Nuclear transport of influenza virus ribonucleoproteins: the viral matrix protein (M1) promotes export and inhibits import. *Cell.* 1991;67(1):117-30.
346. Motta FC, Siqueira MM, Lugon AK, Straliotto SM, Fernandes SB, Krawczuk MM. The reappearance of Victoria lineage influenza B virus in Brazil, antigenic and molecular analysis. *J Clin Virol.* 2006;36(3):208-14.
347. Seo SU, Byun YH, Lee EY, Jung EJ, Jang YH, Kim HA, et al. Development and characterization of a live attenuated influenza B virus vaccine candidate. *Vaccine.* 2008;26(7):874-81.
348. Loving CL, Vincent AL, Pena L, Perez DR. Heightened adaptive immune responses following vaccination with a temperature-sensitive, live-attenuated influenza virus compared to adjuvanted, whole-inactivated virus in pigs. *Vaccine.* 2012;30(40):5830-8.
349. Cheng X, Zengel JR, Suguitan AL, Jr., Xu Q, Wang W, Lin J, et al. Evaluation of the humoral and cellular immune responses elicited by the live attenuated and inactivated influenza vaccines and their roles in heterologous protection in ferrets. *J Infect Dis.* 2013;208(4):594-602.
350. Zhu W, Higgs BW, Morehouse C, Streicher K, Ambrose CS, Woo J, et al. A whole genome transcriptional analysis of the early immune response induced by live attenuated and inactivated influenza vaccines in young children. *Vaccine.* 2010;28(16):2865-76.
351. Reber AJ, Chirkova T, Kim JH, Cao W, Biber R, Shay DK, et al. Immunosenescence and Challenges of Vaccination against Influenza in the Aging Population. *Aging and disease.* 2012;3(1):68-90.
352. Akarsu H, Iwatsuki-Horimoto K, Noda T, Kawakami E, Katsura H, Baudin F, et al. Structure-based design of NS2 mutants for attenuated influenza A virus vaccines. *Virus Res.* 2011;155(1):240-8.
353. Hatta Y, Hatta M, Bilsel P, Neumann G, Kawaoka Y. An M2 cytoplasmic tail mutant as a live attenuated influenza vaccine against pandemic (H1N1) 2009 influenza virus. *Vaccine.* 2011;29(12):2308-12.

354. Victor ST, Watanabe S, Katsura H, Ozawa M, Kawaoka Y. A replication-incompetent PB2-knockout influenza A virus vaccine vector. *J Virol.* 2012;86(8):4123-8.
355. Stech J, Garn H, Herwig A, Stech O, Dauber B, Wolff T, et al. Influenza B virus with modified hemagglutinin cleavage site as a novel attenuated live vaccine. *J Infect Dis.* 2011;204(10):1483-90.
356. Jin H, Zhou H, Lu B, Kemble G. Imparting temperature sensitivity and attenuation in ferrets to A/Puerto Rico/8/34 influenza virus by transferring the genetic signature for temperature sensitivity from cold-adapted A/Ann Arbor/6/60. *J Virol.* 2004;78(2):995-8.
357. Cai Y, Song H, Ye J, Shao H, Padmanabhan R, Sutton TC, et al. Improved hatchability and efficient protection after in ovo vaccination with live-attenuated H7N2 and H9N2 avian influenza viruses. *Virol J.* 2011;8:31.
358. Roscoe B. Jackson Memorial Laboratory., Green EL. *Biology of the laboratory mouse.* 2d ed. New York,: Blakiston Division; 1966. xii, 706 p. p.
359. Wacheck V, Egorov A, Groiss F, Pfeiffer A, Fuereder T, Hoeflmayer D, et al. A novel type of influenza vaccine: safety and immunogenicity of replication-deficient influenza virus created by deletion of the interferon antagonist NS1. *J Infect Dis.* 2010;201(3):354-62.
360. Flandorfer A, García-Sastre A, Basler CF, Palese P. Chimeric influenza A viruses with a functional influenza B virus neuraminidase or hemagglutinin. *J Virol.* 2003;77(17):9116-23.